National Library of Canada
Acquisitions and Bibliographic Services Branch
395 Wellington Street
Ottawa, Ontario
K1A 0N4

Bibliothèque nationale du Canada
Direction des acquisitions et des services bibliographiques
395, rue Wellington
Ottawa (Ontario)
K1A 0N4

Your file Votre référence

Our file Notre référence

NOTICE

The quality of this microform is heavily dependent upon the quality of the original thesis submitted for microfilming. Every effort has been made to ensure the highest quality of reproduction possible.

If pages are missing, contact the university which granted the degree.

Some pages may have indistinct print especially if the original pages were typed with a poor typewriter ribbon or if the university sent us an inferior photocopy.

Reproduction in full or in part of this microform is governed by the Canadian Copyright Act, R.S.C. 1970, c. C-30, and subsequent amendments.

AVIS

La qualité de cette microforme dépend grandement de la qualité de la thèse soumise au microfilmage. Nous avons tout fait pour assurer une qualité supérieure de reproduction.

S'il manque des pages, veuillez communiquer avec l'université qui a conféré le grade.

La qualité d'impression de certaines pages peut laisser à désirer, surtout si les pages originales ont été dactylographiées à l'aide d'un ruban usé ou si l'université nous a fait parvenir une photocopie de qualité inférieure.

La reproduction, même partielle, de cette microforme est soumise à la Loi canadienne sur le droit d'auteur, SRC 1970, c. C-30, et ses amendements subséquents.

Canada

Mechanical, Neural and Vascular Determinants of Diaphragm Function

by

Michael Edward Ward

A Thesis submitted to theFaculty of Graduate Studies and Research
in partial fulfilment of the requirements for the degree of
Doctor of Philosophy

Department of Medicine, Division of Experimental Medicine
McGill University, Montreal, Quebec

ISBN 0-612-00144-X

For Suzanne, Susannah, Andrew and Emily

Acknowledgements

I would like to thank my supervisors, Drs. Macklem and Hussain, whose curiosity, creativity and dedication to the scientific method will always be my greatest source of inspiration. Dr. Macklem has been my supervisor, mentor and friend for the past ten years. Without his continuous support through periods of what often appeared to be overwhelming adversity I would have lost my way many times. Dr. Hussain has taught me, usually by example, the intensity, determination and persistence required to overcome the obstacles facing every scientist.

Abstract

The respiratory muscles play a role in respiratory failure when the efficient performance of the work of ventilation and/or their supply of metabolic substrates is disrupted. In this report a model of inspiratory muscle action is presented. The inflationary pressure applied to the lungs and the lung apposed rib cage is partitioned into two parts. One component is attributable to the action of rib cage muscles and the other is due to the interaction between upper and lower rib cage compartments. These contributions were found to be equal.

The role of afferent impulses travelling in the phrenic nerve in the control of respiratory muscle activity was investigated by electrical stimulation of its central cut end. Activation of these fibres exerts a non-uniform effect on the activities of the upper airway, rib cage and abdominal muscles and may influence respiratory muscle recruitment.

The roles of blood flow and oxygen delivery in determining diaphragm function was investigated. The rate at which diaphragmatic fatigue develops is diminished at high rates of blood flow and this effect is not related to the associated increase in oxygen delivery. The critical oxygen delivery at which oxygen consumption becomes supply dependent is the same for the resting diaphragm as for the rest of the body tissues. Activation of the diaphragm results in a higher critical oxygen delivery, however, this effect is mitigated by an increase in the critical oxygen extraction ratio.

The role of nitric oxide in regulating diaphragmatic blood flow and oxygen uptake was investigated by infusion of N^G-nitro-L-arginine. This treatment increased diaphragmatic vascular resistance, reduced the duration and magnitude of reactive vasodilation and increased the oxygen consumption and critical extraction ratio in the contracting diaphragm.

Résumé

Les muscles respiratoires jouent un rôle dans l'insuffisance respiratoire lorsque la performance du travail de ventilation et(ou) l'approvisionnement en substrats métaboliques sont perturbés. Ce rapport présente un modèle d'action du muscle inspiratoire. La pression dilatatrice appliquée aux poumons et au gril costal apposé aux poumons est divisée en deux parties. Un composant est attribuable à l'action des muscles du gril costal et l'autre à l'interaction entre les compartiments inférieurs et supérieurs du gril costal. Leurs contributions sont apparemment égales.

Le rôle des impulsions afférentes traversant le nerf phrénique dans le contrôle de l'activité des muscles respiratoires a été étudié par stimulation électrique de son extrémité centrale. L'activation de ces fibres exerce un effet non uniforme sur les activités de voies respiratoires supérieures, du gril costal et des muscles abdominaux et semble influencer mobilisation des muscles respiratoires.

Les rôles du débit sanguin et de l'apport en oxygène dans la détermination de la fonction diaphragmatique ont été étudies. Le seuil d'apparition de la fatigue diaphragmatique diminue lorsque le débit sanguin est élevé, phénomène qui n'a aucun rapport avec l'augmentation connexe des apports en oxygène devient dépendante de l'apport est comparable pour le diaphragm au repos et le reste des tissus organiques. L'activation du diaphragme entraine un apport critique d'oxygène supérieur, phénomène néanmoins mitigé par une augmentation du quotient d'extraction d'oxygène critique.

Le rôle de l'oxyge nitrique dans la régulation du débit sanguin diaphragmatique et de la fixation d'oxygène a été étudié par infusion de N^G-nitro-L-arginine. Ce trainement augmente la résistance vasculaire diaphragmatique, réduit la durée et l'ampleur de la vasodilation réactive et augmente la consommation d'oxygène et le quotient d'extraction critique dans le diaphragme contracté.

Preface

The McGill Faculty of Graduate Studies and Research permits the choice of two options in the submission of a thesis. Option A is the conventional format known to all universities whereas option B is in the form of published or publishable papers. This work is submitted in the format of option B according to the thesis guidelines:

> "Candidates have the option, subject to the approval of their Department, of including as part of their thesis, copies of the text of a paper(s) submitted for publication, or the clearly duplicated text of a published paper(s), provided that these copies are bound as an integral part of the thesis. If this option is chosen, connecting texts, providing logical bridges between the different papers are mandatory. The thesis must still conform to all other requirements of the "Guidelines Concerning Thesis Preparation" and should be in a literary form that is more than a mere collection of manuscripts published or to be published. The thesis must include as separate chapters or sections: 1) a Table of Contents, 2) a general abstract in English and French, 3) an introduction which clearly states the rationale and objectives of the study, 4) a comprehensive general review of the background literature to the subject of the thesis, when this review is appropriate, and 5) a final overall conclusion and/or summary. Additional material (procedural and design data as weli as descriptions of equipment used) must be provided in sufficient detail (e.g. in appendices) to allow a clear and precise judgement to be made of the importance and originality of the research reported in the thesis. In the case of manuscripts co-authored by the candidate and others the candidate is required to make an explicit statement on who contributed to such work and to what extent; supervisors must attest to the accuracy of the claims at the Ph.D. Oral Defense. Since the task of the examiners is made more difficult in these cases, it is in the candidates interest to make perfectly clear the responsibilities of the different authors of the co-authored papers."

Seven published papers are presented in this thesis. These include the following:

1. Analysis of human chest wall motion using a two compartment rib cage model. M.E. Ward, J. Ward and P.T. Macklem, Journal of Applied Physiology 1992 72: 1338-1347

2. Effect of phrenic afferent stimulation on pattern of respiratory muscle activation in dogs. M.E. Ward, A. Deschamps, C. Roussos and S.N.A. Hussain, Journal of Applied Physiology 1992 73(2): 563-570

3. Oxygen delivery-independent effect of blood flow on diaphragm fatigue. M.E. Ward, S.A. Magder and S.N.A. Hussain, American Review of Respiratory Disease 1992 145: 1058-1063

4. Systemic and diaphragmatic O_2 delivery-O_2 consumption relationships. M.E. Ward, H.Y. Chang and S.N.A. Hussain. Journal of Applied Physiology 1994 - In Press

5. Regulation of baseline vascular resistance in the canine diaphragm by nitric oxide. M.E. Ward and S.N.A. Hussain. British Journal of Pharmacology 1994 - In Press

6. The role of endothelium-derived relaxing factor in reactive hyperaemia in the canine diaphragm. M.E. Ward, S.A. Magder and S.N.A. Hussain. Journal of Applied Physiology - 74: 1606-1612, 1993

7. Effect of inhibition of nitric oxide release on the diaphragmatic oxygen delivery-consumption relationship. M.E. Ward and S.N.A. Hussain. Journal of Critical Care 1994 - In Press

I am the first author of these papers. I participated in the design of the studies, carried out the experiments, analyzed the data and wrote the manuscripts. J. Ward, a student working in Dr. Macklem's laboratory assisted with performance of experiments and contributed to the data analysis for paper 1. A. Deschamps was a student in the Critical Care Division at McGill University with experience in the technique of carotid sinus isolation. He contributed to the performance of the experiments for paper 2 and taught me this technique. Dr. C. Roussos is a world expert in the role of phrenic afferents in the regulation of breathing and is responsible for much of the pioneering work in this field. He was an invaluable source of information and advice in designing the experiments and interpreting the results obtained and reported in paper 2. Dr. S. Magder is a cardiovascular physiologist with expertise in the study of peripheral vascular responses. He assisted with designing and interpreting the experiments and in preparing the manuscripts for papers 3 and 6. Dr. H.Y Chang was a research fellow in Dr. Hussain's laboratory. He assisted with the performance of the experiments presented in paper 4.

In accordance with the "Guidelines Concerning Thesis Preparation" the text of these papers is duplicated in its original form. As a result, minor variations in style (e.g. reference format) reflecting differences in editorial requirements among journals, may be noted between sections of the thesis which have been previously published.

Table of Contents

CHAPTER 1: Introduction

INTRODUCTION

Spontaneous ventilation depends on the continued action of the respiratory musculature. It follows that failure of these muscles must play an important role in the pathophysiology of respiratory failure. ATP production for the continuance of muscle contraction is largely dependent on O_2 availability (23,78). The respiratory muscles in particular are limited in their ability to function anaerobically (107). The ability of their contractile apparatus to continue to generate the force required to sustain ventilation, therefore, is even more highly dependent on oxidative phosphorylation than other skeletal muscles. This means that imbalance between oxygen availability and the metabolic requirements of these muscles will eventually lead to their dysfunction, manifested clinically by respiratory insufficiency and death. This situation may arise if the metabolic demand of the respiratory muscles exceeds their capacity to augment oxygen availability by decreasing the resistance to blood flow or by increasing the capillary surface for oxygen diffusion. Alternatively, systemic oxygen delivery may be limited or the ability of the muscle to extract the available oxygen may be impaired.

These precepts are intuitively attractive, and are supported by some experimental evidence. During the application of inspiratory resistive loads in humans, McCool et al. (115) found that the time to failure of a breathing task is closely related to the increase in respiratory muscle oxygen consumption (VO_2resp) and suggested that a critical rate of energy utilization determines the endurance of the inspiratory pump. In normal humans, breathing hypoxic gas mixtures shortens the time for which breathing against high inspiratory resistances may be voluntarily sustained and hastens the development of electromyographic features predictive of diaphragmatic fatigue (34,158). In addition, Watchco et al. (194) and others (5) have reported

that diaphragm strength and endurance are reduced when arterial oxygen tension falls below 45 mmHg.

It is well known, however, that hypoxia tonically increases end-expiratory lung volume and alters the distribution of respiratory muscle activation (18,166,200). It is possible that the reported reductions in diaphragm strength during hypoxia reflect changes in diaphragm length and mechanical advantage rather than an effect of hypoxia on diaphragm contractility per se. In preparations in which this variable is eliminated, the effect of hypoxia is much less pronounced. Bark et al. (9) found that in perfused canine diaphragm strips, even severe levels of hypoxia produced no adverse effect on the contractility of the resting diaphragm or following a period of rhythmic contraction at low levels of tension. At high levels of tension development, hypoxemia accelerated the development of fatigue, but this required arterial oxygen tensions less than 35 mmHg.

Direct evidence supporting a role for tissue hypoxia in the development of diaphragm fatigue has also been elusive. Bazzy et al. (13) found no decrease in phrenic venous PO_2 during the application of fatiguing inspiratory resistive loads in non-anesthetized sheep. Pope et al. (137) found that during diaphragmatic fatigue induced by supramaximal phrenic nerve stimulation in dogs, phrenic venous PO_2 remained above 30 mmHg and biochemical evidence of anaerobic metabolism was absent. Similarly, Manohar (164,191) found that, in ponies, the phrenic arterio-venous O_2 content difference remained unchanged during exhaustive exercise.

Biochemical evidence of failure of aerobic metabolism to meet the energy requirements of the respiratory muscles (lactate accumulation, glycogen depletion and depletion of high energy phosphate stores) during the application of inspiratory loads is similarly lacking. In intact

spontaneously breathing dogs, moderate increases in work of breathing are not consistently associated with increased lactate release by the diaphragm (149,155). Bazzy et al. (13) demonstrated that inspiratory flow resistive loads did not result in increased lactate production even though respiratory failure was present by usual criteria (decreased minute ventilation and elevated arterial PCO_2 > 70 mmHg). In spontaneously breathing rabbits whose respiratory pattern was unrestricted, Ferguson et al. (44) found that progressive inspiratory threshold loading to the point of respiratory failure resulted in no increase in diaphragmatic lactate concentration. In rats, Fregosi and Dempsey (49) found exhaustive exercise to produce an increase in diaphragmatic lactate concentration which is similar to the increase in arterial blood and plantaris muscle lactate concentrations except at maximum VO_2tot when the increase in respiratory muscle lactate concentration is less than that in blood or non-respiratory skeletal muscle. In ponies, Manohar et al. (106,107) demonstrated that extreme exertion was not associated with lactate evolution by the diaphragm.

Depletion of glycogen in the diaphragm is correlated with the development of fatigue during direct nerve stimulation, as it is in peripheral skeletal muscles (44). The role which glycolytic depletion of intramuscular carbohydrate stores contributes to respiratory muscle fatigue in vivo, however, is disputed. In rats, glycogen concentration in the diaphragm falls after prolonged exhaustive swimming (60) and treadmill running (121) and slowly returns to normal over the subsequent 12 hours. This suggests that endogenous glycogen is needed by the respiratory muscles during physiologic tasks and that depletion of these stores may contribute to their failure. Evidence conflicting with this view, however, has been presented by Fregosi and Dempsey (49). These investigators reported a lack of significant glycogen utilization in rat

respiratory muscles during normoxic exercise. Only under conditions of extreme metabolic demand coupled with reduced O_2 transport did glycogen utilization increase in the diaphragm and intercostal muscles. In contrast to this report, Ianuzzo et al. (77) carried out studies in which rats were exposed to a similar normoxic exercise regimen and found a significant reduction (43% of control values) in glycogen content in the diaphragm and intercostal muscles. The reduction occurred in both Type I and II fibres. The reason for the discrepancy in the results of these two studies remains unclear. Ferguson et al. (44) studied the effects of incremental inspiratory threshold loads on the biochemistry and function of the diaphragm in ketamine anaesthetized rabbits. They found no evidence of either glycogen depletion nor of contractile failure despite inability of the animals to continue to initiate inspiratory airflow.

No direct evidence is available, furthermore, which supports failure to maintain intramuscular high energy phosphate concentrations in the respiratory muscles during the development of respiratory failure induced by inspiratory loading. In the dog diaphragm, ATP and phosphocreatine concentrations were found to average 3.8μmol/g and 10.2μmol/g respectively during quiet breathing and 3.3 μmol/g and 12.2 μmol/g respectively during resistive loading (153). Similarly, Fregosi and Dempsey (49) found that ATP concentration in rat diaphragm and intercostal muscles was maintained at rest levels during exhaustive exercise under both normoxic and hypoxic conditions.

These results suggest that common assumptions about the processes leading to failure of the respiratory muscles to maintain ventilation are oversimplifications. The cause of respiratory failure is multifactorial. Although exhaustion of biochemical substrate may contribute to loss of force under some conditions (44), other factors, particularly impairment of muscle activation

(15) may account for failure to generate an adequate inflation pressure. Neural inputs arising at the cerebral (199) cerebellar (198) or spinal (48) level may influence respiratory motor output, as may failure of transmission at the neuromuscular junction (12,83,177). Furthermore, the respiratory system adapts as a whole to being loaded so as to avoid supply-critical conditions developing in any given respiratory muscle. Thus, although a pump perfused diaphragm will exhibit the biochemical and electromechanical derangements associated with fatigue when stimulated to near maximum contraction for a prolonged period, similar changes do not occur when the normal adaptive mechanisms are available to protect this muscle (44).

The process of adaptation occurs at a number of levels. Mechanically, the ventilatory load is borne not by a single muscle but by several groups of muscles interacting in a complex and changing manner to inflate the lungs and chest wall. Therefore, the load placed on a given muscle group is determined by the linkage between it and all other elements in the system. Reflex and voluntary adjustments of the pattern of activation of the respiratory muscles (192,200,201) alter the distribution of the load so that groups most able to produce the necessary pressures may be recruited to unload those in which metabolic demands are about to exceed the capacity for oxidative energy production. The effect of such a change in neural activation on the contribution of a specific muscle depends on the nature of the mechanical linkage among muscle groups. The arteriolar network responsible for delivery of oxygen and plasma born substrates to the respiratory muscles responds to increased metabolic demand by vasodilation, thereby increasing the available blood flow. This improves both the extracellular milieu by removing metabolic byproducts detrimental to the contractile apparatus as well as bulk oxygen delivery. Even before these changes can be detected, the capacity of the muscles to extract the

available oxygen is enhanced, presumably by redistribution of intramuscular blood flow so as to maximize the capillary surface for oxygen diffusion (188).

Respiratory Muscle Actions and Interactions

The normal mechanisms which protect the diaphragm from exposure to loads which exceed its capacity to endure may be defeated by directly activating the phrenic nerve or by mechanically altering the chest wall (44). Under these conditions, electromechanical and biochemical changes associated with fatigue occur and are well correlated with each other in their severity (44). In the absence of such measures, however, respiratory failure may develop, during the application of ventilatory loads, without impinging on the limits of diaphragmatic oxygen extraction, accumulation of lactate, depletion of glycogen stores or alteration of the diaphragmatic force-frequency relationship (176, 155). The efficacy of the compensatory mechanisms responsible for distribution of the ventilatory load among respiratory muscle groups, therefore, determine the extent to which failure of diaphragmatic contractility contributes to the development of respiratory failure.

Of particular importance to the process of adaptation is the manner in which the respiratory muscle groups are linked mechanically. For example, using a hydraulic analogue, two pumps of different capacity linked mechanically in series will experience equal volume translations but may contribute in vastly differing proportions to the total pressure change across the system. Conversely, the same pumps coupled in parallel will experience the same pressure change from upstream to downstream locations while contributing different amounts to the total rate at which volume is exchanged. Any process which modifies the nature of these mechanical

interactions will, impact on the role any one component plays in the overall ability of the system to sustain the load imposed. In the respiratory system, the respiratory muscles are linked through their attachments to the bony and cartilaginous elements of the chest wall. A change in chest wall configuration during inspiration alters the energy required for respiratory system inflation (2,59) and the manner in which the ventilatory muscles interact with each other (202). The chest wall, therefore, plays a central role in conversion of respiratory muscle shortening to ventilation of the lungs. The importance this concept is illustrated by the fact that failure of the chest wall to efficiently perform its function, due to trauma or skeletal disease, may result in ventilatory failure even if the lungs and respiratory muscles are completely normal.

In patients with pulmonary disease, the derangement afflicting the respiratory system is far more complex than is represented by the simple addition of added inspiratory resistive or elastic loads. Morphologic and biochemical changes in the respiratory muscles may result from systemic effects of the underlying disease (25,55) or from its treatment (45). In addition, changes in the length and orientation of these muscles (eg: as a result of changes in end-expiratory lung volume) may place these muscles at a mechanical disadvantage and alter their mechanical linkage. It is generally recognized that alterations in chest wall function contribute to the impairment of ventilation in patients with respiratory disease (390). A complete understanding of the role these factors play and how they may be corrected has been impeded, however, by the inability to quantify the contributions of the diaphragm and rib cage muscles to the inspiratory pressures generated and the degree to which these muscle groups are linked by the chest wall. In order to address this problem, a progressive series of models has been developed, which allow the characteristics of the system to be analyzed in a stepwise fashion.

The simplest model, and the first exploited, is a two compartment system, whereby, volume changes must involve expansion of the rib cage compartment or of the abdominal compartment. The rib cage and abdomen are assumed to move with only a single degree of freedom (ie: to conform to their relaxation characteristic). Although this appears to be gross oversimplification, if the ribs are constrained to conform to the path which results in the minimum degree of misfit at the costovertebral joints, the abdomen remains relaxed and the spinal attitude is fixed, the use of this model is not unreasonable. Konno and Mead (93) demonstrated that, in fact, these conditions are met over a limited range of volume changes during spontaneous breathing. This observation allowed the measurement of the elastic properties of rib cage and abdomen, and has formed the basis of most models proposed to explain the actions of the respiratory muscles and their contributions to changes in lung volume.

The limitations of this approach, however, have long been recognized. Crawford et al. (29) found the cross-sectional areas of the upper (axilla) and lower (lower costal margin) rib cages to move during quiet breathing in close, but not exact, approximation to their to their relaxation relationship. McCool et. al.(114) used linearized magnetometers to monitor the relative anterior-posterior displacements of the upper (angle of Louis) and lower (5th rib) rib cages. They found that, although the relationship between these two diameters described a curve close to the relaxation characteristic during quiet breathing, the system was easily distorted by changing the muscle groups recruited during inspiration. Isolated contraction of the diaphragm during diaphragm pacing does not drive the rib cage on its passive characteristic (30,31). Recently, electromyographic studies have confirmed that the parasternal intercostal muscles become active during all but the smallest volume changes and that the absence of rib cage

muscle activation alters the inspiratory configuration of the rib cage (35,36,43,57,161). In dogs, Jiang et al. (81) demonstrated that during isolated diaphragm contraction the relationship between the motion of the upper (lung apposed) rib cage and esophageal pressure fell close to its relaxation line. This finding indicates that in dogs there is little resistance to bending between upper and lower (abdomen apposed) rib cage compartments. The loose mechanical coupling between pulmonary and abdominal rib cage compartments in dogs was confirmed by Krayer et. al. (94) using dynamic spatial reconstruction of computed tomographic images. Such evidence suggests that unitary behaviour of the rib cage is the result of the highly coordinated action of the inspiratory muscles rather than inherent rigidity.

Primiano (139) developed a model of the chest wall which incorporated a factor to account for changes in the action of the diaphragm on the rib cage due to varying degrees of rib cage flexibility. Although this permitted description of normal and paradoxical breathing patterns, no estimates of the flexibility of the rib cage or any method of determining it was proposed. The concept of a two compartment rib cage was also incorporated into a mathematical model by Ben-Haim and Saidel (102) in order to account for the flexibility of the rib cage observed in infants. Their analysis of chest wall mechanics in adult humans, however, assumed a rigid linkage between rib cage compartments.

In chapter 2 the characteristics of a model of chest wall function which incorporates a two compartment rib cage are explored. This model is then exploited in order to quantify the degree to which motion of one part of the rib cage may influence the action of the respiratory muscles on the other components. In this way the pressures generated by the costal and crural parts of the diaphragm and the rib cage muscles are calculated.

Phrenic Afferent Modulation of Respiratory Muscle Activation

The distribution of a ventilatory load among respiratory muscle groups may also be influenced by voluntary and reflex changes in their level of activation. The importance of this mechanism as an adaptive response is illustrated by the fact that if it is defeated during resistive loading, either by directly stimulating the phrenic nerves (44) or by requiring target transdiaphragmatic pressures to be achieved (192), biochemical and electromechanical changes characteristic of muscle fatigue occur in the diaphragm. If the level of respiratory muscle activation is not artificially constrained these changes are not observed (12,44).

Phrenic motoneuron activity is controlled by efferent drive emanating from pontine and medullary respiratory controllers. The activity of these controllers is influenced by inputs from higher centres as well as by afferent inputs from various peripheral effectors. This peripheral afferent input provides the respiratory controllers with essential feedback concerning the functional status of these effectors to aid the respiratory controllers in modulating their output in accordance with the metabolic needs of the peripheral organs. Although several of these inputs such as vagal and skeletal muscle afferent sources had received considerable attention in the past, the functional significance of afferent inputs originating from the respiratory muscles in the modulation of central respiratory output has received much less attention. Moreover, the available data on physiological and morphological properties of phrenic afferents have been a source of considerable debate.

Early studies dismissed reflex feedback from the diaphragm as an important factor in determining respiratory motor output. Sant'Ambrogio and Widdicombe (162) investigated the role of phrenic afferent in anaesthetized rabbits and found that, after sectioning the cervical vagi,

phrenic motor activity was not affected by lung inflation or deflation or in response to airway occlusion. Corda and coworkers (28) in a subsequent study showed that phrenic motor activity was not augmented when phrenic afferents were activated by airway conclusion. In accordance with these findings, morphological studies have documenting the paucity of proprioceptors in the diaphragm (39).

In contrast, Green et al (64) have proposed a role for activation of phrenic afferents in the decline in diaphragmatic activation in response to positive-pressure breathing. In addition, there is increasing evidence that phrenic afferents are involved in respiratory load compensation. Banzett et al. (8), demonstrated that negative pressure applied to the lower body was associated with augmentation of diaphragmatic activation in paraplegic patients and Fryman and Frazier (52) found that the ventilatory response to lower-body negative pressure application was eliminated by sectioning of the cervical dorsal roots in cats. Recently, Teitelbaum et al. (182) showed that selective paralysis of the diaphragm enhances respiratory motor output and that this reflex is lost when the phrenic nerve is sectioned. The responses to changes in diaphragm length result primarily from activation of large fibre (fast conducting myelinated, group I and II) afferents serving golgi tendon organ and to a lesser extent muscle spindle type receptors (26,142,144). These appear to play an important role in the modulation of ventilatory drive during eupnoeic breathing.

Small diameter myelinated and unmyelinated group III and IV afferent fibres (40) are even more abundant in the phrenic nerve, although their importance in the control of breathing has been more difficult to establish. In striated mammalian muscles, the majority of such fibres end as free nerve endings (82,173) which may be activated by a variety of stimuli. Low-

threshold units (ergoreceptors) are activated by non-noxious touch, pressure and routine muscle contraction. High-threshold units (nociceptors) are sensitive to chemical stimuli, noxious agents and ischemia. Sustained muscle contraction is usually associated with activation of about one third of group III and 40% of group IV fibres in limb muscles (88). Small fibre phrenic afferents have been shown to become active in response to similar stimuli in the diaphragm. Jammes and coworkers (79), for example, studied 44 group IV afferent fibres from the cervical branches of phrenic nerves in cats. These fibres were strongly activated in response to intra-arterial injections of lactic acid, hypertonic saline or phenyl diguanide. In a similar experiment, Graham and colleagues (62) recorded spontaneous phrenic afferent activities from 50 fibres in the phrenic nerves of cats. Half of these units were thin-fibres with slow and tonic activity. A significant increase in the activity of these fibres was evident when lactic acid and hypertonic saline were injected intra-arterially and in response to a reduction of diaphragmatic blood flow induced by aortic occlusion.

Most thin fibre afferents enter the spinal cord through the dorsal roots. The ventral roots may be the pathway of spinal cord entry for some thin-fibre phrenic afferents, however, since residual ventilatory responses to selective activation of thin-fibre phrenic afferents with capsaicin have been noted in dogs following dorsal rhizotomy (143). The majority of evidence points to an inhibitory influence on ventilatory motor output at the spinal level. Goshgarian (61) reported ipsilateral diaphragm paralysis in rats following spinal cord hemisection at C2. When the dorsal roots of contralateral C6 to C8 were then sectioned, the paralysed diaphragm recovered partially indicating that phrenic afferents exert an inhibitory effect on the contralateral phrenic motoneurons. Subsequent physiological recordings of Gill and Kuno (56) and Rijlant (145) have

documented segmental phrenic motoneuron inhibition by electrical stimulation of phrenic nerve afferents. More recently, Speck and Revelette (172) described a short-latency inhibition of ipsilateral motor discharge combined with a relatively long-latency inhibition of contralateral phrenic motoneurons in response to electrical stimulation of upper cervical roots of the phrenic nerve in cats. Marlot and coworkers (112) also recorded phrenic motor activity in response to ipsilateral and contralateral phrenic nerve stimulation and found that the duration of inhibition was shorter in response to contralateral than ipsilateral afferent stimulation.

Supraspinal projections from phrenic afferents travelling through the dorsal spinal column extend to the external cuneate nucleus (99), lateral reticular nucleus (104) and dorsal and ventral respiratory neurons (6,103). The types of afferent fibres involved in these projections were not clearly identified in these studies. Based on the latencies of dorsal and ventral neuron and reticular formation activation in response to electrical stimulation of the phrenic nerve, however, it is probable that group III afferents are involved. In cats, potentials may be evoked in the sensorimotor cortex in an area located medial to forelimb and lateral to hindlimb afferent projections by activation of phrenic afferents (32). Marlot and colleagues (110) reported that phrenic afferent activation elicits evoked potentials on the cerebellar cortex as well.

The contribution of supraspinal structures to the inhibitory phrenic-to-phrenic reflex is still debatable. Jammes et al. (79) selectively stimulated group IV phrenic afferents in vagotomized cats and noticed a moderate inhibition of contralateral phrenic motor discharge associated with a 17% reduction in the inspiratory time. These authors argue that the observed changes in respiratory timing favour a supraspinal component. This is also supported by the report of Duron and coworkers in which the transient inhibition of phrenic motoneuron by

phrenic afferent activation was eliminated by decerebration (38). Contradicting these findings is the observation of Speck and Revelette (172) who showed that the short-latency inhibition of phrenic motor discharge by group III phrenic afferent activation persists after decerebration and decerebellation. These findings were reconciled by Speck (171) in a later study which confirmed the existence of two separate reflexes, a short-latency ipsilateral inhibition mediated by a segmental circuits, whereas the long-latency contralateral inhibition of phrenic motor discharge requires the presence of intact supraspinal pathways.

A significant number of investigators have reported that stimulation of phrenic afferents, in intact animals, elicits augmentation rather than inhibition of ventilatory drive. Kohrman and colleagues (148), found an increase in tidal volume and breathing frequency during stimulation of the central end of the cut phrenic nerve in dogs and Marlot et al. (111) reported increased breathing frequency and tidal volume in response to prolonged repetitive stimulation of group III phrenic afferents in vagotomized cats. In addition, Road and coworkers (148) showed that the increase in ventilation during electrical stimulation of the central cut end of the phrenic nerve required stimulation intensities greater than those required to activate large fibre afferents. Since sectioning C5 to C7 dorsal roots abolished the response whereas cold blockade of group I and II fibres did not, these authors concluded that the ventilatory response is mediated by groups III and IV afferents. In support of this contention Revelette and coworkers (143) observed an increase in the phasic activity of diaphragm and hypoglossal muscles combined with an increase in breathing frequency during selective small fibre afferent activation elicited by injection of capsaicin into the phrenic artery of vagotomized dogs. Hussain et al. (74) subsequently confirmed this finding in a vascularly isolated diaphragm preparation in which stimulation of

afferents in other vascular beds by contamination of the systemic circulation was avoided.

Establishment of the function of these reflex pathways is further complicated by the observation of biphasic ventilatory responses during phrenic afferent activation in some preparations. Marlot and colleagues (111) showed that a biphasic ventilatory response (a short inhibition followed by prolonged excitation) was observed when phrenic afferents are activated in vagotomized cats. Moreover, roughly 25% of dorsal respiratory group neurons have been found to be activated at the same time that phrenic motor discharge is inhibited by ipsilateral stimulation of group III phrenic afferents (103). A biphasic ventilatory response has also been to shown to occur in response to limb muscle afferents stimulation (42).

To reconcile these apparently contradictory findings, Speck and Revelette (172) have proposed the existence of two separate reflexes mediated by small fibre afferents. A short-latency inhibitory phrenic-to-phrenic reflex is transient in nature (initial one or two breaths following stimulus onset) and may be manifested as ipsilateral and contralateral inhibition of phrenic motor discharge. As discussed above, this reflex is likely to be mediated mainly through segmental networks. The second reflex is a more prolonged, longer-latency, supraspinal reflex which results in increased inspiratory motor drive to the diaphragm and other respiratory muscles. Since the process of respiratory load compensation, at least as it applies to patients with respiratory disease generally occurs over a relatively long time frame (hours to days), it is this second stimulatory reflex which is of greatest relevance to the pathophysiology of respiratory failure.

During inspiratory resistive loading in normal human volunteers, the development of diaphragmatic fatigue is associated with a progressive increase in activation not only of the

diaphragm but also of the rib cage and accessory muscles (192). Reflex compensation for diaphragmatic failure was proposed to explain this finding, although voluntarily activation of other muscle groups in order to comply with the constraints imposed on the ventilatory pattern cannot be excluded. In chapter 3, direct evidence of the reflex effects of phrenic afferent activation on the ventilatory drive and its distribution among the respiratory muscles is presented. This study demonstrates that activation of thin-fibre afferents in the phrenic nerve not only elicits an increase in respiratory motor output but also alters the pattern of muscle activation and the timing of the respiratory cycle. The influence of these changes, both positive and negative, for the respiratory muscles as a group in overcoming ventilatory loads is considered.

Respiratory Muscle Oxygen Delivery and Extraction

In normal subjects at rest the respiratory muscles use little (~1.5%) of the total oxygen consumption (VO_2tot) or cardiac output (149) and, during exercise, VO_2resp increases in proportion to the increased power output by the respiratory muscles (27,150) to as much as 15% of VO_2tot in some subjects (1). Since the cardiac output may reach 25 to 30 l/min in normal individuals, however, even when the blood flow and oxygen requirements of the respiratory muscles are high, no threat is posed to the body as a whole.

In patients with pulmonary disease, in contrast, VO_2resp at rest may account for 25% of VO_2tot (27,46). As minute ventilation increases in these patients, chest wall deformation, increased end-expiratory lung volume, expiratory muscle pressure development beyond maximum effective pressure, changes in resting muscle length and recruitment of postural and

synergistic accessory muscles which do not directly contribute to ventilation, all contribute to a progressive decrease in respiratory muscle efficiency (work of breathing/VO_2resp) (19,27,50,154). Based on this observation, Otis (109), Margaria (128) and others (147,169,193) have argued that as efficiency deteriorates, the rate of increase of VO_2resp eventually equals the rate of increase in VO_2tot. Further increases in ventilation will not render more energy available for work other than for the work of breathing. The ventilatory value corresponding to this point, therefore, represents the maximum ventilation available for useful external work assuming that the respiratory muscles possess a limited capacity to function anaerobically. This concept of "energy stealing" by the respiratory muscles has been advanced in support of the early institution of mechanical ventilation in patients with respiratory failure, particularly when systemic oxygen delivery may be impaired (193). In patients with co-existent cardiovascular impairment (often as a result of chronic pulmonary disease) or abnormalities of oxygen carrying capacity the situation may be further exacerbated. Viires (189) has shown that during a low cardiac output state, the respiratory muscles of spontaneously breathing dogs commanded 20% of the cardiac output, compared to 3% during mechanical ventilation.

In addition its mechanical arrangement, the maximum efficiency with which a muscle performs a certain type of work is determined, in part, by the intrinsic rate of ATP hydrolysis by the contractile proteins. A fast white (glycolytic) muscle performs more economically when shortening quickly against a light load than slowly against a heavy load, whereas, the opposite holds for a slow red (oxidative) muscle (97,122,183). The mammalian diaphragm is composed of three types of muscle fibre characterized histochemically as slow-twitch oxidative (SO), fast-twitch oxidative-glycolytic (FOG), and fast-twitch glycolytic (FG) (101,146). Corresponding

roughly to these categories is the classification developed by Dubowitz and Brooke (37) which divides fibres into Type I, which stain lightly for myofibrillar ATPase with alkaline preincubation, and all other types which are labelled Type II. Type II fibres are further subdivided, on the basis of their reactions with ATPase following acid preincubation, into IIa, IIb and IIc. IIb are "mirror image" to type I, IIa and IIc demonstrate intermediate staining characteristics. IIc fibres are rare in adults and likely represent an intermediate fetal fibre type of high oxidative capacity (113). In other skeletal muscles, these histochemical distinctions correlate respectively with the physiological characterization of motor units into three types 1) slow-twitch (S) with low recruitment thresholds, high level of fatigue resistance and low force production when activated; 2) fast-twitch fatigue-resistant (FR) units with higher recruitment thresholds, relative resistance to fatigue and higher levels of force production; and 3) fast-twitch fatiguable (FF) which produce the highest levels of force, have the highest thresholds for recruitment, and are highly susceptible to fatigue (22). Large differences in diaphragmatic fibre composition and oxidative enzyme activities have been observed between species (65). Of significance, since much data concerning diaphragmatic metabolism comes from canine studies, Green et al. (65) could identify no classical type IIB fibres in the dog diaphragm. In adult humans, type I fibres constitute approximately 50-55% of the total in the diaphragm, 65% in the intercostal muscles (33,117) and 40% in the vastus lateralis (33). As would be predicted from this fibre type composition, the respiratory muscles in general, and the diaphragm specifically, are quite limited in their ability to function anaerobically (106-108,195).

Since the diaphragm satisfies almost all of its energy requirements by oxidative metabolism over a large range of work output, its energy expenditures can be closely

approximated by the measurement of its oxygen consumption. During mechanical ventilation the O_2 uptake of the resting canine diaphragm is between 0.2 and 0.8 ml/min/100g (150,152) which is similar to the values for other resting skeletal muscles. During unobstructed hyperventilation, diaphragmatic O_2 consumption increases to 1.7-3.0 ml/min/100g (150,152). The highest values for diaphragmatic O_2 uptake occur with resistive loading. During the application of the highest resistance tested by Robertson et al. (151) the diaphragm consumed 24 ml/min/100g. No similar direct measurements are available for the other respiratory muscles, however, during the application of inspiratory resistances total body O_2 consumption increased to 200 ml/min/100g from a control value of 150 ml/min/100g (151). If all of this increase is attributed to increased extraction by the respiratory muscles, it would appear that the diaphragm and the other respiratory muscles contribute approximately equally to the energy cost of overcoming resistive loads.

To meet these high levels of energy expenditure, oxygen availability to metabolically active regions of the diaphragm must be enhanced. The most well known mechanism by which this is achieved is a decrease in vascular resistance which increases delivery and ameliorates the supply critical conditions. The capacity to increase diaphragmatic blood flow is large. Reid and Johnson (141) determined the maximal conductance of the diaphragm using work, pharmacologic agents and hypoxia to produce vasodilation. These investigators assumed that the driving pressure for blood flow was the difference between arterial pressure and right atrial pressure, ignoring the existence of zero flow pressure. As a result they obtained a polynomial relationship between Qdi and perfusion pressure. The dependence of conductance on driving pressure was felt to reflect autoregulation, (the tendency to maintain constant flow in the face of changes in

perfusion pressure) in their preparation. Magder (105) subsequently fit their pressure flow data to a linear relationship, however, and obtained a slope (conductance) of $3.41 \cdot 10^{-2}$ ml/min/g with a predicted zero-flow pressure of 43 mmHg. This value for maximum conductance is comparable to that reported by Magder (105) during maximum vasodilation produced by nitroprusside and electrophrenic stimulation ($3.13 \cdot Pa \cdot 10^{-2}$) although the zero flow pressure intercept was lower in this study (17 mmHg) than that calculated from the data reported by Reid and Johnson (141). Therefore, although higher maximum flows are predicted from the data during combined pharmacologic and metabolic vasodilation, this difference appears to reflect a difference in critical closing pressure rather than failure to achieve maximum conductance with physiologic stimuli. The relationship between pressure and flow reported by Magder (105) predicts a flow of 3.65 ml/min/g at a mean arterial pressure of 100 mmHg and 2.09 ml/min/g at 50 mmHg. Sharf et al. (164) measured the changes in diaphragmatic blood flow over a pressure range of 60 to 100 mmHg using an electromagnetic flow meter on the left inferior phrenic artery in dogs during haemorrhage. They found the pressure-flow relationship to be linear during spontaneous breathing and 60 to 90 mmHg during loaded breathing. This range of pressures may have been to narrow to observe autoregulation in this circulation, however, since, in a subsequent study in spontaneously breathing dogs, Hussain et al. (364) found that the relationship between inferior phrenic artery flow and pressure remained relatively constant until perfusion pressure fell below 80 mmHg and then declined more rapidly.

In addition to perfusion pressure, blood flow to the respiratory muscles is determined by their level of activity. When the inspiratory muscles are at rest their blood flow averages 55% of the level measured during quiet spontaneous breathing (25,118,150,152,189). Unobstructed

hyperventilation is associated with moderate increases in diaphragm blood flow, with the average reported increase being about 45% per 100% increase in ventilation (7,25,118,150,152,154,156). Far higher levels are seen when resistance to inspiratory airflow is increased. Rochester and Bettini (80) reported a linear increase in diaphragmatic blood flow with resistive loading to about 0.6 to 1.1 ml/min/g. Robertson et al. (149), on the other hand, reported an exponential increase in diaphragm blood flow, up to 2.1 ml/min/g, as inspiratory airflow resistance increased. Reid and Johnson (141) also measured diaphragmatic blood flow during high resistive loads and found a linear increase in blood flow with increasing diaphragmatic O_2 consumption up to levels obtained with maximum pharmacologic vasodilation.

The timing and intensity of muscle contraction also influence the blood flow available to the diaphragm. Anrep et al. (4) and Bellemare et al. (16) demonstrated that at maximal work loads, diaphragmatic blood flow may be inhibited. Buchler et al. (20) studied diaphragmatic blood flow, using radioactive microspheres, during sustained and intermittent diaphragmatic contractions in anaesthetized dogs. During sustained contractions with the abdomen bound, blood flow increased up to transdiaphragmatic pressure (Pdi) of 40 cmH_2O (max Pdi = 80-90 cmH_2O) and then declined. At a given Pdi, diaphragmatic blood flow was higher with the chest closed and the abdomen left unrestrained than with the chest open and the abdomen bound during both sustained and intermittent contraction. These authors reasoned that raising the intra-abdominal pressure influences flow by raising both the downstream pressure and the resistance of the intramuscular vasculature. Lowering pleural pressure, however, should have the opposite effect. During supramaximal stimulation (which produces a higher Pdi with the abdomen bound), however, maximum blood flow was no different between the two conditions.

They, therefore, concluded that the distribution of pressure between pleural and abdominal surfaces is of less importance during intermittent contractions since inhibition of flow during contraction is compensated by an increase in flow during the relaxation phase. Increasing the duty cycle of contraction (ratio of contraction duration to total cycle time) at maximum Pdi resulted in a progressive decrease blood flow in this study. In a subsequent paper (21) these same authors studied the effect of changing the frequency of intermittent contraction on diaphragm blood flow during supramaximal phrenic nerve stimulation with the abdomen bound. Keeping duty cycle constant at either 0.25 or 0.75, increasing contraction frequency up to 70-80 per minute resulted in an increase in blood flow. After this point, however, further increases in frequency produced no further increment in blood flow. In a diaphragmatic muscle strip preparation, Bark et al. (10) studied the effect of isometric contraction on diaphragmatic blood flow. They quantified muscle activity by the tension-time index (TTI) which was calculated as the product of tension (as a fraction of maximum tension) and duty cycle. Blood flow increased with increases in TTI, peaked when TTI reached 0.2-0.3 and then fell. When the TTI exceeded 0.3, increasing the duty cycle, keeping TTI constant by adjusting tension, was associated with a linear decrease in Qdi. The effect of changes in the timing of contraction on diaphragmatic blood flow was progressively greater at higher values of TTI. The most consistently offered explanation for the effects of contraction intensity and timing on diaphragm blood flow is that diaphragmatic vascular resistance is influenced by intramuscular pressure. Using a catheter-balloon system, Supinski et al. (180) found a linear relationship between force and intramuscular pressure and also concluded that this pressure is a major determinant of diaphragmatic blood flow. Muscle shortening, a major determinant of intramuscular pressure because of its effect

on muscle thickness (170), however, was prevented in their study. In a subsequent study, Hussain et al. (75) measured intramuscular pressure using a Millar microtransducer in the hemidiaphragm during intermittent contractions (duty cycle = 0.5, rate = 15/min) associated with shortening comparable to that observed during spontaneous breathing. They found that intramuscular pressure increased linearly with tension (and shortening) to an average maximum value of 113.5 mmHg. Blood flow to the preparation initially increased as tension and intramuscular pressure increased, however, when intramuscular pressure exceeded 20 mmHg, (tension approximately 30% of maximum) total blood flow increased no further. Flow during the contraction phase decreased progressively above this level while relaxation phase flow increased in compensation.

During reductions in muscle oxygenation, enhancement of oxygen extraction occurs long before compensatory changes diaphragmatic vascular resistance may be recorded (119,140,178). This provides an additional mechanism by which cellular oxygen availability may be maintained in proportion to the metabolic requirements of the contracting muscle. In the diaphragm, maximum oxygen extraction has been reported to be greater than 90% (141). Based on this observation and estimates of maximum blood flow, calculations of maximum oxygen availability, and hence maximum aerobic output of the respiratory muscles have been presented (157). Maximum levels of oxygen extraction do not generally occur, however, until after dependence of oxygen consumption on oxygen delivery has developed (24,89,90,125,127,130,165,167,190). That is, as oxygen delivery is reduced, a critical level of delivery, and a corresponding critical level of oxygen extraction, is reached beyond which further reductions in oxygen delivery result in a fall in oxygen consumption. Oxygen extraction, under these conditions, continues to

increase and is not independent of oxygen delivery as this calculation implies.

In the model of tissue oxygenation originally proposed by August Krogh (95), the amount of oxygen available to a tissue is dependent on the oxygen tension gradient between the capillary lumen and the mitochondria, and the diffusive conductance for oxygen through the tissue. The oxygen tension gradient for diffusion in this model may be influenced by the level of convective oxygen flow, the affinity of the haemoglobin molecule for oxygen and the rate of tissue metabolism. The critical oxygen extraction ratio, does not appear to depend on haemoglobin affinity, however, since altering the oxyhemoglobin dissociation relationship by exposure of the perfusing blood to carbon monoxide has no effect on the critical level of oxygen delivery or extraction (165). Furthermore, Stein and Ellsworth (175,176) found that lowering haemoglobin P_{50} (PO_2 at haemoglobin saturation = 50%) by chronic cyanate treatment does not measurably alter the decrease in oxygen saturation across the capillary network in striated muscle until oxygen supply is severely compromised. The absence of an effect of carbon monoxide treatment on critical oxygen delivery also argues against the driving pressure for oxygen diffusion being the factor limiting extraction at this point, since at a given oxygen delivery capillary PO_2 would vary markedly between the two conditions. A similar conclusion is obtained from studies comparing methods of reduction in oxygen delivery. Theoretically, the driving pressure for oxygen diffusion should be greater during anemia than during hypoxia at equal O_2 deliveries (71). Cain (24), however, found that whether oxygen delivery was reduced by hypoxia or by anemia the critical oxygen delivery was the same, despite a higher mixed venous PO_2 at the critical point during anemia. This finding alone, however, does not eliminate diffusion as a factor limiting oxygen extraction, since Hogan et al. (70) have presented evidence that the

diffusive conductance for oxygen may be reduced in maximally contracting muscle when the haemoglobin of the perfusing blood is lowered.

Convective oxygen delivery to a given capillary network unit may not correlate with bulk blood flow or oxygen delivery. Rapaport et al. (419) suggested that the opening of shunt vessels not participating in nutrient exchange accounted for the lack of increase in tracer clearance from leg muscle despite increased total muscle blood flow following lumbar sympathetic blockade. Similarly, Covino et al. (420) found increased femoral blood flow in hypothermic dogs not associated with increased in nutrient vessel flow and Hyman et al. (421) demonstrated that electrical stimulation of the hypothalamus resulted in increased total muscle blood flow, without changing radioiodide clearance in the cat hindlmb. Bolme and Edwall (422) found directionally opposite changes in tracer transport and limb muscle blood flow during partial arterial occlusion and Renkin et al. (423) reported dissociation between capillary permeability-surface area and total vascular resistance with increasing metabolic rate. More recently, increased capillary red cell content, has been demonstrated in the earliest phases of tissue hypoxia (72,73,87) before increases in vascular conductance have a measurable effect on bulk flow. These findings suggest that optimization of oxygen uptake at a given oxygen delivery requires the active redistribution of flow between nutritive and non-nutritive capillary channels. Direct evidence in support of this notion has been accumulating. In rat limb muscle, Potter and Groom (28) found capillary diameters to conform to a bimodal distribution with a large population (87%) clustered around 5.5 μm and a smaller population (13%) with a modal diameter of 7.5 μm. Harrison (29) has, subsequently, measured capillary flow in skeletal muscle and documented a comparable bimodal distribution. Calculations based on these measurements suggest that despite their smaller

numbers, the large diameter (high flow) capillaries which contribute little to gas exchange may carry up to 71% of the total flow. Thus, a large margin for compensation exists through redistribution of flow before an increase in bulk flow is necessary. In hamster cremaster muscle, Sarelius (163) recently studied the heterogeneity in red blood cell and oxygen flow in the arterioles that control perfusion into adjacent capillary network units arising consecutively from a single transverse arteriole. Under control conditions, oxygen flows were not different between branches, whereas, during maximal vasodilation with adenosine both cell and oxygen flow into these arterioles varied in a systematic way dependent upon their relative branch position. The maintenance of uniform oxygen delivery, therefore, requires active regulation of precapillary arteriolar tone in order to overcome architectural and hemodynamic variables within the microcirculation which tend to produce flow patterns unrelated to metabolic need. A determinant of the critical oxygen extraction ratio, therefore, may be the capacity of local mechanisms regulating arteriolar tone to accomplish this task.

It is of interest that although increased O_2 extraction is the earliest response to hypoxia, maximum extraction is not achieved until levels of tissue hypoxia sufficient to impair oxygen consumption are reached. The mechanisms regulating the distribution of capillary perfusion may, therefore, vary in their sensitivity to hypoxic and metabolic stimuli. Alternatively, Granger (63) has suggested that, since the arteriolar network represents as a series of progressive resistances, maximum perfusion of the nutritive capillary surface may not be possible until the upstream resistance and conductance vessels are recruited. The implication of this finding for the adaptation to a ventilatory load is that the oxygen consumption of the respiratory muscles, is limited not only by the maximum available blood flow but also by the capacity for oxygen

extraction at a particular level of oxygen delivery and muscle activity. This information has not previously been available for the diaphragm or other respiratory muscles.

In chapter 4 two studies are presented. In the first of these the effect of changing diaphragm blood flow independent of oxygen delivery on diaphragmatic fatiguability is explored. In the second the relationships between systemic and diaphragmatic oxygen delivery and diaphragmatic oxygen uptake are determined and the critical diaphragmatic oxygen extraction is calculated.

Role of Nitric Oxide

Recently, modulation of endothelial release of nitric oxide (NO) or a related nitroso compound has emerged as one of the most important mechanisms by which vascular tone is regulated. NO is synthesized in the endothelium from the guanido nitrogen of L-arginine and molecular oxygen by the NADPH and calmodulin dependent action of a constitutive NO synthase. Citrulline is a coproduct of this reaction. FMN, FAD, heme and tetrahydrobiopterin are co-factors (126). Substrate levels adequate to support ongoing NO synthesis are maintained by the uptake of extracellular L-arginine and through the synthesis of L-arginine from the peptidyl L-arginine pool by a process linked to the release of NO (116,184) and through recycling of accumulated L-citrulline to L-arginine (68,168). In large conduit vessels evidence suggests that NO synthesis and release is stimulated in response to shear stress, endothelial deformation, acetylcholine, bradykinin, histamine, 5-HT, thrombin, substance P, ATP and ADP (120). The role of nitric oxide in regulation of tone in smaller arterioles appears to vary with the size of the vessel. In near-resistance arterioles ($\sim 100\mu$), Sun et al. (179) found that N^G-

nitro-L-arginine (LNA), an L-arginine analogue which inhibits synthesis of NO from L-arginine, reduces baseline diameter and inhibits L-arginine induced vasodilation. In cat skeletal muscle, Ekelund and Mellander (41) found that monomethyl-L-arginine (LNMMA), another L-arginine analogue, increases resistance preferentially in arterioles with baseline diameters > 25μ. Persson (131) found that superfusion of rat cremaster muscle with LNMMA reduced terminal arteriolar diameter, but did not influence the post contraction change in diameter of these vessels.

The nitric oxide pathway is likely involved in the regulation of diaphragmatic oxygen availability at several levels. It may play an effector role in the regulation of baseline vascular tone, in the local response to decreased luminal PO_2 (hypoxic vasodilation), as a final common pathway in the dilation which accompanies accumulation of metabolic byproducts (active and reactive hyperaemia), and in modulating the changes in flow during perturbations in perfusion pressure (autoregulation).

Basal release of NO has been detected by bioassay from isolated vessels (85,159). In vivo studies have demonstrated increased baseline arterial pressure following systemic infusion of L-arginine analogues in rats (54), guinea pigs (3), cats (14) and dogs (86). Regional treatment with analogues of L-arginine have been found to increase baseline vascular resistance in isolated rabbit hearts (98), rabbit hindlimb (123) dog hindlimb (196) and human forearm (186). In rat cremaster muscle, arteriolar vasoconstriction has been demonstrated following light-dye injury to the endothelium (91) and following topical application of L-arginine analogues (84). Similarly, Persson et al. (131) have shown LNMMA to reduce baseline microvascular diameters in rabbit tenuissimus muscle. Although these findings represent the majority of

studies, a few investigators have also described intact endothelium-dependent dilation or non-selective inhibition of agonist-induced dilation following the infusion of L-arginine analogues (123,183). The source of L-arginine on which the endothelial cell depends for substrate in the synthesis of NO also varies. In some isolated vessel preparations (58,84) and in the pial circulation in vivo (122) availability of extracellular L-arginine appears to limit basal NO formation. In other preparations (47,53,97,183) administration of exogenous L-arginine has no effect on vascular tone. These vessels presumably depend on intracellular synthesis of L-arginine and on the recycling of L-citrulline formed in the process of NO synthesis (68,168). Such discrepant results indicate that conclusions drawn from these studies, must be restricted to the vascular bed under study. The results obtained from previous studies, therefore, cannot be extrapolated to the diaphragm and the role of the nitric oxide pathway in this circulation must be specifically determined.

The role of the NO pathway in hypoxic vasodilation is also controversial. The activity of endothelial nitric oxide synthase is dependent on its oxygenated heme moiety, therefore, its role under hypoxic conditions would be expected to be minimal. Consistent with this prediction, a pressor response is elicited by hypoxia in some large vessel preparations and inhibition of basal NO release by hypoxia has been proposed as the underlying mechanism (124). Recently, Hashimoto et al. (67) have shown that endothelium dependent dilation of porcine coronary arteries is inhibited by hypoxic perfusate. In contrast, however, Pohl and Busse (134) have shown that vasodilation in rabbit aortic and femoral arterial rings in response to luminal hypoxia is inhibited by the NO inhibitors haemoglobin and dithiothreitol. In the isolated guinea pig heart(51,129) the coronary vasodilator response to perfusion with hypoxic buffer is also at least

in part mediated by the NO pathway since it is attenuated by L-arginine analogues. These observations are compatible with a variable role for the NO pathway, depending on the severity of hypoxia. Accordingly, NO release may be enhanced during mild hypoxia facilitating an increase in perfusion through conductance vessel dilation. During more severe hypoxia, however, NO synthase may be inhibited, whereas other vasodilators of metabolic origin become increasingly important. In the early stages of reductions in diaphragmatic oxygen availability, therefore, NO may play a role in maintaining tissue oxygenation, eventually losing effectiveness and being supplanted by other vasodilatory mediators as the hypoxic stimulus increases in intensity.

Increased muscular activity (active hyperaemia) and transient vascular occlusion (reactive hyperaemia) are the most well known stimuli to vasodilation in which a major role for mediators of metabolic origin has been proposed. Many of the chemicals which have previously been proposed to mediate metabolic control of vascular tone are now known influence endothelial release of NO (120). It is not surprising, therefore, that modulation of NO release has been proposed as a contributor to the vascular response to these stimuli (17,160,197). Most studies have demonstrated some effect of inhibition of NO synthesis on the active response. In the rat cremaster muscle, however, Persson (131) failed to show a change in the degree of microvessel dilation during muscle activation following treatment with LNMMA. In the hamster cremaster muscle, in contrast, Hester et al. (69) found NO inhibition with N^G-nitro-L-arginine methyl ester (LNAME), to decrease both resting diameter and functional dilation (active hyperaemia) of first order (65μ) arterioles, resting diameter but not active dilation in 2nd order (45μ) arterioles, and neither resting diameter nor active dilation in 3rd order (30μ) arterioles. A longitudinal gradient

in role for NO in the vasodilatory response to increased O_2 demand, therefore, appears to exist. In the canine diaphragm Hussain et al. (76) found that infusion of the L-arginine analogue arginino-succinic acid attenuated by approximately 20% the reduction in vascular resistance during phrenic nerve stimulation. Studies of the role of NO in reactive hyperaemia, have also yielded conflicting results. Chemical de-endothelialization (saponin) in dog hindlimb (160) and light-dye injury of arteriolar endothelium (92) in rat cremasteric muscle have been reported to reduce peak post occlusive vasodilation. Inhibition of EDRF synthesis by N^G-monomethyl-L-arginine infusion, in contrast, has not been found to alter peak post-occlusive changes in microvascular resistance in cat hindlimb muscle (17) nor to affect the increase in arteriolar diameter following a 15 second occlusion in rat cremaster muscle (197). The finding of an effect of NO inhibition on the active hyperaemic response in the diaphragm (76) suggests that the NO pathway may also play a role in the response to transient vascular occlusion, to the extent that it is dependent on metabolic mediation. This response is of greater physiologic significance in the diaphragm than in most organs, since, during the application of heavy loads, diaphragmatic blood flow is characterized by intermittent interruption and augmentation of relaxation phase flow is important to the preservation of its nutrient supply.

Autoregulation is the tendency to maintain blood flow constant despite changes in arterial perfusion pressure. This tendency is most strongly expressed in tissues with high levels of basal metabolic activity. It is felt to reflect the effects of vasoactive chemical and reflex neural influences superimposed on the intrinsic myogenic response to changes in vascular transmural pressure. The net effect of these influences is to impose a sigmoid shape on the relationship between perfusion pressure and blood flow (11,174,187). Accordingly, as perfusion pressure

is raised above the working range, increments in flow are resisted by myogenic enhancement of vascular smooth muscle tone. Eventually, a point is reached where this increase in resistance is overcome and flow increases in proportion to perfusion pressure. Conversely, as perfusion pressure is reduced below the working range, vascular tone and resistance to flow decrease because of myogenic relaxation triggered by decreasing vascular transmural pressure and because of the accumulation of vasodilator substances of metabolic origin. Eventually, a state of maximum vasodilation is achieved and blood flow falls linearly with further decreases in perfusion pressure. Nitric oxide has been shown to play a role in the process of autoregulation in several preparations. In the rabbit ear, inhibition of NO release converts a normally linear pressure-flow relationship to one conforming to a sigmoid shaped curve (66) indicating that the autoregulatory capacity of this circulation is normally suppressed by endothelial release of NO. In the renal and coronary circulations L-arginine analogues have been shown to reduce baseline blood flow without altering the range over which flow is maintained independent of changes in perfusion pressure (11,187). Reduction of the slope of the upper part of the pressure-flow relationship (above the autoregulated range of perfusion pressures) has also been observed in the isolated guinea pig heart following treatment with LNA (185). As with other aspects of vascular regulation, therefore, the importance of NO pathway appears to vary among the preparations in which it has been investigated.

The intraarterial infusion of NO inhibitors has been shown to reduce tissue oxygenation in several preparations (133,135,136). This reduction is due, in part, to inhibition of resistance vessel dilation in response to increased metabolic activity (76). In pump perfused preparations (136), however, this variable is obviated and an effect independent of bulk oxygen flow must

be hypothesized. As discussed above, oxygen uptake is determined by the driving pressure for oxygen diffusion and the diffusive conductance for oxygen. An effect of abluminally released nitric oxide on the tissue permeability to oxygen diffusion remains speculative. In fact, agreement on a normal value of this parameter cannot even be achieved. Kuo and Pittman (96) and Swain and Pittman (181), used a microspectrophotometric technique for determining O_2 transport in the arteriolar network of hamster retractor muscle. When the data on the precapillary longitudinal gradient in O_2 saturation was analyzed using an in-vitro value for the diffusion coefficient, the predicted O_2 flux from the arterioles turned out to be an order of magnitude smaller than the experimental values (138). The error in available estimates of O_2 diffusivity may, therefore, be up to an order of magnitude. Longmuir et al. (100) have suggested the existence of rapid diffusion O_2 channels within striated muscle cells. Such an inhomogeneity in tissue oxygen diffusion could reconcile these findings and the possibility of a regulatory role for NO at this site remains to be investigated. NO is avidly bound to haemoglobin, however, it seems unlikely that an effect on oxyhemoglobin dissociation could account for changes in oxygen extraction given the low levels of luminal NO release (85) and the relative insensitivity of O_2 extraction to changes in haemoglobin oxygen affinity (175). Inhibition of NO release has been shown to influence terminal arteriolar diameter in the resting rabbit tenuissimus muscle (131,132). It is attractive, therefore, to speculate that NO release by the microvascular endothelium may play a role in the local regulation of convective oxygen flow.

In chapter 5, the role of NO in regulation of the delivery of blood and oxygen to the diaphragm is investigated. This includes evaluation the importance of this regulatory mechanism in the maintenance of baseline blood flow and the vascular response to transient vascular

occlusion. In addition, the effect of inhibiting NO synthesis on the diaphragmatic oxygen delivery-consumption relationship is determined.

Summary

Failure of the chest wall to efficiently convert muscle contraction into ventilation of the lungs both increases the load placed on the respiratory muscles as a group and reduces the capacity of the individual muscles to generate the required output because of changes in their resting length, orientation and mechanical linkage to other components of the system. The capacity of the respiratory muscles to sustain ventilation is also reduced if the mechanisms by which they adapt to the demand for increased mechanical output are impaired. These adaptive responses are extensive. They include reflex changes in the timing and intensity of their contraction resulting from consciously and unconsciously perceived sensory input, changes in conductance of their vasculature, augmentation of their capacity for oxygen and substrate exchange and the metabolic adaptations by which they optimize energy production from the available substrates. This thesis presents a series of studies which explore the nature of some of these adaptive mechanisms and evaluate the manner in which they contribute to the function of the respiratory system.

REFERENCES

1. Aaron, E.A., K.C. Seow, B.D. Johnson and J.A. Dempsey. Oxygen cost of exercise hyperpnea: implications for performance. *J. Appl. Physiol.* 72: 1818-1825, 1992.

2. Agostoni, E., P. Mognoni, G. Torri and F. Saracino. Relation between changes of rib cage circumference and lung volume. *J. Appl. Physiol.* 20: 1179-1186, 1985.

3. Aisaka, K., S.S. Gross, O.W. Griffith and R. Levi. N^G-methylarginine, a potent pressor agent in the guinea pig: does nitric oxide regulate blood pressure in vivo? *Biochem. Biophys. Res. Commun.* 160: 881-886, 1989.

4. Anrep, G.V., S.. Cerqua and A. Samaan. The effect of muscular contraction upon the blood flow in the skeletal muscle, in the diaphragm and in the small intestine. *Proc. R. Soc. Lond. Ser.* 114: 245-257, 1934.

5. Arnold, J.S., A. Oliven and S.G. Kelson. Effect of hypoxia on transdiaphragmatic pressure in intact hamsters. *Fed. Proc.* 44: 1004, 1985.

6. Ashton, H. Critical closing pressure in human peripheral vascular beds. *Clin. Sci.* 22: 79-87, 1962.

7. Axen, C. and P.O. Janson. Diaphragmatic blood flow at various levels of ventilation in the rabbit. *Acta Physiol. Scand.* 106: 1-3, 1979.

8. Banzett, R.B., G.F. Inbar, R. Brown, M. Goldman, R. rossier and J. Mead. Diaphragm electrical activity during negative lower torso pressure in quadriplegic men. *J. Appl. Physiol.* 51: 654-659, 1981.

9. Bark, H., G. Supinski, R. Bundy and S. Kelsen. Effect of hypoxia on diaphragm blood flow, oxygen uptake and contractility. *Am. Rev. Respir. Dis.* 138: 1535-1541, 1988.

10. Bark, H., G.S. Supinski, J.C. Lamanna and S.G. Kelsen. Relationship of changes in diaphragmatic muscle blood flow to muscle contractile activity. *J. Appl. Physiol.* 62: 291-299, 1987.

11. Baumann, J.E., P.B. Persson, H. Ehmke, B. Nafz and H.R. Kirchleim. Role of endothelium-derived relaxing factor in renal autoregulation in conscious dogs. *Am. J. Physiol.* 263: F208-F213, 1992.

12. Bazzy, A.R. and D.F. Donnelly. Diaphragmatic failure during loaded breathing: role of neuromuscular transmission. *J. Appl. Physiol.* 74: 1679-1683, 1993.

13. Bazzy, A.R., L.M. Pang, S.R. Akabas and G.G. Haddad. O_2 metabolism of the sheep diaphragm during flow resistive loaded breathing. *J. Appl. Physiol.* 66: 2305-2311, 1989.

14. Bellan, J.A., R.K. Minkes, D.B. McNamara and P.J. Kadowtiz. N^W-nitro-L-arginine selectively inhibits vasodilator responses to acetylcholine and bradykinin in cats. *Am. J. Physiol.* 260: H1025-H1029, 1991.

15. Bellemare, F. and B. Bigland-Ritchie. Central components of diaphragmatic fatigue assessed by phrenic nerve stimulation. *J. Appl. Physiol.* 62: 1307-1316, 1987.

16. Bellemare, F., D. Wight, C.M. Lavigne and A. Grassino. The effect of tensin and pattern of contractions on the blood flow of the canine diaphragm. *J. Appl. Physiol.* 54: 1597-1606, 1983.

17. Bjornberg, J., U. Alberta and S. Mellander. Resistance responses in proximal arterial vessels, arterioles and veins during reactive hyperaemia in skeletal muscle and their underlying regulatory mechanisms. *Acta Physiol. Scand.* 139: 535-550, 1990.

18. Bouverot, P. and R.S. Fitzgerald. Role of the arterial chemoreceptors in controlling lung volume in the dog. *Respir. Physiol.* 7: 203-215, 1969.

19. Brancatisano, A., L.A. Engel and S.H. Loring. Lung volume and effectiveness of inspiratory muscles. *J. Appl. Physiol.* 74: 688-694, 1993.

20. Buchler, B., S. Magder, H. Katsardis, Y. Jammes and C. Roussos. Effects of pleural pressure and abdominal pressure on diaphragmatic blood flow. *J. Appl. Physiol.* 58: 691-697, 1985.

21. Buchler, B., S. Magder and C. Roussos. Effects of contraction frequency and duty cycle on diaphragmatic blood flow. *J. Appl. Physiol.* 58: 265-273, 1985.

22. Burke, R.E., D.N. Levine, F.E. Zajac, P. Tsairis and W.K. Engel. Mammalian motor units: physiological-histochemical correlation in three types of cat gastrocnemius. *Science* 174: 709-712, 1971.

23. Bylund-Fellenius, A.C., P.M. Walker, A. Elander, S. Holms and T. Schersten. Energy metabolism in relation to oxygen partial pressure in human skeletal muscle during exercise. *Biochem.* 200: 247-255, 1991.

24. Cain, S.M. Oxygen delivery and extraction in dogs during anemic and hypoxic hypoxia. *J. Appl. Physiol.* 42: 228-234, 1977.

25. Campbell, J.A., R.L. Hughes, V. Sahgal, J. Frederiksen and T.W. Shields. Alterations in intercostal muscle morphology and biochemistry in patients with obstructive lung disease. *Am. Rev. Respir. Dis.* 122: 679-686, 1980.

26. Cheeseman, M. and W.R. Revelette. Phrenic afferent contribution to reflexes elicited by changes in diaphragm length. *J. Appl. Physiol.* 69: 640-647, 1990.

27. Cherniack, R.M. The oxygen consumption and efficiency of the respiratory muscles in health and emphysema. *J. Clin. Invest.* 38: 494-499, 1959.

28. Corda, M., C. Von Euler and G. Lennerstrand. Proprioceptive innervation of the diaphragm. *J. Physiol. Lond.* 178: 161-177, 1965.

29. Crawford, A.B., D. Dodd and L.A. Engel. Changes in rib cage shape during quiet breathing, hyperventilation and single inspirations. *Resp. Physiol.* 54: 197-209, 1983.

30. D'Angelo, E. and G. Sant'Ambrogio. Direct action of contracting diaphragm on the rib cage in rabbits and dogs. *J. Appl. Physiol.* 36: 715-719, 1974.

31. Danon, J., W.S. Druz, N.B. Goldberg and J.T. Sharp. Function of the isolated paced diaphragm and the cervical accessory muscles in C1 quadriplegics. *Am. Rev. Respir. Dis.* 119: 909-918, 1979.

32. Davenport, P.W., F.J. Thompson, R.L. Reep and A.N. Freed. Projection of phrenic nerve afferents to the cat sensorimotor cortex. *Brain Research* 328: 150-153, 1985.

33. Decramer, M., A. DeTroyer, S. Kelly, L. Zocchi and P.T. Macklem. Regional differences in abdominal pressure swings in dogs. *J. Appl. Physiol.* 56: 1682-1687, 1984.

34. Deschamps, A. and S. Magder. Baroreflex control of regional capacitance and blood flow distribution with or without α-adrenergic blockade. *Am. J. Physiol.* 32: H1755-H1763, 1992.

35. DeTroyer, A. and M. Estenne. Coordination between rib cage muscles and diaphragm during quiet breathing in humans. *J. Appl. Physiol. : Respirat. Environ Exercise Physiol.* 57: 899-906, 1984.

36. DeTroyer, A. and M.G. Sampson. Activation of the parasternal intercostals during breathing efforts in human subjects. *J. Appl. Physiol. : Respirat. Environ Exercise Physiol.* 52: 524-529, 1982.

37. Dubowitz, F. and Brooke, M.H. Muscle Biopsy: A Modern Approach. In: , London: W.B. Saunders, 1973, p. 49-60.

38. Duron, B., Jung-Caillol, M.C. and Marlot, D. Reflexe inhibiteur phrenico-phrenique. In: *Respiratory Centres and Afferent Systems*, edited by Duron, B. Paris: INSERM, 1976, p. 193-197.

39. Duron, B., M.C. Jung-Caillol and D. Marlot. Myelinated nerve fiber supply and muscle spindles in the respiratory muscles of cas: Quantitative study. *Anat. Embryol.* 152: 171-192, 1978.

40. Duron, B. and D. Marlot. The non-myelinated fibers of the phrenic and the intercostal nerves in the cat. *Z. Mikrosk. anat. Forsch, Leipzig* 2: 257-268, 1980.

41. Ekelund, U. and S. Mellander. Role of endothelium-derived nitric oxide in the regulation of tonus in large-borearterial resistance vessels, arterioles and veins in cat skeletal muscle. *Acta Physiol. Scand.* 140: 301-309, 1990.

42. Eldridge, G.L., P. Gill-Kumar, D.E. Millhorn and T.G. Waldrop. Spinal inhibition of phrenic motoneurones by stimulation of afferents from peripheral muscles. *J. Physiol.* 311: 67-79, 1981.

43. Estenne, M. and A. DeTroyer. Relationship between respiratory muscle electromyogram and rib cage motion in tetraplegia. *Am. Rev. Respir. Dis.* 132: 53-59, 1985.

44. Ferguson, G.T., C.G. Irvin and R.M. Cherniack. Relationship of diaphragm glycogen, lactate and function to respiratory failure. *Am. Rev. Respir. Dis.* 141: 926-932, 1990.

45. Ferguson, G.T., C.G. Irvin and R.M. Cherniack. Effect of corticosteroids on diaphragm function and biochemistry in the rabbit. *Am. Rev. Respir. Dis.* 141: 156-163, 1990.

46. Field, S., S.M. Kelly and P.T. Macklem. The oxygen cost of breathing in patients with cardiorespiratory disease. *Am. Rev. Respir. Dis.* 126: 9-13, 1982.

47. Fortes, Z.B., M.A. Oliviera, R. Scivoleto, M.H.C. Carvalho, G. De Nucci and D. Nigro. Nitric oxide release may be involved in the microcirculatory response to acetylcholine. *Eur. J. Pharmacol.* 182: 143-147, 1990.

48. Frazier, D.T., F. Xu, L.Y. Lee and R.F. Taylor. Respiratory load compensation III. Role of spinal cord afferents. *J. Appl. Physiol.* 75: 682-687, 1993.

49. Fregosi, R.F. and J.A. Dempsey. Effects of exercise in normoxia and acute hypoxia on respiratory muscle metabolites. *J. Appl. Physiol.* 60: 1274-1283, 1986.

50. Fritts, H.W., J. Filler, A.P. Fishman and A. Cournand. The efficiency of ventilation during voluntary hyperpnea: studies in normal subjects and in dyspneic patients with either chronic pulmonary emphysema or obesity. *J. Clin. Invest.* 38: 1339-1348, 1959.

51. Fritz, L.B., D.G. Davis, R.H. Holtrop and H. Dunder. Fatty acid oxidation by skeletal muscle during rest and activity. *Am. J. Physiol.* 194: 377-386, 2000.

52. Fryman, D.L. and D.T. Frazier. Diaphragm afferent modulation of phrenic motor drive. *J. Appl. Physiol.* 62: 2436-2441, 1981.

53. Gardiner, S.M., A.M. Comptom, T. Bennett, R.M.J. Palmer and S. Moncanda. Control of regional blood flow by endothelium-derived nitric oxide. *Hypertension Dallas* 15: 486-492, 1990.

54. Gardiner, S.M., A.M. Compton, P.A. Kemp and T. Bennett. Regional and cardiac hemodynamic responses to glyceryl trinitrate, acetylcholine, bradykinin and endothlin-1 in conscious rats: effects of N^G-nitro-L-arginine. *Br. J. Pharmacol.* 101: 632-639, 1989.

55. Gertz, I., G. Hedenstierna, G. Hellers and J. Wahren. Muscle metabolism in patients with chronic obstructive lung disease and acute respiratory failure. *Clin. Sci. Mol. Med.* 52: 395-403, 1977.

56. Gill, P.K. and M. Kuno. Excitatory and inhibitory actions on phrenic motoneurons. *J. Physiol. Lond.* 168: 274-289, 1963.

57. Gilmartin, J.J. and G.J. Gibson. Mechanisms of paradoxical rib cage motion in patients with chronic obstructive pulmonary disease. *Am. Rev. Respir. Dis.* 134: 683-687, 1986.

58. Gold, M.E., K.S. Wood, G.M. Buga, R.E. Byrns and L.J. Ignarro. L-arginine causes whereas L-argininosuccinic acid inhibits endothelium-dependent vascular smooth muscle relaxation. *Biochem. Biophys. Res. Commun.* 161: 536-543, 1989.

59. Goldman, M., G. Grimby and J. Mead. Mechanical work of breathing derived from rib cage and abdominal VP partitioning. *J. Appl. Physiol.* 41: 752-763, 1976.

60. Gorski, J., Z. Namiot and J. Giedroje. Effect of exercise on metabolism of glycogen and triglycerides in the respiratory muscles. *Pflugers Arch.* 377: 251-254, 1978.

61. Goshgarian, H.G. The role of cervical afferent nerve fiber inhibition of the crossed phrenic phenomenon. *Exper. Neurol.* 72: 211-225, 1981.

62. Graham, R., Y. Jammes, S. Delpierre, C. Grimaud and Ch. Roussos. The effects of ischemia, lactic acid and hypertonic sodium chloride on phrenic afferent discharge during spontaneous diaphragmatic contraction. *Neurosci. Lett.* 67: 257-262, 1986.

63. Granger, H.J., A.H. Goodman and B.H. Cook. Metabolic models of microcirculatory regulation. *Fed. Proc.* 34: 2025-2030, 1975.

64. Green, M., J. Mead and T.A. Sears. Muscle activity during chest wall restriction and positive pressure breathing in man. *Respir. Physiol.* 35: 283-300, 1978.

65. Green, N.J., H. Reichmann and D. Pette. Inter- and intraspecies comparisons of fibre type distribution and of succinate dehydrogenase activity in type I, IIA and IIB fibres of mammalian diaphragms. *Biochem.* 81: 67-73, 1984.

66. Griffith, T.M. and D.H. Edwards. Myogenic autoregulation of flow may be inversely related to endothelium-derived relaxing factor activity. *Am. J. Physiol.* 258: H1171-H1180, 1990.

67. Hashimoto, M., L.A. Close, Y. Ishida and R.J. Paul. Dependence of endothelium-mediated relaxation on oxygen and metabolism in porcine coronary arteries. *Am. J. Physiol.* 265: H299-H306, 1993.

68. Hecker, M., W.C. Sessa, H.J. Haris, E.E. Anggard and J.R. Vane. The metabolism of L-arginine and its significance for the biosynthesis of endothelium-derived relaxing factor: Cultured endothelial cells recycle L-citrulline to L-arginine. *Proc. Natl. Acad. Sci. U. S. A.* 87: 8612-8616, 1990.

69. Hester, R.L., A. Eraslan and Y. Saito. Differences in EDNO contribution to arteriolar diameter at rest and during functional dilation in striated muscle. *Am. J. Physiol.* 265: H146-H151, 1993.

70. Hogan, M.C., D.E. Bebout and P.D. Wagner. Effect of hemoglobin concentration on maximal O_2 uptake in canine gastrocnemius muscle in situ. *J. Appl. Physiol.* 70: 1105-1112, 1991.

71. Hogan, M.C., J. Roca, P.D. Wagner and J.B. West. Limitation of maximal O_2 uptake and performance by acute hypoxia in dog muscle in situ. *J. Appl. Physiol.* 65: 815-821, 1988.

72. Honig, C.R., J.L. Frierson and T.E.J. Gayeski. Anatomical determinants of O_2 flux density at coronary capillaries. *Am. J. Physiol.* 256: H375-H382, 1989.

73. Honig, C.R., C.L. Odoroff and J.L. Frierson. Capillary recruitment in exercise: rate, extent, uniformity, and relation to blood flow. *Am. J. Physiol.* 238: H31-H32, 1980.

74. Hussain, S.N.A., S. Magder, A. Chatillon and Ch. Roussos. Chemical activation of thin-fiber phrenic afferents: respiratory responses. *J. Appl. Physiol.* 69: 1002-1011, 1990.

75. Hussain, S.N.A. and S.A. Magder. Diaphragmatic intramuscular pressure in relation to tension, shortening, and blood flow. *J. Appl. Physiol.* 71: 159-167, 1991.

76. Hussain, S.N.A., D.J. Stewart, J.P. Ludemann and S.A. Magder. Role of endothelium-derived relaxing factor in active hyperemia of the canine diaphragm. *J. Appl. Physiol.* 72: 2393-2401, 1992.

77. Ianuzzo, C.D., M.J. Spalding and H. Williams. Exercise-induced glycogen utilization by the respiratory muscles. *J. Appl. Physiol.* 62: 1405-1409, 1987.

78. Idstrom, J.P., V.H. Subramanian, B. Chance, T. Schersten and A.C. Bylund-Fellenius. Oxygen dependence of energy metabolism in contracting and recovering rat skeletal muscle. *Am. J. Physiol.* 248: H40-H48, 1985.

79. Jammes, Y., B. Buchler and S. Delpierre. Phrenic afferents and their role in inspiratory control. *J. Appl. Physiol.* 60: 854-860, 1986.

80. Jaspers, S.R. and M.E. Tischler. Role of glucocorticoids in the response of rat leg muscles to reduced activity. *Muscle Nerve* 9: 554-561, 1986.

81. Jiang, T.X., M. Demedts and M. Decramer. Mechanical coupling of upper and lower canine rib cages and its functional significance. *J. Appl. Physiol.* 64: 620-626, 1988.

82. Johnson, P.C. and M. Intaglietta. Contributions of pressure and flow sensitivity to autoregulation in mesenteric arterioles. *Am. J. Physiol.* 231: 1686-1698, 1976.

83. Jones, D.A., B. Bigland-Ritchie and R.H.T. Edwards. Excitation frequency and muscle fatigue: Mechanical response during voluntary and stimulated contractions. *Exp. Neurol.* 64: 401-413, 1979.

84. Kaley, G., A. Koller, J.M. Rodenbrug, E.J. Messina and M.S. Wolin. Regulation of arteriolar tone and responses via L-arginine pathway in skeletal muscle. *Am. J. Physiol.* 262: H987-H992, 1992.

85. Kelm, M. and J. Schrader. Control of coronary vascular tone by nitric oxide. *Circ. Res.* 66: 1561-1575, 1990.

86. Klabunde, R.E., R.C. Ritger and M.C. Helgren. N^G-monomethyl-L-arginine causes systemic vasoconstriction and cardiac depression in anesthetized dogs. *Pharmacologist* 32: 145, 1990.

87. Klitzman, B., D.N. Damon, R.J. Gorczynski and B.R. Duling. Augmented tissue oxygen supply during striated muscle contraction in the hamster. *Circ. Res.* 51: 711-721, 1982.

88. Kniffki, K.D., S. Mense and R.F. Schmidt. Muscle receptors with fine afferent fibers which may evoke circulatory reflexes. *Circ. Res.* 48: 25-31, 1981.

89. Kohzuki, H., Y. Enoki, Y. Ohga, S. Shimizu and S. Sakata. Oxygen consumption in resting dog gracilis muscle perfused at varying oxygen delivery. *Jap. J. Physiol.* 41: 23-34, 1991.

90. Kolar, F. and L. Jansky. Oxygen consumption in rat skeletal muscle at various rates of oxygen delivery. *Experientia* 40: 353-354, 1984.

91. Koller, A. and G. Kaley. Role of endothelium in reactive dilatation of skeletal muscle arterioles. *Am. J. Physiol.* 259: H1313-H1316, 1990.

92. Koller, A., E.J. Messina, M.S. Wolin and G. Kaley. Effects of endothelial impairment on arteriolar dilator response in vivo. *Am. J. Physiol.* 257: H1485-H1489, 1989.

93. Konno, K. and J. Mead. Measurement of the separate volume changes of rib cage and abdomen during breathing. *J. Appl. Physiol.* 22: 407-422, 1967.

94. Krayes, S., M. Decramer, J. Vetterman, E.L. Rittman and K. Kehder. Volume quantification of chest wall motion in dogs. *J. Appl. Physiol.* 65: 2213-2220, 1988.

95. Krogh, A. The number and distribution of capillaries in muscles with calculations of the oxygen pressure necessary for supplying the tissue. *J. Physiol. Lond.* 52: 409-415, 1919.

96. Kuo, L. and R.N. Pittman. Effect of hemodilution on oxygen transport in arteriolar networks of hamster striated muscle. *Am. J. Physiol.* 254: H331-H339, 1988.

97. Lahera, V., M.G. Salom, M.J. Fisken-Olsen, L. Raij and J.C. Romero. Effects of N^G-monomethyl-L-arginine and L-arginine on acetylcholine renal response. *Hypertension Dallas* 15: 659-663, 1990.

98. Lamontagne, D., U. Pohl and R. Busse. N^G-Nitro-L-arginine antagonizes endothelium-dependent dilator responses by inhibiting endothelium-derived relaxing factor release in the isolated rabbit heart. *Pflugers Arch.* 418: 266-270, 1991.

99. Larnicol, N., D. Rose and B. Duron. Identification of phrenic afferents to the external cuneate nucleus: a fluorescent double-labelling study in the cat. *Neurosci. Lett.* 62: 163-167, 1985.

100. Longmuir, I.S. Channels of oxygen transport from blood to mitochondria. *Adv. Physiol. Sci.* 25: 19-22, 1980.

101. Macklem, P.T., D. Gross, A. Grassino and C. Roussos. Partitioning of inspiratory pressure swings between diaphragm and intercostal/accessory muscles. *J. Appl. Physiol. : Respirat. Environ Exercise Physiol.* 44: 200-208, 1978.

102. Macklem, P.T., D.M. Macklem and A. DeTroyer. A model of inspiratory muscle mechanics. *J. Appl. Physiol. : Respirat. Environ Exercise Physiol.* 55: 547-557, 1983.

103. Macron, J.M. and D. Marlot. Effects of stimulation of phrenic afferent fibers on medullary respiratory neurons in cat. *Neurosci. Lett.* 63: 231-236, 1986.

104. Macron, J.M., D. Marlot and B. Duron. Phrenic afferent input to the lateral medullary reticular formation of the cat. *Respir. Physiol.* 59: 155-167, 1985.

105. Magder, S. Pressure-flow relations of diaphragm and vital organs with nitroprusside-induced vasodilatation. *J. Appl. Physiol.* 61: 409-416, 1986.

106. Manohar, M., T.E. Goetz, L.C. Holste and D. Nganwa. Diaphragmatic O_2 and lactate extraction during submaximal and maximal exertion in ponies. *J. Appl. Physiol.* 64: 1203-1209, 1988.

107. Manohar, M. and A.S. Hassan. Diaphragm does not produce ammonia or lactate during high-intensity short-term exercise. *Am. J. Physiol.* 259: H1185-H1189, 1990.

108. Manohar, M. and A.S. Hassan. Diaphragmatic energetics during prolonged exhaustive exercise. *Am. Rev. Respir. Dis.* 144: 415-418, 1991.

109. Margaria, R., G. Milic-Emili, J.M. Petit and G. Cavagna. Mechanical work of breathing during muscular exercise. *J. Appl. Physiol.* 15: 354-358, 1960.

110. Marlot, D., J.M. Macron and B. Duron. Projection of phrenic afferents to the cat cerebellar cortex. *Neurosci. Lett.* 44: 95-98, 1984.

111. Marlot, D., J.M. Macron and B. Duron. Inhibitory and excitatory effects on respiration by phrenic nerve afferent stimulation in cats. *Respir. Physiol.* 69: 321-333, 1987.

112. Marlot, D., J.M. Macron and B. Duron. Effects of ipsilateral and contralateral cervical phrenic afferent stimulation on phrenic motor unit activity in the cat. *Brain Research* 450: 373-377, 1988.

113. Maxwell, L.C., R.J.M. McCarter, T.J. Kuehl and J.L. Robotham. Development of histochemical and functional properties of baboon respiratory muscles. *J. Appl. Physiol.* 54: 551-561, 1983.

114. McCool, F.D., S.H. Loring and J. Mead. Rib cage distortion during voluntary and involuntary breathing acts. *J. Appl. Physiol.* 58: 1703-1712, 1985.

115. McCool, F.D., G.E. Tzelepis, D.E. Leith and F.G. Hoppin. Oxygen cost of breathing during fatiguing inspiratory resistive loads. *J. Appl. Physiol.* 66: 2045-2055, 1989.

116. Mitchell, J.A., M. Hecker and J.R. Vane. The generation of L-arginine in endothelial cells is linked to the release of endothelium-derived relaxing factor. *Eur. J. Pharmacol.* 176: 253-254, 1990.

117. Mizuno, M. and N.H. Secher. Histochemical characteristics of human expiratory and inspiratory intercostal muscles. *J. Appl. Physiol.* 67: 592-598, 1989.

118. Mognoni, P., F. Saibene and G. Sant'Ambrogio. Contribution of the diaphragm and other inspiratory muscles to different levels of total volumes and static inspiratory effort in the rabbit. *J. Appl. Physiol.* 202: 517-534, 1969.

119. Mohrman, D.E. and R.R. Regal. Relation of blood flow to VO_2, PO_2 and PCO_O in dog gastrocnemius muscle. *Am. J. Physiol.* 255: H1004-H1010, 1988.

120. Moncada, S., R.M.J. Palmer and E.A. Higs. Nitric oxide physiology, pathophysiology and pharmacology. *Pharmacol. Rev.* 43: 109-143, 1991.

121. Moore, R.L. and P.D. Gollnick. Response of ventilatory muscles of the rat to endurance training. *Pflugers Arch.* 392: 268-271, 1982.

122. Morikawa, E., S. Rosenblatt and M.A. Moskowitz. L-arginine dilates rat pial arterioles by nitric oxide-dependent mechanisms and increases blood flow during focal cerebral ischaemia. *Brit. J. Clin. Pharmacol.* 905-907, 1992.

123. Mugge, A., J.A.G. Lopez, D.J. Piegors, K.R. Breese and D.G. Heistad. Acetylcholine-induced vasodilation in rabbit hindlimb in vivo is not inhibited by analogues of L-arginine. *Am. J. Physiol.* 260: H242-H247, 1991.

124. Muramatsu, M., Y. Iwama, K. Shimizu, et al. Hypoxia-elicited contraction of aorta and coronary artery via removal of endothelium-derived nitric oxide. *Am. J. Physiol.* 263: H1339-H1347, 1992.

125. Nagano, K., S. Gelman, D.A. Parks and E. Bradley. Hepatic oxygen supply-uptake relationship and metabolism during anesthesia in miniature pigs. *Anesthesiology* 72: 902-910, 1990.

126. Nathan, C. Nitric oxide as a secretory product of mammalian cells. *FASEB J.* 6: 3051-3064, 1992.

127. Nelson, D.P., C.E. King, S.L. Dodd, P.T. Shcumacker and S.M. Cain. Systemic and intestinal limits of O_2 extraction in the dog. *J. Appl. Physiol.* 63: 387-394, 1987.

128. Otis, A.B., W.O. Fenn and H. Rahn. Mechanics of breathing in man. *J. Appl. Physiol.* 2: 592, 1950.

129. Park, K.H., L.E. Rubin, S.S. Gross and R. Levi. Nitric oxide is a mediator of hypoxic coronary vasodilatation: relation to adenosine and cyclooxygenase-derived metabolites. *Circ. Res.* 71: 992-1001, 1992.

130. Perry, M.A., P. Bulkley, P.R. Kvietys and D.N. Granger. Regulation of oxygen uptake in resting and pentagastrin-stimulated canine stomach. *Am. J. Physiol.* 242: G565-G569, 1982.

131. Persson, M.G., L.E. Gustafsson, N.P. Wiklund, P. Hedqvist and S. Moncada. Endogenous nitric oxide as a modulator of rabbit skeletal muscle microcirculation in vivo. *Br. J. Pharmacol.* 100: 463-466, 1990.

132. Persson, M.G., N.P. Wiklund and L.E. Gustafsson. Nitric oxide requirement for vasomotor nerve-induced vasodilation and modulation of resting blood flow in muscle microcirculation. *Acta Physiol. Scand.* 141: 49-56, 1990.

133. Pohl, U. and Busse, R. Reduced nutritional blood flow in autoperfused rabbit hindlimbs following inhibition of endothelial vasomotor function. In: *Resistance Arteries*, edited by

Halpern, W., Pegram, B., Bryaden, J., Mackey, K., Mclaughlin, M. and Osol, G. New York: Ithaca, Perinatology, 1988, p. 10-16.

134. Pohl, U. and R. Busse. Hypoxia stimulates release of endothelium-derived relaxant factor. *Am. J. Physiol.* 256: H1595-H1600, 1989.

135. Pohl, U. and D. Lamontagne. Impaired tissue perfusion after inhibition of endothelium-derived nitric oxide. *Basic Res. Cardiol.* 86: 97-105, 1991.

136. Pohl, U., D. Lamontagne, E. Bassenge and R. Busse. EDRF antagonizes myogenic autoregulation in the vasculature of isolated rabbit hearts. *Am. J. Physiol.* 1992.(In Press)

137. Pope, A., S.M. Scharf and R. Brown. Diaphragm metabolism during supramaximal phrenic nerve stimulation. *J. Appl. Physiol.* 66: 567-572, 1989.

138. Popel, A.S., R.N. Pittman and M.L. Ellsworth. Rate of oxygen loss from arterioles is an order of magnitude higher than expected. *Am. J. Physiol.* H921: H924, 1989.

139. Primiano, F.P.,Jr. Theoretical analysis of chest wall mechanics. *J. Biomechanics* 15: 919-931, 1982.

140. Reid, M.B. and R. Johnson. Efficiency, maximal blood flow and aerobic work capacity of canine diaphragm. *Am. J. Physiol.* 54: 763-772, 1983.

141. Reid, M.B. and R.L. Johnson,Jr.. Efficiency, maximal blood flow, and aerobic work capacity of canine diaphragm. *J. Appl. Physiol.* 54: 763-772, 1983.

142. Revelette, R., S. Reynolds, D. Brown and R. Taylor. Effect of abdominal compression on diaphragmatic tendon organ activity. *J. Appl. Physiol.* 72: 288-292, 1992.

143. Revelette, W.R., L.A. Jewell and D.T. Frazier. Effect of diaphragm small-fiber afferent stimulation on ventilation in dogs. *J. Appl. Physiol.* 65: 2097-2106, 1988.

144. Rexed, B. Contributions to the knowledge of the postnatal development of the peripheral nervous system in man. *Acta Psychiat. Neurol. Suppl.* Suppl. No. 33: 1944.

145. Rijlant, P. Contribution a letude de controle reflexe de la respiration. *Bull. Acad. Med. Belg.* 7: 58-107, 1942.

146. Riley, D.A. and A.J. Berger. A regional histochemical and electromyographic analysis of the cat respiratory diaphragm. *Exp. Neurol.* 66: 636-649, 1979.

147. Riley, R.L. The work of breathing and its relation to respiratory acidosis. *Ann. Int. Med.* 41: 172-176, 1954.

148. Road, J.D., N.H. West and B.N. Van Vliet. Ventilatory effects of stimulation of phrenic afferents. *J. Appl. Physiol.* 63: 1063-1069, 1987.

149. Robertson, C.H., G.H. Foster and R.L. Johnson. The relationship of respiratory failure to the oxygen consumption of, lactate production by, and the distribution of blood flow among respiratory muscles during increasing inspiratory resistance. *J. Clin. Invest.* 59: 31-42, 1977.

150. Robertson, C.H., M.A. Pagel and R.L. Johnson. The distribution of blood flow, oxygen consumption and work output among the respiratory muscles during unobstructed hyperventilation. *J. Clin. Invest.* 59: 43-50, 1977.

151. Robertson, C.H.,Jr., G.H. Fortis and R.L. Johnson,Jr.. The relationship of respiratory failure to the oxygen consumption of lactate production by, and distribution of blood flow among respiratory muscles during increasing respiratory resistance. *J. Clin. Invest.* 59: 31-42, 1977.

152. Rochester, D.F. Measurement of diaphragmatic blood flow and oxygen consumption in the dog by the Kety-Schmidt technique. *J. Clin. Invest.* 53: 1126-1132, 1974.

153. Rochester, D.F. Respiratory muscle blood flow and metabolism. In: *The Thorax*, edited by Lenfant, C. and Roussos, Ch. New York: Marcel Dekker Inc., 1985, p. 393-436.

154. Rochester, D.F. and G. Bettini. Diaphragmatic blood flow and energy expenditure in the dog, effects of inspiratory airflow resistance and hypercapnia. *J. Clin. Invest.* 57: 661-672, 1976.

155. Rochester, D.F. and A.M. Briscoe. Metabolism of the working diaphragm. *Am. Rev. Respir. Dis.* 119: 101-106, 1979.

156. Rochester, D.F. and M. Pradel-Guena. Measurement of diaphragmatic blood flow in dogs from xenon-133 clearance. *J. Appl. Physiol.* 34: 68-74, 1973.

157. Roussos, Ch. Energetics. In: *The Thorax*, edited by Lenfant, C. and Roussos, Ch. New York: Marcel Dekker Inc., 1985, p. 437-492.

158. Roussos, Ch. and P.T. Macklem. Diaphragmatic fatigue in man. *J. Appl. Physiol.* 43: 189-197, 1978.

159. Rubanyi, G.M., R.R. Lorenz and P.M. Vanhoutte. Bioassay of endothelium-derived relaxing factor. *Am. J. Physiol.* 215: H1077-H1080, 1985.

160. Sagach, V.F. and M.N. Tkachenko. Role of the endothelium in the development of reactive hyperemia. *Biull. Eksp. Biol. Med.* 108: 431-423, 1989.

161. Sampson, M.G. and A. DeTroyer. Role of intercostal muscles in the rib cage distortions produced by inspiratory loads. *J. Appl. Physiol. : Respirat. Environ Exercise Physiol.* 52: 517-523, 1982.

162. Sant'Ambrogio, G. and J.G. Widdicombe. Respiratory reflexes acting on the diaphragm and inspiratory intercostal muscles of the rabbit. *J. Physiol. Lond.* 180: 766-779, 1965.

163. Sarelius, I.H. Cell and oxygen flow in arterioles controlling capillary perfusion. *Am. J. Physiol.* 34: H1628-H1687, 1993.

164. Scharf, S.M., H. Bark, S. Einhorn and A. Tarasiuk. Blood flow to the canine diaphragm during hemorrhagic shock. *Am. Rev. Respir. Dis.* 133: 205-211, 1986.

165. Schumacker, P.T., G.R. Long and L.D.H. Wood. Tissue oxygen extraction during hypovolemia: role of hemoglobin P_{50}. *J. Appl. Physiol.* 62: 1801-1807, 1987.

166. Sears, T.A., A.J. Berger and E.A. Phillipson. Reciprocal tonic activation of inspiratory and expiratory motoneurons by chemical dries. *Nature* 299: 728-730, 1982.

167. Segal, J.M., T. Phang and K. Walley. Low-dose dopamine hastens onset of gut ischemia in a porcine model of hemorrhagic shock. *J. Appl. Physiol.* 73(3): 1159-1164, 1992.

168. Sessa, W.C., M. Hecker, J.A. Mitchell and J.A. Vane. the metabolism of L-arginine and its significance for the biosynthesis of endothelium-derived relaxing factor: L-glutamine inhibits the generation of L-arginine by cultured endothelial cells. *Proc. Natl. Acad. Sci. U. S. A.* 87: 8607-8611, 1990.

169. Shepherd, R.J. The oxygen cost of breathing during vigorous exercise. *Q. J. Exp. Physiol.* 51: 336-350, 1966.

170. Skalak, R. Approximate formulas for myocardial fiber stresses. *J. Biomech. Eng.* 104: 162-163, 1982.

171. Speck, D.F. Supraspinal involvement in the phrenic-to-phrenic inhibitory reflex. *Brain Research* 414: 169-172, 1987.

172. Speck, D.F. and W.R. Revelette. Attenuation of phrenic motor discharge by phrenic nerve afferents. *J. Appl. Physiol.* 62: 941-945, 1987.

173. Stacey, M.J. Free nerve endings in skeletal muscle of the cat. *J. Anat.* 105: 231-254, 1969.

174. Stainsby, W.N. and A.B. Otis. Blood flow, blood oxygen tension, oxygen uptake, and oxygen transport in skeletal muscle. *Am. J. Physiol.* 206: 858-866, 1964.

175. Stein, J.C. and M.L. Ellsworth. Microvascular oxygen transport: impact of a left shifted dissociation curve. *Am. J. Physiol.* 262: H517-H522, 1992.

176. Stein, J.C. and M.L. Ellswroth. Capillary oxygen transport during severe hypoxia: role of hemoglobin oxygen affinity. *J. Appl. Physiol.* 75: 1601-1607, 1993.

177. Stephens, J.A. and A. Taylor. Fatigue of maintained voluntary muscle contraction in man. *J. Physiol. Lond.* 220: 1-18, 1972.

178. Stowe, D.F., T.L. Owen, D.K. Anderson, F.J. Haddy and J.B. Scott. Interaction of O_2 and CO_2 in sustained exercise hyperemia of canine skeletal muscle. *Am. J. Physiol.* 229: 28-33, 1975.

179. Sun, D., E.J. Messina, A. Koller, M.S. Wolin and G. Kaley. Endothelium dependent dilation to L-arginine in isolated rat skeletal muscle arterioles. *Am. J. Physiol.* 262: H1211-H1216, 1992.

180. Supinski, G.S., A.F. DiMarco and A. Altose. Effect of diaphragmatic contraction on intramuscular pressure and vascular impedence. *J. Appl. Physiol.* 68: 1486-1493, 1990.

181. Swain, D.P. and R.N. Pittman. Oxygen exchange in the microcirculation of hamster retractor muscle. *Am. J. Physiol.* 256: H247-H255, 1989.

182. Teitelbaum, J., C.O. Borel, S. Magder, R.J. Traystman and S.N.A. Hussain. Effect of selective diaphragmatic paralysis on the inspiratory motor drive. *J. Appl. Physiol.* 72: 288-292, 1992.

183. Thomas, G., E.A. Cole and P.W. Ramwell. N^G-monomethyl-L-arginine is a nonspecific inhibitor of vascular relaxation. *Eur. J. Pharmacol.* 170: 123-124, 1989.

184. Thomas, G. and P.W. Ramwell. Peptidyl arginine diminase and endothelium dependent relaxation. *Eur. J. Pharmacol.* 153: 147-148, 1988.

185. Ueeda, M., S.K. Silvia and R.A. Olsson. Nitric oxide modulates coronary autoregulation in the guinea pig. *Circ. Res.* 70: 1296-1303, 1992.

186. Vallance, P., J. Collier and S. Moncada. Effects of endothelium-derived nitric oxide on peripheral arteriolar tone in man. *Lancet* 2: 997-1000, 1989.

187. Van Citters, R.L. Occlusion of lumina in small arterioles during vasoconstriction. *Circ. Res.* 18: 199-204, 1966.

188. Vetterlein, F., U. Keitel and G. Schmidt. Capillary filling kinetics in the rabbit heart during normoxemia and hypoxemia. *Am. J. Physiol.* 264: H287-H293, 1993.

189. Viires, N., G. Sillye, M. Aubier, A. Rassidakis and Ch. Roussos. Regional blood flow distribution in dog during induced hypotension and low cardiac output. *J. Clin. Invest.* 72: 935-947, 1983.

190. Walley, K.R., C.J. Becker, R.A> Hogan, K. Teplinsky and L.D.H. Wood. Progressive hypoxemia limits left ventricular oxygen consumption and contractility. *Circ. Res.* 63: 849-859, 1988.

191. Ward, M.E., H.Y. Chang and S.N.A. Hussain. Systemic and diaphragmic O_2 delivery-O_2 consumption relationships. *J. Appl. Physiol.* 1993.(In Press)

192. Ward, M.E., D. Eidelman, D.G. Stubbing, F. Bellemare and P.T. Macklem. Respiratory sensation and pattern of respiratory muscle activation during diaphragm fatigue. *J. Appl. Physiol.* 65: 2181-2189, 1988.

193. Ward, M.E. and Ch. Roussos. Respiratory muscles in shock: Service or disservice. *Intensive and Critical Care Digest* 4: 3-5, 1985.

194. Watchko, J.F., W.A. LaFramboise, T.A. Standaert and D.E. Woodrum. Diaphragmatic function during hypoxemia: neonatal and developmental aspects. *J. Appl. Physiol.* 60: 1599-1604, 1986.

195. Wermers, B.W., H.M. Cavert, J.O. Harris and C.F. Quello. Glycogen metabolism in perfused contracting white rat hemidiaphragm muscle. *Am. J. Physiol.* 219: 1434-1439, 1970.

196. White, D.G., G.M. Drew, J.M. Gurden, D.M. Penny, A.G. Roach and I.S. Watts. The effect of N^G-nitro-L-arginine methyl ester upon basal blood flow and endothelium-dependent vasodilatation in the dog hindlimb. *Br. J. Pharmacol.* 108: 763-768, 1993.

197. Wolin, M.S., J.M. Rodenburg, E.J. Messina and G. Kaley. Similarities in the pharmacological modulation of reactive hyperemia and vasodilation to hydrogen peroxide in rat skeletal muscle arterioles: Effects of probes for endothelium-derived mediators. *J. Pharmacol. Exp. Ther.* 253: 508-512, 1990.

198. Xu, F., R.F. Taylor, L.Y. Lee and D.T. Frazier. Respiratory load compensation II. Role of the cerebellum. *J. Appl. Physiol.* 75: 675-681, 1993.

199. Xu, F., T. Taylor, T. McLarney, L.Y. Lee and D.T. Frazier. Respiratory load compensation. I. Role of the cerebrum. *J. Appl. Physiol.* 74: 853-858, 1993.

200. Yan, S., I. Lichros, S. Zakynthinos and P.T. Macklem. Effect of diaphragmatic fatigue on control of respiratory msucles and ventilation during CO_2 rebreathing. *J. Appl. Physiol.* 75: 1364-1370, 1993.

201. Yan, S., P. Sliwinski, A.P. Gauthier, I. Lichros, S. Zakynthinos and P.T. Macklem. Effect of global inspiratory muscle fatigue on ventilatory and respiratory muscle responses to CO_2. *J. Appl. Physiol.* 75: 1371-1377, 1993.

202. Zocchi, L., N. Garzaniki, S. Newman and P.T. Macklem. Effect of hyperventilation and equalization of abdominal pressure on diaphragmatic action. *J. Appl. Physiol.* 62: 1655-1664, 1987.

CHAPTER 2: Respiratory Muscle Actions and Interactions

Foreword to Chapter 2

Analysis of the integrated movement of chest wall is infinitely more complex than a description of the motion of its component parts. The chest wall contains 46 bones (24 ribs, 19 vertebrae, sternum, manubrium and pelvis). If all could move independently, each would posess 6 degrees of freedom, corresponding to 3 directions of translation and 3 axes of rotation. In addition, the soft tissue elements (right and left costal and crural diaphragm, abdominal free wall) may undergo distortion in three dimensions. Fortunately, the geometry of the joints and the muscular attachments place additional constraints on the way in which each element can move, thereby reducing the degrees of mechanical freedom. These constraints allow simplified models to be developed, which allow motion of the respiratory system to be described in terms of a few simple varibles. As long as the assumptions concerning the constraints are valid, these models allow predictions concerning the mechanical behavior of the system to be made which then may be tested experimentally. The goal of developing such models, therefore, is not to precisely duplicate the behaviour of the chest wall under all conditions but to understand, in a stepwise fashion, progressively more complex aspects of its function.

In this chapter a model of the chest wall is described which incorporates a two compartment rib cage. The actions of the diaphragm are exerted primarily on the abdominal rib cage, whereas the rib cage muscles exert their force primarily on the pulmonary rib cage. The crucial determinant of the interaction between the diaphragm and rib cage muscles, therefore, is the strength of the mechanical linkage between the two compartments. The experiments described, performed in normal individuals, illustrate use of the model to quantify the linkage between rib cage components and several other aspects of respiratory muscle interaction which were previously unmeasurable. This work opens the way for characterization of the mechanical abnormalities which contribute to respiratory system dysfunction in disease states.

Analysis of Human Chest Wall Motion Using a Two Compartment Rib Cage Model

Michael E. Ward, Joel W. Ward, and Peter T. Macklem
Journal of Applied Physiology 72: 1338-1347, 1992

Abstract

We present a model of rib cage mechanics which extends that described previously by Macklem et. al. (J. Appl. Physiol. 55:547-557, 1983) and incorporates a two compartment rib cage. We divide the rib cage into that apposed to the lung (RCpul) and that apposed to the diaphragm (RCab). We apply this model to determine rib cage distortability, the mechanical coupling between RCpul and RCab, the contribution of the rib cage muscles (RCM) to the pressure change during spontaneous inspiration (Prcm) and the insertional component of transdiaphragmatic pressure (Pdi,ins) in humans. Distortion is defined as the perpendicular displacement of the relationship between the cross-sectional areas of RCpul and RCab off of their relaxation line, distortability as the relationship between distortion and transdiaphragmatic pressure (Pdi) and mechanical coupling as the relationship between distortion and the pressure acting to restore the rib cage to its relaxed configuration (Plink), all assessed during bilateral transcutaneous phrenic nerve stimulation. Plink was significant even during quiet breathing. Prcm was calculated at end inspiration as the component of the pressure displacing RCpul not accounted for by Plink or pleural pressure. Prcm and Plink were approximately equal during quiet breathing. Pdi,ins was measured as the pressure acting on RCab not accounted for by the change in abdominal pressure during an inspiration without rib cage distortion and was 33% $\pm$ 10%(SEM) of total Pdi.

Introduction

Previously proposed models of chest wall motion have considered the rib cage as a single compartment with a single degree of freedom (25,27,28). Available evidence suggests, however, that such unitary behaviour is the result of the highly coordinated action of the inspiratory muscles (18) rather than inherent rigidity of the rib cage. In this paper we present a model which incorporates a two compartment rib cage as originally proposed by Agostini and D'Angelo (1). The rib cage is separated into that part apposed on its inner surface to the lung (RCpul) and that part apposed to the diaphragm (RCab). We show that using this approach it is possible to determine the following parameters: 1) the strength of the mechanical linkage between the two rib cage compartments; 2) The relationship between the pressure producing the rib cage distortions and the magnitude of distortion. 3) The contribution of the pressures resulting from distortion to inspiration; 4) the inspiratory pressure developed by the rib cage muscles (RCM); and 5) the contribution of the insertional action of the diaphragm to inflation of RCab.

The model represents an extension of that proposed by Macklem et. al. (28). The major differences ensue from treating the chest wall as three compartments which results in a different mechanical arrangement of the diaphragm and RCM.

Theory: Analysis of Pressures aplied to RCpul and RCab:

We assume that the important inspiratory RCM are the scalenes and parasternal msucles (15,20). The former are inserted into ribs 1 and 2; the latter into ribs 2 - 6 inclusive. The 6th rib attaches to the sternum at its ventral end. Thus the direct actions of the major RCM are almost exclusively on RCpul. The costal part of the diaphragm originates from the lower end of the sternum and from ribs 7 - 12 inclusive. The area of diaphragmatic apposition to the rib cage (Aap) at functional residual capacity (FRC) extends cranially to about the level of the xiphisternum. Thus the action of the diaphragm is almost exclusively on RCab.

Because the two parts of the rib cage are anatomically distinct and the pressures acting on them are different, it is reasonable to treat them as separate compartments. The pressures acting to displace RCpul are therefore: 1) The pleural pressure over the surface of the lung (Ppl,L); 2) the pressure developed by the rib cage muscles (Prcm) and 3) the pressure acting on RCpul resulting from mechanical coupling between the 2 rib cage compartments and any distortion that is present (Plink). Under equilibrium conditions, the pressures acting to displace RCpul are counterbalanced by its elastic recoil pressure, (Prc,pul).

Therefore:

$$P_{rc,pul} = P_{pl,L} + P_{rcm} + P_{link} \quad \ldots\ldots\ldots\ldots 1$$

The pressures acting to displace RCab are: 1) the pleural pressure in the area of apposition (Ppl,ap) which is close to abdominal pressure (Pab) (2,29,38); 2) the pressure resulting from the insertional action of the diaphragm on RCab independent of changes in Pab; 3) Plink when distortion is present; 4) the pressure resulting from the direct action of the abdominal muscles on RCab (12) independent of changes in Pab (Pmus,ab). As in the case of

RCpul, at equilbrium the pressures acting to displace RCab are counterbalanced by its elastic recoil pressure.

Therefore:

$$Prc,ab = Pab + xPdi + Plink + Pmus,ab \quad .....2$$

where Prc,ab is the elastic recoil pressure of RCab and xPdi represents the insertional action of Pdi on RCab ($1 > x > 0$). The pressure producing distortion is the difference between the pressures acting on RCab and RCpul. During pure diaphragmatic contraction when Prcm and Pmus,ab are zero, this is the difference between equations 2 and 1 or:

$$Pab + xPdi + Plink - Ppl,L\text{-}Plink = (x + 1)Pdi \quad ..... \ 3$$

In this paper we deal only with inspiration and assume that expiratory Prcm is zero. We ignore flow-resistive pressure losses.

The Mechanical Model: Figure 1 is a mechanical diagram of the model in lateral projection. The structure shaped like an inverted hockey-stick with a detached handle represents the rib cage. RCpul extends to the upper level of the costal fibers and is apposed to the lung. The pressure at its inner surface is Ppl,L. With contraction of the rib cage muscles it is displaced upward and anteriorly, rotating around the hinge at its attachment to the rest of the bony skeleton. It is connected to RCab by a spring which resists deformation. In agreement with equation 1, the pressures acting on RCpul are Ppl,L, Prcm and any pressure resulting from displacement of the spring (Plink). RCab is represented by the "handle" of the hockey stick and is directly apposed to the costal fibers. The pressure at its inner surface is Ppl,ap. The diaphragm, as in the previous model (28) is depicted as two muscles, the costal and crural parts, arranged mechanically in parallel so that Pdi is the sum of the pressure developed by the costal

part (Pdi,cos) and that developed by the crural part (Pdi,cru). Pdi is also the sum of xPdi and (1 - x)Pdi where (1 - x)Pdi is the non-insertional component of Pdi. Note that unlike in the previous model (28) xPdi and Pdi,cos are not necessarily equal.

When the diaphragm contracts in isolation, Pab increases displacing the abdominal wall anteriorly. Pab is transmitted (with or without some gain change) to the inner surface of RCab as Ppl,ap and results in displacement of RCab anteriorly and cranially. At the same time Ppl,L falls tending to displace RCpul inward and altering the position of RCpul relative to RCab thereby distorting the rib cage. The spring exerts a pressure, Plink, on both compartments which acts to minimize the distortion. Thus, in the model, the pressures acting on RCab are Ppl,ap, which we assume to be close to Pab, the pressure resulting from the insertional action of Pdi,cos which we equate with xPdi and Plink in agreement with equation 2.

If one assumes that Ppl,ap = Pab, then the pressure producing the distortion is Pab + xPdi - Ppl,L or (x + 1)Pdi in agreement with equation 3. Thus Pdi is directly proportional to the pressure producing distortion and can be used as an index of it. Note that the pressure producing distortion is distinct from the restoring force or Plink resulting from the distortion.

In the model depicted in figure 1 the spring above RCpul represents the elastic properties of the rib cage; the springs between RCpul, the rest of the skeleton and the central tendon represent the elastic properties of the lung; the springs between the central tendon, the skeleton and the anterior abdominal wall represent the elastic properties of the abdomen.

The Hydraulic or Electrical Analogue: Figure 2 gives the hydraulic or electrical analogue of the mechanical model presented in figure 1. Structures which are dislaced and which consist of elastic, frictional and inertial elements are represented by rectangles, namely the lung, RCpul,

RCab and the abdomen. Muscles, modeled as generators or pumps are represented as circles. The spring, S, linking RCpul and RCab which gives rise to Plink is also represented as a pump or generator. According to equations 1 and 2 the pressures (or voltages in the electrical analogue) acting on RCpul and RCab are the sum of 2 or more different pressures. In the analogue model this is accomplished by summing junctions.

In this model, in contrast to that previously described by Macklem et. al. (28), RCM and the diaphragm are hydraulically and electrically in parallel (mechanically in series).

As in the previous model, the costal and crural parts of the diaphragm are arranged hydraulically and electrically in series (mechanically in parallel) so that Pdi is the sum of Pdi,cos and Pdi,cru.

The pressure balance equation across the lung and RCpul pathway in figure 2 is given by:

$PB - Ppl, L + Ppl,L - Py + Py - (Py+Plink) + (Py+Plink) - PB = 0$

where Py is the pressure between RCM and the summing junction and PB is the ambient pressure. Since $Py - Ppl,L = Prcm$ and since

$(Py + Plink) - PB = Prc,pul$, substituting and taking PB to be 0, simplifies this equation to:

$- Ppl,L - Prcm - Plink + Prc,pul = 0$

This is identical to equation 1.

The pressure balance equation across the lung and RCab pathway is given by:

$PB - Ppl,L + Ppl,L - Px + Px - (Px - Ppl,L + Pab + Plink) + (Px - Ppl,L + Pab + Plink) - PB = 0$

where Px is an imaginary pressure between the costal and crural daphragms (*28). Since Pdi,cos

= Px - Ppl and since

Prc,ab = (Px - Ppl,L + Pab + Plink) - PB, substituting and taking PB to be 0, simplifies this equation to:

-Pdi,cos - Pab - Plink + Prc,ab = 0

Assuming Pmus,ab to be 0 and Pdi,cos equal to xPdi this is identical to equation 2.

The pressure balance equation across the lung and abdomen pathway is given by:

PB - Ppl,L + Ppl,L - Px + Px - Pab + Pab - PB = 0

which simplifies to:

- Ppl,L - Pdi + Pab = 0 4

During relaxation when all pressures developed by the muscles are zero and assuming no passive diaphragmatic tension, equations 1, 2 and 4 simplify to:

Prc,pul = Ppl,L + Plink

Prc,ab = Pab + Plink

Pab = Ppl,L

Because the pressures acting on both parts of the rib cage are equal there is no rib cage distortion and Plink = 0. Therefore the relationship between the cross-sectional areas of RCpul and RCab (Arc,pul and Arc,ab respectively) during relaxation represents the configuration existing when the pressures acting on both compartments are identical and defines the undistorted configuration of the rib cage. During relaxation, therefore, equation 1 simplifies to:

Prc,pul = Ppl,L

By measuring Ppl,L one can then determine Prc,pul as a function of Arc,pul. If we assume that the relationship between Arc,pul and Prc,pul is constant and is not influenced by muscle

contraction or rib cage distortion, Prc,pul may be determined if Arc,pul is known.

When the diaphragm is the only muscle contracting, equation 1 becomes:

$Prc,pul = Ppl,L + Plink.$

If Arc,pul is known, Prc,pul can be estimated, Ppl,L measured and thus Plink determined. The distortion can be quantified by the displacement of Arc,pul and Arc,ab away from the undistorted relaxation configuration, therefore, the relationship between Plink and distortion may be defined. Thus, during spontaneous breathing, if Arc,pul and the magnitude of the distortion are known, the only unknown in equation 1 is Prcm.

Similarly, during spontaneous breathing with no distortion and with the abdominal muscles relaxed, equation 2 simplifies to:

$Prc,ab = Pab + xPdi.$

Since Prc,ab can be estimated from the measurement of Arc,ab and its relationship with Prc,ab during relaxation, and since Pab can be measured, the only remaining unknown in this equation is xPdi.

Note that during undistorted active inspiration Prc,pul must equal Prc,ab or, assuming abdominal muscle relaxation:

$Pab + xPdi = Ppl,L + Prcm$

$(x + 1)Pdi = Prcm$

Thus, in order to prevent distortion, the rib cage muscles must be recruited just sufficiently to cancel the distorting action of $(x = 1)Pdi$.

Calculation of Prcm and xPdi in equations 1 and 2 are illustrated below in the Methods section.

Methods

Subjects and Instrumentation: Studies were performed in 5 normal male volunteers 32 to 54 years of age recruited from among laboratory personel. 5 subjects were used in each measurement protocol. All subjects were experienced in physiologic studies and in the performance of respiratory manoeuvres. Measurements were performed with the subjects seated breathing through a mouthpiece attached to a Hans-Rudolf valve. Esophageal pressure (Pes), an index of Ppl,L and gastric pressure (Pga), an index of Pab, were measured using catheter balloon systems. Pdi was measured by electronic subtraction of Pes from Pga. A respiratory inductance plethysmograph (Respitrace™, Ambulatory Monitoring Inc.) operating in the DC mode was used to obtain a signal proportional to the cross-sectional area of the rib cage at the levels of the nipples and the xiphoid cartilage (Arc,pul and Arc,ab respectively). During measurement of the insertional component of Pdi, the anterior-posterior abdominal dimension was measured using a pair of linearized magnetometers (Peterson) with the coils positioned just superior to the level of the umbilicus. Flow was measured using a pneumotachograph (Fleish No. 3) and a differential pressure transducer (Validyne MP 45 + 2cm H_2O). Inspired and expired volume were obtained by electronic integration of the flow signal. An esophageal electrode was used to record the rectified integrated diaphragmatic electromyogram (EMG) to assist in identifying relaxation conditions. Signals were recorded on an 8 channel strip chart recorder and through an analogue-digital converter board (Data Translations DT2821) to a desktop computer at 1 KHz per channel. The signals were later plotted (see below) and calculations performed graphically as illustrated in figures 3-5. During the experiments Pes, Pga, Arc,pul and Arc,ab were plotted against each other as required on a storage oscilloscope

(Techtronics 5103N) and recorded photographically for later reference. Bilateral transcutaneous phrenic nerve stimulation was performed using a stimulating unit (TECA Co. Pleasantville, NY.). Diaphragmatic mass action potentials were recorded during the stimulations from surface electrodes placed on the lower costal margin and in the 5th intercostal space bilaterally.

Procedures: Relaxation Relationships: At the beginning and end of each study protocol, subjects performed 3 to 5 relaxed expirations against a high alinear expiratory resistance after having inspired to a lung volume near total lung capacity (TLC). To evaluate the mechanical linkage between RCpul and RCab at lung volumes near functional residual capacity (FRC), relaxation curves below FRC were obtained by having the subjects expire to residual volume (RV) and passively inspire against a high alinear resistance attached to the inspiratory limb of the Hans-Rudolf valve. Relaxation was judged adequate if Pdi remained zero above FRC, Pes and Pga returned smoothly and reproducibly to their static equilibrium pressures, the relationships between Pes and Arc,pul and between Pab and Arc,ab were reproducible from manouevre to manouevre and the diaphragmatic EMG remained silent. The relaxation relationships among Pes, Pga, Arc,pul and Arc,ab were compared before and after each study to ensure that no change in experimental conditions had occurred which may have altered these relationships.

Assessment of the mechanical linkage between RCpul and RCab: The mechanical linkage between RCpul and RCab was assessed during isolated diaphragmatic contraction produced by bilateral transcutaneous phrenic nerve stimulation. We wished to examine the interaction between the two compartments over a wide range of distortions, therefore, variation in twitch intensity

was accomplished in 3 ways 1) single twitches at supramaximal voltage (stimulus duration = 1 msec) relying on the natural variability in the the intensity of contraction which accompanies changing lung volume (35); 2) paired twitches separated by 0.1 to 0.05 seconds (10-20 Hz, stimulus duration = 1 msec) allowing varying degrees of summation and therefore varying contraction intensities; and 3) in some subjects, single submaximal twitches during which the voltage outputs to each side were adjusted independently to maintain the mass action potentials in constant proportion and so produce symmetrical low intensity contractions. All stimulations were applied during relaxation (Pdi =0, silent diaphragmatic EMG) against an occluded airway at lung volumes between FRC and 1 litre above FRC (over which range the relaxation relationship between Arc,pul and Arc,ab was linear in all subjects). Pdi was measured and distortion and Plink were calculated for each stimulation as described below and illustrated in figure 3. The curves, passing through the origin, which best described the relationships between Pdi and distortion and between distortion and Plink, were then generated for each subject. Only when stimulation resulted in a diaphragmatic mass action potential did the esophageal pressure change, suggesting that the diaphragm was the only inspiratory muscle significantly activated by this procedure.

Assessment of the contribution of the rib cage muscles to inspiration: After the pattern of ventilation had stabilized on the mouthpiece and without forewarning the subjects, 10 consecutive spontaneous breaths were recorded and ensemble averaged. Rib cage distortion at the end inspiratory point of zero flow was calculated by comparison with the relaxation curve. From this measurement and the relationship between distortion and Plink, Plink and Prcm were calculated for each of 5 subjects as described below and illustrated in figure 4.

Calculation of the insertional component of transdiaphragmatic pressure: The relaxation relationships between Arc,ab and Arc,pul and between Pga and abdominal displacement were recorded on the storage oscilloscope. The subjects were then asked to inspire through the mouthpiece while maintaining these relationships in their relaxation configuration by targetting to the curves displayed on the oscilloscope screen. Maintaining relaxation of the abdominal muscles was important to ensure that abdominal muscle contraction did not influence the relationship between Pga and Arc,ab. In practice most subjects conformed to this pattern naturally (ie: did not contract their abdominal muscles during inspiration) as has been described previously (21) and the plots served only as a check on adequate performance of the manouevre. After a practice period, when the subjects were able to inflate the rib cage without distorting it and without contracting the abdominal muscles. 5 efforts of the same inspired volume were recorded and ensemble averaged. The insertional component of Pdi was calculated at 5 equal intervals between FRC and the maximum volume inspired during the manoeuvres for each of 5 subjects as described below and illustrated in figure 5.

Data Analysis: In figure 3 the relationships, in one of the subjects, between Arc,ab and Arc,pul during relaxation (left panel) gives the undistorted configuration of the rib cage. The relationship between Pes and Arc,pul during relaxation (right panel) gives Prc,pul as a function of Arc,pul. Deviation from the relaxation relationships during an isolated diaphragmatic contraction are also illustrated.

In the left panel of figure 3 displacements off the relaxation line for RCpul and RCab indicate distortions. These distortions, expressed in arbitrary units, were measured as the shortest

(ie: perpendicular) distance to the relaxation line from the point at which the change in Arc,pul was maximal (ie: the end of the twitch). This allowed measurements of distortion within an individual but did not allow comparisons between individuals.

In the right panel of figure 3 Plink is estimated. If Ppl,L (as estimated by Pes) had been the only agency acting on RCpul during the twitch Arc,pul would have decreased along its relaxation pressure-area relationship with Arc,ab to point A. The fact that Arc,pul decreased only to point B is due to the restoring force represented by Plink so that the net deflating pressure (Prc,pul) was less than would occur in the absence of mechanical coupling between the rib cage compartments. According to equation 1, because Prcm is zero Plink is given by: As Prc,pul (distance DC) - Ppl,L (distance DB) = distance BC. The relationship between Plink and distortion was obtained by plotting our arbitrary measure of distortion against Plink. This assumes that Plink is independent of the pathway by which a given distortion was reached. Similarly the distortability of the rib cage was obtained by plotting our index of distortion against Pdi.

In figure 4 the relationships between Arc,pul and Arc,ab and between Pes and Arc,pul during a spontaneous breath compared to relaxation are shown. As illustrated in the left panel of figure 4, distortion was measured at end-inspiration. Using our calibration curve Plink was then calculated.

In the right panel of figure 4, the relationship between Pes and Arc,pul is shown during spontaneous breathing and relaxation. In this instance, Arc,pul increased even though Ppl,L became more negative because of the combined action of Plink and the pressures developed by the rib cage muscles. We know the total pressure acting on RCpul (Prc,pul) as the distance BC

and the change in Pes as the distance BA, therefore, since $P_{rc,pul} = P_{es} + P_{rcm} + P_{link}$, Prcm was calculated as the distance AC minus Plink.

For the calculation of the insertional component of Pdi (xPdi) we plotted Pga vs Arc,ab during inspirations in which Plink was zero and the abdominal muscles were relaxed. An example is shown in figure 5. Since the change in Pga during active inspiration could not account for all of the change in Arc,ab there must have been another agency inflating the rib cage which we took to be the insertional component of Pdi. This was measured as the distance AB in figure 5.

Results:

Mechanical linkage between RCpul and RCab: The relationships between distortion and Plink and between Pdi and distortion are illustrated for each of 5 subjects in figures 6 and 7. In all subjects isolated diaphragmatic contraction resulted in displacement of Arc,pul and Pes significantly off of their relaxation line resulting in a positive value for Plink. This indicates a significant resistance to bending between RCpul and RCab in humans. The curve relating Pdi and distortion indicates that the rib cage becomes progresssively more difficult to distort with increasing distortion. As a result the increment in restoring force (represented by Plink) for a given increase in distortion increases progressively with increasing degrees of distortion. It should be realized that our arbitary index of distortion does not allow comparison of distortability between individuals. Changes within an individual can, however, be estimated.

Calculation of the pressures developed by the rib cage muscles to spontaneous inspiration: All subjects demonstrated some deviation from the relaxation relationship between Arc,pul and Arc,ab during quiet breathing. In all subjects this distortion was within the range over which the relationship between distortion and Plink was assessed.

The values for Prcm and Plink and their values as a fraction of the total pressure required to both inflate the lung and displace RCpul are presented in Table 1. On average, Plink and Prcm contributed equally to this pressure.

Calculation of the insertional component of transdiaphragmatic pressure: Pdi,ins is plotted against the volume at which it was measured in each of 5 subjects in figure 8. In figure 9 these are expressed as a fraction of the total Pdi. With increasing volume, and increasing Pdi, the magnitude of the insertional component of Pdi increased. The fraction of the total Pdi which

comprised the insertional component, however, remained approximately constant overall. The insertional component of Pdi was significant and represented 33 + 10SE percent of total Pdi when averaged over all lung volumes in all subjects.

Discussion

Comparison with other approaches: Early analyses of chest wall motion (6,39) assumed the displacements of the abdomen to be attributable to the diaphragm, the rib cage to RCM, and treated the chest wall as a two compartment system. While the first two assumptions are untenable (21,25,27,28) the third has proven useful. Konno and Mead (25) presented evidence that the rib cage and abdomen behaved as compartments each with a single degee of freedom within fairly narrow limits of respiratory effort. To the extent that these limits are observed, the volume changes of each compartment can be described from knowlege of changes in a single dimension of the rib cage and abdomen. This was a major advance in the study of respiratory kinematics and in addition allowed measurement of the elastic properties of rib cage and abdomen. The limitations of this approach, however, have long been recognized. Crawford et al (11) found the cross-sectional areas of the upper (axilla) and lower (lower costal margin) rib cages to move during quiet breathing in close, but not exact, approximation to their to their relaxation relationship . McCool et. al. (31) used linearized magnetometers to monitor the relative anterior-posterior displacements of the upper (angle of Louis) and lower (5th rib) rib cages. They found that while during quiet breathing the relationship between these two diameters described a curve close to that during relaxation, the system was easily distorted by changing the muscle groups recruited during inspiration. Isolated contraction of the diaphragm during diaphragm pacing does not drive the rib cage on its passive characteristic (12). Recently, electromyographic studies have confirmed that the parasternal intercostal muscles become active during all but the smallest volume changes and that the absence of RCM activation alters the inspiratory configuration of the rib cage (15,18,33). It is apparent,therefore, that further insights

into the nature of inspiratory muscle action reguire additional sophistication.

Primiano (32) developed a mathematical model of the chest wall which incorporated a factor to account for changes in the action of the diaphragm on the rib cage due to varying degrees of rib cage flexibility. While abie to describe normal and paradoxical breathing patterns, no estimates of the flexibility of the rib cage or any method of determining it was proposed. Agostoni and D'Angelo proposed division of the rib cage into pulmonary and abdominal apposed compartments (1). This concept was incorporated into a mathematical model by Ben-Haim and Saidel (5). Their analysis of chest wall mechanics in adult humans, however, assumes a rigid rib cage (3,4). Their consideration of the diaphragm as single muscle interacting with the rib cage only through its effect on abdominal pressure also limits the application of their model since the costal part possesses an action distinct from that of the crural part attributable to its direct insertion on the rib cage (16).

In dogs, Jiang et al. (23) developed a 2 compartment rib cage model upon which ours is based. They demonstrated that during isolated diaphragm contraction the relationship between Arc,pul and Ppl,L and between Arc,ab and Pab fell close to their respective relaxation lines. These findings indicate that in dogs there is little resistance to bending between rib cage compartments. The loose mechanical coupling between pulmonary and abdominal rib cage compartments in dogs was confirmed by Krayer et. al. (26) who, using computed tomography to create a dynamic reconstruction of the motion of the chest wall, found that diaphragm contraction contributed nothing to the volume displaced by the lung apposed rib cage.

In the current paper we present a more comprehensive model than previously proposed which maintains the dual nature of diaphragmatic action, and whose power to represent the

behaviour of the chest wall is enhanced by incorporation of a two compartment rib cage. Our experimental results emphasize the importance in humans of determining the forces of interaction between compartments in predicting the behaviour of the chest wall under any given set of experimental conditions. Thus, while as in previous studies (11,31) the observed deviation of Arc,pul and Arc,ab from their relaxation line during quiet breathing may be small, the importance of this distortion depends on the degree of coupling between compartments. In contrast to previous findings in dogs (23,26), we have found in humans that this coupling is sufficiently tight that the small distortions accompanying a spontaneous breath contributed significantly to the inflationary force which is transmitted via the pulmonary rib cage to the lung. These results indicate a major difference between the two species in chest wall function and therefore in the mechanical interactions between the respiratory muscles.

By measuring the insertional component of Pdi, we have divided the diaphragm's action on the rib cage functionally rather than anatomically, ie: into that part which acts through the diaphragmatic insertions on the costal margin and that which acts through transmission of pressure across the area of rib cage apposition. Jiang et. al. (23) found in dogs that isolated diaphragm contraction displaced the lower rib cage close to its relaxation relationship with Pab and concluded that the majority of the diaphragm's action on the rib cage is attributable to its effect on abdominal pressure so that the insertional component of Pdi is small. In addition to the differences in species which may account for the difference between their results and ours, the maneoeuvre performed by our subjects in assessing the insertional component of Pdi was not a spontaneous breath but an inspiration during which rib cage configuration was fixed by active contraction of the muscles of the upper rib cage.

Critique: Although the 2 compartment rib cage model allows estimates of parameters that have not previously been measurable this approach contains assumptions whose limitations must be considered. In reality the rib cage is continuous and therefore consists of an infinite number of compartments each able to change shape along any diameter. Our simplification of this complex structure to two compartments whose motion is fully described by changes in their cross sectional areas allows us to limit the number of degrees of freedom and permits the development of equations describing its behaviour.

In dividing the rib cage we ignore any action of the intercostal and levatores costae muscles on RCab. Their action on RCpul is included with that of other inspiratory RCM. DeTroyer et. al. (19) showed that when contracting alone in a single interspace, both sets of intercostal muscles could produce an inspiratory displacement of the ribs depending on the relative impedances of the rib cage to caudal and cephalad motion. Except during increased chemical drive, however, the internal intercostal muscles in humans are active only during expiration (24). During spinal cord stimulation in dogs Budzinska et. al. (9) found that sectioning of the parasternal and external intercostals eliminated inflation of the rib cage despite activation of the remaining internal intercostals. They also found the inflationary effect of the external intercostal muscles to decrease caudally. DeTroyer et. al. (20) found that even in the cranial interspaces most of the shortening the external intercostal muscle could be attributed to the simulatneous contraction of the parasternal. Others have found in humans that the external intercostals in the lower intercostal spaces are inactive during quiet breathing below the 4th interspace but that these muscles became active late in inspiration with increasing ventilation (24,36,42). Therefore, although the external intercostals, inserting, on RCab may become active

at increased levels of ventilation and may limit application of our model under these conditions, they are unlikely to have had an important influence on our results during quiet breathing or slow inspiratory manouevres. Litle information is available on the levatores costae muscles during quiet breathing in humans.

Our model as illustrated in figures 1 and 2 makes no provision for the action of the abdominal muscles on RCab although this is taken into account in euqation 2. In the current study as in the study of Goldman et. al. (21) the abdominal wall was displaced along its passive characteristic with regard to Pab during quiet breathing. We ensured abdominal muscle relaxation during manouevres other than quiet breathing by continuously monitoring this relationship. Therefore, any effect of the abdomen on displacement of RCab would have been due to passive coupling. Deschamps et. al. (14) have found such coupling to be small and we, like many others, neglect it.

The anatomical limits of RCpul and RCab are continuously changing as the area of apposition changes with posture and degree of diaphragmatic shortening. To a large extent the rationale for dividing the rib cage into pulmonary and abdominal components is fortuitous. At FRC the important rib cage inspiratory muscles act above the area of apposition and the costal part of the diaphragm originates from ribs into which the parasternal and scalene muscles do not insert. This distinction becomes blurred at low lung volumes when the area of apposition extends into the "pulmonary" rib cage, and at high volumes when Ppl,L acts on the "abdominal" rib cage. Our use of the model therefore strictly applies only over a limited range of lung volumes.

We represent the mechanical coupling between RCpul and RCab by a spring in figure 1 and as a pressure generator (equivalent to a muscle) in figure 2. Obviously, the mechanical

coupling between the two rib cage compartments does not have its own inherent energy source. This must be supplied by external agencies, namely the mucles which produce rib cage deformations. It should be kept in mind that the generator in figure 2 requires an external source.

In our application of the model to analysis of the motion of the human rib cage, we assume that the relationship between pleural surface pressure at the level of the plethysmograph band and the midesophageal pressure is constant during relaxation, isolated diaphragm contraction and spontaneous inspiration. While regional differences in pleural pressure swings are known to occur (8,22) and to be influenced by the muscle groups contributing to inflation, these mostly affect the craniocaudal pressure distribution. Since the distortions and pressure swings during our measurements were relatively small (of the same order of magnitude as those during spontaneous breathing) we feel that the use of midesophageal pressure is a reasonable best estimate.

Similarly, we use the changes in gastric pressure to estimate the pleural pressure swings in the area of diaphragmatic apposition. Decramer et. al. (13) have demonstrated regional variation in intraabdominal pressure during separate contraction of the costal and crural parts of the diaphragm. Since under all conditions in the current study both parts of the diaphragm contracted simultaneously and symmetrically such pressure gradients should be small. Pleural pressure in the area of apposition has been demonstrated, on average, to approximate that of abdominal pressure although at individual points in the area of apposition there can be considerable random variation (29,38). On balance the available evidence supports our use of Pab as an approximation of the Ppl,ap.

Marginot-Lagarde et.al. (30) found that the output of the respitrace inductance plethysmograph for ellipses and rectangles was a function of cross sectional area but could also be influenced by changes in shape. In our studies, the changes in cross sectional area of the rib cage were small in proportion to the total area so that the changes in AP and lateral dimensions as a proportion of the total magnitude of these dimensions would be correspondingly small. For this reason we neglected the change in the ratio of these dimensions, and the error so induced. Newer Respitrace™ models have subsequently shown good correlation between cross-sectional area and inductance plethysmograph output over the physiologic range of areas and shapes (40).

We have assessed the distortability of the rib cage during diaphragmatic twitches. Since the time to peak transdiaphragmatic pressure following a single supramaximal phrenic nerve stimulation is approximately 50 msec with similar time courses for both pleural and abdominal pressure changes, the frequency responses of the devices used in measurement and of the chest wall itself become important variables. We performed power spectral analysis of the esophageal pressure change during such stimulations in one subject. The peak of this function was at 9 Hz with dissipation of 99% of the signal at 15 Hz. The frequency response of our pressure transducers (Validyne MP45 + 200 cmH_2O) is flat to 60 Hz (10). The frequency response of the Respitrace™ has been evaluated to 32 Hz (7) and was flat over that range.

All of the twitches in this study were performed during airway occlusion. Under these conditions the time constant of the respiratory system is the product of the compliance of the respiratory system and its contained air and the the resistance of the tissues of the chest wall and lung. Assigning a value for respiratory system compliance of 0.1 l/cmH_20, for gas compliance of $0.0014/cmH_20$ and a respiratory system resistance of $3cmH_20/lps$ yields a time constant for

the respiratory system response to phrenic shocks of approximately 4.5 msec. As the time for maximum pressure deveopment is at least 10 times this amount, there was adequate time for full respiratory system response to phrenic twitches.

Predictions Arising from the Model: Under conditions when the area of apposition becomes small or non-existant, Plink should approach zero because the force acting on RCab will decrease. proportionately to the decrease in area over which Pab acts. Such states include hyperinflation, pneumothorax and pleural effusion. Under these circumstances our model predicts that the burden of inflating RCpul will be placed on RCM. Since dyspnea appears to be related to the activation of RCM (34,41), this may have important implications in the symptomatology of these conditions.

Our model also predicts that a similar situation exists when the mechanical coupling between RCpul and RCab is very loose. This situation may exist in infants (37), some animals (23) and in flail chest. When this happens RCM recruitment is essential to prevent inward rib cage displacement.

Our findings suggest that the insertional component of diaphragmatic action is not trivial in man. Zocchi et. al. (43) have shown changes in mechanical coupling between costal and crural parts of the diaphragm during hyperinflation and with substitution of abdominal viscera with an equal volume of fluid. These changes are related to changes in orientation of diaphragmatic fibers and distribution of abdominal pressure over the inferior surface of the diaphragm. Equalization of abdominal pressure changes by ascites should improve the insertional component of Pdi in that the forces generated by crural contraction is transmitted to the costal diaphragm and crural shortening should then contribute to rib cage expansion (28).

In contast to the previous model, RCM and diaphragm in the present model are pneumatically and electrically in parallel (figure 2). Thus, in principle the tidal volume can be partitioned into a component due to RCM contraction and that due to diaphragmatic contraction. The quantification of the volume changes attributable to each muscle group, however presents difficulties because it requires estimates of the changes in lung volume attributable to both Plink and the insertional component of Pdi. It is not clear how these volume changes can be calculated.

References:

1. Agostoni E, D'Angelo E, Statics of the chest wall. In The Thorax Part A. pp 259-295 Eds. C Roussos & PT Macklem. Vol 29. Lung Biology in Health, Marcel Dekker Inc. New York, 1988

2. Agostoni E, Zocchi L, Macklem PT,. Transdiaphragmatic pressure and rib motion in area of apposition during paralysis. J Appl Physiol 65: 1296-1300, 1988

3. Ben-Haim SA, Lichtenstein O, Saidel GM, Mechanical analysis of extrapulmonary volume displacements in the thorax and abdomen. J. Appl. Physiol. 67:1785-1790, 1989

4. Ben-Haim SA, Saidel GM, Chest wall mechanics: Effects of acute and chronic lung disease, J. Biomechanics 22:559-564, 1989

5. Ben-Haim SA, Saidel G, Mathemmatical model of chest wall mechanics: A phenomenological approach. Annals of Biomedical Engineering, 18:37-56, 1990

6. Bergofsky EH, Relative contributions of the rib cage and the diaphragm to ventilation in man. J. Appl. Physiol. 19:698-706,1964

7. Boynton BR, Glass G, Frantz ID, Fredberg JJ, Rib cage vs abdominal displacement in dogs during forced osciliation to 32 Hz. J. Appl. Physiol. 67:1472-1478, 1989

8. Brown R, Scharf SM, Ingram R, Nonhomogeneous alveolar pressure swings: effect of different respiratory muscles. J. Appl. Physiol. 52:638-641, 1960

9. Budzinska K, Supinski G, DiMarco AF, Inspiratory action of separate external and parasternal intercostal muscle contraction. J. Appl. Physiol. 67:1395-1400, 1989

10. Butler JP, Leith DE, Jackson AC, Principles of measurement: applications to pressure, volume and flow. Handbook of Physiology - The Respiratory System III. Ch.2, p 15-33, Ed. 1987, Waverly Press Inc., Baltimore, Md. 21202

11. Crawford ABH, Dodd D, Engel LA, Changes in rib cage shape during quiet breathing, hyperventilation and single inspirations. Respiration Physiol. 54:197-209, 1983

12. Dannon J, Druz WS, Goldberg NB, Sharp JT, Function of isolated paced diaphragm and the cervical accessory muscles in C1 quadraplegics. Am. Rev. Respir. Dis. 119:909-919, 1979

13. Decramer M, DeTroyer A, Kelly S, Zocchi L, Macklem PT, Regional differences in abdominal pressure swings in dogs. J. Appl. Physiol. 56:1682-1687, 1984

14. Deschamps C, Rodarte JR, Wilson TA, Coupling between rib cage and abdominal compartments of the relaxed chest wall. J. Appl. Physiol. 65:2265-2269, 1988

15. DeTroyer A, MG Sampson, Activation of the parasternal intercostals during breathing efforts in human subjects. J Appl Physiol 52: 524-529, 1982

16. DeTroyer A, Sampson M, Sigrist S, Macklem PT, Action of costal and crural parts of the diaphragm on the rib cage in dog. J. Appl. Physiol. 53:30-39, 1982

17. DeTroyer A and M Estenne. Coordination between rib cage muscles and diaphragm duirng quiet breathing in humans. J Appl Physiol 57: 899-904, 1984

18. DeTroyer A, Estenne M, Coordination between rib cage muscles and diaphragm during quiet breathing in humans. J Appl Physiol 57: 899-904, 1984

19. DeTroyer A, Kelly S, Macklem PT, Zin WA, Mechanics of intercostal space and actions of external and internal intercostal muscles. J. Clin. Invest. 75:850-857, 1985

20. DeTroyer A, Farkas GA, Linkage between parasternals and external intercostals during resting breathing. J. Appl. Physiol. 69:509-516, 1990

21. Goldman MD, Mead J, Mechanical interaction between the diaphragm and rib cage. J. Appl. Physiol. 35:197-204, 1973

22. Irvin CG, Sampson M, Engel L, Grassino AE, Effect of breathing pattern on esophageal

pressure gradients in humans. J. Appl. Physiol. 57:168-175, 1984

23. Jiang TX, Demedts M and Decramer M. Mechanical coupling of upper and lower cannine rib cages and its functional significance. J Appl Physiol 64: 620-626, 1988

24. Koepke GH, Smith EM, Murphy AJ, Dickinson DG, Sequence of action of the diaphragm and intercostal muscles during respiration. I. Inspiration. Arch Phys. Med. Rehabil. 39:426-430, 1958

25. Konno K, Mead J, Measurement of separate volume changes of rib cage and abdomen during breathing. J. Appl. Physiol. 22: 407-422, 1967

26. Krayer S, Decramer M, Vettermann J, Ritman EL, Rehder K, Volume qauantification of chest wall motion in dogs. J. Appl. Physiol. 65:2213-2220, 1988

27. Loring SH, Mead J, Action of the diaphragm on the rib cage inferred from a force balance analysis. J Appl Physiol 53: 756-760, 1982

28. Macklem PT, Macklem DM, DeTroyer A, A model of inspiratory muscle mechanics. J Appl Physiol 55:547-557, 1983

29. Macklem PT, Zocchi L, Agostoni E, Pleural pressure between diaphragm and rib cage

duirng inspiratory muscle activity. J Appl Physiol 65: 1286-1295, 1988

30. Marginot-Lagarde P, Sartene R, Mathieu M, Durand G, What does inductance plethysmography really measure. J. Appl. Physiol. 64:1749-1756, 1988

31. McCool FD, Loring SH, Mead J, Rib cage distortion during voluntary and involuntary breathing acts. J. Appl. Physiol. 58:1703-1712, 1985

32. Primiano FP, Theoretical analysis of chest wall mechanics. J. Biomechanics. 15:919-931, 1982

33. Sampson MG, DeTroyer A, Role of intercostal muscles in the rib cage distortions produced by inspiratory loads. J. Appl. Physiol. 52:517-523, 1982

34. Sharp JT, Drutz WS, Moisan T, Foster MT, Machnack W, Postural relief of dyspnea in severe chronic obstructive pulmonary disease. Am. Rev. Respir. Dis. 122:201-210, 1980

35. Smith J, Bellemare F, Effect of lung volume on twitch contraction intensity during phrenic nerve stimulation. J. Appl. Physiol., 1988

36. Taylor A. The contribution of the intercostal muscles to the effort of respiration in man. J. Physiol. Lond. 151:390-402, 1960

37. Tusiewicz K, Moldofsky H, Bryan AC, Bryan MH, Mecahnics of the rib cage and diaphragm during sleep. J. appl. Physiol. 43:600-602, 1977

38. Urmey WF, A DeTroyer, KB Kelly and SH Loring. Pleural pressure increases during inspiration in the zone of apposition of diaphragm to rib cage. J Appl Physiol 65: 2207-2212, 1988

39. Wade OL, Movements of the thoracic cage and diaphragm in respiration. J. Physiol. Lond. 124:193-212, 1954

40. Watson HL, Poole DA, Sackner MA, Accuracy of respiratory inductive plethysmographic cross-sectional areas. J. Appl. Physiol. 65:306-308, 1988

41. Ward ME, D Eidelman, DG Stubbing, F Bellemare and PT Macklem. Respiratory sensation and pattern of respiratory msucle activation during diaphragm fatigue. J Appl Physiol 65: 2181-2189, 1988

42. Whitelaw WA, Feroah T, Patterns of intercostal muscle activity in humans. J. Appl. Physiol. 67:2087-2094, 1989

43. Zocchi L, Garzaniti N, Newman, Macklem PT, Effect of hyperinflation and equalization of abdominal pressure on diaphragmatic action. J. Appl. Physiol. 62:1655-1664, 1987

Figure Legends

Figure 1

Diagram illustrating how we model the rib cage mechanically, the mechanical linkages of the rib cage muscles, the elastic properties of the respiratory system and the agencies acting to displace and distort the rib cage. For further description see text.

Figure 2

Hydraulic or electrical analogue of the mechanical model presented in figure 1. RCM = rib cage muscles, cos = costal diaphragm; CRU = crural diaphragm; AB = abdomen; S = spring linking the two rib cage compartments. Circles containing Σ are summing junctions. Other circles represent pressure or voltage generators including the spring, the source of energy for which must come from RCM, COS, and CRU. Rectangles represent structures which are displaced and which consist of elastic (capacitive), frictional (resistive) and inertial (inductive) elements. For further description see text.

Figure 3

Left Panel: Relationship between cross-sectional areas of the abdominal (Arc,ab) and pulmonary (Arc,pul) rib cages during relaxation and phrenic nerve stimulation. Distortion is the perpendicular distance from the relaxation line to the point representing the end of the twitch. Right Panel: Relationship between esophageal pressure (Pes) and Arc,pul during relaxation and phrenic nerve stimulation. Point A is the point to which Arc,pul would have decreased had there been no mechanical coupling between rib cage compartments. The net pressure acting on RCpul (Prc,pul) is the distance DC. The change in Pes is the distance DB. The inflationary pressure on RCpul resulting from the interaction between RCpul and RCab (Plink) is given by the difference between DB and DC ie: the distance BC.

Figure 4

Left Panel: Relationship between cross-sectional areas of the abdominal (Arc,ab) and pulmonary (Arc,pul) rib cages during a spontaneous breath and relaxation. Distortion was measured as the perpendicualar distance from the relaxation line to the point representing end inspiration.

Right Panel: Relationship between esophageal pressure (Pes) and Arc,pul during a spontaneous breath and relaxation. The total pressure acting on RCpul (Prc,pul) is given by the distance BC. The distance BA gives the change in Pes. The distance AC gives the sum of the pressure generated by the rib cage muscles (Prcm) and the pressure resulting from the interaction between rib cage compartments (Plink). Plink for a given distortion is known. Prcm is therefore obtained by subtracting Plink from the distance AC.

Figure 5

Relationship between abdominal pressure Pab and the cross-sectional area of the abdominal rib cage (Arc,ab) during relaxation and during inspiration while actively maintaining an undistorted rib cage. The insertional component of Pdi is given by the distance AB.

Figure 6

Relationship between distortion and the inflationary pressure exerted on the pulmonary rib cage attributable to mechanical coupling between rib cage compartments (Plink) during phrenic nerve stimulation in 5 subjects.

Figure 7

Relationship between transdiaphragmatic pressure (Pdi) and distortion during phrenic nerve stimulation in 5 subjects.

Figure 8

The insertional component of transdiaphragmatic pressure (Pdi,ins) is plotted against lung volume at which it was measured. Symbols represent different subjects.

Figure 9

The insertional component of transdiaphragmatic pressure (Pdi,ins) as a function of total transdiaphragmatic pressure (Pdi) is plotted against the lung volume at which it was measured. Symbols represent different subjects.

FIGURE 1

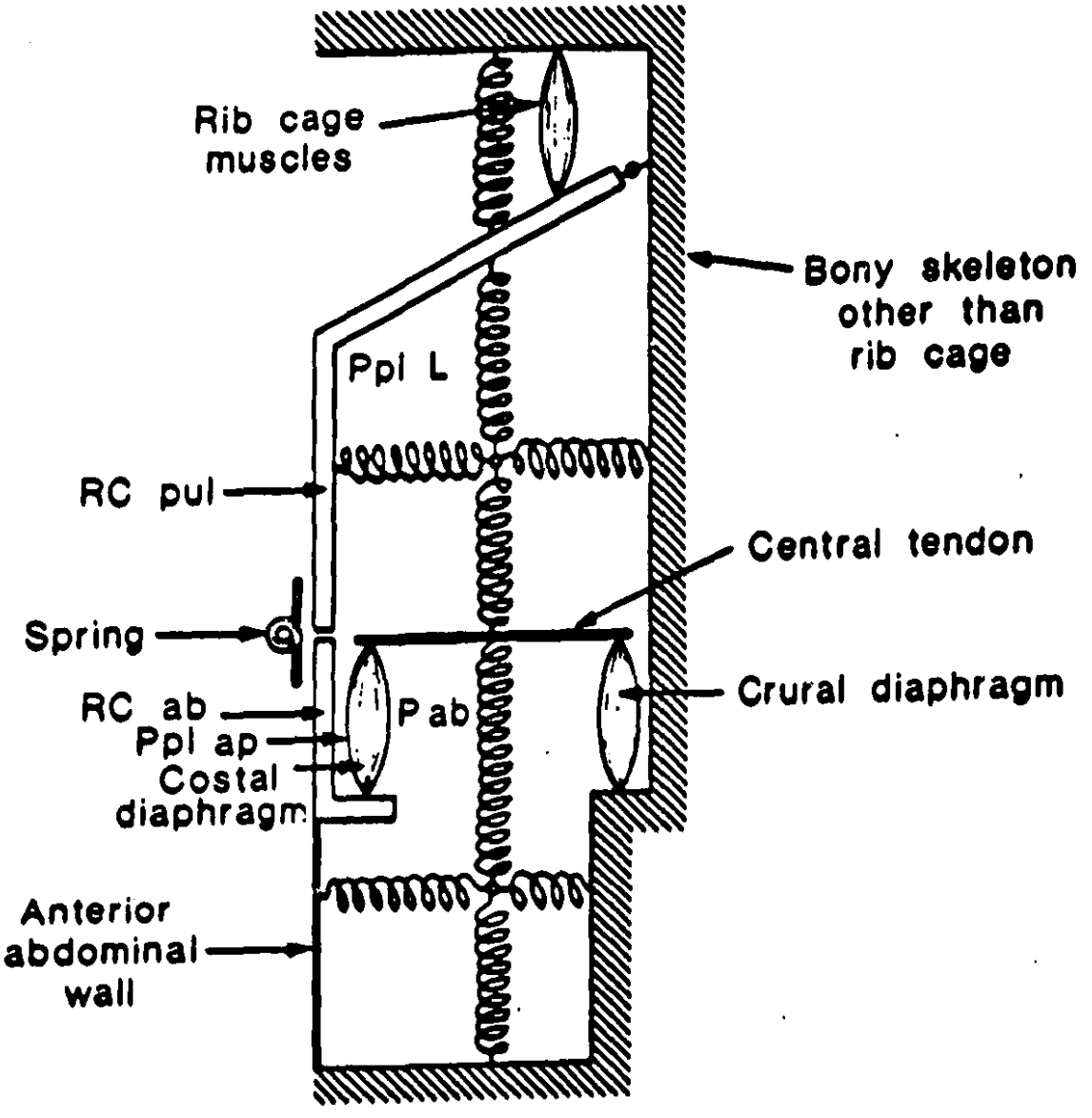
Rib cage muscles
Bony skeleton other than rib cage
Ppl L
RC pul
Central tendon
Spring
Crural diaphragm
RC ab
Ppl ap
Costal diaphragm
P ab
Anterior abdominal wall

FIGURE 2

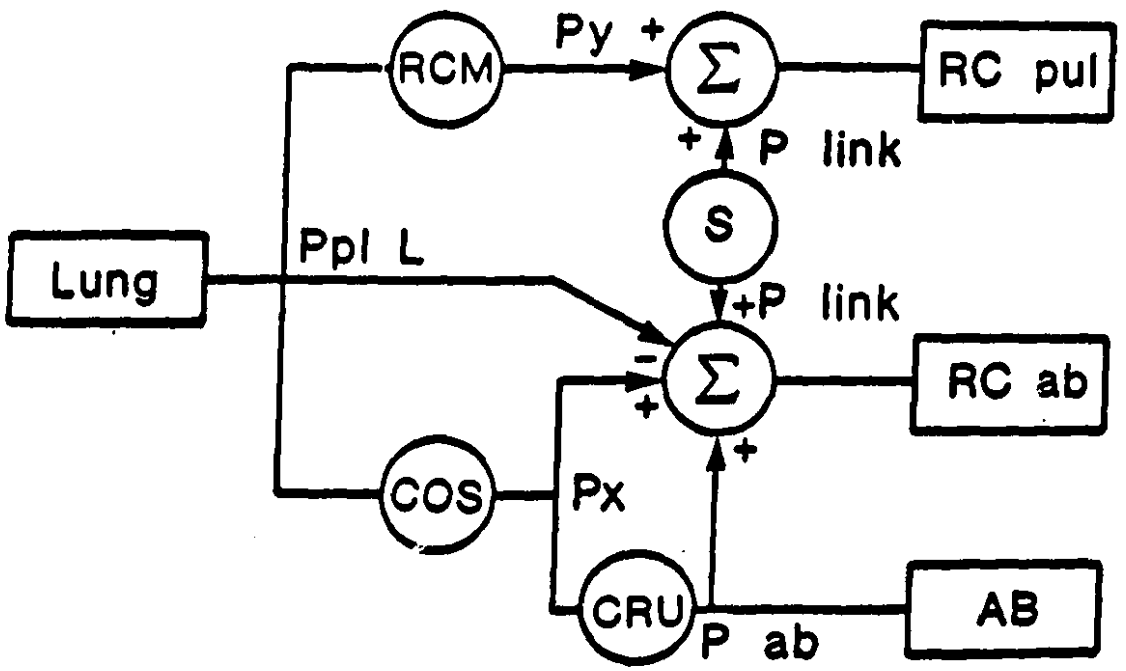

FIGURE 3

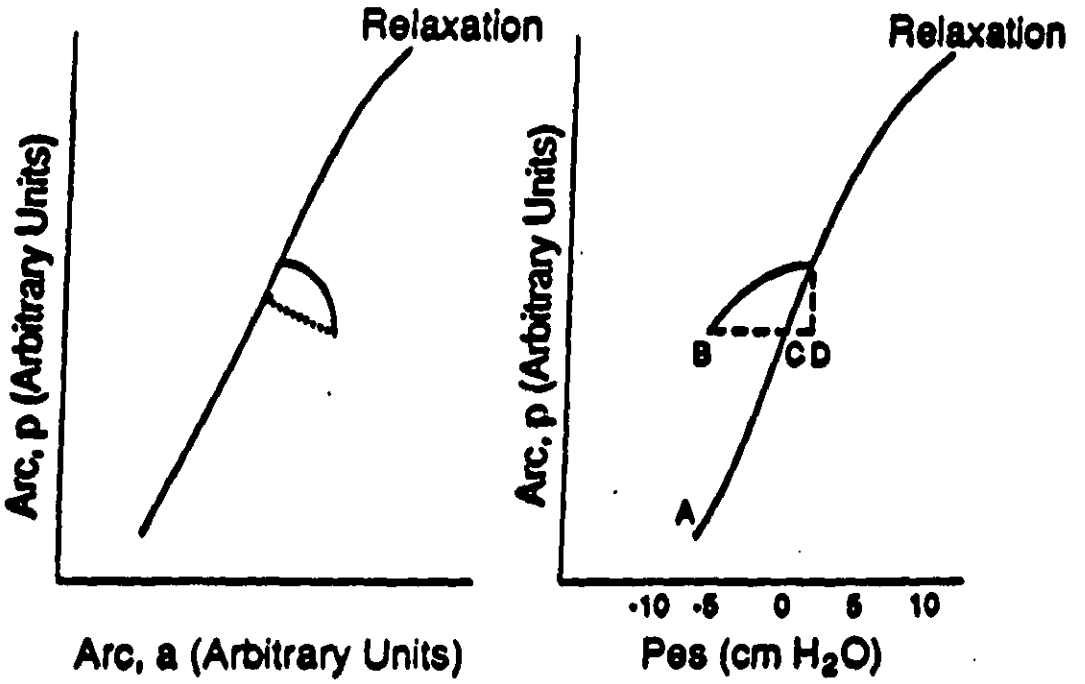
Relaxation
Arc, p (Arbitrary Units)
Arc, a (Arbitrary Units)
Relaxation
Arc, p (Arbitrary Units)
B
CD
A
-10
-5
0
5
10
Pes (cm H2O)

FIGURE 4

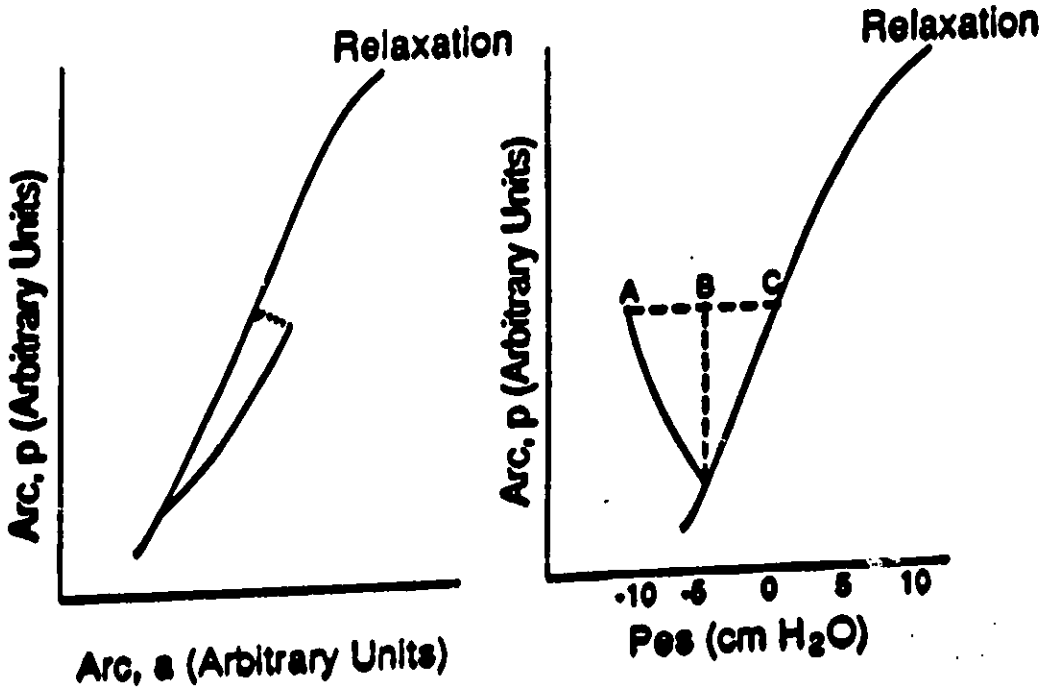
Relaxation
Arc, p (Arbitrary Units)
Arc, s (Arbitrary Units)
Relaxation
Arc, p (Arbitrary Units)
A
B
C
-10
-5
0
5
10
Pes (cm H2O)

FIGURE 5

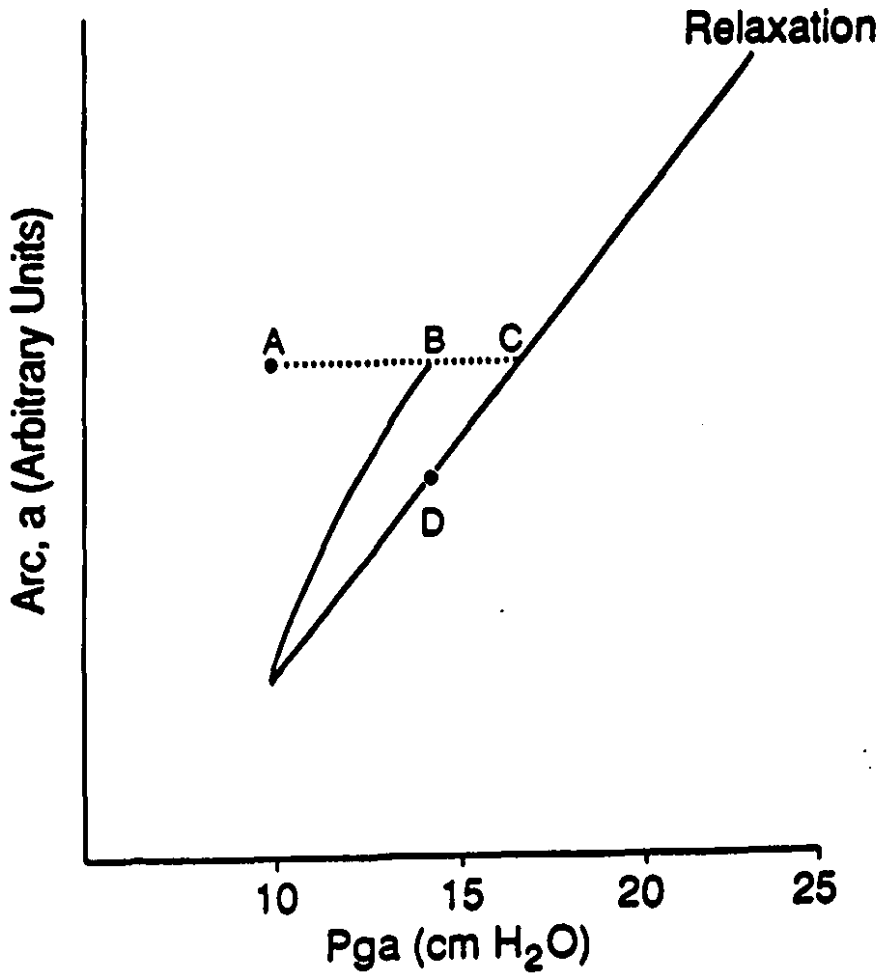

FIGURE 6

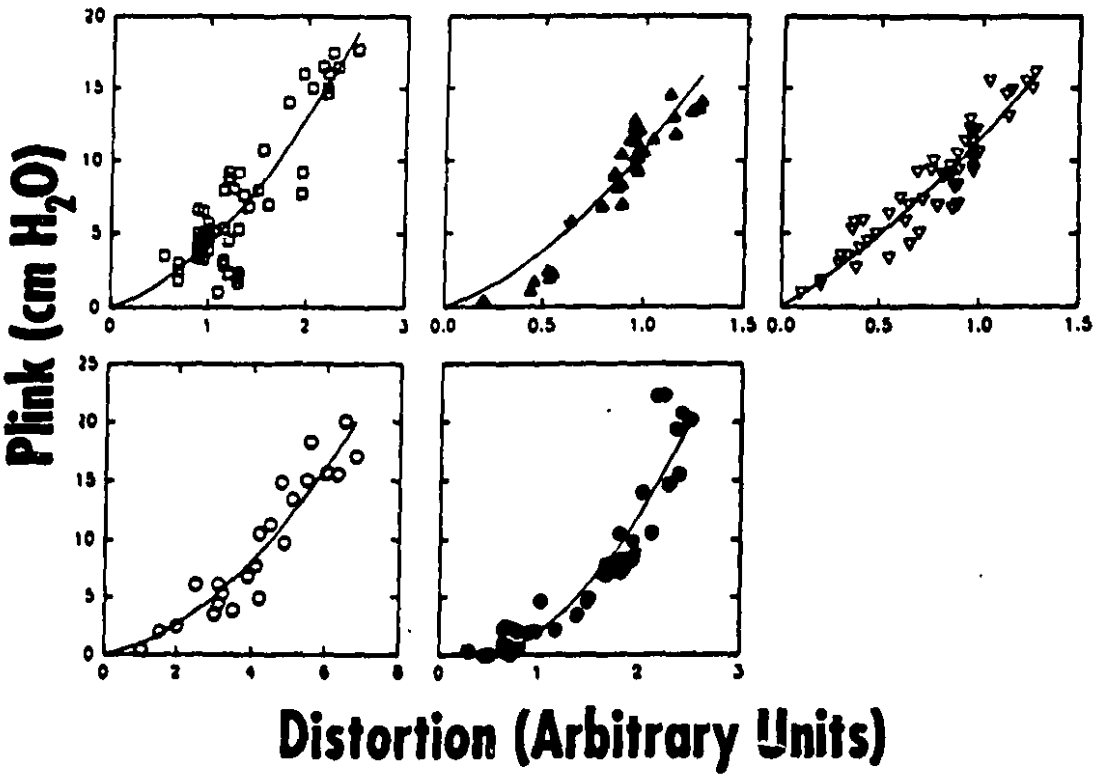

FIGURE 7

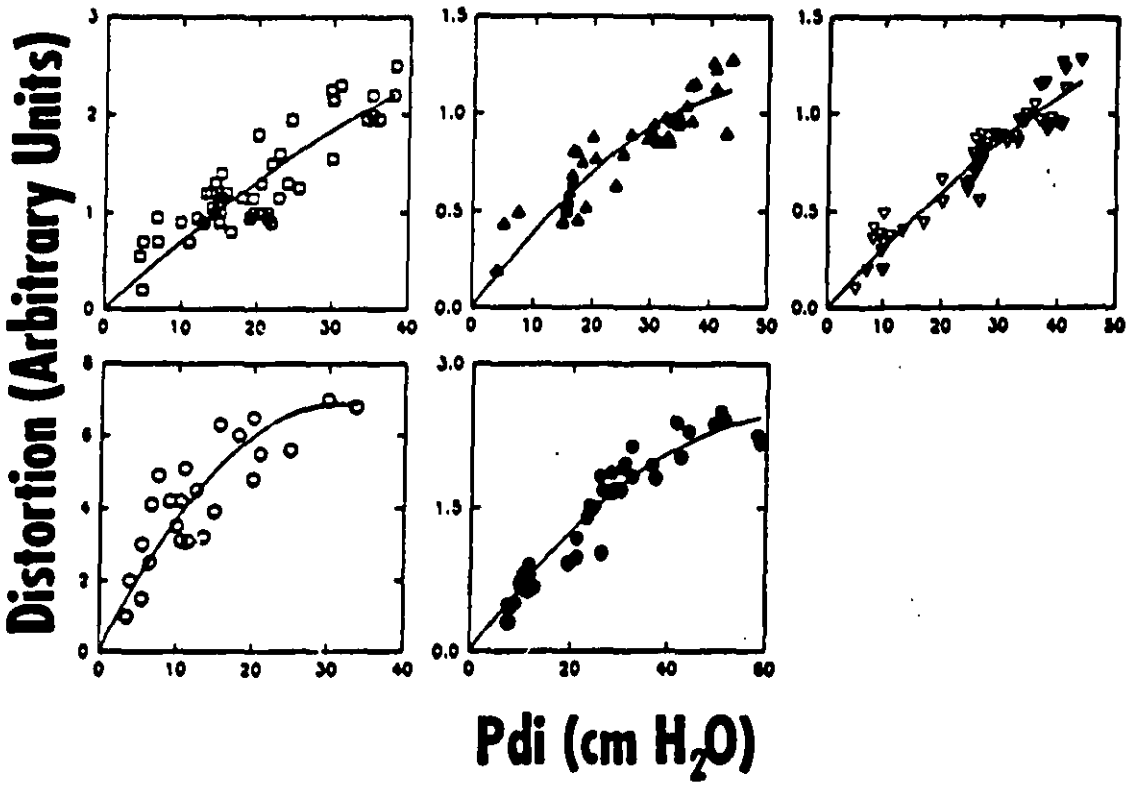

FIGURE 8

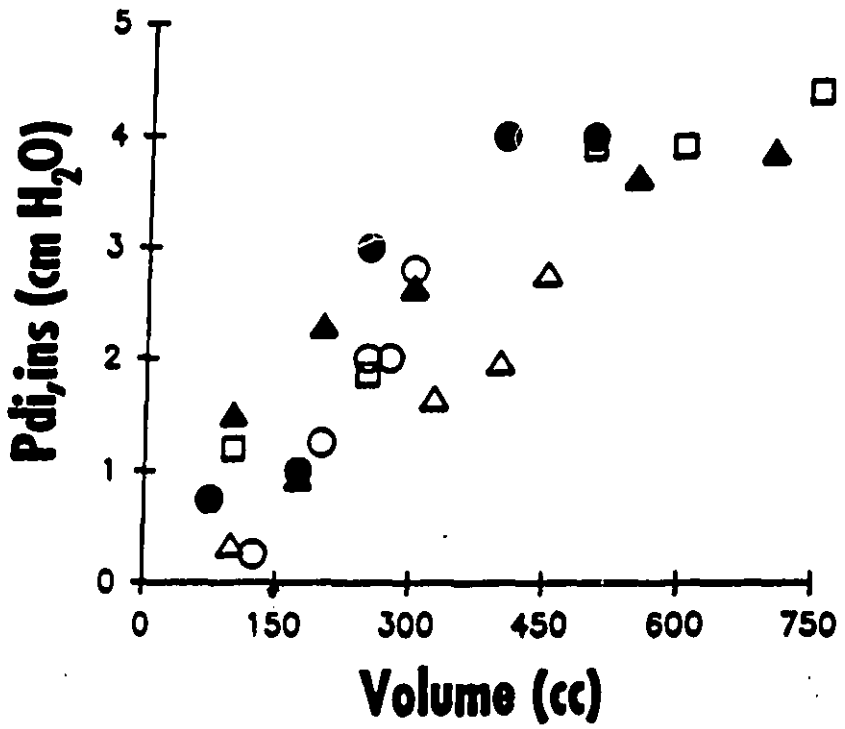

FIGURE 9

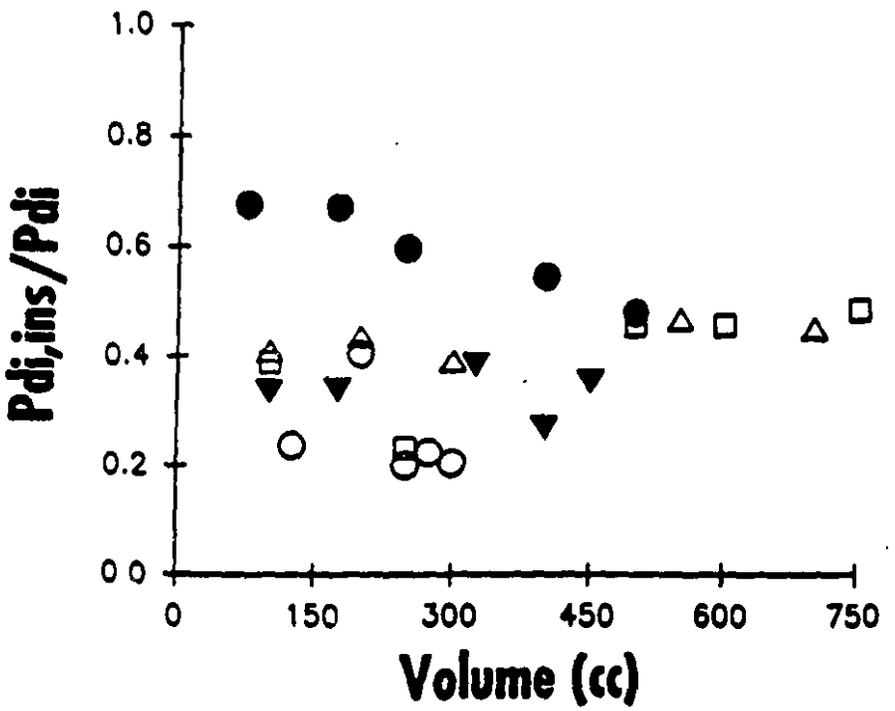

CHAPTER 3: Phrenic Afferent Modulation of Respiratory Muscle Activation

Foreword to Chapter 3

Recently, attention has focused on the functional importance of the abundant small diameter myelinated and unmyelinated afferent fibres in the phrenic nerve in the regulation of phrenic motor output. There is now overwhelming evidence that activation of these fibres elicits profound changes in the respiratory and cardiovascular systems. The study presented in this chapter evaluates the changes in minute ventilation, pattern of respiratory muscle activation and respiratory timing which occur during stimulation of small fibre phrenic afferents. The pattern of muscle activation will determine how the ventilatory load is distributed among respiratory muscle groups. For example, strong recruitment of abdominal muscles may represent a mechanism by which, through facilitation of high expiratory flow rate and reduction of diaphragmatic shortening, the diaphragm is placed at a better mechanical advantage with respect to its force-length and force-velocity characteristics. The influence of impulses arising from the diaphragm on ventilatory timing may be of even greater significance to the process of ventilatory load compensation since they will alter the velocity of diaphragm contraction and the ability of the muscle to meet its requirements for enhanced blood flow. The role of these fibres in determining the capacity to sustain spontaneous ventilation, therefore, is potentially large.

Effect of Phrenic Afferent Stimulation on Pattern of Respiratory Muscle Activation

Michael E. Ward, Alain Deschamps, Charis Roussos and Sabah N. A. Hussain
Journal of Applied Physiology 73: 563-570, 1992

ABSTRACT

Ventilation and EMG activities of the right hemidiaphragm, parasternal intercostal, triangularis sterni, transversus abdominis, genioglossus and alae nasi muscles were measured before and during central stimulation of the left thoracic phrenic nerve in 10 α-chloralose anaesthetized, vagotomized dogs. Pressure in the carotid sinuses was fixed so as to maintain baroreflex activity constant. The nerve was stimulated for 1 minute with a frequency of 40 Hz, stimulus duration of 1 msec at voltages of 5, 10, 20 and 30 times twitch threshold (TT). At 5 times TT no change in ventilation or EMGs occurred. At 10-30 times TT a progressive increase in ventilation was achieved through increases in both breathing frequency and tidal volume. This was accompanied by progressive and approximately equal increases in the activity of the diaphragm, parasternal and alae nasi muscles. The increase in genioglossus activity was much greater than that of the other inspiratory muscles. Phrenic nerve stimulation also elicited inhomogeneous activation of the expiratory muscles. Whereas the transversus abdominis activity rose progressively with increasing stimulation intensity; the activity of the triangularis sterni remained unchanged. The high stimulation intensities required suggest that activation of afferent fiber groups III and IV is involved in the response. We conclude that thin-fiber phrenic afferent activation exerts a non-uniform effect on the activities of the upper airway, rib cage and abdominal muscles and may play a role in the control of respiratory muscle recruitment.

Key Words: Phrenic Nerve, Afferents, Ventilation, Diaphragm, Respiratory Muscle Recruitment, Control of Breathing

INTRODUCTION

Activation of phrenic afferents has been shown to influence ventilatory drive and the timing of the respiratory cycle (16,18,22,25). Consequently, this pathway has been proposed as a means by which feedback from the diaphragm may modify the intensity and timing of diaphragmatic contraction (12,16). Since such changes impact on the load which must be overcome by the diaphragm and on its nutrient supply, a role has also been suggested for such reflexes in the pathophysiology of diaphragm fatigue (12,16).

Afferent inputs from peripheral skeletal muscle result in inhomogeneous activation of the chest wall muscles (13,20). If this is true of afferents in the phrenic nerve their activation may also be an important determinant of the pattern of respiratory muscle recruitment. As such they may further influence the diaphragm's function through alterations in it's configuration, shortening velocity and operating length.

In this study the changes in activation of the diaphragm and the muscles of the rib cage, abdomen and upper airway during electrical stimulation of the proximal phrenic nerve were examined in order to assess the potential for participation of phrenic afferent mediated reflexes in the control of respiratory muscle recruitment.

METHODS

Surgical Preparation: Ten mongrel dogs (weight 25.5 $\pm$ 2.8 kg, mean $\pm$ SEM) were anaesthetized initially with sodium thiopental (20 mg/kg i.v.) and then maintained with α-chloralose (60 mg/kg i.v.). Supplemental doses of α-chloralose were given as needed to eliminate jaw tone but maintain knee reflexes. This dose regimen depresses but does not eliminate the

corneal reflex. The animals were intubated with cuffed endotracheal tubes and were mechanically ventilated during the surgical procedure. Blood pressure in the descending aorta (Part) was measured using a catheter inserted through the right femoral artery. Bilateral cervical vagotomies were performed through a midline incision in the neck. This was done to eliminate the ventilatory effects of vagally mediated aortic (19) and atrial (1) baroreflex and pulmonary stretch and irritant receptor activation (9). The removal of vagal afferent inputs, however, may have resulted in reduction of the spontaneous activation of the abdominal muscles (5) (see discussion).

The rib cage was opened through a left thoracotomy in the fifth or sixth interspace and the left phrenic nerve was dissected away from the pericardium. A pair of insulated stainless steel stimulating electrodes were applied to the nerve near its exit from the diaphragm and connected through an isolation unit (Grass S1U5) to a stimulator (Grass S48). Twitch threshold (TT) was determined using single pulses of 1.0 msec duration at increasing voltage until a visible diaphragmatic twitch was elicited. The phrenic nerve was cut distal to the stimulating electrode and the thoracotomy incision was closed tightly in three layers. The left pleural space was evacuated of residual air by closed chest tube drainage. Five cmH_2O positive end-expiratory pressure (PEEP) was applied throughout the study by submersion of the expiratory line.

Carotid Sinus Preparation: Activation of baroreceptors has been shown to influence the pattern of respiratory muscle recruitment (23). In order to avoid the changes in carotid baroreceptor activity which would otherwise have accompanied the systemic pressor response to phrenic afferent stimulation (18,22) the carotid sinuses were isolated by ligating the internal carotid arteries approximately 1 cm distal to the sinus and the external carotid arteries just distal to the

lingual artery. The common carotid arteries were cannulated in the direction of the sinuses with a Y-connector. Flow through the carotid sinuses (and therefore the pressure within them) was controlled by a non-pulsatile pump with inflow from the right common carotid artery. The left common carotid artery was ligated and the pressure within the carotid sinuses (Psinus) was measured from a port on the Y-connector.

Measurements: Air flow was measured using a pneumotachograph (Fleisch No. 1) and a differential pressure transducer (Validyne MP45 $\pm$ 2 cmH_2O) connected in series with the endotracheal tube and a Hans-Rudolph valve. Supplemental oxygen was delivered through the inspiratory line as needed to maintain arterial PO_2 above 100 mmHg. Pairs of teflon coated stainless steel wire electrodes were implanted transcutaneously into the alae nasi (8 dogs) and transmucosally into the posterior paramedian portion of the genioglossus (8 dogs). Electrodes were also implanted under direct vision, after removing the skin and underlying muscles, into the parasternal intercostal muscles in the fourth or fifth intercostal space (8 dogs), into the triangularis sterni in the sixth intercostal space (5 dogs) and into the external oblique 5 to 6 cm below the costal margin in the anterior axillary line (2 dogs). A pair of fish hook electrodes (0.8 cm apart) were placed via an abdominal incision into the right costal diaphragm (8 dogs) and into the right transversus abdominis (7 dogs) midway between the costal margin and the iliac crest. The electromyographic (EMG) activity from each muscle was filtered (0.02-1 KHz) and amplified (DISA 05A0L). The signals were then full-wave rectified and integrated through an RC integrator with a time constant of 100 msec. Flow, volume, mean Part, Psinus and the integrated EMG signals were recorded on two 8 channel strip chart recorders (Graphtech Mark 8 WR3500).

Experimental Protocol: After a 30 minute stabilization period, arterial blood samples for blood gas analysis were drawn and control measurements of all variables were made during spontaneous breathing. The proximal end of the transected left phrenic nerve was then stimulated for one minute at a frequency of 40 Hz with a stimulus duration of 1 msec. Voltages were set at 5, 10, 20 and 30 times TT in random order. Stimulation at 30 times TT was performed in 7 dogs only. A 5 to 10 minute recovery period was allowed between stimulations.

Data Collection and Statistical Analysis: Mean Part, heart rate (HR, measured from the arterial pressure tracing) and mean Psinus were calculated in 10 second blocks for one minute before and during phrenic stimulation. The values obtained during the minute prior to onset of each stimulation were averaged and designated as controls. Tidal volume (V_T) was obtained by electronic integration of the flow signal. The inspiratory and expiratory times (Ti and Te, respectively) and total respiratory cycle duration (Ttot) were measured from the flow signal. Breathing frequency (f) was calculated from Ttot and minute ventilation (V_E) was calculated as the product of V_T and f. The EMG activities were taken as the peaks of the integrated signals.

Two-way analysis of variance (ANOVA, with respect to time and animals) was done to compare individual breaths during phrenic nerve stimulation with control values (mean of 5 pre-stimulation breaths). If the time effect was found significant ($p < 0.05$), we then performed Student-Newman-Keuls test for multiple comparison between the mean values of each respective time and the control values. The residual mean squares of the ANOVA and its associated number of degrees of freedom were used in the Student-Newman-Keuls test. The ventilatory response

to phrenic nerve stimulation peaked 6 to 7 breaths after the onset of phrenic nerve stimulation (figure 1). We, therefore, averaged the ventilatory variables and EMG activities of breaths 8 to 10 (designated as peak values) and compared them with control values.

RESULTS

Arterial pH, PO_2 and PCO_2 before stimulation with stimulus intensity of 5 times TT averaged 7.30 ± 0.02, 223.0 ± 7.51 mmHg and 40.6 ± 3.7 mmHg, respectively (mean ± SEM). These values were not different from those measured before stimulation at 10 times (7.29 ± 0.02, 221.1 mmHg ± 70.1 mmHg, 42.1 ± 4.6 mmHg), 20 times (7.30 ± 0.02, 182.1 ± 78 mmHg, 38.0 ± 2.7 mmHg) and 30 times TT (7.27 ± 0.02, 238.6 ± 83.5 mmHg, 43.9 ± 6.0 mmHg).

Psinus averaged 107 ± 10 mmHg, 109 ± 5 mmHg, and 107 ± 7 mmHg and 108 ± 7 mmHg (mean ± SEM) prior to stimulation at 5, 10, 20 and 30 times TT respectively. These values were maintained throughout the stimulation periods by adjusting the speed of the pump perfusing the carotid sinuses as required.

Table 1 lists the values of Part and HR during control and stimulation periods. Stimulation at 5 and 10 times TT elicited no change in either of these variables. Stimulation at 20 and 30 times TT produced a 16 % ($p < 0.05$) and 21 % ($p < 0.05$) increase in Part respectively. HR increased by 8 % ($p < 0.05$) at both of these stimulation intensities.

Figure 1 illustrates the breath by breath changes in V_E (absolute values) with increasing intensity of phrenic nerve stimulation. Control V_E before stimulation at 5, 10, 20 and 30 times TT averaged 6.15 ± 0.87, 6.81 ± 1.36, 6.73 ± 1.06 and 5.00 ± 0.86 l/min, respectively (mean±SEM). Stimulation at 5 times TT elicited no significant change in V_E compared to the

control value. In response to 10 times TT stimulation, V_E rose to levels significantly greater than control from breath 8 onward. A progressively greater increase in V_E was observed in response to phrenic nerve stimulation at 20 and 30 times TT.

Figure 2 illustrates the peak changes in V_E (percentage of control values) in response to phrenic nerve stimulation at different intensities. Stimulation at 5 times TT elicited no change in ventilation, whereas V_E rose by 31.7% ($p < 0.05$), 58.2% ($p< 0.01$) and 66.5% ($p < 0.01$) of the control value in response to stimulation at 10, 20 and 30 times TT, respectively.

Table 2 shows the control and peak stimulation values for V_T, f, Ti and Te. The changes in V_E with central phrenic nerve stimulation are the result of significant increases in both V_T and f. At stimulation intensities of 20 and 30 times TT there was a decrease in Te by 39 % ($p < 0.05$) and 53 % ($p < 0.05$) respectively, whereas Ti shortened by 13 % ($p < 0.05$) and 16.5% ($p < 0.05$), respectively.

Figure 3 illustrates the increase in peak integrated EMG activity relative to control values of the alae nasi and genioglossus muscles with increasing stimulation intensity. In all animals, phasic inspiratory activity of the alae nasi and genioglossus was evident under control conditions. Stimulation at 5 times TT elicited no significant change in the activity of either of these muscles. While the EMG activity of both muscles increased in response to stimulation at 10 times the TT only the change in genioglossus activity reached statistical significance ($p < 0.05$). Stimulation at 20 and 30 times TT elicited a 45 and 50 percent increase in alae nasi activity ($p < 0.05$) respectively. This contrasts with 3 and 6 fold increases in genioglossus activity at the same stimulation intensities.

In figure 4 the increase in peak inspiratory EMG activity relative to control of the right

diaphragm and parasternal intercostal muscle with increasing stimulation intensity is illustrated. No statistically significant change in the activities of these muscles occurred at 5 or 10 times TT. Stimulation of the proximal phrenic nerve at 20 and 30 times TT elicited 67% ($p < 0.05$) and 59% ($p < 0.05$) increases in right diaphragm activity and 60% and 72% increases in parasternal activity, respectively.

In all animals, phasic expiratory activity of triangularis sterni and transversus abdominis was evident at all times while external oblique only became active under control conditions in the presence of 5 cm H_2O of PEEP. Figure 5 illustrates the changes in peak expiratory EMG activities of the transversus abdominis and triangularis sterni muscles with increasing stimulus intensity. Stimulation at 5 times TT produced no significant change in the activity of either transversus abdominis or external oblique muscles. At stimulation intensities of 10, 20 and 30 times TT, activity of the transversus abdominis underwent a 2 ($p < 0.05$), 3 ($p < 0.05$) and 12 ($p < 0.01$) fold increase, respectively, while that of the external oblique increased by 37%, 90% and 115%, respectively (not shown). The activity of the triangularis sterni, in contrast, remained unchanged at all stimulation intensities.

DISCUSSION

The main findings of this study are:

1. In vagotomized, α-chloralose anaesthetized dogs, electrical stimulation of the central cut end of the left thoracic phrenic nerve resulted in an increase in minute ventilation achieved by an increase in both tidal volume and breathing frequency.
2. The increase in inspiratory muscle activity evoked by phrenic afferent stimulation was not

homogeneous. While the EMG activity of the right costal diaphragm, parasternal intercostal and alae nasi muscles increased to approximately the same extent, the increase in genioglossus activity was disproportionately large.

3. There was dissociation between rib cage and abdominal expiratory muscle activation. Triangularis sterni activity was unaffected by phrenic afferent stimulation while the transversus abdominis was strongly recruited.

Critique: The studies were performed in anaesthetized dogs which had undergone vagotomy, carotid sinus isolation, and laparotomy. Our findings must, therefore, be interpreted in the context of the experimental preparation.

Vagotomy was performed in order to eliminate confounding reflex alterations of the ventilatory response to phrenic afferent stimulation. This interrupted phasic changes in vagal activity resulting from pulmonary stretch and irritant receptor activation (9) as well as changes in tonic vagal activity (21) such as accompany aortic (1) and atrial (19) baroreflex stimulation. While eliminating these variables, vagotomy may also have influenced the degree of expiratory muscle activation. Early reports allege the vagus to be the principle if not exclusive activator of the abdominal muscles (2,3). Kelson et. al. (17), however, found expiratory electrical activity of the external oblique muscle to be abolished by vagotomy in only 4 of 11 α-chloralose anaesthetized dogs. In 6 of the 7 animals in their study in which external oblique activity persisted following vagotomy, the increase in its level of activation during increased chemical drive (hypoxia and hypercapnia) remained intact. De Troyer and Ninane (5) found the expiratory activity of the triangularis sterni to increase in some animals and to decrease in others following

vagotomy while the activity of the external oblique was uniformly inhibited. If in our study expiratory muscle activity were suppressed under control conditions the response to phrenic afferent stimulation may have been exaggerated when expressed as a percent of control. This effect would have been, at least in part, offset since the stimulatory effect of increased vagal activity associated with baroreflex and pulmonary volume related reflex activation was prevented. Furthermore, since no significant increase in triangularis sterni activity was observed during stimulation, inhibition of transversus abdominis activity could only account for the difference between these two muscles if triangularis sterni were maximally activated under control conditions. This is unlikely since the activity of this muscle in vagotomized dogs has been shown to increase in response to postural changes (5).

In the intact animal, carotid baroreflex inputs to the respiratory control centres would also act to modify the responses to phrenic afferent activation. Changes in carotid sinus pressure of the same magnitude as the changes in arterial pressure observed during phrenic nerve stimulation in the current study have been shown to reduce tidal volume and breathing frequency (4). In addition, an increase in carotid sinus pressure would be expected to suppress hypoglossal nerve activity relative to that of the phrenic nerve (23). These effects, would reduce the increases in ventilation and genioglossus activity which we observed under conditions of constant carotid sinus pressure. It is of note that in previous studies of the ventilatory effects of phrenic (18,22) and limb muscle afferent (13,20) stimulation the influence of carotid baroreflex activation have not been taken into account.

Our preparation has not eliminated input from non vagally innervated aortic baroreceptors. These effects, however, appear to be small. Dove et. al. (6) found that maintaining Part constant

had no effect on the ventilatory response to brief carotid sinus pressure changes. Similarly, Brunner et. al. (4) found that preventing reflex changes in Part during steady state carotid sinus stimulation resulted in only minor differences in breathing frequency compared to when these changes were permitted.

Placement of EMG electrodes in the costal diaphragm and transversus abdominis muscle required a limited laparotom. In pentobarbital anaesthetized dogs, Farkas and De Troyer (8) found suppression of transversus abdominis activity compared with that of the triangularis sterni and external oblique muscles following incision of the abdomen from xiphoid process to symphysis pubis or following incision from xiphoid process to umbilicus with cholecystectomy. Their study differs from ours in both the anaesthetic used and the extent of the abdominal procedure. That these factors played an important role in the observed inhibition and that the effect on our animals was much less pronounced is supported by the fact that we consistently observed phasic activity of this muscle during spontaneous ventilation in the absence of PEEP. In the study of Farkas and De Troyer (8), in contrast, its activity was completely abolished under these conditions. Any error related to lower control activity of the transversus abdominis, moreover, would be offset by the negative influence on its recruitment during the stimulation periods.

Arterial PCO_2 and pH were similar at the onset of each stimulation period. We wished to observe the effect of stimulation on minute ventilation and ventilatory timing, therefore, no effort was made to fix ventilation so as to maintain PCO_2 constant. As a result, depending on the minute ventilation achieved, varying degrees of hypocapnia would be expected to accompany the stimulations. Smith et. al. (24) found that when hypocapnia was allowed to occur during

moderate hypoxic hyperventilation (2 to 3 fold increase in ventilation) or in response to almitrine infusion in conscious dogs, the activity of both triangularis sterni and transversus abdominis remained unchanged or declined, whereas that of the crural diaphragm increased progressively. Accordingly, a larger increase in the activities of these muscles (but not a change in their relative activations) might have been observed if arterial PCO_2 had been maintained constant during the stimulation period.

Changes in ventilation may also accompany changes in cardiac output and pulmonary blood flow (29). As in previous reports (18), however, the animals in the current study demonstrated changes in ventilation beginning several seconds before the onset of the hemodynamic response. It is, therefore, unlikely that the changes in ventilation, timing or distribution of drive which we observed were secondary to hemodynamic effects.

Afferent Fiber Type: The phrenic nerve contains numerous large (Group I and II) and small (group III and IV) diameter afferents (18), all of which are likely to have been activated by the stimulation parameters used in this study. The ventilatory effects of these various afferent groups remains controversial owing to varying effects in different experimental preparations. In studies on dogs in which the supraspinal pathways have been preserved (18,22), as in the current study, central stimulation of the thoracic phrenic nerve has produced a purely stimulatory effect on ventilation. Since the increase in ventilation required high stimulation intensities (10 - 40 times motor activation threshold) and since sectioning the C5 - C7 dorsal roots abolished the response while cold blockade of group I and II afferent fibers did not, Road et. al. (22) concluded that the increase in ventilation was due to activation of thin (group III and IV) fiber afferents. This

conclusion is compatible with the finding that chemical activation of these fibers by capsaicin injection into the phrenic circulation is stimulatory to ventilation (15).

Consistent with these reports, we observed significant increases in ventilation and respiratory muscle activation only at high stimulation intensities (10 - 30 times motor activation threshold). All group I and most group II fibers should have been activated well before this level had been reached (7,10). It is likely, then, that the changes in ventilation and pattern of muscle activation which we observed were due primarily to activation of thin-fiber phrenic afferents.

Pattern of Muscle Activation: Inhomogeneous activation of the abdominal and ribcage expiratory muscles is a feature of many ventilatory stimuli. In addition to differences in the importance of vagal afferent inputs, the triangularis sterni has been reported to be less responsive to hypercapnia (28) and to skeletal muscle afferent stimulation (20) than the transversus abdominis. The independence of the mechanisms responsible for neural control of these two muscle groups has been underscored by observations of directionally opposed changes in their activities during oesophageal distention (28) and their separate isolated activation during chemoreceptor stimulation (24). Our findings, therefore, add phrenic afferent activation to the list of stimuli associated with differential recruitment of these muscles.

We also found differences between the response of the genioglossus muscle and that of the other muscles active with inspiration. Phrenic afferent mediated spinal inhibitory reflexes (25) have been described and would be expected to affect the diaphragm and parasternal muscles but not the cranially innervated genioglossus. Since the activity of the alae nasi, innervated by the facial nerve, increased in proportion to the increase in diaphragm activity, however, we cannot

account for the preferential activation of the genioglossus on this basis. The activity of the genioglossus muscle has been found to be more sensitive than that of the diaphragm to chemical and electrical stimulation of the brainstem reticular activating system (27,28) and to various pharmacologic agents which suppress or enhance reticular formation activity (27). Based on these findings, St. John (28) has suggested that the hypoglossal nerve is more dependent upon reticular mechanisms for its respiratory activity than are phrenic motoneurons. Thus, projection of collaterals from phrenic sensory neurons onto the reticular formation may account for the preferential activation of this muscle during phrenic afferent stimulation.

The effect of limb muscle afferent stimulation on the pattern of chest wall muscle activation has been studied. Haxhiu et al. (13) stimulated the central cut end of the sciatic nerve in dogs and observed a greater increase in the activation of upper airway dilator (genioglossus, alae nasi and posterior cricoarytenoid) muscles in comparison with the diaphragm. In a similar preparation, Oliven et al. (20) described a significantly greater increase in expiratory abdominal muscle activity as compared with that of the triangularis sterni in response to sciatic nerve stimulation. Similarly, we (14) found that the activities of the genioglossus and transversus abdominis muscles increased to a greater extent than those of the diaphragm, parasternal intercostals and alae nasi, in response to gastrocnemius afferent stimulation while the activity of triangularis sterni increased only at high intensities of nerve stimulation. The similarity in the pattern of respiratory muscle recruitment elicited by phrenic afferent activation in the present study to that observed during limb muscle afferent stimulation suggests that the central projections of thin-fiber phrenic afferents and those of afferents arising from limb muscles may be alike.

Implications: Thin fiber muscular afferents are activated by polymodal receptors sensitive to mechanical distortion, ischemia and the accumulation of metabolic byproducts. This suggests that in the diaphragm, these fibers may play a role in determining the ventilatory response to high ventilatory loads, inadequate diaphragm blood flow and diaphragm fatigue. Our finding that activation of phrenic thin fiber afferents is associated with strong recruitment of the expiratory abdominal muscles may be relevant in this context. In addition to facilitating high expiratory flow rates, this may reduce the degree of diaphragmatic shortening placing the diaphragm at a better mechanical advantage with respect to its force-length and force-velocity characteristics. Abdominal muscle activation will also tend to lower the end expiratory position of the rib cage. While shortening of Te, as observed in the current study, may limit this effect, the potential result is greater passive expansion of the rib cage in early inspiration and end expiratory lengthening of the inspiratory rib cage muscles.

The intensity of inspiratory muscle contraction appears to be predictive of arousal during airway obstruction in sleep (11). Our current results suggest that afferent activation by receptors within the diaphragm sensitive to mechanical stimulation could participate in the termination of obstruction through selective enhancement of upper airway dilator muscle contraction.

ACKNOWLEDGEMENTS

The authors thank Stephen Nuara for his technical assistance. The study was funded by a grant from the Heart and Stroke Foundation of Canada. M. Ward is a fellow of the Medical Research Council of Canada. S. Hussain is a scholar of the Heart and Stroke Foundation of Canada.

REFERENCES

1. Aviado, D., and C. Schmidt. Cardiovascular and respiratory reflexes from the left side of the heart. Am. J. Physiol. 164:726-730, 1959

2. Bishop, B. Diaphragm and abdominal muscle responses to elevated airway pressures in the cat. J. Appl. Physiol. 22:959-965, 1967

3. Bishop, B. and H. Bachofen. Comparison of neural control of diaphragm and abdominal muscle activities in the cat. J. Appl. Physiol. 32:798-805, 1972

4. Brunner, M.J., M.S. Sussman, A.S. Greene, C.H. Kallman and A.A. Shoukas. Carotid sinus baroreceptor reflex control of respiration. Circ. Res. 51:624-636, 1982

5. De Troyer, A., and Ninane. Effect of posture on expiratory muscle use during breathing in the dog. Respir. Physiol. 67:311-322, 1987.

6. Dove, E.L., and P.G. Katona. Respiratory effects of brief baroreceptor stimuli in anaesthetized dog. J. Appl. Physiol. 59:1258-1265, 1985

7. Eccles, R.M., and A. Lundberg. Synaptic actions in motoneurons by afferents which may evoke the flexion reflex. Rev. Arch. Ital. Biol. 97:199-221, 1959

8. Farkas, G. and A. De Troyer. Effects of midline laparotomy on expiratory muscle activation in anaesthetized dogs. J. Appl. Physiol. 67:599-605, 1989

9. Fishman, N.H., E.A. Phillipson and J.A. Nadel. Effect of differential vagal cold blockade on breathing pattern in conscious dogs. J. Appl. Physiol. 34:754-758, 1973

10. Gasser, H.S. Unmedullated fibres originating in dorsal root ganglion. J. Gen. Physiol. 33:651-690, 1950

11. Gleeson, K., C.W. Zwillich, D.P. White. The influence of increasing ventilatory effort on arousal from sleep. Am. Rev. Respir. Dis. 142:295-300, 1990

12. Graham, R., Y. Jammes, S. Delpierre, C. Grimaud, and Ch. Roussos. The effects of ischemia, lactic acid and hypertonic sodium chloride on phrenic afferent discharge during spontaneous diaphragmatic contraction. Neurosc. Letters 67:257-262, 1986

13. Haxhiu, M.A., E. Van Lunteren, J. Mitra, N.S. Cherniack, and K. Strohl. Comparison of the responses of the diaphragm and upper airway muscles to central stimulation of the sciatic nerve. Respir. Physiol. 58:65-76, 1984

14. Hussain, S.N.A., M.E. Ward, A.G. Gatensby, Ch. Roussos and A. Deschamps. Effects of limb muscle afferent stimulation on ventilatory muscle activation in anaesthetized dogs.

Respir. Physiol. In press.

15. Hussain, S.N.A, S. Magder, A. Chatillon and Ch. Roussos. Chemical activation of thin-fiber phrenic afferents: respiratory responses. J. Appl. Physiol. 69(3):1002-1011, 1990.

16. Jammes, Y., B. Buchler, S. Delpierre, A. Rasidakis, C. Grimaud and Ch. Roussos. Phrenic afferents and their role in inspiratory control. J. Appl. Physiol 60:854-860, 1986

17. Kelsen, S.G., M.D. Altose and N.S. Cherniack. Interaction of lung volume and chemical drive on respiratory muscle EMG and respiratory timing. J. Appl. Physiol. 42:287-294, 1977

18. Kohrman, R.M., J.B. Nolasco, and C.J. Wiggers. Types of afferent fibres in the phrenic nerve. Am. J. Physiol. 151:547-553, 1947

19. Levy, M., M. Ng, and H. Zieske. Cardiac and respiratory effects of aortic arch baroreceptor stimulation. Circ. Res. 19:930-939, 1966

20. Oliven, A., M.A. Haxhiu, and S.G. Kelsen. Distribution of motor activity to expiratory muscles during sciatic nerve stimulation in the dog. Respir. Physiol. 81:165-176, 1990

21. Phillipson, E.A., Vagal control of breathing pattern independent of lung inflation in conscious dogs. J. Appl. Physiol. 37:183-189, 1974

22. Road, J.D., H.C. West, and B.N. Van Vliet BN. Ventilatory effects of stimulation of phrenic afferents. J. Appl. Physiol. 63:10063-1069, 1987

23. Salamone, J.A., K.P. Strohl, D.M. Weiner, J. Mitra, and N.S. Cherniack. Cranial and phrenic nerve responses to changes in systemic blood pressure. J. Appl. Physiol. 55:61-68, 1983

24. Smith, C.A., D.M. Ainsworth, K.S. Henderson and J.A. Dempsey. Differential responses of expiratory muscles to chemical stimuli in awake dogs. J. Appl. Physiol. 66:384-391, 1989

25. Speck, D.F.,and W.R. Revelette. Attenuation of phrenic motor discharge by phrenic nerve afferents. J. Appl. Physiol. 62:941-945, 1987

26. St. John, W., and T.A. Bledsoe. Comparison of respiratory-related trigeminal hypoglossal and phrenic activities. Respir. Physiol. 62:61-78, 1985

27. St. John, W.M. Influence of reticular mechanisms upon hypoglossal, trigeminal and phrenic activities. Respir. Physiol. 66:27-40, 1986

28. Van Lunteren, E., M.A. Haxhiu, N.S. Cherniack, and J.S. Arnold. Rib cage and abdominal expiratory muscle responses to CO2 and oesophageal distension. J. Appl. Physiol. 64:846-853, 1988

29. Wasserman, K., B.J. Whipp, and J. Castagna. Cardiodynamic hyperpnoea: hyperpnoea secondary to cardiac output increase. J. Appl. Physiol. 36:457-464, 1974

Table 1: Effect of central phrenic nerve stimulation on mean arterial pressure and heart rate.

Stimulation Intensity (X TT)	Mean Arterial Pressure (mmHg)		Heart rate (beats/min)	
	Control	Peak	Control	Peak
5	134±7	137±8	147±6	147±6
10	134±+7	146±10	150±6	158±6
20	132±6	154±7*	151±6	162±4*
30	128±6	154±8*	151±6	162±4*

Values are means ± SEM. XTT, multiples of twitch threshold.

* $p < 0.05$ in comparison with control.

Table 2: **Effect of central phrenic nerve stimulation on tidal volume and respiratory timing.**

Stimulation Intensity (X TT)	**Tidal Volume (litres)**		**Frequency (breaths/min)**	
	Control	Peak	Control	Peak
5	0.52±0.04	0.58±0.04	12.5±2.2	12.3±2.3
10	0.59±0.06	0.65±0.06	12.0±2.3	14.0±2.1
20	0.60±0.05	0.73±0.06*	11.3±1.4	14.0±1.8*
30	0.50±0.05	0.68±0.05*	10.5±2.1	14.5±1.5*

Stimulation Intensity	**Inspiratory Time (seconds)**		**Expiratory Time (seconds)**	
(X TT)	Control	Peak	Control	Peak
5	1.60±0.21	1.77±0.20	4.80±+1.59	4.71±1.77
10	1.94±0.21	1.78±0.23	5.55±+1.10	3.85±0.86
20	1.93±0.11	1.68±0.14*	5.89±1.27	3.59±0.77*
30	2.00±0.23	1.67±0.13*	7.81±2.20	3.70±0.80*

Values are means ± SEM. XTT, multiples of twitch threshold

* $P < 0.05$ in comparison with control.

FIGURE LEGENDS:

Figure 1

Breath by breath changes in minute ventilation in response to phrenic nerve stimulation at 5, 10, 20 and 30 times twitch threshold. The vertical lines indicate the beginning of phrenic nerve stimulation. The horizontal lines indicate the breaths which were averaged and designated as peak values.

Figure 2

Minute ventilation as a percent of the corresponding control value during stimulation at 5, 10, 20 and 30 times twitch threshold. *, ** $p < 0.05, 0.01$ in comparison with control values.

Figure 3

Percent increase from the control value of the peak integrated inspiratory EMG activity of the genioglossus and alae nasi during stimulation at 5, 10, 20 and 30 times twitch threshold. Note the difference in y axis ranges. *, ** $p < 0.05, 0.01$ in comparison with control values.

Figure 4

Percent increase from the control value of the peak integrated inspiratory EMG activity of the right hemidiaphragm and parasternal intercostal muscle during stimulation at 5, 10, 20 and 30 times twitch threshold. * $p < 0.05$ in comparison with control values.

Figure 5

Percent increase from the control value of the peak integrated expiratory EMG activity of the transversus abdominis and triangularis sterni. Note difference in y axis ranges. *, ** $p < 0.05$, 0.01 in comparison with control values.

FIGURE 1

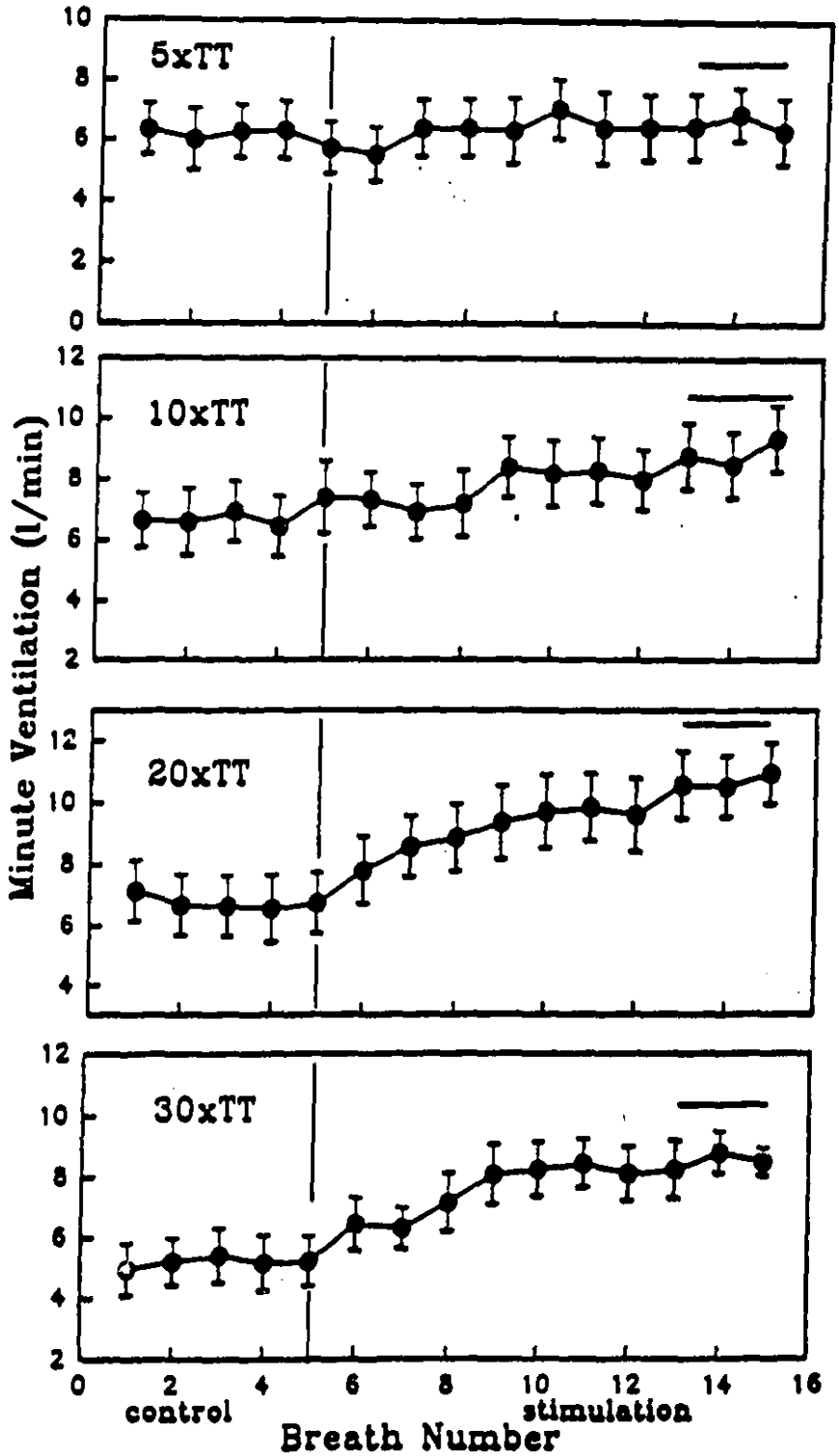
5xTT
10xTT
20xTT
30xTT
Minute Ventilation (l/min)
control
stimulation
Breath Number

FIGURE 2

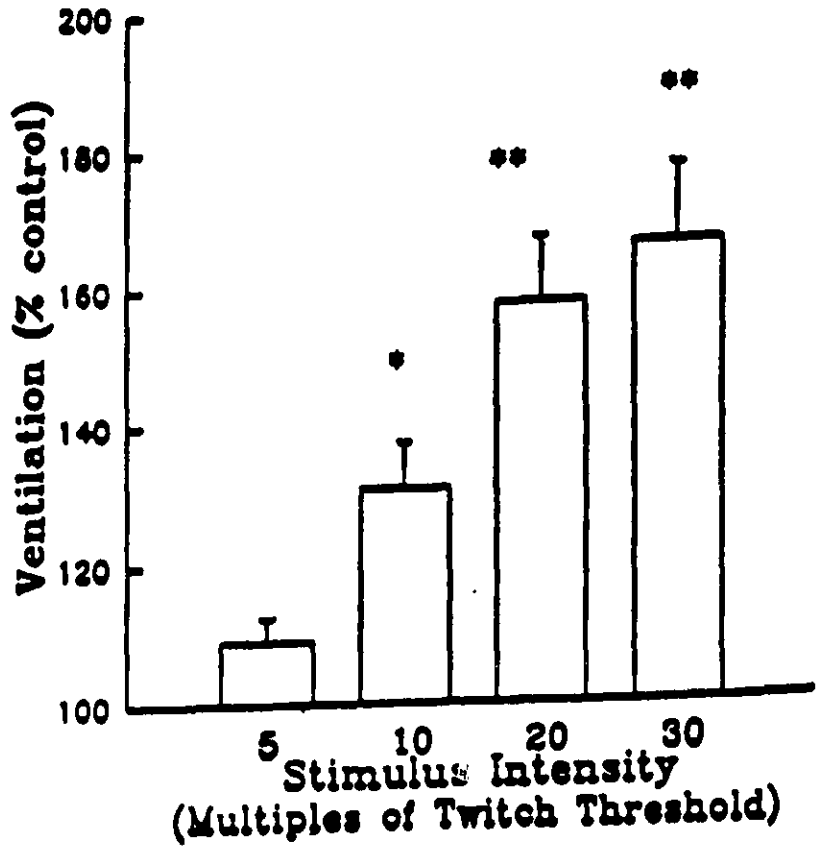
200
180
160
140
120
100
Ventilation (% control)
*
**
**
5
10
20
30
Stimulus Intensity
(Multiples of Twitch Threshold)

FIGURE 3

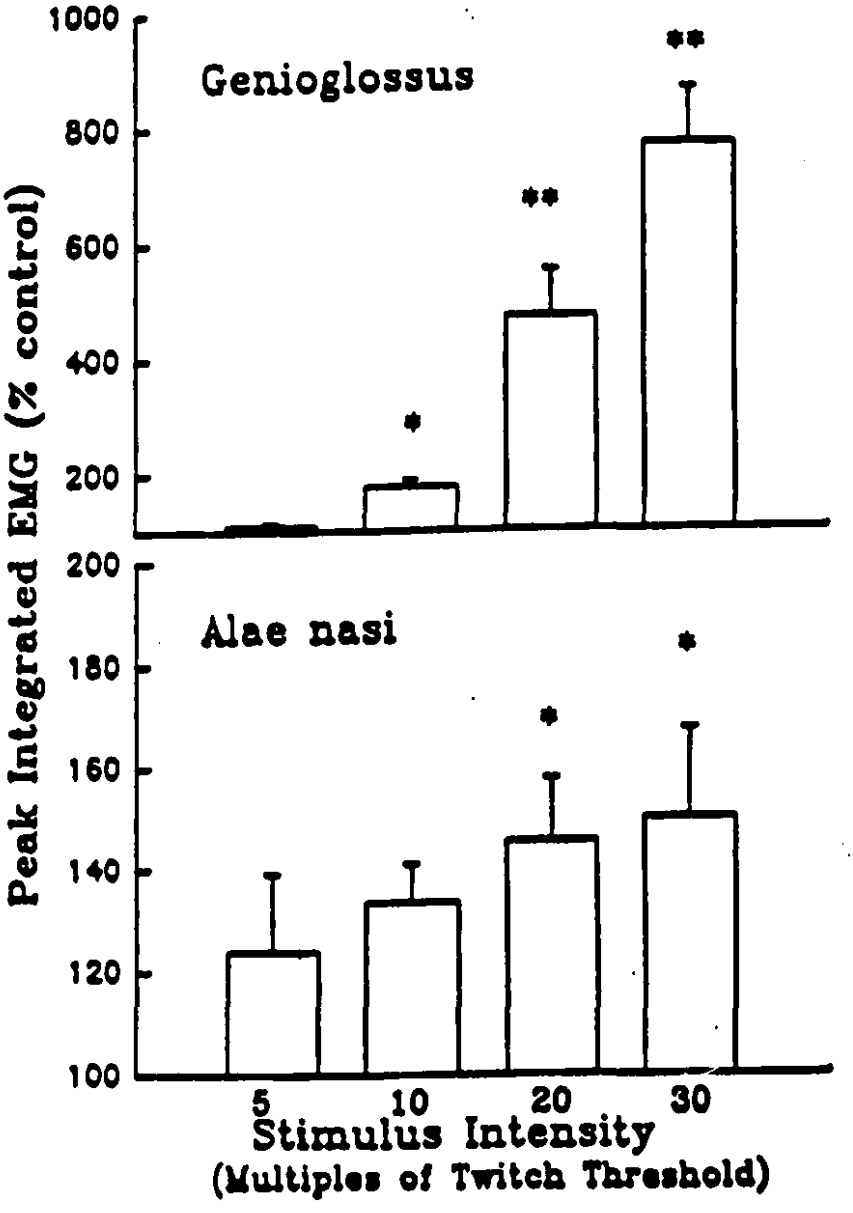
Genioglossus
Alae nasi
Peak Integrated EMG (% control)
1000
800
600
400
200
180
160
140
120
100
*
**
**
*
*
*
5
10
20
30
Stimulus Intensity
(Multiples of Twitch Threshold)

FIGURE 4

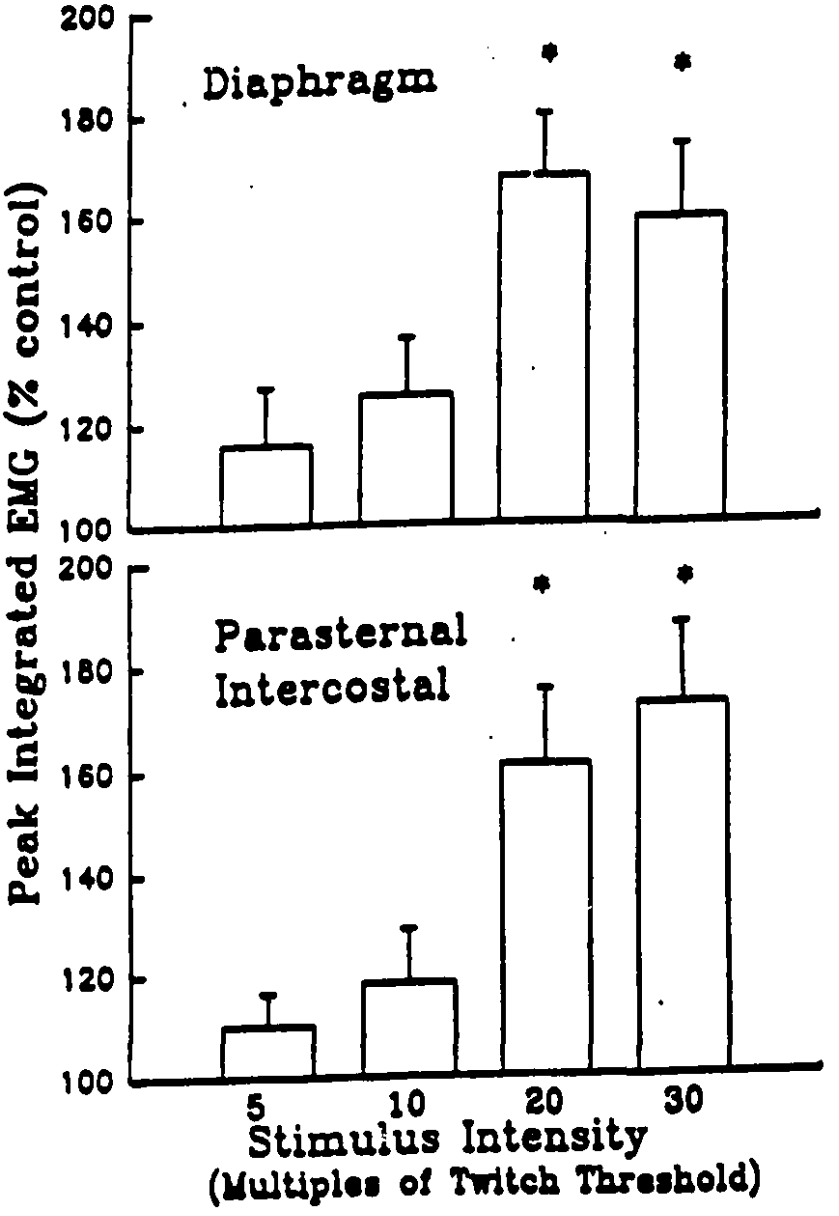
Diaphragm
Parasternal
Intercostal
Peak Integrated EMG (% control)
200
180
160
140
120
100
5
10
20
30
Stimulus Intensity
(Multiples of Twitch Threshold)

FIGURE 5

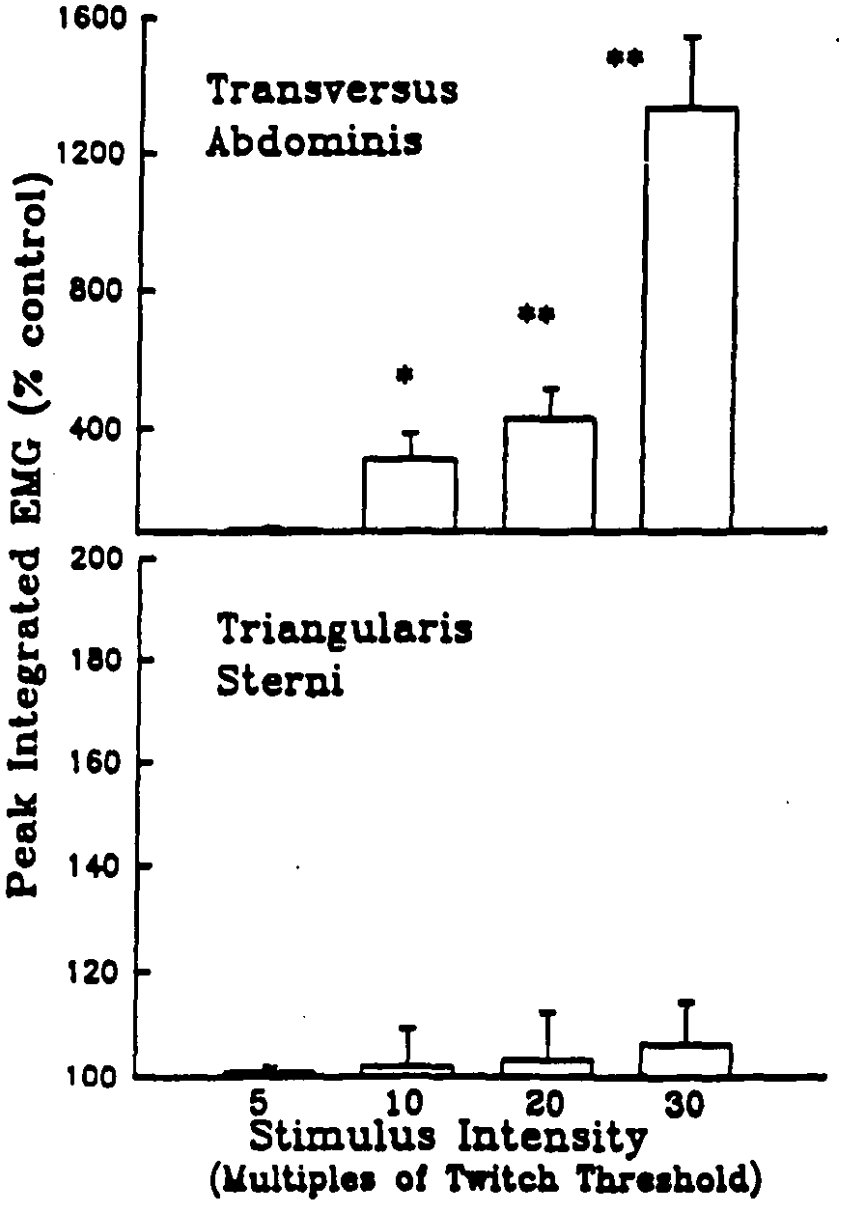
1600
1200
800
400
200
180
160
140
120
100
Transversus
Abdominis
Triangularis
Sterni
*
**
**
Peak Integrated EMG (% control)
5
10
20
30
Stimulus Intensity
(Multiples of Twitch Threshold)

CHAPTER 4: Respiratory Muscle Oxygen Delivery and Extraction

Foreword to Chapter 4

Using near infrared spectroscopy, Mancini et al. (12) demonstrated progressive deoxygenation of the accessory muscles of respiration, associated with a reduction in minute ventilation compared with normals, during maximal bicycle exercise in patients with congestive heart failure. This suggests that, at least in some patients, limitation of respiratory muscle oxygen delivery may play a role in the capacity to maintain a required level of ventilation. When the ability to augment oxygen delivery is limited, the respiratory muscles must depend on increased extraction to meet their metabolic needs. The extent to which oxygen consumption may be maintained in the face of diminishing oxygen delivery through this mechanism is a characteristic of the tissue and varies widely among organs having different levels of basal metabolic activity (4,8,9,13,15,17,19-21). Understanding the factors limiting the capacity of the diaphragm to sustain ventilation under such conditions, therefore, requires specific evaluation of the relationship between its oxygen delivery and its oxygen consumption.

As important as the relationship between local oxygen delivery and diaphragmatic oxygen consumption is, it is the systemic oxygen delivery at which the oxygen uptake of the diaphragm becomes limited that determines how a given degree of hemodynamic impairment will be tolerated. In addition to the ability of the diaphragm to increase its oxygen extraction, this parameter also depends on the how blood flow is redistributed during reductions in systemic oxygen delivery. Although preferential perfusion of the ventilatory muscles during shock states has been proposed (18), the existence of such a protective mechanism and its role in maintaining respiratory muscle oxygenation has not been documented experimentally.

Adequate respiratory muscle blood flow is also important for reasons beyond simply

providing the tissue with a continuous source of oxygen and substrate. The deterioration of muscle function in-vitro has been linked to the intracellular accumulation of metabolic byproducts, particularly hydrogen ion and inorganic phosphate (5-7,11,14,16,22). The primary determinant of the intracellular concentrations of these elements is the extracellular H^+ concentration (10). Experiments in limb muscle have yielded evidence that these mechanisms may be active in vivo as well (1-3). The contractility of the respiratory muscles may, therefore, be influenced by blood flow through mechanisms unrelated to oxygen transport such as maintenance of the extracellular milieu.

In this chapter, the effect of reductions in diaphragmatic blood flow, independent of the usually associated reduction in oxygen and plasma borne substrate is determined. In addition, the changes in diaphragmatic oxygen consumption during reductions in oxygen delivery by progressive hemorrhage are evaluated. From this data, the critical diaphragmatic oxygen delivery and extraction ratio are calculated and related to changes in the systemic oxygen delivery. These calculations allow prediction of the impact of reductions in systemic oxygen delivery on the capacity of the diaphragm to meet its metabolic requirements aerobically.

REFERENCES

1. Barclay, J.K. A delivery-independent blood flow effect on skeletal muscle fatigue. *J. Appl. Physiol.* 61: 1084-1090, 1986.

2. Barclay, J.K., C.M. Boulianne, B.A. Wilson and S.J. Tiffin. Interaction of hyperoxia and blood flow during fatigue of canine skeletal muscle in situ. *J. Appl. Physiol.* 47: 1018-1024, 1979.

3. Barclay, J.K. and W.M. Stainsby. The role of blood flow in limiting maximal metabolic rate in muscle. *Med. Sci. Sports* 7: 116-119, 1975.

4. Cain, S.M. Oxygen delivery and extraction in dogs during anemic and hypoxic hypoxia. *J. Appl. Physiol.* 42: 228-234, 1977.

5. Fabiato, A. and F. Fabiato. Effects of pH on the myofilaments and the sarcoplasmic reticulum of skinned cells from cardiac and skeletal muscles. *J. Physiol. Lond.* 276: 233-255, 1978.

6. Fuchs, F., Y. Reddy and F.N. Briggs. The interaction of cations with the calcium-binding site of troponin. *Biochim. Biophys. Acta* 221: 407-409, 1970.

7. Inesi, G. and T.L. Hill. Calcium and proton dependence of sarcoplasmic reticulum ATPase. *Biophys. J.* 44: 271-280, 1983.

8. Kohzuki, H., Y. Enoki, Y. Ohga, S. Shimizu and S. Sakata. Oxygen consumption in resting dog gracilis muscle perfused at varying oxygen delivery. *Jap. J. Physiol.* 41: 23-34, 1991.

9. Kolar, F. and L. Jansky. Oxygen consumption in rat skeletal muscle at various rates of oxygen delivery. *Experientia* 40: 353-354, 1984.

10. Kowalchuk, J.M., G.J.F. Heigenhauser, M.I. Lindinger, J.R. Sutton and L. Jones. Factors influencing hydrogen ion concentration in muscle after intense exercise. *J. Appl. Physiol.* 5: 2080-2089, 1986.

11. Mainwood, G.W. and J.M. Renaud. The effect of acid-base balance on fatigue of skeletal muscle. *Can. J. Physiol. Pharmacol.* 63: 403-416, 1985.

12. Mancini, D.M., N. Ferraro, D. Nazzaro, B. Chance and J.R. Wilson. Respiratory muscle deoxygenation during exercise in patients with heart failure demonstrated with near-infrared spectoroscopy. *J. Am. Coll. Cardiol.* 18: 492-498, 1991.

13. Nagano, K., S. Gelman, D.A. Parks and E. Bradley. Hepatic oxygen supply-uptake relationship and metabolism during anesthesia in miniature pigs. *Anesthesiology* 72: 902-910, 1990.

14. Nakamaru, Y. and A. Schwartz. The influence of hydrogen ion on the sarcoplasmic reticulum. *J. Gen. Physiol.* 59: 22-32. 1972.

15. Nelson, D.P., C.E. King, S.L. Dodd, P.T. Shcumacker and S.M. Cain. Systemic and intestinal limits of O_2 extraction in the dog. *J. Appl. Physiol.* 63: 387-394, 1987.

16. Nosek, T.M., K.Y. Fender and R.E. Godt. It is diprotonated inorganic phosphate that depresses force in skinned skeletal muscle fibres. *Science* 236: 191-193, 1987.

17. Perry, M.A., P. Bulkley, P.R. Kvietys and D.N. Granger. Regulation of oxygen uptake in resting and pentagastrin-stimulated canine stomach. *Am. J. Physiol.* 242: G565-G569, 1982.

18. Schini, V.B. and P.M. Vanhoutte. Inhibitors of calmodulin impair the constitutive but not the inducible nitric oxide synthase activity in the rat aorta. *J. Pharmacol. Exp. Ther.* 261: 553-559, 1992.

19. Schumacker, P.T., G.R. Long and L.D.H. Wood. Tissue oxygen extraction during hypovolemia: role of hemoglobin P_{50}. *J. Appl. Physiol.* 62: 1801-1807, 1987.

20. Segal, J.M., T. Phang and K. Walley. Low-dose dopamine hastens onset of gut ischemia in a porcine model of hemorrhagic shock. *J. Appl. Physiol.* 73(3): 1159-1164, 1992.

21. Walley, K.R., C.J. Becker, R.A. Hogan, K. Teplinsky and L.D.H. Wood. Progressive hypoxemia limits left ventricular oxygen consumption and contractility. *Circ. Res.* 63: 849-859, 1988.

22. Wilson, J.R., K.K. McCully, D.M. Mancini, B. Boden and B. Chance. Relationship of muscular fatigue to pH and diprotonated Pi in humans: a ^{31}P-NMR study. *J. Appl. Physiol.* 64: 2333-2339, 1988.

Oxygen Delivery-Independent Effect of Blood Flow on Diaphragm Fatigue

Michael E. Ward, Sheldon A. Magder and Sabah N.A. Hussain
American Review of Respiratory Disease 145: 1058-1063, 1992

ABSTRACT:

To determine the effect of blood flow on diaphragm fatigue independent of oxygen delivery, the left hemidiaphragm was vascularly isolated in 14 pentobarbital anaesthetized, mechanically ventilated dogs. Fatigue (decline in tension generation) of the left diaphragm was induced by phrenic nerve stimulation at 10 Hz, 12/min, duty cycle of 0.5 for 8 minutes. Two stimulation periods separated by 30 minutes of rest were performed in each animal. Diaphragmatic O_2 delivery during the two periods was the same. In group 1 (n=8), the diaphragm was autoperfused from the femoral artery (High O_2-Low Flow) during the first stimulation period. The tension generated by the diaphragm during this period declined progressively to 47.7% of initial values. In the second period in this group, the diaphragm was pump perfused with arterial blood, diluted with an equal volume of 6% dextran at a flow rate twice that of the first period (Low O_2-High Flow). Tension in this period declined to 76% of initial tension ($P<0.05$ compared with High O_2-Low Flow). In group 2 (n=6), stimulation performed while perfusing the diaphragm in the first period with diluted arterial blood at a flow rate twice that recorded during autoperfusion (Low O_2-High Flow) produced a decline in tension to 70% of the initial values. In the second period, the diaphragm was perfused with undiluted arterial blood at flow rate equal 50% of that of the first period (High O_2-Low Flow). Tension during this period declined to 56% of initial values ($P<0.05$ compared with Low O_2-High Flow). At any time during stimulation in both groups, the relative tension in the Low O_2-High Flow periods was higher than that of High O_2-Low Flow periods. These results indicate that increasing blood flow retards the development of diaphragm fatigue by mechanisms independent of oxygen delivery.

INTRODUCTION:

The importance of maintaining diaphragm oxygen and substrate delivery in the management of respiratory failure, in which respiratory muscle dysfunction may be playing a role, has recently been emphasized (1) and supported by experimental evidence. Aubier et al. (2) reported that, in patients with respiratory failure, dopamine infusion increased diaphragmatic blood flow (and therefore oxygen delivery) and improved diaphragm function. Supinski et al. (3) have found that increasing blood flow partially reversed the loss of force generating capacity induced by repetitive high intensity isometric contractions in an isolated diaphragm strip preparation. In limb muscle, tension developed during twitch contractions can be increased by increasing blood flow (4) and fatigue during repetitive twitch (4) and tetanic (5) contractions is retarded.

Others suggest, however, that these effects may involve more complex mechanisms than the simple maintenance of adequate substrate for aerobic metabolism. In limb muscle, Barclay (6) has demonstrated that hyperperfusion is associated with a reduction in the rate of fatigue, which was independent of oxygen and plasma born substrate delivery. Delivery-independent factors, such as alterations in perfusion pressure, extracellular fluid composition or the capillary surface available for substrate and metabolite exchange may, therefore, also play a role in the improvement in diaphragm function observed with augmentation of blood flow. Since O_2 and substrate delivery may be manipulated independent of changes in diaphragm blood flow (by changing their concentrations), the development of a rational management strategy requires determination of the relative importance of these factors.

The purposes of this study are: 1) to study the effect of augmentation of diaphragm

blood flow on the rate of development of diaphragm fatigue during intermittent, submaximal contractions; and 2) to determine whether modification of the rate of fatigue by hyperperfusion is attributable to increased oxygen and substrate delivery or if delivery-independent mechanisms also play a significant role.

METHODS:

Animal Preparation: Fourteen mongrel dogs weighing 25-34 kg were anaesthetized with sodium pentobarbital (initial dose 25 mg/kg i.v.) which was supplemented as necessary. The animals were supine, intubated with a cuffed endotracheal tube and mechanically ventilated (tidal volume 17 ml/kg, frequency of 15 per minute). Supplemental O_2 was supplied through the inspiratory line and arterial PO_2 was maintained above 100 mmHg. Positive end-expiratory pressure (PEEP) (5 cmH_2O) was applied at the expiratory line. A catheter was placed in the aorta via the right carotid artery to monitor arterial pressure (P_{art}) and arterial blood gases. Blood O_2 contents were measured with a co-oximeter (Instrumentation Laboratory IL-182). Another catheter was placed in the right femoral vein to administer fluids. Core body temperature was kept constant at approximately 37° C by a heating pad placed under the animal.

Isolated left hemidiaphragm: In all animals, we used the in-situ innervated and vascularly isolated left hemidiaphragm preparation developed by Hussain et al (7). The lower six ribs and interspaces on the left side were exposed by dissecting the abdominal rectus, external oblique and latissimus dorsi muscles. Each interspace was incised (5-10 cm long) and the incision was extended as near as possible to the origin of the costal diaphragm. Intercostal vessels were then

ligated and the ribs were removed. A midline incision was made in the xiphisternal cartilage to expose the left internal mammary artery, which was then ligated. A lateral abdominal incision was made just caudal to the inferior margin of the costal diaphragm. This incision extended from the midline to the inferior margin of the last rib, which was cut at the left costophrenic angle. The two halves of the diaphragm were divided by an incision extending from the xiphisternal cartilage to the central tendon. The ribs and cartilages of the now free costal margin were secured by silk threads to 3 metal bars, 5 cm long. Each bar was attached through its centre to a force transducer (Grass model FT10). To ensure independent movement of each bar, we severed the interconnecting rib portions (1 cm). Each transducer was mounted on a rack-and-pinion adjustable clamp which allowed adjustment of diaphragmatic length. These clamps were attached horizontally to a rigid metal frame surrounding the animal's thorax. Force transducers were calibrated with weights (100-500 g). The temperature of the diaphragm was monitored continuously using a temperature probe fixed to the surface of the isolated hemidiaphragm (Mon-a-therm, Model 6000, Zimmer of Canada Ltd., Mississauga, Ont.).

After the lower six ribs were removed and before the abdomen was opened, three pairs (one in each segment) of piezoelectric crystals (2.5 mm diam) were placed in the costal diaphragm. Each pair was placed 10-25 mm apart and oriented longitudinally along the segment. The crystals were connected to a four channel ultrasonic device (Sonomicrometer 120, Triton Technology, San Diego, CA) via fine insulated wires. The distance between crystals measured after the lower six ribs were removed was designated as the resting length at functional residual capacity. After isolation of the left diaphragm was completed, the resting length of each diaphragmatic segment was adjusted to the length at functional residual capacity.

At the end of the experiment, the length of each segment was measured from the rib attachment to the central tendon. The diaphragm was then disconnected and surgically removed. The weight of each of the three diaphragmatic segments (anterior, middle, and posterior) was measured. Segmental cross sectional areas were calculated as the ratio of muscle weight to length (8). Segmental tension was expressed as force per unit cross-sectional area. Mean diaphragmatic tension was obtained by averaging the three segmental tensions.

Phrenic blood flow measurement: The stomach, liver, spleen, and left kidney were retracted through the abdominal incision to expose the left phrenic artery. This artery was dissected free from the surrounding tissue 4 to 6 cm above the adrenal gland. The proximal part of the artery was ligated, and a polyethylene catheter (PE 160, 1.14 mm ID, 1.57 mm OD, 3 cm long) was introduced into the distal portion. A side port was placed at the entrance of the catheter into the phrenic artery from which blood was drawn for measurement of blood gases and O_2 content of the blood perfusing the diaphragm and for measurement of phrenic perfusion pressure (P_{phr}). The catheter was connected to an electromagnetic flow probe (Carolina Medical Electronics, 1.91 mm ID). The other side of the probe was connected to a 15-cm-long polyethylene tube (4 mm ID, 6 mm OD), which, in turn was connected to a Y-shaped connection. One arm of the Y connector was connected to a catheter in the left femoral artery so that arterial flow could be diverted from the left femoral artery through the catheter-probe system to the left phrenic artery. The other arm of the Y connection was secured via two three-way stopcocks and an extension, to a pump (Cole Palmer Instruments, model 7523-00) which was used to perfuse the left phrenic artery at a fixed rate with either arterial blood from the right femoral artery or with diluted

arterial blood stored in a glass container. Diaphragmatic O_2 delivery (DO_2phr) was calculated as the product of the phrenic arterial O_2 content and phrenic arterial flow (Qphr). All animals were heparinized (10,000 IU i.v.) after catheterizing the phrenic artery.

Phrenic Nerve Stimulation: Bipolar electrodes were placed around the left phrenic nerve close to its exit from the diaphragm. The electrodes were connected through a Grass isolation unit (SIU5) to a Grass stimulator (S48). Maximum stimulation of the left diaphragm was achieved by delivering a single stimulus (0.2 ms duration) with progressively increasing voltage. The voltage output was then set 2 volts higher than the last voltage found to produce an increment in diaphragm tension. During contraction periods, the left phrenic nerve was stimulated intermittently 12 times per minute at 10 Hz, duty cycle of 0.5 for 8 minutes.

Experimental Protocol: In each animal, fatigue of the isolated left diaphragm was induced twice. Each fatigue run consisted of a 5 minute control period, an 8 minute stimulation period and a 30 minute recovery period. Samples of the blood perfusing the hemidiaphragm were drawn during the control period, at the end of each minute during the contraction period and at the end of the recovery period of each run. During the fatigue runs in which hemidiaphragm was pump perfused, blood flow was set such that DO_2phr was the same as that recorded during two minutes of stimulation while the muscle was perfused by the natural flow from the left femoral artery. DO_2phr was, therefore, the same in all runs. The animals were divided into two groups. In the first group (n=8), autoperfusion with undiluted blood (High O_2-Low Flow) was compared with pump perfusion with diluted blood (Low O_2-High Flow). In the second

group (n=6), pump perfusion with undiluted blood (High O_2-Low flow) was compared with pump perfusion with diluted blood (Low O_2-High flow).

Group 1 (n=8): During the control, stimulation and recovery periods of the first run (autoperfusion, High O_2-Low Flow) the left diaphragm was perfused by blood redirected from the left femoral artery. During the second run (pump perfusion, Low O_2-High Flow,) the left hemidiaphragm was pump perfused with the animals own arterial blood diluted with an equal volume of 6% dextran that was contained in a glass container, continuously stirred and maintained at the same temperature as the diaphragm. The flow rate of the pump was set to match the DO_2phr that was achieved during the first two minutes of the stimulation period of the autoperfusion run.

Group 2 (n=6): To calculate the steady state values of diaphragmatic O_2 delivery during the stimulation period, the left phrenic nerve was stimulated intermittently (10 Hz, 12/min, duty cycle = 0.5) for two minutes while the hemidiaphragm was perfused from the left femoral artery. The flow rate of the pump during both runs was adjusted to match DO_2phr that was achieved during this period. During the first run (Low O2-High Flow) the left diaphragm was pump perfused with arterial blood diluted with an equal volume of 6% dextran (see above). After the five minute control period, the left phrenic nerve was stimulated for 8 minutes followed by 30 minutes of recovery. During the second run (High O_2-Low Flow) the left diaphragm was pump perfused with undiluted left femoral arterial blood at the same the steady-state value of DO_2phr.

Data analysis: Tension, Qphr and DO_2phr were averaged during the last 15 seconds of each

minute during stimulation period. Blood flow and O_2 delivery were expressed as ml/100g/minute, whereas the developed tension during each stimulation period was expressed as percentage of tension developed after 30 seconds of stimulation (relative tension). All data are presented as mean $\pm$ SEM. We compared the changes in tension, blood flow, and O_2 delivery for the two runs within each group and for the first runs of each group using analysis of variance (ANOVA). Changes found to be significantly different by ANOVA were further evaluated by the Student-Newman-Keuls test. P values of 0.05 or less were considered significant.

RESULTS:

Group 1: The phrenic arterial blood gases in the group 1 animals are listed in table 1. PO_2 and pH were not significantly different between the two conditions studied in this group. Phrenic arterial $PaCO_2$ in the pump perfusion, Low O_2-High Flow run was lower than that during the autoperfusion, High O_2-Low Flow run ($P<0.05$). Control values of mean P_{art}, mean P_{phr}, phrenic arterial O_2 contents, and haematocrit in the autoperfusion run averaged 106 $\pm$ 4 mmHg, 97 $\pm$ 3 mmHg, 19.7 $\pm$ 1.1 ml/dl, and 45.1 $\pm$ 1.7%, respectively. These values did not change during the stimulation period. Comparable values during the control period of the pump perfusion run averaged 112 $\pm$ 6 mmHg, 164 $\pm$ 19 mmHg ($P<0.01$ in comparison with autoperfusion), 10.3 $\pm$ 0.5 ml/dl ($P<0.01$), and 23.6 $\pm$ 0.6% ($P<0.01$), respectively. These parameters remained unchanged during the stimulation period.

Figure 1 illustrates the changes in diaphragmatic blood flow (top panel) and diaphragmatic O_2 delivery (bottom panel) during both runs in the group 1 animals. Control

values of Qphr and DO_2phr in the autoperfusion run averaged 15.5 $\pm$ 2.4 and 3.16 $\pm$ 0.6 ml/100g/min, respectively. These values increased to 28.6 $\pm$ 2.3 and 5.78 $\pm$ 0.7 ml/100g/min, respectively, after 1 minute of stimulation ($P<0.01$ in comparison with control values) with no change thereafter. Control values of Qphr and DO_2phr in the pump perfusion run averaged 54.1 $\pm$ 5.7 and 5.6 $\pm$ 0.7 ml/100g/min, respectively. These values remained unchanged during the stimulation period. Qphr during the stimulation period of the pump perfusion run was, therefore, double that of the autoperfusion run ($P<0.01$), whereas DO_2phr was not significantly different.

Diaphragmatic tension during autoperfusion and pump perfusion is plotted against time in figure 2. After 30 seconds of stimulation in the autoperfusion run, tension averaged 124.1 $\pm$ 17.2 g/cm^2 and then declined significantly after 4 minutes of stimulation reaching 47.7% of that developed at 30 s ($P<0.01$) by the end of the stimulation period. After 30 seconds of stimulation in the pump perfusion run, diaphragmatic tension averaged 83.7 $\pm$ 14.1 g/cm^2 (66.2% of that in the autoperfusion, High O_2-Low Flow run, $P<0.05$). Relative diaphragmatic tension in the pump perfusion run increased significantly after 2 minutes ($P<0.01$ in comparison with that at 30 s) and then declined reaching 76.5% of that developed at 30 s ($P<0.01$) by the end of the stimulation period. At any given time during the stimulation periods, the relative tension in the autoperfusion run was significantly lower than that in the pump perfusion run ($P<0.01$).

Group 2: Control values of phrenic arterial blood gases obtained in group 2 are listed in table 1. PaO_2 and pH were similar in the two runs, whereas $PaCO_2$ was significantly lower in the Low O_2-High Flow run in comparison with the High O_2-Low Flow run. Control values of

mean P_{art}, mean P_{phr}, arterial O_2 contents, and haematocrit in the low O_2-high flow run averaged 110 $\pm$ 6 mmHg, 198 $\pm$ 25 mmHg, 9.8 $\pm$ 1.1 ml/dl, and 20.1 + 2.8%, respectively. These values did not change during the stimulation period. Comparable values during the control period of High O_2-Low Flow run averaged 108 $\pm$ 5 mmHg, 153 $\pm$ 24 mmHg ($P<0.05$), 19.0 $\pm$ 2.2 ml/dl ($P<0.05$), and 37.7 $\pm$ 4.5% ($P<0.05$), respectively.

Figure 3 shows the changes in Qphr (top panel) and DO_2phr (bottom panel) in group 2. Control values of Qphr and DO_2phr in the Low O_2-High Flow run averaged 58.2 $\pm$ 4.2 and 5.6 $\pm$ 0.9 ml/100g/min, respectively. These values remained unchanged during the stimulation period. In comparison, control values of Qphr and DO_2phr of the High O_2-Low Flow run averaged 30.4 $\pm$ 3.8 and 5.6 $\pm$ 1.0 ml/100g/min, respectively with no change during the stimulation period. Qphr was significantly higher in the Low O_2-High Flow run compared to the High O_2-Low flow experiments ($P<0.01$) whereas DO_2phr was not significantly different.

Diaphragmatic tension (as a percent of that after 30 seconds of stimulation) during the High O_2-Low Flow and Low O_2-High Flow runs are plotted against time in figure 4. After 30 seconds of stimulation in the Low O_2-High Flow run tension averaged 165.1 $\pm$ 25.5 g/cm^2 and then declined significantly after 4 minutes ($p<0.05$) reaching 70% of that developed at 30 s ($P<0.01$) by the end of the stimulation period. In the High O_2-Low Flow run diaphragmatic tension generated after 30 seconds of stimulation averaged 163.5 $\pm$ 26.5 g/cm^2 (97% of that in the Low O_2-High Flow run) then declined significantly by minute 3 ($p<0.05$) and reached 56% of that developed at 30 s ($P<0.01$) by the end of the stimulation period. From minute 4 onward, relative tension developed at any given time was significantly lower in the High O_2-Low Flow experiments in comparison with Low O_2-High Flow experiments ($P<0.01$).

We also compared the rate of decline in tension during the first run group 1 with that of group 2 (ie: High O_2-Low Flow in group 1 with Low O_2-High Flow in group 2). DO_2phr was comparable between these two conditions (5.78 $\pm$ 0.7 and 5.6 $\pm$ 0.9 ml/100g/min respectively). Initial tension in the group 1 animals was lower than that in the group 2 animals (124 $\pm$ 17.2 vs. 165.1 $\pm$ 25.5 g/cm^2 respectively). The rate of loss of tension was significantly ($P<0.05$) greater and the relative tension at the end of the run significantly ($P<0.05$) lower (46.7 $\pm$ 3.8 vs. 70.0 $\pm$ 5.5 percent of that at 30 seconds respectively) in group 1 (High O_2-Low Flow) than in group 2 (Low O_2-High Flow).

DISCUSSION:

The main findings of this study are:

1) Increasing diaphragm blood flow retards development of diaphragmatic fatigue induced by intermittent submaximal contractions.

2) This effect results from the increase in blood flow itself and is independent of alterations in diaphragmatic oxygen delivery.

Critique:

Several criticisms may apply to these findings.

Within each group, the rate of loss of tension in fresh muscle was compared to that of muscle which had previously been fatigued. Loss of force following fatiguing contractions can persist for long periods of time and may, therefore, have impaired muscle performance in the second run. This effect, would have led to an underestimation of the improvement attributable to increased flow in group 1, and an overestimation in group 2. The high flow condition,

however, was associated with improvement in diaphragm tension whether it preceded (group 2) or followed (group 1) the low flow run. Furthermore, comparison of the rate of fatigue during the first runs of each group shows that despite comparable values for oxygen delivery and in the absence of previous fatigue, the group in which the muscle was pump perfused at a higher flow rate fatigued more slowly.

In the group 1 animals, the absolute value of the initial diaphragmatic tension during the second stimulation period (low O_2-High Flow) was lower than that during the first stimulation period (High O_2-Low Flow). Since the rate of muscle energy expenditure is dependent upon the generated tension (9), the lower rate of fatigue during Low O_2-High Flow perfusion in this group could have been due to higher oxygen delivery relative to the metabolic rate. This mechanism cannot, however, account for the difference between the initial runs of the two groups since, despite higher absolute tension, the diaphragm fatigued more slowly and to a lesser extent under Low O_2-High Flow conditions.

Whereas the pH and PO_2 were comparable under all conditions, the PCO_2 of the diluted blood perfusing the contracting diaphragm during the Low O_2-High Flow periods was significantly lower than that of the undiluted blood in the High O_2-Low Flow periods. This may have resulted from dilution of dissolved CO_2 and bicarbonate and from equilibration with gas in the mixing chamber during the dilution procedure. The possibility that hypocapnia may have contributed to the decrease in the rate of diaphragmatic fatigue with hyperperfusion through alterations in intracellular pH must be considered.

In resting skeletal muscle Bettice (10) has shown small changes in intracellular pH to accompany changes in extracellular PCO_2 comparable to that observed in the current study. In

resting muscle, however, the rate of CO_2 production is very low. Intracellular PCO_2 would therefore also be low and changes in extracellular PCO_2 would be expected to significantly alter the gradient for diffusion and therefore CO_2 clearance. Although intracellular PCO_2 has not been measured in exercising skeletal muscle, Kowalchuk et al. (11) found the PCO_2 of the venous effluent from human leg muscle to average 106 mmHg 30 seconds post exercise. Since the venous PCO_2 decayed rapidly once exercise had ceased, it is likely that the intracellular PCO_2 was much higher than this during the muscle contractions. Under these conditions, changes in arterial PCO_2, which are small in comparison, are unlikely to alter the gradient for CO_2 clearance enough to have a significant effect on intracellular pH.

The diaphragm also appears to be relatively insensitive to increases in intracellular pH in contrast to cardiac muscle in which intracellular alkalosis usually has a positive inotropic effect. In vivo in humans (12) and in dogs (13) hypocapnia has been shown to have no effect on diaphragmatic contractility. Similarly, in rat diaphragm strips in vitro, Shee and Cameron (14) found even extreme hyopocapneic alkalosis (PCO_2 7 mmHg, extracellular pH 8.15, intracellular pH 7.56) to have no effect on twitch height and to produce no change in contractile force during stimulation at 10 Hz. There was slowing of relaxation (therefore increased fusion and increased tension) at stimulation frequencies between 20 and 50 Hz at this pH but until this extreme level of alkalosis was reached, there was no effect on the force frequency curve. Therefore, although it cannot be excluded, a significant change in intracellullar pH is unlikely to have occurred and there is strong evidence that such a change would not have enhanced diaphragm performance.

Vascular isolation of an organ system, alters the pattern of blood flow delivery and could

potentially impair oxygen delivery. In this case, the intercostal and internal mammary contributions have been eliminated and the entire hemidiaphragm perfused by the inferior phrenic artery. In the canine diaphragm, however, extensive head to head anastomoses between the phrenic and internal mammary and intercostal systems have been demonstrated (15) and normal perfusion has been shown to persist despite occlusion of the internal mammary arteries (16). Hussain et al. (7) have shown, in the same preparation as used in the current study, that lissamine green B injection into the inferior phrenic artery results in coloration of the entire hemidiaphragm. Finally, resting diaphragmatic blood flow in this preparation was not lower than that reported in intact dogs (17,18).

Comparison with previous studies:

In canine gastrocnemius muscle, Barclay (6) studied the effect of hyperperfusion with constant O_2 delivery on the rate of fatigue during a 20 minute continuous isometric contraction induced by stimulation of the sciatic nerve at 5 Hz. Under these conditions, fatigue was most rapid when the muscle was autoperfused. Maintaining constant muscle blood flow during the contraction by pump perfusion was associated with a slower fatigue rate. Increasing blood O_2 content at the same rate of blood flow by increasing the inspired oxygen concentration to 100% had no further effect. Hyperperfusion while maintaining a constant rate of O_2 delivery (either by haemodilution or by administration of a hypoxic gas mixture) further retarded the rate of force loss. While differences in the type of contraction induced hampers direct comparison of these findings with our current results, the observations are compatible.

Supinski et al. (3) studied the effect of mechanical hyperperfusion with undiluted fully saturated blood on the force-frequency relationship of canine diaphragm strips in which fatigue

had been induced by rhythmic (15/min., duty cycle = 0.5) high intensity (80% maximum) isometric contractions. They found that increasing perfusion pressure partially restored the tension generated at both high and low frequencies of stimulation. No effort was made by these investigators to determine what component of this effect was related to changes in blood flow independent of oxygen delivery. The results of our current study, therefore, extend their finding of a beneficial effect of hyperperfusion on contractility of diaphragmatic muscle with established fatigue to the process of fatigue development in the fresh non-isometrically contracting muscle. We further demonstrate that, as in limb muscle, this improvement is not related to changes in total muscle oxygen or plasma born substrate delivery (assuming plasma dilution proportional to the change in haematocrit).

Mechanisms of improved diaphragm function:

The mechanisms underlying the development of fatigue in skeletal muscle are unknown. The disruption of cellular organelles involved in excitation-contraction coupling, have been identified, but are unlikely to be influenced by the level of blood flow. Similarly, central factors may contribute to the loss of force generation during voluntary contractions in conscious subjects but are unlikely to be important determinants of the rate of diaphragm fatigue during electrophrenic stimulation in anaesthetized animals. Failure of excitation is known to contribute to fatigue during stimulation at high frequencies (100 Hz) (19). Recovery occurs quickly, however, when the stimulus rate is reduced to 20 Hz (20), therefore this mechanism is unlikely to account for changes in contraction intensity during stimulation at 10 Hz in the current experiments.

Other mechanisms which are more likely to have played a role in the blood flow related

changes in contractility include the following:

1) Improved availability of O_2 and substrate at the cellular level. The availability of O_2 and plasma-born substrate to the contracting muscle cells is not purely a function of total muscle delivery. Compensatory increases in tracer transport during partial arterial occlusion (21), dissociation between permeability-surface area and total vascular resistance with increasing metabolic rate (22) and changes in the site of local microvascular control with changes in venous O_2 tension (23) have been demonstrated in skeletal muscle. These findings indicate that factors under local control may affect solute exchange and play a role in the maintenance of tissue oxygenation. Therefore, whereas changes in total muscle oxygen and substrate delivery cannot account for the observed improvement in diaphragm function, the relationship between substrate availability and demand may have been modified on a regional level as a consequence of changes in flow.

2) Increased perfusion pressure. Since P_{phr} was significantly higher in the Low O_2-High Flow runs than in the High O_2-Low Flow runs in both groups of animals, our experiments do not differentiate between pressure and flow dependent mechanisms. The effect of perfusion pressure, independent of blood flow on skeletal muscle function has not been investigated. In the myocardium, however, a relationship between coronary artery pressure and myocardial oxygen consumption (24) and contractility (25) has been demonstrated. Perfusion pressure may influence muscle metabolism in several ways. In resting canine skeletal muscle, Appelgren (26) has demonstrated that the homogeneity of blood flow (as reflected by capillary diffusion capacity for iodide) is related to perfusion pressure. A more homogeneous flow pattern may increase proportion of total muscle flow directed through nutrient vessels and the recruitment of new

capillary channels would shorten the radius for oxygen diffusion.

In contracting muscle, intraluminal pressure may be of additional importance. Petrofsky et al. (27) have demonstrated improved endurance of canine limb muscle when perfusion pressure was maintained above intramuscular pressure and suggested that the autoregulatory mechanisms which permit matching of blood flow to metabolic requirements require sufficient transmural pressure to maintain vascular patency.

Recently, perfusion pressure has also been shown to influence the magnitude of flow dependent changes in resistance of coronary arterioles (28). It is likely, therefore, that perfusion pressure interacts with endothelium dependent and metabolic factors in the control of the capillary surface available for diffusion of oxygen and plasma born substrate.

In addition to metabolic effects, changes in perfusion pressure may alter the mechanical properties of the muscle. Distention of the vessels may lengthen the muscle fibers producing an apparent increase in contractility through internal preloading (25).

*3) **Changes in the extracellular milieu.*** The extracellular ionic composition is highly sensitive to changes capillary perfusion. For example, Mainwood et al. (29) found extracellular pH to be highly dependant on the ratio of metabolic load to perfusion. As a result, changes in perfusion cause rapid alterations in the transmembrane efflux of H^+ (29). Intracellular H^+ accumulation negatively influences contraction at several levels. These include inhibition of the Na^+/K^+ pump on which the resting membrane potential (and therefore excitability) of the sarcoplasmic reticulum (SR) depends (30), impaired Ca^{++} release from the SR (31), competitive inhibition of Ca^{++} binding to troponin C (32) and direct inhibition of the interaction between actin and myosin (33).

Inorganic phosphate (Pi) has also received attention as an ion whose accumulation may contribute to force loss through direct effects on the contractile process. In skinned muscle fibres (34) and in human forearm muscle (35) a unique relationship can be demonstrated between force generation and the concentration of the diprotonated form of Pi ($H_2PO_4^-$) even when the effect of pH is extracted or altered by prior fatiguing exercise. Since high concentrations of intracellular H^+ favour the existence of Pi in its diprotonated form, this provides another mechanism whereby perfusion related changes in the extracellular environment may exert a potent influence on the rate of fatigue.

Implications:

Traditionally, respiratory muscle fatigue has been thought to occur and contribute to respiratory failure when the supply of nutrients to these muscles is insufficient to meet their metabolic demand (1). Not surprisingly, therefore, steps to increase oxygen, and other substrate, delivery to the ventilatory muscles have been advocated in the management of patients (2,3). Our findings indicate that this concept needs modification. Increased oxygen delivery may be accomplished by increasing blood flow or oxygen content. We suggest that the latter approach is less likely to achieve the desired goal of improving respiratory muscle function than are measures to increase cardiac output and specifically, respiratory muscle blood flow.

Acknowledgements:

The authors thank S. Nuara for his technical assistance. M. Ward is a fellow of the Medical Research Council of Canada, S. Magder is a scholar of the Fonds de Research en Santé du Quebec, S. Hussain is a scholar of the Canadian Heart and Stroke Foundation. The study was funded by a grant from the Medical Research Council of Canada.

References:

1. Macklem PT, Roussos CS, Respiratory muscle fatigue: a cause of respiratory failure? Clin Sci Mol Med. 1977; 53:419-422
2. Aubier M, Murciano D, Menu Y, Boczkowski J, Mal H, Pariente R, Dopamine effects on diaphragmatic strength during acute respiratory failure in chronic obstructive pulmonary disease. Ann Int Med 1989; 110:17-23
3. Supinski G, Dimarco A, Ketai L, Hussein F, Altose M, Reversibility of diaphragm fatigue by mechanical hyperperfusion. Am Rev Respir Dis 1988; 138:604-609
4. Barclay JK, Stainsby WM, The role of blood flow in limiting maximal metabolic rate in muscle. Med Sci Sports 1975; 7:116-119
5. Barclay JK, Boulianne CM, Wilson BA, Tiffin SJ, Interaction of hyperoxia and blood flow during fatigue of canine skeletal muscle in situ. J Appl. Physiol 1979; 47:1018-1024
6. Barclay JK, A delivery-independent blood flow effect on skeletal muscle fatigue. J Appl Physiol 1986; 61:1084-1090
7. Hussain SNA, Roussos C, Magder S, In situ isolated perfused and innervated left hemidiaphragm preparation. J Appl Physiol 1989; 67:2141-2146
8. Close RI, The dynamic properties of mammalian skeletal muscles. Physiol Rev 1972; 52:129-197
9. Gladden LB, MacIntosh BR, Stainsby WN, O_2 uptake and developed tension during and after fatigue, curare block and ischemia. J Appl Physiol 1978; 45:751-755
10. Bettice JA, Effect of hypocapnia on intracellular pH during metabolic acidosis.

Respiration Physiol 1979 38: 257-266

11. Kowalchuk JM, Heigenhauser GJF, Lindinger MI, Sutton JR, Jones L, Factors influencing hydrogen ion concentration in muscle after intense exercise. J Appl Physiol 198 65: 2080-2089

12. Juan G, Calverly P, Talamo C, Schnader J, Roussos C, Effect of carbon dioxide on diaphragmatic function in human beings. N Engl J Med 1984; 310:874-879

13. Schnader JY, Juan G, Howell S, Fitzgerald R, Roussos C, Arterial CO_2 partial pressure affects diaphragmatic function. J Appl Physiol 1985; 58:823-829

14. Shee CD, Cameron IR, The effect of pH and hypoxia on function and intracellular pH of the rat diaphragm. Respiration Physiol 1990 79: 57-68

15. Comptois A, Gorczyca W, Grassino A, Anatomy of diaphragmatic circulation. J Appl Physiol 1987 62: 238-244

16. Lockhat D, Magder S, Roussos C, Collateral sources of costal and crural diaphragmatic blood flow. J Appl Physiol 1985 59: 1164-1170

17. Rochester DF, Bettini G, Diaphragmatic blood flow and energy expenditure in the dog. Effects of inspiratory airflow resistance and hypercapnia. J Clin Invest 1976 57: 661-672

18. Robertson CH, Pagel MA, Johnson RL, The distribution of blood flow, oxygen consumption and work output among the respiratory muscles during unobstructed hyperventilation. J Clin Invest 1977 59: 43-50

19. Krnjevic K, Miledi R, Failure of neuromuscular propagation in rats. J. Physiol Lond. 1958; 140:440-461

20. Jones DA, Bigland-Ritchie B, Edwards RHT, Excitation frequency and muscle fatigue:

Mechanical response during voluntary and stimulated contractions. Exp. Neurol. 1979; 64:401-413

21. Bolme P, Edwall L, Dissociation of tracer disappearance rate and blood flow in isolated skeletal muscle during various vascular reactions. Acta Physiol Scand 1971; 82:17-21

22. Renkin EM, Hudlicka O, Sheehan RM, Influence of metabolic vasodilation on blood-tissue diffusion in skeletal muscle. Am J Physiol 1966, 211:87-98

23. Granger HJ, Goodman AH, Granger DN, Role of resistance and exchange vessels in local microvascular control of skeletal muscle oxygenation in the dog. Circ Res 1976; 38:379-385

26. Gregg DE, Effect of coronary perfusion pressure or coronary flow on oxygen usage of the myocardium. Circulation Research 1963; 13:497-500

25. Scharf SM, Bromberger-Barnea B, Influence of coronary flow and pressure on cardiac function and coronary vascular volume. Am J Physiol 1973 224:918-925

26. Appelgren KL, Effect of perfusion pressure and haematocrit on capillary flow and transport in hyperaemic skeletal muscle of the dog. Microvascular research 1972; 4:231-246

27. Petrofsky JS, Hendershot DM, The interrelationship between blood pressure, intramuscular pressure and isometric endurance in fast and slow twitch skeletal muscle in the cat. Eur J Appl Physiol 1984; 53:106-111

28. Kuo L, Davis MJ, Chilian WM, Endothelium-dependent, flow-induced dilation of isolated coronary arterioles. Am J Physiol 1990; 259 (Heart Circ. Physiol. 28): H1063-H1070

29. Mainwood GW and Renaud JM, The effect of acid-base balance on fatigue of skeletal muscle. Can. J. Physiol. Pharmacol. 1985; 63:403-416

30. Inesi G and Hill TL, Calcium and proton dependence of sarcoplasmic reticulum ATPase. Biophys J. 1983; 44:271-280

31. Nakamaru Y and Schwartz A, The influence of hydrogen ion on the sarcoplasmic reticulum. J. Gen. Physiol 1972; 59:22-32

32. Fuchs F, Reddy Y, Briggs FN, The interaction of cations with the calcium-binding site of troponin. Biochim. Biophys. Acta 1970; 221:407-409, 1970

33. Fabiato A, Fabiato F, Effects of pH on the myofilaments and the sarcoplasmic reticulum of skinned cells from cardiac and skeletal muscles. J. Physiol. Lond. 1978; 276:233-255

34. Nosek TM, Fender KY, Godt RE, It is diprotonated inorganic phosphate that depresses force in skinned skeletal muscle fibres. Science 1987; 236:191-193

35. Wilson JR, McCully KK, Mancini DM, Boden B, Chance B, Relationship of muscular fatigue to pH and diprotonated Pi in humans: a ^{31}P-NMR study. J Appl Physiol 1988; 64:2333-2339

Table 1.

Control values of phrenic arterial blood gases in groups 1 and 2.

Group	Run	pH	PaO_2	$PaCO_2$
Group 1				
	Autoperfusion High O_2-Low flow	7.28 ± 0.02	132.0 ± 21.4	34.5 ± 2.4
	Pump perfusion Low O_2-High flow	7.28 ± 0.02	130.1 ± 17.5	19.1 ± 2.8**
Group 2				
	Low O_2-High Flow	7.31 ± 0.03	145.8 ± 22.8	14.3 ± 2.8
	High O_2-Low Flow	7.30 ± 0.03	152.7 ± 32.0	35.3 ± 5.1**

Values are mean ± SEM. PaO_2 and $PaCO_2$ are expressed in mmHg. ** $P<0.01$ between runs in a given group.

FIGURE LEGENDS:

Figure 1: Changes in diaphragmatic blood flow (Qphr, top panel) and oxygen delivery (DO_2phr, bottom panel) with time during autoperfusion (High O_2-Low Flow) and pump perfusion (Low O_2-High Flow) in the group 1 animals. Note that the initial rise in Qphr and DO_2phr in the autoperfusion run corresponds with the onset of stimulated contraction. Values are means ± SEM.

Figure 2: Diaphragmatic tension as a fraction of that generated after 30 seconds of stimulation is plotted against time during autoperfusion (High O_2-Low Flow) and pump perfusion (Low O2-High Flow) in the group 1 animals. Values are means ± SEM.

Figure 3: Changes in diaphragmatic blood flow (Qphr, top panel) and oxygen delivery (DO_2phr, bottom panel) with time during pump perfusion with undiluted blood at low flow rate (High O_2-Low Flow) and with diluted blood at high flow rate (Low O_2-High Flow) in the group 2 animals. Values are means ± SEM.

Figure 4: Diaphragmatic tension as a fraction of that generated after 30 seconds of stimulation is plotted against time during pump perfusion with undiluted blood at low flow rate (High O_2-Low Flow) and with diluted blood at high flow rate (Low O_2-High Flow) in the group 2 animals. Values are means ± SEM.

FIGURE 1

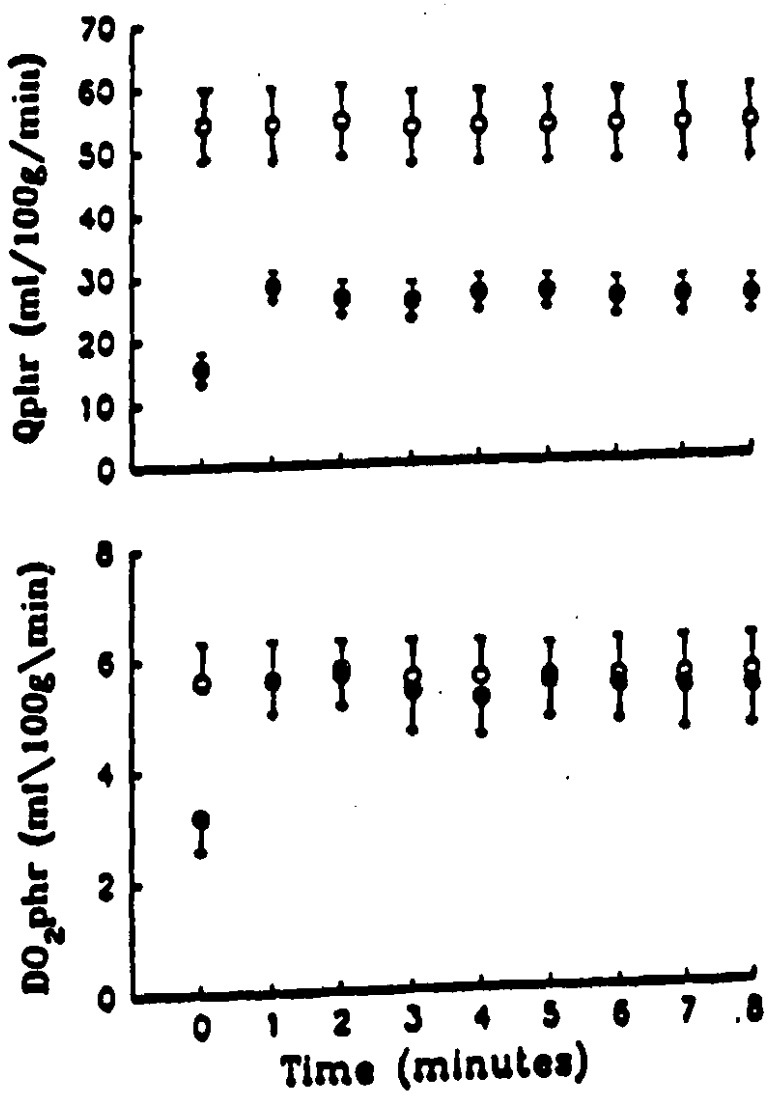
Qphr (ml/100g/min)
70
60
50
40
30
20
10
0
DO_2phr (ml\100g\min)
8
6
4
2
0
0 1 2 3 4 5 6 7 8
Time (minutes)

FIGURE 2

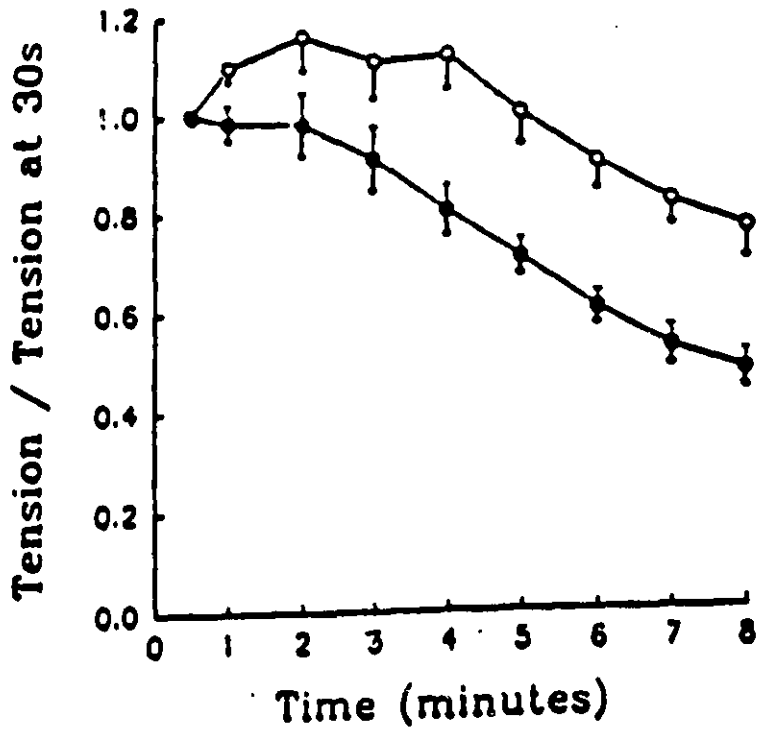
Tension / Tension at 30s
1.2
1.0
0.8
0.6
0.4
0.2
0.0
0
1
2
3
4
5
6
7
8
Time (minutes)

FIGURE 3

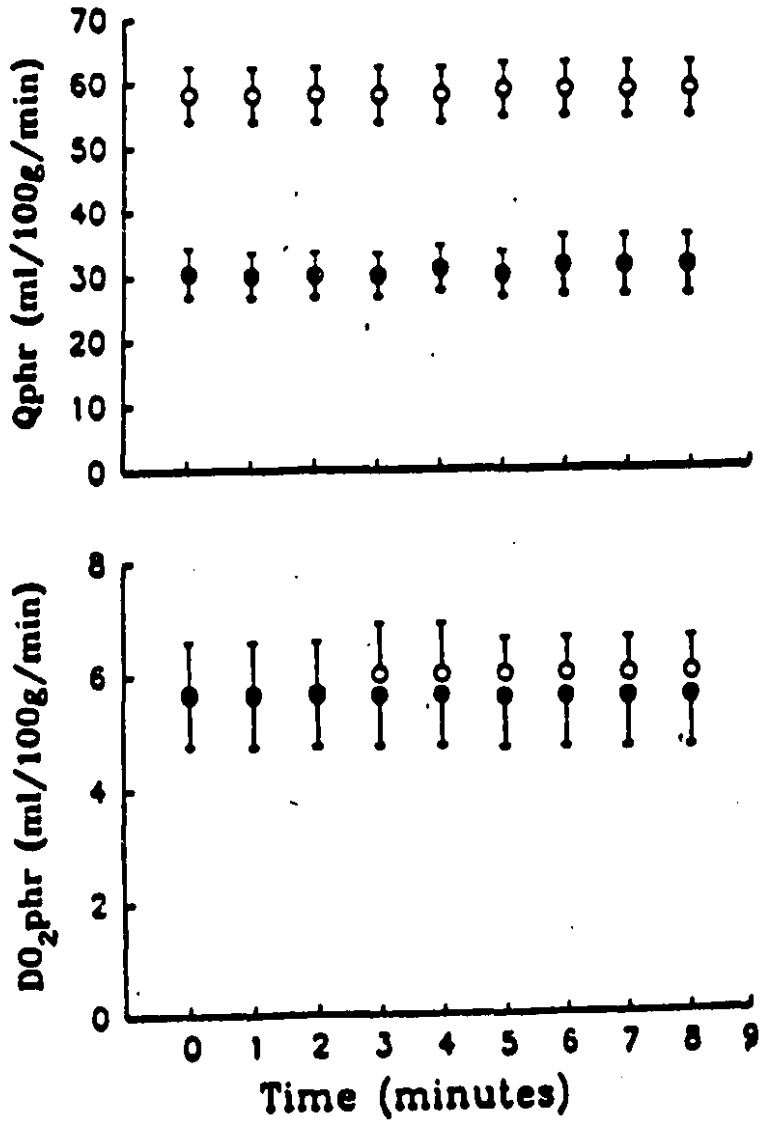
70
60
50
40
30
20
10
0
Qphr (ml/100g/min)
8
6
4
2
0
DO_2phr (ml/100g/min)
0 1 2 3 4 5 6 7 8 9
Time (minutes)

FIGURE 4

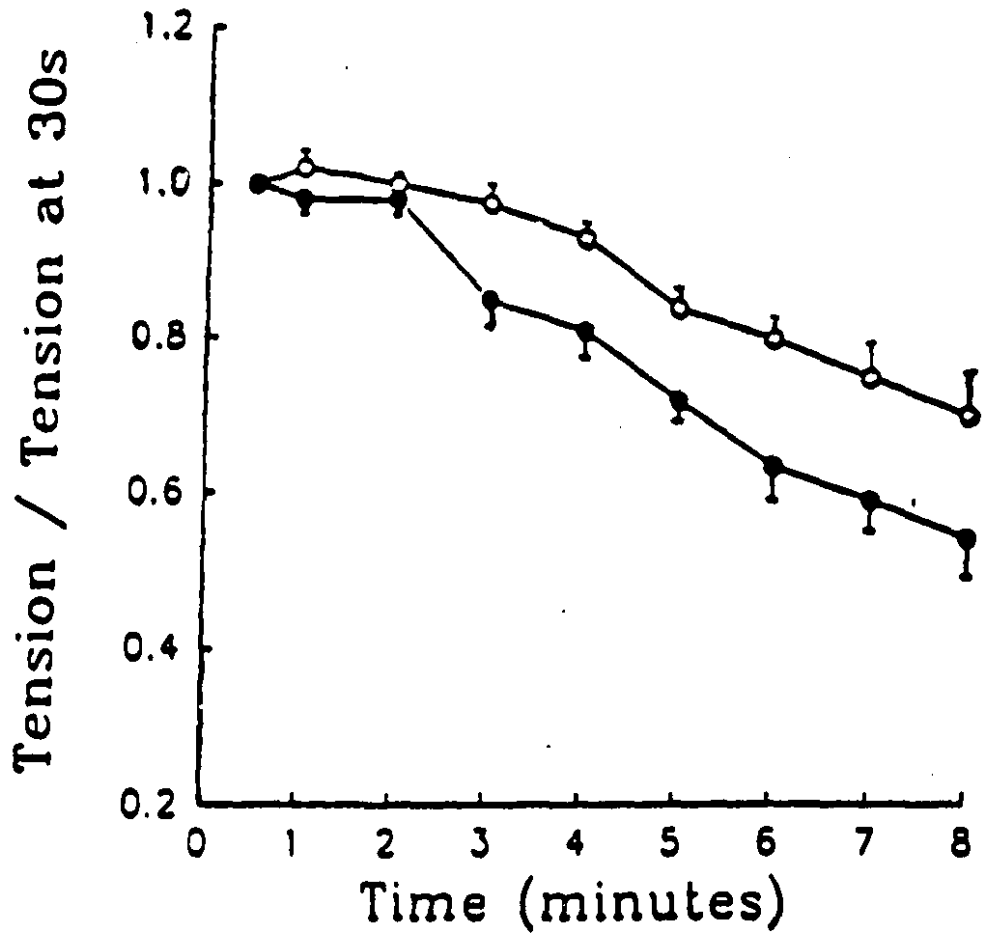
Tension / Tension at 30s
1.2
1.0
0.8
0.6
0.4
0.2
0
1
2
3
4
5
6
7
8
Time (minutes)

Systemic and Diaphragmatic Oxygen Delivery-Consumption Relationships during Haemorrhage

Michael E. Ward, Han Chang, Filippo Erice and Sabah N. A. Hussain
Journal of Applied Physiology 1994 - In Press

ABSTRACT

When tissue oxygen delivery falls below a critical threshold, tissue oxygen uptake becomes limited. In this study, we compared the critical O_2 delivery and the critical and maximum O_2 extraction ratios of the resting and contracting left hemidiaphragm with those of the non-diaphragmatic tissues in 7 dogs. The left hemidiaphragm was perfused through the left inferior phrenic artery with arterial blood from the left femoral artery. Phrenic venous blood was sampled through a catheter in the inferior phrenic vein. Systemic O_2 delivery was reduced in stages by controlled haemorrhage. Left diaphragm O_2 consumption during rest and during 3 minutes of continuous (3Hz) stimulation of the left phrenic nerve, and the O_2 consumption of the remaining non-left hemidiaphragmatic tissues were measured at each stage. Critical diaphragmatic O_2 delivery for the resting diaphragm averaged 0.8 ± 0.16 ml/min/100g with a critical O_2 extraction ratio of $65.5 \pm 6\%$. In the contracting diaphragm, the critical diaphragmatic O_2 delivery and critical O_2 extraction ratio averaged 5.1 ± 0.9 ml/min/100g and $81 \pm 5\%$ respectively. Whole body O_2 delivery at which resting diaphragm O_2 consumption became supply limited was similar to that for non-diaphragmatic tissues. By comparison, supply limitation of O_2 consumption occurred at a higher systemic O_2 delivery in the contracting diaphragm than in the rest of the body despite the increase in critical diaphragmatic extraction ratio. Thus, oxygenation of the isolated diaphragm does not appear to be preferentially preserved during generalized reductions in O_2 delivery. These results suggest that in diseases associated with increased work of breathing and decreased O_2 delivery, the diaphragm may become metabolically impaired before limitation of O_2 consumption is observed systemically.

Key Words: respiratory muscles, diaphragm, blood flow, oxygen consumption

INTRODUCTION

At normal levels of O_2 delivery, tissue O_2 uptake (VO_2) remains largely independent of O_2 delivery because of compensatory changes in O_2 extraction (6,33). In tissues with high metabolic requirements the ability to meet their metabolic needs is protected by two mechanisms. Regional changes in resistance vessel tone redistribute blood flow away from low extraction tissues toward more metabolically active areas (7,33). Simultaneously, an increase in capillary density allows extraction to lower end capillary O_2 contents without producing areas of tissue anoxia due to diffusion limitation (20). However, if O_2 delivery decreases below a critical threshold, VO_2 is depressed because the increase in extraction is no longer proportional to the fall in delivery (8). The onset of delivery dependence of O_2 consumption does not occur simultaneously in all tissues (22). Differences in maximal capillary density, intensity of myogenic reactivity to changes in vascular transmural pressure and sensitivity of the microvasculature to metabolic feedback among different organ systems may all contribute to this variation.

Maintenance of substrate supply to the respiratory muscles in proportion to their metabolic requirements is necessary to survival. Moreover, the diaphragmatic circulation must maintain this balance despite the fluctuations in transmural pressure (14) which occur during the respiratory cycle. On the basis of these considerations, and the finding that respiratory muscle oxygen delivery is preferentially maintained during circulatory shock, Viires et al. (35) suggested that the regulatory mechanisms responsible for the matching of oxygen supply to oxygen demand may be more developed in these muscles than in other tissues. In their study, however, diaphragm work was changing and increases in blood flow may have been in response

to changes in metabolic rate. Diaphragmatic O_2 consumption, furthermore, was not monitored so its relationship to oxygen delivery could not be determined. Others (3,26-29,32) have measured diaphragmatic oxygen consumption during respiratory loading and during hypotension, but the relationship between diaphragmatic O_2 delivery and O_2 consumption was not addressed. This is because the lack of an isolated diaphragm preparation placed technical limitations on the measurement of diaphragm blood flow. The use of radioactive microspheres does not permit sufficient sequential measurements to plot the entire relationship and, since the diaphragm derives its blood supply from multiple sources, oxygen delivery cannot be determined from measurements of flow through easily accessible arteries.

In this study, we used the in-situ isolated left diaphragm to determine the critical diaphragmatic O_2 delivery and the critical and maximum diaphragmatic O_2 extraction ratios. These were compared to those of the rest of the body to determine whether local compensatory mechanisms may exist to protect the diaphragm from the onset of tissue hypoxia during generalized reductions in oxygen availability.

METHODS

Animal Preparation: Seven mongrel dogs (28.8 $\pm$ 0.97 kg SD) were anaesthetized with sodium thiopental (10 mg/kg) followed by α-chloralose (60-80 mg/kg). Supplemental doses of α-chloralose were given as needed to eliminate the jaw tone but maintain knee reflexes. The animals were supine, intubated with a cuffed endotracheal tube and mechanically ventilated (tidal volume 15 ml/kg, frequency of 15 /min). Supplemental O_2 was supplied through the inspiratory line and arterial PO_2 maintained above 100 mmHg. Positive end-expiratory pressure (PEEP)

(5 cm) was applied at the expiratory line. A catheter was placed in the aorta through the right carotid artery to monitor arterial pressure (P_{art}) and another catheter was placed in the right femoral vein to administer fluids. A balloon tipped thermodilution pulmonary artery catheter (Edwards Laboratories, Santa Ana, Ca) was placed into the pulmonary artery through the right internal jugular vein and used to measure cardiac output (CO) by thermodilution and to draw samples of mixed venous blood. Core body temperature was kept constant at approximately 37° C by a heating pad placed under the animal.

Isolated left hemidiaphragm: In all animals, we used the in-situ vascularly isolated left hemidiaphragm preparation previously reported in detail (16). Briefly, the intercostal vessels and the left internal mammary artery were ligated and the lower left ribs were removed. Through an abdominal incision, the two halves of the diaphragm were divided. The ribs and cartilages of the free costal margin were secured by silk threads to 3 metal bars attached through their centers to force transducers (Grass model FT10). To ensure independent movement of the bars, we severed the interconnecting rib portions. The stomach, liver, spleen, and left kidney were retracted to expose the left phrenic artery. This artery was ligated proximally and a polyethylene catheter (PE 160, 1.14 mm ID, 1.57 mm OD, 3 cm long) was introduced into the distal portion. A side port in the catheter was used for measurement of phrenic perfusion pressure (P_{phr}). The catheter was connected to an electromagnetic flow probe (Carolina Medical Electronics, 1.91 mm ID). The pressure-flow relationship of the catheter-probe system was linear over the range of flows in the study with conductance = 2.6 ml/min/mmHg. Phrenic arterial flow measured by the probe was designated as Q_{phr}. The other side of the probe was

connected to a catheter in the left femoral artery, thereby, perfusing the diaphragm with blood flow diverted from the left femoral artery. All animals were heparinized after catheterizing the phrenic artery.

To sample phrenic venous blood, a polyethylene catheter (PE280, 2.15 mm ID, 3.25 mm OD) was introduced into the left inferior phrenic vein through the left femoral vein and secured by a silk suture through the central tendon. The venous blood was collected in a container and reinfused through the femoral venous line.

The temperature of the diaphragm was monitored continuously using a temperature probe fixed to the surface of the isolated hemidiaphragm (Mon-a-therm, Model 6000, Zimmer of Canada Ltd., Mississauga, Ont.) and maintained between 37.5 and 38.5°C using a heat lamp if required. At the end of the experiment the animals were exsanguinated and the diaphragm was dissected free and weighed.

Phrenic nerve stimulation: Bipolar electrodes were placed around the left phrenic nerve close to its exit from the diaphragm. The electrodes were connected through an isolation unit (Grass SIU5) to a stimulator (Grass S48). Maximum stimulation of the left diaphragm was achieved by delivering a single stimulus (0.2 ms duration) with progressively increasing voltage. The voltage output was then set 2 volts higher than the last voltage found to produce an increment in diaphragm tension. During contraction periods, the left phrenic nerve was stimulated continuously at 3 Hz for 3 minutes.

Oxygen Delivery and Consumption Measurements: Systemic arterial, mixed venous, and phrenic venous blood O_2 contents (CaO_2, CvO_2, CvO_2,di, respectively) were measured with a co-oximeter (Instrumentation Laboratory IL-182). The arterial O_2 content was multiplied by CO to obtain the systemic (whole body) oxygen delivery, by CO minus Q_{phr} to obtain the O_2 delivery to tissues other than the left hemidiaphragm and by Q_{phr} to obtain left hemidiaphragm O_2 delivery. The oxygen consumption of the left hemidiaphragm (VO_2,di) was calculated as:

$VO_2,di = (CaO_2 - CvO_2,di) \cdot Q_{phr}$.

Non-left hemidiaphragm oxygen consumption (VO_2) was calculated as:

$VO_2 = (CaO_2 - CvO_2) \cdot (CO - Q_{phr})$.

All values were normalized for tissue weight.

Note that the right hemidiaphragm in these anaesthetized, mechanically ventilated animals was resting. Its blood flow and O_2 delivery are, therefore, similar to those recorded in the left hemidiaphragm at rest. These are very small in comparison to the cardiac output and to the systemic O_2 delivery ($<0.5\%$) even during the final stage of the experiments. Therefore, although the systemic O_2 delivery, calculated as the product of CaO_2 and CO minus Q_{phr}, and the O_2 consumption, calculated as CaO_2-CvO_2 times CO-Q_{phr}, include contributions of the right hemidiaphragm, changes in these parameters reflect, overwhelmingly, the O_2 delivery to and the O_2 consumption of the non-diaphragmatic tissues.

Experimental Protocol: Thirty minutes after the surgery was completed, with the animal in steady state, cardiac output was measured, P_{phr} and Q_{phr} were recorded and arterial, mixed venous and phrenic venous blood samples were drawn for determination of blood gas tensions

and O_2 content. Stepwise haemorrhage was then begun by withdrawing blood in 50 to 100 ml aliquots from the left femoral arterial line. Haemorrhage was continued until the animal could no longer maintain a stable blood pressure. This resulted in the performance of eight to 12 stages of haemorrhage in each animal. After steady state was reached at each stage, cardiac output, P_{phr}, Q_{phr} were then recorded and arterial, mixed venous and phrenic venous blood samples were drawn. The phrenic nerve was then stimulated as described above and the measurements were repeated at the end of the contraction period at each stage.

Data Analysis: The following critical O_2 deliveries were determined: 1) The whole body O_2 delivery ($CaO_2 \cdot CO$) at which VO_2 and VO_2,di (resting and contracting) became supply dependent, 2) The non-diaphragmatic O_2 delivery ($CaO_2 \cdot CO \cdot Q_{phr}$) at which VO_2 became supply dependent, and 3) The diaphragmatic O_2 delivery at which VO_2,di (resting and contracting) became supply dependent. For each calculation, the appropriate O_2 delivery was plotted on the x axis against the corresponding O_2 consumption on the y axis (see figures 1 & 2). For each animal, the data were sorted as O_2 delivery and O_2 consumption pairs with increasing O_2 delivery. All possible regression lines were then calculated as the data was grouped pair by pair into high and low O_2 delivery subsets. The pair of lines that resulted in the smallest sum of squared residuals was used in further calculations (31). The critical O_2 delivery was then determined by solving the equations describing the regression lines for the values of these variables at the point of intersection.

The critical O_2 extraction ratios at the point of onset of delivery dependence of VO_2,di with the muscle at rest and during phrenic nerve stimulation were calculated as the ratios of the

respective phrenic arteriovenous O_2 content differences to the arterial O_2 content when the critical point corresponded to a direct measurement of O_2 delivery. When this was not the case, the critical extraction ratio was estimated by linear interpolation using values measured during the two stages bracketing the point of critical O_2 delivery. The maximum O_2 extraction ratios for the diaphragm (resting and contracting) were calculated as the ratios of the respective arteriovenous O_2 content differences to the arterial O_2 content during the final stage of each experiment. Similarly, when possible, the critical O_2 extraction ratio for the whole body (excluding the left diaphragm) was calculated as CaO_2-CvO_2 divided by CaO_2 at the point of onset of delivery dependence of VO_2 and otherwise by interpolation.

Differences among mean values for the whole body and for the resting and contracting diaphragmatic variables were evaluated using one way analysis of variance (ANOVA). If the ANOVA revealed significant ($p < 0.05$) differences among the means, the differences between individual means were assessed using paired t-tests. P values less than 0.05 were considered significant. All values are reported as means $\pm$ SEM.

RESULTS

Values for haemoglobin, P_{art}, cardiac output and arterial blood gases prior to beginning the haemorrhage protocol and during the final stage of the experiments are presented in table 1. Values of PvO_2,di, phrenic arteriovenous O_2 content difference and VO_2,di prior to beginning the haemorrhage protocol, during the stage just prior to the onset of O_2 delivery dependence of VO_2,di and during the final stage of the experiments are presented in table 2. The phrenic perfusion pressure at the onset of delivery dependence of VO_2di was 73.6$\pm$7.5 and 108.6$\pm$8.4

mmHg for the resting and contracting diaphragm respectively. The tension generated by the contracting diaphragm averaged 45.8 ± 5.8 g prior to haemorrhage and 41.2 ± 5.5 g during the final stage. This difference was not statistically significant.

Figures 1 and 2 display data obtained from one representative animal. In figure 1 the relationship between QO_2di and VO_2,di during stimulated contraction is compared with that obtained while the diaphragm was at rest. In figure 2, the relationships between whole body O_2 delivery and VO_2 (top panel) and between whole body O_2 delivery and VO_2,di (resting and contracting, bottom panel) are plotted. The regression lines calculated for each relationship in this animal are also included to illustrate the method for determination of critical O_2 delivery.

The critical diaphragmatic oxygen delivery and the critical and maximal oxygen extraction ratios for the resting and the contracting diaphragm are presented in figure 3. The diaphragmatic O_2 delivery and the O_2 extraction ratio at the point of onset of O_2 supply dependence of VO_2,di were both significantly higher for the contracting than for the resting diaphragm.

In figure 4, the whole body O_2 deliveries at which VO_2 and VO_2,di (resting and contracting) became dependent on O_2 supply are plotted. The O_2 consumption of the resting diaphragm and the non-diaphragmatic tissues became delivery dependent at the same level of whole body O_2 delivery. In contrast, the O_2 consumption of the contracting diaphragm became supply limited at a whole body O_2 delivery well above that at which non-diaphragmatic O_2 consumption became supply dependent.

The critical diaphragmatic O_2 delivery with the diaphragm at rest was 0.8±0.16 ml/min/100g which did not differ significantly from the critical non-diaphragmatic O_2 delivery

(0.7±0.08 ml/min/100g). Similarly the critical O_2 extraction ratio for the resting diaphragm (0.65±0.08) was not significantly different from the critical O_2 extraction ratio for the non-diaphragmatic tissues (0.62±0.08).

The maximum recorded O_2 extraction ratio for the whole body was 0.91±0.022. This value is significantly higher than that of the resting diaphragm but not different from that of the contracting diaphragm.

DISCUSSION

The main findings of this study are:

1) During 3 Hz contractions, the critical diaphragmatic O_2 delivery and extraction ratio increased above those of the resting diaphragm.

2) During 3Hz diaphragmatic contractions, the whole body O_2 delivery at which diaphragmatic O_2 consumption became supply dependent was higher than that at which the oxygen consumption of the non-diaphragmatic tissues became supply dependent.

3) Critical diaphragmatic O_2 delivery and the critical O_2 extraction ratio for the resting diaphragm did not differ from those of the non-diaphragmatic tissues.

Considerations of Methods:

Certain aspects of the experimental preparation and protocol require consideration. First: it is known that the internal mammary and intercostal arteries contribute to the arterial supply of the intact diaphragm (9). It is, therefore, possible that ligation of these arteries in our

preparation might have resulted in hypoperfusion of the diaphragm. Blood flow and O_2 consumption of the resting and contracting diaphragm measured at the initial arterial pressure, however, were comparable to those reported for the intact diaphragm during mechanical ventilation and resistive breathing, respectively (26-29). In addition, resting diaphragmatic blood flow values measured at low arterial pressure are similar to those reported by Viires et al. (35) for the intact diaphragm during mechanical ventilation and hypotension. In spite of these results and in spite of the fact that maximum diaphragmatic O_2 extraction in our study is similar to that reported for the intact diaphragm (26), we cannot exclude the possibility that we may have restricted the total cross sectional area of diaphragmatic vascular bed and increased maldistribution of intradiaphragmatic blood flow. It is, therefore, likely that the isolation procedure may have elicited a state of increased diaphragmatic O_2 demand which in turn may alter the point of critical O_2 delivery. These possibilities should be considered before one makes any extrapolation of our results to the condition of intact diaphragm.

Second: the use of artificial stimulation to increase diaphragmatic O_2 demands can be criticized on the basis that the pattern of motor unit recruitment is different from that occurring during spontaneous diaphragmatic contractions. Although preferable, the use of spontaneous contractions as a mean to alter diaphragmatic metabolic demands is difficult to control especially when arterial pressure is changing as in our study. Reduction of arterial pressure is usually associated with a significant augmentation of diaphragmatic recruitment. Accordingly, changes in arterial pressure may result in significant alterations in diaphragmatic O_2 uptake irrespective of diaphragmatic O_2 delivery. Based on this, we chose to stimulate the diaphragm artificially to maintain diaphragmatic O_2 demands constant so that changes in diaphragmatic O_2 uptake can

be related to alterations in diaphragmatic O_2 delivery. We also sectioned the left phrenic nerve proximally to eliminate spontaneous diaphragmatic contractions. The choice of continuous 3 Hz stimulation of the phrenic nerve is based on our previous study (15) in which we have demonstrated that low frequency phrenic nerve stimulation elicits moderate increases in diaphragmatic blood flow and O_2 uptake whereas high frequency stimulations are associated with the generation of high intramuscular pressure resulting in compression of blood vessels and reduction of blood flow and O_2 uptake during muscle contractions (15). In addition, we chose 3Hz stimulation to avoid muscle fatigue and reduction in diaphragmatic tension which, in turn, may alter diaphragmatic O_2 uptake at a given level of O_2 delivery.

Comparison with previous findings in the diaphragm:

Our preparation permits control of the arterial supply to the diaphragm and access to its entire venous drainage. This allows the simultaneous measurement of VO_2,di and total diaphragmatic blood flow. Analysis of the relationship between VO_2,di and O_2 delivery in this way has not previously been undertaken. Therefore, comparison with previous results is limited. Rochester and Bettini (29) found that increases in work of breathing were accompanied by increased blood flow and O_2 extraction. The arteriovenous O_2 content difference plateaued, however, at approximately 13 ml/100ml at high work loads while diaphragmatic blood flow continued to increase. Robertson et al. (27,28) measured the relationship between the arteriovenous O_2 content difference and diaphragm blood flow during resistive loading and CO_2 rebreathing. Initially both the arteriovenous O_2 content difference and blood flow to increased with workload. At high workloads, during resistive loading but not during CO_2 rebreathing, a

plateau was reached in the arteriovenous O_2 content difference, after which further increases in O_2 consumption were achieved by increases in blood flow alone. This occurred when the arteriovenous O_2 content difference reached approximately 11 ml/100ml and diaphragm blood flow was approximately 50 ml/min/100g.

The data required to compute the corresponding O_2 deliveries and extraction ratios are not provided in these reports. If it is assumed, however, that the arterial O_2 contents are not different from ours, these values would compare with our findings of an arteriovenous O_2 content difference of 16.9 ± 1.5 ml/100ml, a diaphragm blood flow of 24.4 ± 2.5 ml/min/100g and a diaphragmatic VO_2 of 4.12 ± 0.62 ml/min/100g just prior to the onset of O_2 delivery dependence of VO_2,di in the contracting diaphragm. The differences in these findings may be explained by differences in the conditions studied; ie: resistive loading with unrestricted blood flow compared with tissue hypoxia induced by reduced oxygen delivery. It appears that under conditions of limited O_2 availability, the ability of the tissue to extract oxygen is greater than suggested by these previous studies.

Although not directly addressing the issue of supply limitation of oxygen uptake, Reid and Johnson (26) found that, during resistive loading, respiratory failure occurred in dogs when the phrenic venous PO_2 fell below 10-12 torr (venous O_2 content of 1 ml/100ml) and proposed this as the point beyond which tissue hypoxia limits diaphragm function. In a diaphragm strip preparation, however, Bark et al. (3) found fatigue to be associated with phrenic venous PO_2s of 15-20 Torr despite no change in diaphragmatic VO_2. The phrenic venous PO_2 did not reach as low a level in our animals as in these previous studies, presumably because the metabolic stress was not as great. We may have observed a lower phrenic venous PO_2 if the plateau

diaphragmatic VO_2 were raised further by increasing the contraction intensity.

Of the available reports of diaphragm O_2 delivery and uptake, the protocol used in the study of Scharf et al. (32) resembles that of our current experiments most closely. In that study, which was designed primarily to examine the relationship between arterial pressure and blood flow, the arterial and phrenic venous O_2 tensions and contents were measured during haemorrhage. At a systemic blood pressure of 55 mmHg, during spontaneous breathing and resistive loading, these investigators found the venous PO_2 to be 29 ± 8.5 and 21 ± 9.3 mmHg and the venous O_2 contents to be 9.9 ± 1.9 and 5.9 ± 1.9 ml/100ml, respectively (arteriovenous O_2 content difference = 7.9 and 12.6 ml/100mls, respectively). Although, this data does not allow determination of the critical O_2 delivery, the phrenic venous PO_2 during the final stage of their experiments is similar to those in our animals following the onset of O_2 delivery dependence of VO_2di.

Comparison with other tissues:

The critical O_2 delivery for whole body (excluding the left diaphragm) was 0.7 ± 0.08 ml/min/100g in our animals. The critical systemic O_2 delivery values during haemorrhage in dogs and pigs are listed in table 3. Higher critical O_2 deliveries have been noted during hypoxic and anemic hypoxia (9.8 ml/min/kg, table 3), central venous obstruction (11.7 ml/min/kg (23)) and during the application of PEEP (13.6 ml/min/kg (23)). The relationship between O_2 delivery and O_2 consumption has only been studied in resting limb muscle. In the isolated canine hindlimb, Samsel et al. (30) found the VO_2 to become supply limited at a systemic O_2 delivery of 5.2 ml/kg/min and an extraction ratio of 67% during haemorrhage (plateau VO_2 = 3.9

ml/min/kg). Table 3 lists the mean values of critical O_2 delivery and critical O_2 extraction ratio of various peripheral muscles. Our current results in the dog diaphragm, therefore, do not suggest a difference between the resting diaphragm and limb muscle in the capacity to increase oxygen extraction in response to reduced oxygen supply. In the heart the O_2 extraction ratio is high (65%, 30) even at normal myocardial oxygen delivery. As a result, myocardial VO_2 does not remain constant during reductions in oxygen delivery. Walley et al. (36), however, found that during progressive hypoxemia, coronary blood flow increases to a maximum value. After this point, further reductions in arterial O_2 content were associated with increases in O_2 extraction ratio, accelerated reduction in myocardial VO_2, altered lactate metabolism and deterioration in left ventricular function. These findings suggest a greater qualitative similarity between the heart and other tissues than has previously been appreciated. A biphasic relationship between O_2 delivery and uptake, similar to that which we describe in the diaphragm has also been demonstrated in the stomach (24), intestine, mesentery and liver (table 3). The difference in critical O_2 delivery appears to be related to differences in baseline O_2 consumptions of various tissues.

Effect of contraction:

The O_2 consumption of the contracting diaphragm became limited at a higher O_2 delivery than was observed in the resting muscle. This is the expected finding considering the increase in O_2 uptake which accompanied muscle contraction. The onset of supply dependence would have occurred even earlier, however, were it not for a concurrent increase in the critical O_2 extraction ratio. The extraction ratio continued to increase as diaphragmatic O_2 delivery was

further compromised.

The onset of delivery dependence of oxygen consumption has been attributed to the development of tissue hypoxia as the limits of oxygen extraction are reached (6). Within the framework of this interpretation, the fact that the extraction ratio is submaximal at this point suggests the existence of some form of variable arteriovenous shunt. This may arise because of 1) interregional inhomogeneity in the degree to which tissue O_2 delivery is matched to metabolic demand, 2) variation in the relative affinity of intracellular and intravascular oxygen binding elements or 3) intraregional variation in nutritive relative to non-nutritive capillary flow. The improvement in critical oxygen extraction ratio with contraction may reflect a compensatory adjustment in one or more of these factors in response to increased metabolic demand.

With regard to the first of these mechanisms, as overall O_2 delivery is reduced, one would expect greater regional homogeneity in the relationship between O_2 delivery and metabolic demand (and greater overall O_2 extraction) as well oxygenated areas are eliminated. Hurtado et al. (13), however, have measured regional tissue O_2 tension in the rabbit hindlimb during hypotension. They found that, if anything, the tissue PO_2 histograms widened as blood flow was reduced, suggesting that intraregional factors must account for the increase in extraction ratio.

With regard to the second mechanism, if the onset of O_2 supply dependence reflects limitation of molecular diffusion due to extraction below a critical end capillary PO_2, altered haemoglobin O_2 avidity due to local changes in pH and temperature might be expected to influence the critical extraction ratio. Schumacker et al. (33) addressed this issue in a study of the effect of experimental reduction in haemoglobin P_{50} on the systemic oxygen delivery-consumption relationship. They found no change in either the critical O_2 delivery or the

extraction ratio at the point of onset of O_2 supply dependence and suggested that other factors limit O_2 consumption before blood-tissue diffusion becomes important.

In the models proposed by Granger (10), differential sensitivity to metabolic mediators of vasodilation among microvessels of differing diameter results initially in an increase in capillary density and an improvement in extraction ratio in response to hypoxia with upstream resistance vessels being recruited later on. Anatomically (25) and functionally (11), two populations of capillaries have since been identified in skeletal muscle. Potter and Groom (25) found capillary diameters to conform to a bimodal distribution clustered around 5.5 μm and 7.5 μm in diameter. Harrison et al. (11) calculated that, despite their smaller numbers, the large diameter (high flow) capillaries, which contribute little to gas exchange, may carry up to 71% of the flow. Thus, a large margin for compensation exists through intraregional redistribution of capillary flow. This would, therefore, appear to be the most likely explanation for the observed increase in extraction ratio during muscle contraction and during progressive ischaemia.

Implications:

Our findings do not support a difference between the resting diaphragm and other tissues in the regulatory mechanisms involved in the response to reductions in oxygen availability. On the other hand, our experiments suggest that when the O_2 consumption of the diaphragm is augmented by low frequency stimulation, critical diaphragmatic O_2 delivery increases to a level greater than that of the whole body. These results imply that diaphragmatic metabolic requirements during a moderate increase in O_2 demands (VO_2di of 3.85 $\pm$0.62 ml/100g/min) which is comparable to that reported in intact dogs breathing against a mild or moderate resistive

load (26,29) may be comprised when systemic O_2 delivery reaches 10 ml/kg/min (figure 4). At this systemic O_2 delivery, systemic O_2 uptake remained independent of O_2 supply. We also speculate that critical systemic O_2 delivery at which diaphragmatic O_2 uptake becomes supply dependent is influenced by the pattern of muscle contraction. It is likely that at a given level of metabolic demands, strong or tetanic contractions will be associated with greater critical systemic O_2 delivery than low frequency contractions. This is because, unlike low frequency stimulation, increased intramuscular pressure during strong diaphragmatic contractions compromise blood flow and leads to a greater reliance on O_2 extraction to achieve the O_2 demands. Accordingly, critical O_2 extraction ratio will be reached at a greater systemic O_2 delivery than during low frequency stimulation. The implication of our data is that in disease states associated with decreased O_2 delivery and increased work of breathing, the diaphragm may become metabolically impaired before limitation of O_2 consumption is observed systemically. Our results can also explain the impairment of diaphragmatic contractile performance, the development of hypercapneic respiratory failure and increased respiratory muscle contribution to systemic lactic acidosis during cardiogenic and septic shock (1,2,17). In both these conditions, diaphragmatic metabolic demands are increased moderately as a result of hyperventilation whereas perfusion pressure and presumably systemic O_2 delivery decline significantly.

ACKNOWLEDGEMENTS

The authors thank S. Nuara for his technical assistance. M. Ward is a fellow of the Parker B. Francis Foundation, S. Hussain is a scholar of the Canadian Heart and Stroke

Foundation.

REFERENCES:

1. Aubier, M. T. Trippenbach, and C. Roussos. Respiratory muscle fatigue during cardiogenic shock. J. Appl. Physiol. 51:499-508, 1981.

2. Aubier, M., N. Viires, G. Syllie, R. Mozes and C.Roussos. Respiratory muscle contribution to lactic acidosis in low cardiac output. Am. Rev. Resp. Dis. 126:648-652, 1982.

3. Bark H., G. Supinski, R. Bundy, and S. Kelson, Effect of hypoxia on diaphragm blood flow, oxygen uptake and contractility. Am. Rev. Respir. Dis. 138: 1535-1541, 1988

4. Bredle, D.L., and S.M. Cain. Systemic and muscle oxygen uptake/delivery after dopexamine infusion in endotoxic dogs. Critical Care Medicine 19:198-204, 1991

5. Bredle, D.L., R.W. Samsel, P.T. Schumacker, and S.M. Cain. Critical O2 delivery to skeletal muscle at high and low PO2 in endotoxemic dogs. J.Appl. Physiol. 66(6):2553-2558, 1989.

6. Cain S.M. Peripheral oxygen uptake and delivery in health and disease. Clin. Chest. Med. 4: 139-148, 1983

7. Cain S.M., and C.K. Chapler. O_2 extraction by canine hindlimb during alpha-adrenergic blockade and hypoxic hypoxia. J. Appl. Physiol. 48:630-635, 1980

8. Cain S.M. Oxygen delivery and extraction in dogs during anemic and hypoxic hypoxia. J. Appl. Physiol. 42: 228-234, 1977

9. Comtois, A., W. Corczy and A. Grassino. Anatomy of diaphragmatic circulation. J. Appl. Physiol. 62:238-244, 1987.

10. Granger, H.J., A.H. Goodman, and B.H. Cook. Metabolic models of microcirculatory regulation. Fed Proc. 34: 2025-2030, 1975

11. Harrison, D.K., S. Birkenhake, S.K. Knauf, and M. Kessler. Local oxygen supply and blood flow regulation in contracting muscle in dogs and rabbits. J. Physiol. 422: 227-243, 1990.

12. Heard, S.O., T.D. Baum, H. Wang, H.R. Rothschild and M.P. Fink. Systemic and Mesenteric O2 metabolism in endotoxic pigs: Effects of graded hemorrhage. Cir. Shock 35:44-52, 1991

13. Hurtado, F.J., A.M. Gutierrez, N. Silva, E. Fernandez, A.E. Khan, and G. Gutierrez, Role of tissue hypoxia as the mechanism of lactic acidosis during E. Coli endotoxemia.

J. Appl. Physiol. 72: 1895-1901, 1992.

14. Hussain, S.N.A. and S.A. Magder, Diaphragmatic intramuscular pressure in relation to tension, shortening and blood flow. J. Appl. Physiol. 71(1):159-167 , 1991

15. Hussain, S.N.A., C. Roussos and S. Magder. The selective effects of tension, duty cycle and arterial pressure on diaphragmatic blood flow. J. Appl. Physiol. 66:968-976, 1989.

16. Hussain S.N.A., C. Roussos, S. Magder. In situ isolated perfused and innervated left hemidiaphragm preparation. J. Appl. Physiol. 67:2141-2146, 1989.

17. Hussain, S.N.A., G. Simkus and C. Roussos. Respiratory muscle fatigue: a cause of ventilatory failure during septic shock. J. Appl. Physiol. 58:2033-2040, 1985.

18. Kohzuki, H., Y. Enoki, Y. Ohga, S. Shimizu, and S. Sakata, Oxygen consumption in resting dog gracilis muscle perfused at varying oxygen delivery. Jap. J. Physiol. 41: 23-34, 1991.

19. Kolar, F. and L. Jansky, Oxygen consumption in rat skeletal muscle at various rates of oxygen delivery. Experientia 40:353-354 1984.

20. Lindbom, L., R.F. Tuma and K.E. Arfors. Influence of oxygen on perfused capillary density and capillary red cell velocity in rabbit skeletal muscle. Microvasc. Res. 19: 197-208, 1980.

21. Nagano, K., S. Gelman, D.A. Parks, and E. Bradley, Hepatic oxygen supply-uptake relationship and metabolism during anesthesia in miniature pigs. Anesthesiology 72: 902-910, 1990.

22. Nelson, D.P., C.E. King, S.L. Dodd, P.T. Schumacker, and S.M. Cain. Systemic and intestinal limits of O_2 extraction in the dog. J. Appl. Physiol. 63: 387-394, 1987.

23. Pepe, D.E., and B.H. Culver. Independently measured oxygen consumption during reductions of oxygen delivery by positive end-expiratory pressure. Am. Rev. Respir. Dis. 132:788-792, 1985.

24. Perry, M.A., P. Bulkley, P.R. Kvietys, and D.N. Granger. Regulation of oxygen uptake in resting and pentagastrin-stimulated canine stomach. Am. J. Physiol. 242: G565-G569, 1982.

25. Potter, R.F., and A.C. Groom. Capillary diameter and geometry in cardiac and skeletal muscle studied by means of corrosion casts. Microvascular Res. 25: 68-84, 1983

26. Reid, M.B., and R.L. Johnson, Jr., Efficiency, maximal blood flow, and aerobic work capacity of canine diaphragm. J. Appl. Physiol. 54:763-772, 1983

27. Robertson, C.H.Jr., G.H. Fortis, and R.L. Johnson Jr., The relationship of respiratory failure to the oxygen consumption of lactate production by, and distribution of blood flow among respiratory muscles during increasing inspiratory resistance. J. Clin. Invest. 59: 31-42, 1977

28. Robertson, C.H.Jr., M.A. Pagel, and R.L. Johnson Jr., The distribution of blood flow, oxygen consumption, and work output among the respiratory muscles during unobstructed hyperventilation. J. Clin. Invest. 59: 43-50, 1977.

29. Rochester, D.F., and G. Bettini, Diaphragmatic blood flow and energy expenditure in the dog. J. Clin. Invest. 57: 661-672, 1976

30. Samsel, R.W., D.P. Nelson, W.M. Sanders, L.D.H. Wood, and P.T. Schumacker, Effect of endotoxin on systemic and skeletal muscle O_2 extraction. J. Appl. Physiol. 65:1377-1382, 1988.

31. Samsel R.W. and P.T. Schumacker. Determination of the critical oxygen delivery from experimental data: sensitivity to error. J. Appl. Physiol. 64: 2074, 1988.

32. Scharf S.M., H. Bark, S. Einhorn, and A. Tarasiuk, Blood flow to the canine diaphragm during hemorrhagic shock Am Rev Respir Dis 133:205-211, 1986

33. Schumacker P.T., G.R. Long, and L.D.H. Wood. Tissue oxygen extraction during hypovolemia: role of haemoglobin P_{50}. J. Appl. Physiol. 62: 1801-1807, 1987.

34. Segal, J.M., T. Phang and K. Walley. Low-dose dopamine hastens onset of gut ischemia in a porcine model of hemorrhagic shock. J. Appl. Physiol. 73(3):1159-1164, 1992.

35. Viires, N., G. Sillye, M. Aubier, A. Rassidakis and C. Roussos. Regional blood flow distribution in dog during induced hypotension and low cardiac output. J. Clin. Invest. 72: 935-947, 1983.

36. Walley, K.R., C.J. Becker, R.A. Hogan, K. Teplinsky and L.D.H. Wood, Progressive hypoxemia limits left ventricular oxygen consumption and contractility. Circ. Res. 63:849-859, 1988

TABLE 1

Values for selected systemic parameters prior to haemorrhage and during the final stage of the experiments.

	Initial	Final
Haemoglobin (g)	14.2 ± 1.1	13.8 ± 1.16
Arterial Pressure (mmHg)	151.4 ± 11.8	36.4 ± 3.85
Cardiac Output (L/min)	3.99 ± 0.43	0.50 ± 0.07
arterial PO_2 (mmHg)	118.8 ± 9.8	112.0 ± 6.12
arterial PCO_2 (mmHg)	38.0 ± 1.8	36.1 ± 2.3
arterial pH	7.405 ± 0.017	7.298 ± 0.028

Initial, values prior to haemorrhage; Final, values during final stage of haemorrhage protocol

TABLE 2

Phrenic arterial blood flow (Q_{phr}), phrenic venous PO_2 (PvO_2,di), phrenic arteriovenous O_2 content difference ((Ca-Cv)O_2di) and diaphragmatic O_2 consumption (VO_2di) prior to beginning the hemorrhage protocol (Initial), during the stage just before to onset of O_2 delivery dependence of diaphragmatic O_2 consumption (Critical) and during the final stage (Final) of the experiments in the resting and contracting (3 Hz continuous stimulation) diaphragm.

	Qphr (ml/min/100g)	PvO_2di (mm Hg)	(Ca-Cv)O_2di (ml O_2/100ml)	VO_2di (ml O_2/min/100g)
RESTING				
Initial	23.5±4.5	58.6±3.8	1.26±0.4	0.27±0.08
Critical	4.6±0.5	35.0±2.5	10±1.6	0.45±0.1
Final	2.2±0.3	32.7±1.8	12.5±2	0.26±0.05
CONTRACTING				
Initial	39.6±5.4	32.9±2.7	11.7±1.4	4.53±0.53
Critical	24.4±2.5	24.7±2.2	15.6±1.7	3.85±0.62
Final	9.1±1.3	20.5±1.5	16.9±1.5	1.53±0.34

Table 3: Mean values of critical O_2 delivery and critical O_2 extraction ratio (ER) for whole body and different organs reported in the literature.

Authors	Reference	Animal	Organ	Critical O_2 Delivery	Critical O_2 ER
Cain, 1977	8	Dogs	Whole Body	9.8 ml/kg/min	
Pepe & Culver, 1985	23	Dogs	Whole Body	13.6 ml/kg/min	
Pepe & Culver, 1985	23	Dogs	Whole Body	11.7 ml/kg/min	
Nelson et al., 1987	22	Dogs	Whole Body	7.4 ml/kg/min	71%
Schumacker et al.,1987	33	Dogs	Whole Body	8.1 ml/kg/min	73%
Samsel et al., 1988	30	Dogs	Whole Body	8.0 ml/kg/min	70%
Walley et al., 1988	36	Dogs	Whole Body	9.3 ml/kg/min	
Heard et al., 1991	12	Pigs	Whole Body	12.8 ml/kg/min	71%
Segal et al., 1992	34	Pigs	Whole Body	7.1 ml/kg/min	72%
Kolar & Jansky, 1984	19	Rats	Gracilis muscle	16 ml/min/kg	62%
Bredle & Cain, 1991	4	Dogs	Hindlimb	4.6 ml/kg/min	81%
Kohzuki et al., 1991	18	Dogs	Gracilis muscle	4.5 ml/kg/min	67%
Bredle et al., 1989	5	Dogs	Hindlimb	6.0 ml/kg/min	72%
Nelson et al., 1987	22	Dogs	Intestine	35.7 ml/kg/min	69%
Nagano et al., 1990	21	Pigs	Liver	63 ml/kg/min	
Heard et al., 1991	12	Pigs	Mesentery	1.47 ml/kg/min	75%

FIGURE LEGENDS

Figure 1.

Relationships between diaphragmatic O_2 delivery and O_2 consumption with the diaphragm at rest and during 3 Hz stimulation.

Figure 2.

Relationships between O_2 consumption and O_2 delivery for whole body (excluding the left diaphragm (top panel)) and for the resting and contracting left hemidiaphragm (bottom panel).

Figure 3.

Top: Critical diaphragmatic oxygen delivery for the resting and contracting (3 Hz) diaphragm. Bottom: Oxygen extraction ratios at the onset of delivery dependence of diaphragmatic oxygen consumption (Critical) and during the final stage of the haemorrhage protocol (Maximal).

* significant difference ($p < 0.05$) compared to the value for the resting diaphragm.

Figure 4.

Critical values for whole body oxygen delivery below which the oxygen consumption of the left diaphragm and whole body (excluding the left diaphragm) became dependent on O_2 delivery.

* significant difference ($p < 0.05$) compared to the value for the resting diaphragm.

+ significant difference ($p < 0.05$) compared to the value for the resting diaphragm.

Figure 1

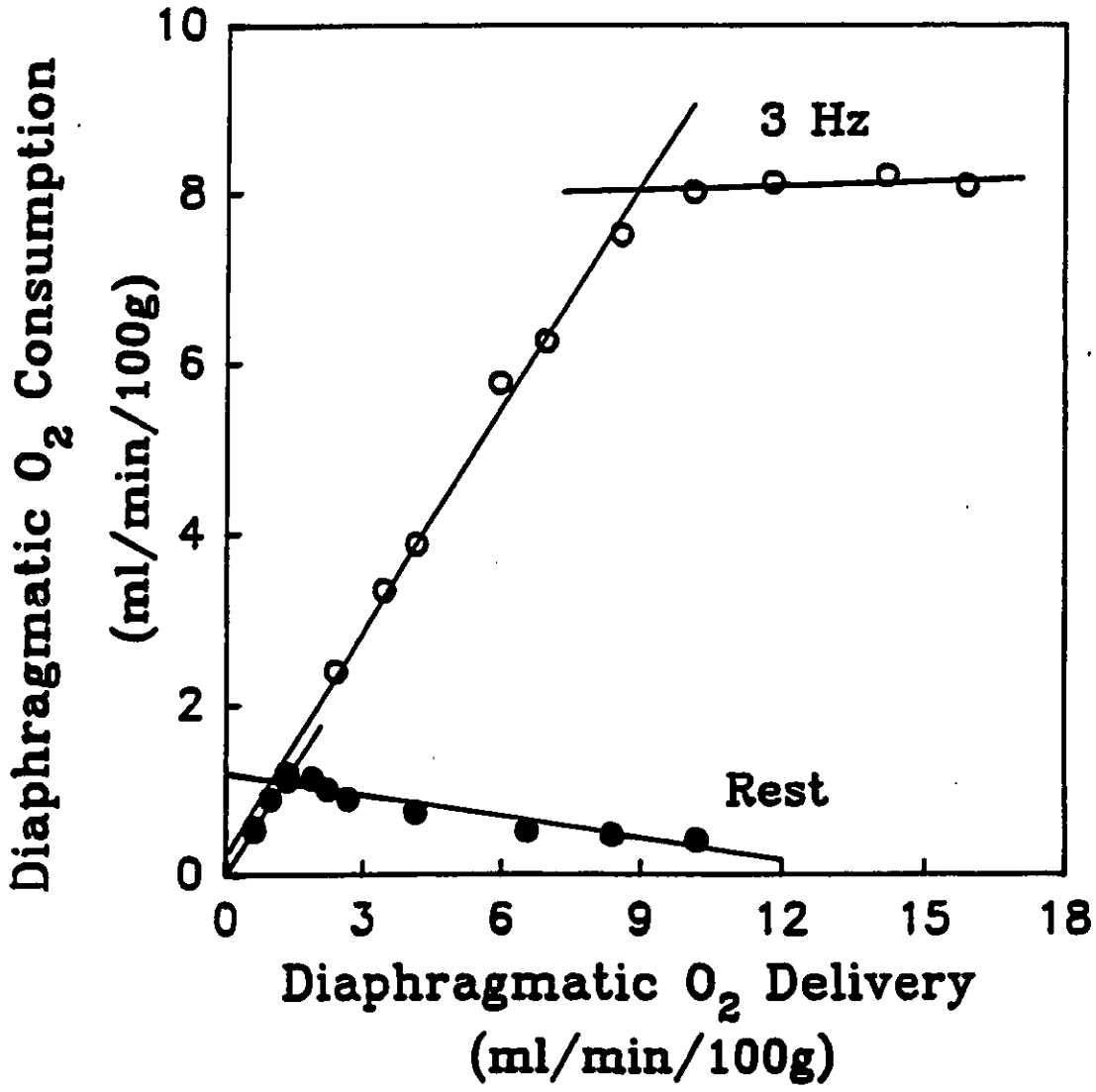
Diaphragmatic O_2 Consumption
(ml/min/100g)
10
8
6
4
2
0
3 Hz
Rest
0
3
6
9
12
15
18
Diaphragmatic O_2 Delivery
(ml/min/100g)

Figure 2

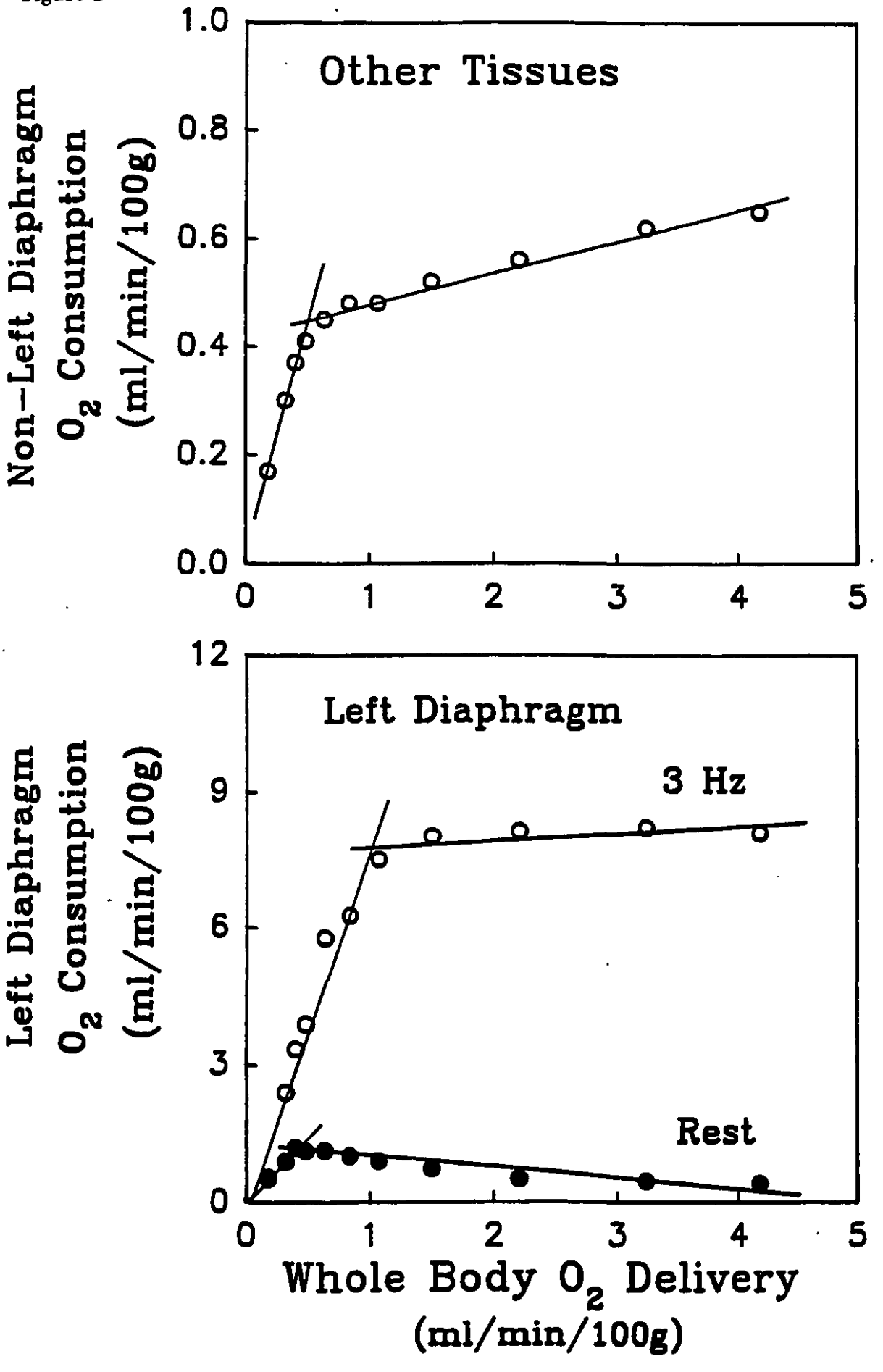
Other Tissues
Non-Left Diaphragm
O_2 Consumption
(ml/min/100g)
1.0
0.8
0.6
0.4
0.2
0.0
0
1
2
3
4
5
Left Diaphragm
3 Hz
Rest
Left Diaphragm
O_2 Consumption
(ml/min/100g)
12
9
6
3
0
0
1
2
3
4
5
Whole Body O_2 Delivery
(ml/min/100g)

Figure 3

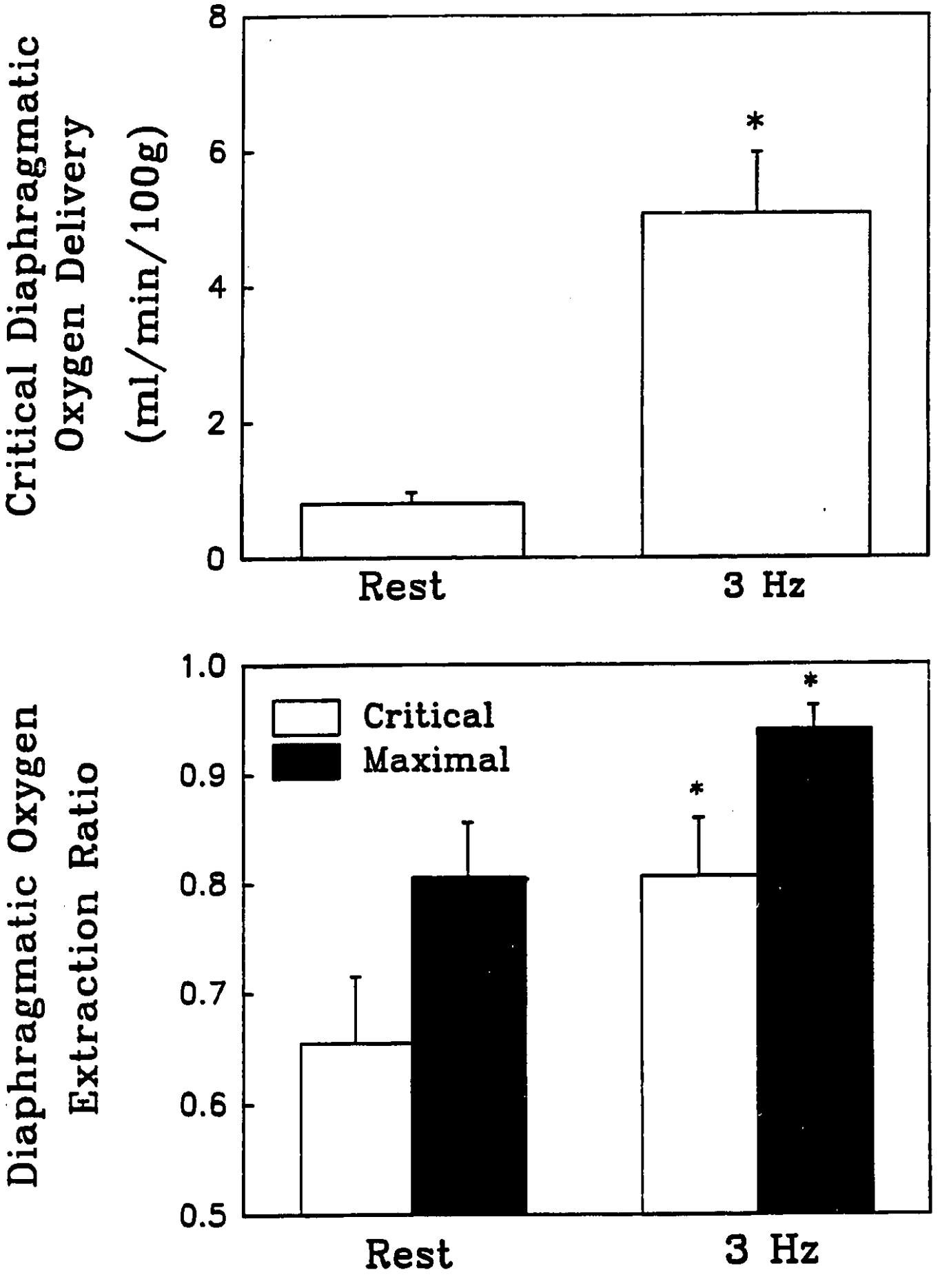
Critical Diaphragmatic Oxygen Delivery (ml/min/100g)
8
6
4
2
0
*
Rest
3 Hz
Diaphragmatic Oxygen Extraction Ratio
1.0
0.9
0.8
0.7
0.6
0.5
Critical
Maximal
*
*
Rest
3 Hz

Figure 4

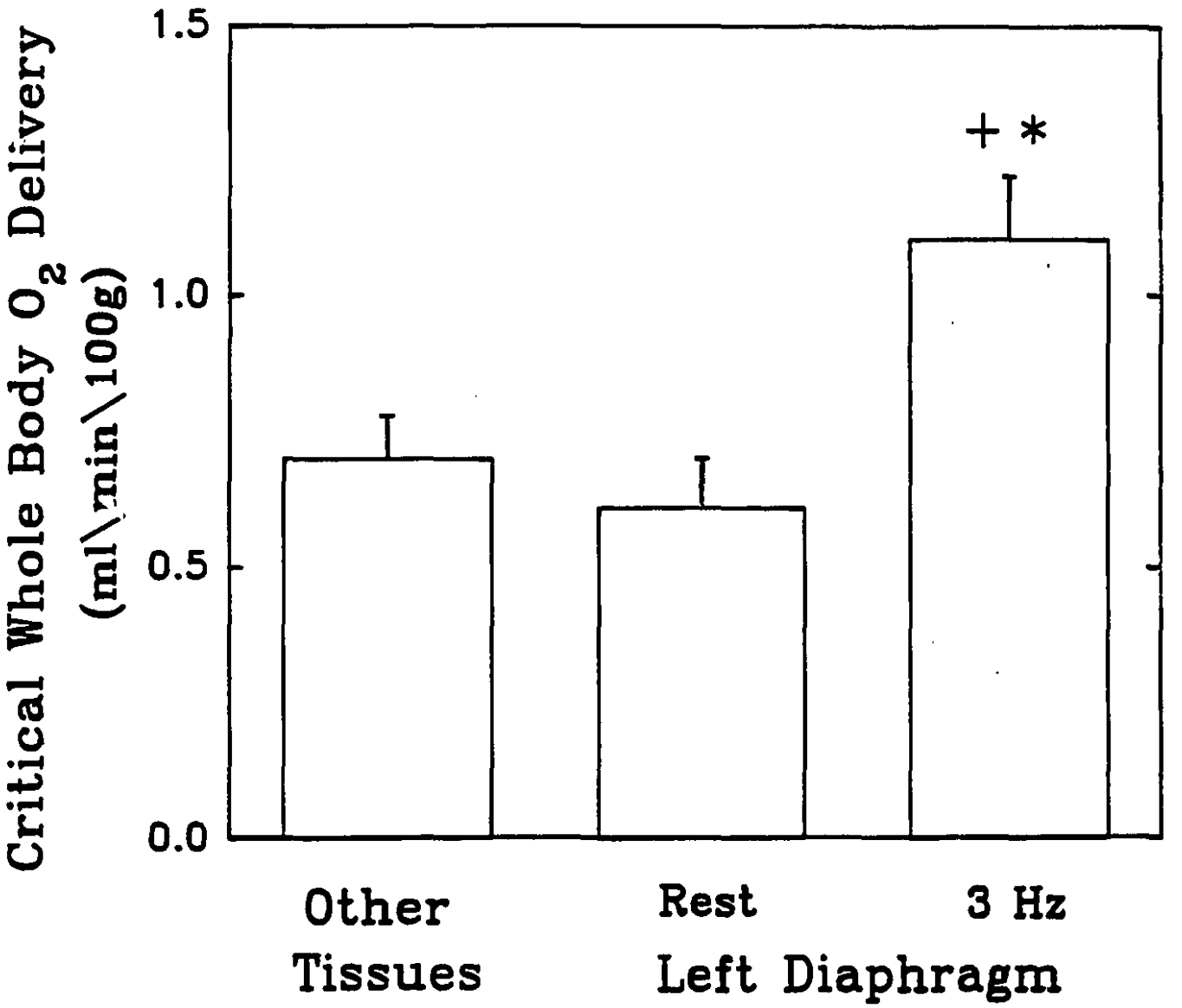
Critical Whole Body O_2 Delivery
(ml\min\100g)
1.5
1.0
0.5
0.0
+ *
Other Tissues
Rest
3 Hz
Left Diaphragm

CHAPTER 5: Regulation of Diaphragmatic Blood Flow and Oxygen Uptake by Nitric Oxide

Foreword to Chapter 5

Several investigators have suggested that endothelial release of nitric oxide plays a role in the coupling of oxygen delivery to metabolic rate in highly aerobic tissues. Evidence of reduced tissue oxygen tension, an index of the degree to which a tissue's oxygen delivery is adequately matched to its oxygen requirements, during inhibition of NO release has been presented in support of this contention. Pohl and Busse (1) found that inhibition of NO synthesis in the rabbit hindlimb lowered tissue PO_2. Furthermore, Gossypol (NO inhibitor) has been shown to decrease rabbit peroneus muscle O_2 consumption (2). In these autoperfused preparations inhibition of the NO pathway may have reduced altered vascular tone in resistance or conductance vessels impairing the capacity to increase bulk oxygen delivery in proportion to metabolic demand. More recently, Pohl and colleagues (3) have reported a decline in O_2 uptake in an isolated heart preparation following infusion of LNA. Alterations in bulk blood flow are obviated in pump perfused preparations, therefore the effect of NO inhibition must be attributed to changes in the factors limiting oxygen extraction. It is likely, therefore, that the NO pathway is involved in the regulation of tissue oxygen availability at many levels. In this chapter, studies are presented which examine the importance of endothelial NO release in the regulation of baseline vascular tone, autoregulation of blood flow, reactive hyperaemia and in determining the critical level of oxygen delivery and extraction at which oxygen consumption becomes dependent on delivery in the canine diaphragm. The results indicate that modulation of endothelial NO release represents a major control mechanism by which the process of matching diaphragmatic oxygen availability to its rate of metabolic activity may be regulated.

REFERENCES

1. Pohl, U. and Busse, R. Reduced nutritional blood flow in autoperfused rabbit hindlimbs following inhibition of endothelial vasomotor function. In: *Resistance Arteries*, edited by Halpern, W., Pegram, B., Bryaden, J., Mackey, K., Mclaughlin, M. and Osol, G. New York: Ithaca, Perinatology, 1988, p. 10-16.

2. Pohl, U. and D. Lamontagne. Impaired tissue perfusion after inhibition of endothelium-derived nitric oxide. *Basic Res. Cardiol.* 86: 97-105, 1991.

3. Pohl, U., D. Lamontagne, E. Bassenge and R. Busse. EDRF antagonizes myogenic autoregulation in the vasculature of isolated rabbit hearts. *Am. J. Physiol.* 1992. (In Press).

Regulation of Baseline Vascular Resistance in the Canine Diaphragm by Nitric Oxide

Michael E. Ward and Sabah N. A. Hussain
British Journal of Pharmacology, 1994 - In Press

ABSTRACT

1. The role played by nitric oxide (NO) in the regulation of blood flow to the isolated, canine hemidiaphragm was evaluated by determining a) the effects of the L-arginine analogues N^G-nitro-L-arginine methyl ester (LNAME), N^G-nitro-L-arginine (LNA), and Argininosuccinic acid (ArgSA) on baseline vascular resistance and of the latter two agents on endothelium dependent (acetylcholine, Ach) and endothelium independent (Sodium nitroprusside, SNP) vasodilation; b) the effects of L- and D-arginine on baseline vascular resistance; and c) the effects of L-glutamine, an inhibitor of intracellular recycling of L-citrulline to L-arginine, on baseline resistance and on the response to Ach and SNP.

2. LNAME, LNA and ArgSA ($6 \cdot 10^{-4}$ M final concentrations) increased baseline diaphragmatic vascular resistance to a similar extent ($28.6 \pm 4.2\%$, $26.7 \pm 4.3\%$ and $32.8 \pm 4.6\%$ respectively). LNA and ArgSA reversed the vasodilatory effect of Ach but not of SNP.

3. L- and D-arginine had no effect on vascular resistance.

4. L-glutamine (10^{-3}M) increased baseline vascular resistance by $10 \pm 1.9\%$ ($p < 0.05$) but did not alter either Ach or SNP responses.

5. Basal NO release plays a role in the regulation of baseline diaphragmatic vascular resistance. L-arginine analogues tested potently and specifically inhibited this process. Moreover, extracellular L-arginine appears to have no effect on baseline diaphragmatic vascular resistance.

Key Words: EDRF, nitroarginine, argininosuccinic acid, L-arginine, L-glutamine, blood flow, respiratory muscles

INTRODUCTION

Endothelial release of vasodilator substances, including nitric oxide (NO) has been shown to play a pivotal role in the regulation of blood flow in a number of vascular beds. The importance of the L-arginine-NO pathway in the regulation of resting vascular tone and as a mediator of endothelium-dependent vasodilation has been evaluated by observing the effects of inhibiting nitric oxide synthase activity using L-arginine analogues. The effect of these false substrates, however, has varied among experimental preparations. Although in the majority of studies, an increase in baseline vascular resistance and inhibition of endothelium-dependent dilation have been observed, a few investigators have also described no inhibition of endothelium-dependent dilation or non-selective inhibition of agonist-induced dilation following the infusion of L-arginine analogues (Mugge *et al.*, 1991; Thomas *et al.*, 1989). Such discrepant results obtained in apparently similar experimental preparations indicate that conclusions drawn from these studies, must be restricted to the vascular bed under study. In addition, L-arginine analogues have been shown to differ in their potency (Vargas *et al.*, 1991), specificity (Thomas *et al.*, 1988), reversibility by L-arginine (Bogle *et al.*, 1992), method of endothelial cell entry (Bogle *et al.*, 1992) and mechanism of action (Gross *et al.*, 1990). Such pharmacologic differences may, therefore, contribute to the conflicts which currently complicate interpretation of this literature.

The source of L-arginine on which the endothelial cell depends for substrate in the synthesis of NO also varies. In some isolated vessel preparations (Kaley *et al.*, 1992, Gold *et al.*, 1989) and in the pial circulation in vivo (Morikawa *et al.*, 1992) availability of extracellular L-arginine appears to limit basal NO formation. In other preparations (Fortes *et al.*, 1990;

Gardiner *et al.*, 1990; Lahera *et al.*, 1990; Thomas *et al.*, 1989) administration of exogenous L-arginine has no effect on vascular tone. These vessels presumably depend on intracellular synthesis of L-arginine and on the recycling of L-citrulline formed in the process of NO synthesis (Hecker *et al.*, 1990, Sessa *et al.*, 1990).

Failure to maintain substrate supply to the diaphragm in proportion to its metabolic requirements results in muscle failure (Supinski *et al.*, 1988; Macklem & Roussos, 1977). Study of the mechanisms by which diaphragm blood flow is regulated has, therefore, been of high priority among physicians seeking to develop rational treatment strategies for patients with respiratory failure (Aubier *et al.*, 1989). Since, for the reasons discussed above, the results obtained from previous studies cannot be extrapolated to the diaphragm, further progress in this field requires that the role of the nitric oxide pathway in this circulation be specifically determined.

We have, therefore, evaluated the role of NO in the regulation of blood flow in the canine diaphragm by determining a) the effects of three L-arginine analogues, N^G-nitro-L-arginine methyl ester (LNAME), N^G-nitro-L-arginine (LNA) and Argininosuccinic acid (ArgSA) on baseline vascular resistance and of the latter two agents on endothelium-dependent (acetylcholine, Ach) and -independent (Sodium nitroprusside, SNP) vasodilation; b) the effects of L- and D-arginine on baseline vascular resistance; and c) the effects of L-glutamine, an inhibitor of L-arginine synthesis from L-citrulline (Sessa et al, 1990) on baseline resistance and on Ach and SNP induced vasodilation.

METHODS

Animal Preparation: Studies were performed on mongrel dogs (weight = 27.8 ± 1.27 kg SD). The animals were anaesthetized with sodium thiopental (10 mg/kg) followed by α-chloralose (60-80 mg/kg). Supplemental doses of α-chloralose were given as needed to eliminate the jaw tone but maintain knee reflexes. All animals were treated with indomethacin 5mg/kg to block prostaglandin synthesis. The animals were supine, intubated with cuffed endotracheal tubes and mechanically ventilated (tidal volume 15 ml/kg, frequency adjusted to maintain the arterial PCO_2 from 38 to 42 mmHg). Supplemental oxygen was supplied through the inspiratory line and arterial PO_2 maintained above 100 mmHg. Positive end-expiratory pressure (5 cm H_2O) was applied at the expiratory line. A catheter was placed in the aorta through the right carotid artery to monitor arterial pressure (P_{ar}) and another catheter was placed in the right femoral vein to administer supplemental anaesthetic. Core body temperature was kept constant at approximately 37° C by a heating pad placed under the animal.

Isolated left hemidiaphragm: In all animals, we used the in-situ, vascularly isolated left hemidiaphragm preparation previously reported in detail (Hussain *et al.*, 1989). Briefly, through an abdominal incision, silk sutures were placed 1 cm apart in the left hemidiaphragm to be used for future reference in adjusting the muscle's resting length. The intercostal vessels and the left internal mammary artery were ligated and the lower left ribs were removed. The diaphragm was divided into two halves and the ribs and cartilages of the lower costal margin were freed and suspended vertically from metal bars. Resting diaphragm length was adjusted to that in situ using the reference sutures. The stomach, liver, spleen, and left kidney were retracted to expose the left phrenic artery. This artery was ligated proximally and a polyethylene catheter (PE 160,

1.14 mm ID, 1.57 mm OD, 3 cm long) was introduced into the distal portion. A side port in the catheter was used for measurement of phrenic perfusion pressure (P_{phr}). The catheter was connected to an electromagnetic flow probe (Carolina Medical Electronics, 1.91 mm ID) in order to measure phrenic arterial flow (Q_{phr}). The pressure-flow relationship of the catheter-probe system was linear over the range of flows in the study with conductance = 2.6 ml/min/mmHg. The other side of the probe was connected to a Y shaped connector, one arm of which was connected to a catheter in the left femoral artery, thereby allowing the diaphragm to be perfused with blood diverted from this source. The other arm of the Y was connected via a constant perfusion pump to a catheter in the right femoral artery. The diaphragm could, thereby, be pump perfused using a constant flow pump (Cole-Parmer Masterflex No. 7523-00, head No. 7016-20, No. 16 tubing) with blood from the right femoral artery by clamping the left femoral arterial catheter. Drugs were administered to the phrenic circulation through a side port in the Y connector using a Harvard infusion pump. All animals were heparinized after catheterizing the phrenic artery.

The temperature of the diaphragm was monitored continuously using a temperature probe fixed to the surface of the isolated hemidiaphragm (Mon-a-therm, Model 6000, Zimmer of Canada Ltd., Mississauga, Ont.) and maintained between 37.5 and 38.5°C using a heat lamp if required. At the end of the experiment the animals were exsanguinated and the diaphragm was dissected free and weighed.

Experimental Protocols:

Baseline vascular resistance:

Studies were performed on separate groups of animals, each group (6 animals in each group) receiving a different inhibitor of NO release. In each experiment, the left diaphragm was autoperfused from the left femoral artery for 30 minutes. Following this stabilization period, pump perfusion was begun, as described above, at the flow rate identical to that recorded during the period of autoperfusion. The Harvard pump was then used to infuse saline into the phrenic circulation at a rate equal to $1/100^{th}$ of the phrenic arterial blood flow. After 20 minutes of infusion, control measurements of P_{art} and P_{phr} were made. The saline syringe was then removed from the Harvard pump and replaced with one containing one of the following solutions: N^G-nitro-L-arginine (LNA), $6 \cdot 10^{-2}$ M; N^G-nitro-L-arginine methyl ester (LNAME), $6 \cdot 10^{-2}$ M; Argininosuccinic acid (ArgSA), $6 \cdot 10^{-2}$ M; L-glutamine, 10^{-1}M. The test agent was infused for 20 minutes, at which time measurements of P_{art} and P_{phr} were repeated. All agents, except LNA, were dissolved in normal saline with correction of pH to 7.4. LNA solution of $6 \bullet 10^{-2}$M was prepared by dissolving LNA in 0.5 ml of 1N HCl and 19.5 ml of normal saline. We then added enough NaOH to correct the pH to 7.4. Infusion of the LNA vehicle elicited no changes in diaphragmatic vascular resistance.

Response to Ach and SNP

In 3 animals, the dose response curves for Ach and SNP were determined. Increasing concentrations of these agents were infused into the phrenic circulation, each at $1/100^{th}$ of the total phrenic arterial flow rate. The final concentrations found to produce 80% of maximal vasodilation averaged 10^{-5}M for Ach and 2μg/ml for SNP respectively. These concentrations were then used in the following studies of the effects of the test agents on the responses to these

vasodilators.

Studies were performed on separate groups of animals (6 per group), each receiving a different inhibitor of NO release. Following an initial 30 minute stabilization period of autoperfusion, the diaphragm was pump-perfused at the same rate as that recorded during autoperfusion. A dual syringe pump was loaded with two syringes containing saline. Saline from both syringes was then infused into the phrenic circulation at a rate equal to $1/100^{th}$ of the phrenic arterial flow per syringe. After 20 minutes, baseline measurements of P_{art} and P_{phr} were performed. One of the saline syringes was then removed from the pump and replaced with one containing either Ach (10^{-3}M) or SNP (200 μg/ml), and infusion was continued at the same rate. After 20 minutes of simultaneous infusion of saline and either Ach or SNP, by which time a steady state vascular resistance had been achieved in all animals, measurements of P_{art} and P_{phr} were repeated. The second saline syringe was then removed and replaced with a syringe containing one of the following solutions: LNA, $6 \cdot 10^{-2}$M; ArgSA, $6 \cdot 10^{-2}$M, *L-glutamine*, 10^{-1}M. After 20 minutes of simultaneous infusion of either Ach or SNP and the test agent, measurements of P_{art} and P_{phr} were repeated.

L-arginine and D-arginine:

In 2 separate groups of animals (6 per group) the left hemi-diaphragm was autoperfused for 30 minutes and then pump perfused at the natural flow rate as described above. The Harvard pump was subsequently used to infuse saline into the phrenic circulation at a rate equal to $1/100^{th}$ of the phrenic arterial blood flow. After 20 minutes of infusion, control measurements of P_{art} and P_{phr} were made. The saline syringe was then removed from the Harvard pump and

replaced with one containing either L-arginine or D-arginine (pH = 7.4) and infusion was continued at the same rate. The initial concentration in the syringe was $0.6 \cdot 10^{-1}$ M to yield a final concentration of $0.6 \cdot 10^{-3}$M in the phrenic arterial blood. This syringe was replaced sequentially with syringes containing solutions which yielded final concentrations of $3 \cdot 10^{-3}$M and $6 \cdot 10^{-3}$M. The test agent was infused for 10 minutes at each concentration, at which time repeat measurements of P_{art} and P_{phr} were performed.

Data Analysis:

Results are expressed as mean ± SEM. Two mean comparisons were performed using two tailed paired t-tests. Comparisons of multiple means were performed using analysis of variance (ANOVA) corrected for multiple measures when appropriate and analyzed post-hoc using the Neuman-Keuls procedure. Differences were deemed significant when $p < 0.05$.

RESULTS

Effect on baseline vascular resistance:

Baseline Q_{phr} before LNA, LNAME, ArgSa and L-glutamine infusion averaged 20.8, 26.4, 29.2 and 28.5 ml/100g/min, respectively. Figure 1 illustrates the mean values of P_{phr} measured at baseline and after 20 minutes infusion of these agents. LNAME ($6 \bullet 10^{-4}$M), LNA ($6 \bullet 10^{-4}$M) and ArgSA ($6 \bullet 10^{-4}$M) significantly ($p < 0.01$) increased phrenic vascular resistance (28.6±4.2%, 26.7±4.3% and 32.8±4.6% respectively compared to baseline), whereas L-glutamine (10^{-3}M) increased vascular resistance by a statistically significant ($p < 0.05$) but much smaller amount (10±1.9 %, figure 1). The increase in phrenic vascular resistance in response

to all of these agents reached a steady state level within 10 minutes of the infusion with no change thereafter. In addition, the pressor response to LNA, LNAME and L-glutamine was well maintained and persisted for over 60 minutes after the cessation of infusion . By comparison, phrenic vascular resistance recovered completely after 20 minutes of the cessation of ArgSA infusion. Figure 2 illustrates an example of the changes in phrenic perfusion pressure in response to $6 \bullet 10^{-4}$M LNAME infusion. The increase in phrenic vascular resistance plateaued within 10 minutes of LNAME infusion. Infusion of normal saline into the phrenic artery over 20 minute period elicited no significant alterations in phrenic vascular resistance.

Effect on response to Ach and SNP:

Figure 3 illustrates the effects of LNA (top), ArgSA (middle) and L-glutamine (bottom) on the vasodilator response to Ach and SNP. Infusion of LNA and ArgSA completely reversed the vasodilation induced by Ach while having no significant effect on the SNP response. L-glutamine had no effect on the magnitude of vasodilation produced by either Ach or SNP.

Effect of L-arginine and D-arginine:

Figure 4 presents the values of P_{phr} during infusion of L-arginine and D-arginine. Neither isomer had any effect on diaphragmatic vascular resistance at any of the concentrations tested.

DISCUSSION

The main findings of this study are: 1) Infusion of the L-arginine analogues LNA,

LNAME and ArgSA increased the baseline vascular resistance of the phrenic circulation in vivo. 2) Infusion of LNA or ArgSA attenuated the vasodilatory effect of Ach infusion while having no effect on vasodilation in response to SNP. 3) L-arginine and D-arginine at physiological pH have no effect on baseline diaphragmatic vascular resistance. 4) L-glutamine (10^{-3}M) increased baseline vascular resistance but had no effect on either Ach or SNP induced vasodilation.

Basal NO release:

Basal release of EDRF has been detected by bioassay from isolated vessels (Rubanyi *et al.*, 1985; Kelm & Schrader, 1990). In vivo studies have demonstrated increased baseline arterial pressure following systemic infusion of L-arginine analogues in rats (Gardiner *et al.*, 1989), guinea pigs (Aisaka *et al.*, 1989), cats (Bellan *et al.*, 1991) and dogs (Klabunde *et al.*, 1990). Regionally, treatment with analogues of L-arginine have been found to increase vascular resistance in isolated rabbit hearts (Lamontagne *et al.*, 1991), rabbit hindlimb (Mugge *et al.*, 1991) dog hindlimb (White *et al.*, 1993) and human forearm (Vallance *et al.*, 1989). In rat cremaster muscle, arteriolar vasoconstriction has been demonstrated following light-dye injury to the endothelium (Koller & Kaley, 1990) and following topical application of L-arginine analogues (Kaley *et al.*, 1992). Similarly, Persson *et al.* (1990) have shown LNMMA to reduce microvascular diameters in rabbit tenuissimus muscle. Consistent with this evidence, we have found the baseline resistance of the diaphragmatic vasculature to increase significantly following the administration of L-arginine analogues. This effect could not have been due to suppression of vasodilatory prostanoid synthesis (Koller *et al.*, 1990) since all animals had been pretreated with indomethacin. These results, therefore, suggest a role for modulation of basal endothelial

release of NO in the control of resting smooth muscle tone in this vascular bed as well.

Endothelium-dependent and -independent vasodilation:

The results of studies of the role of NO in agonist induced vasodilator responses have been less consistent than those concerning its role in regulation of baseline vascular tone. Some studies have shown that the in vivo responses to endothelium-dependent agents are selectively inhibited by treatment with L-arginine analogues, while responses to endothelium-independent agents are not significantly decreased (Aisaka *et al.*, 1989; Gold *et al.*, 1989; Gardiner *et al.*, 1989; Bellan *et al.*, 1991; Kaley *et al.*, 1992; Bellan *et al.*, 1993; White *et al.*, 1993). Other studies, however, have shown either no decrease in responses to endothelium-dependent vasodilators (Mugge *et al.*, 1991, Ross *et al.*, 1991) or a non-selective inhibition of both endothelium-dependent and -independent vasodilation (Thomas *et al.*, 1989; Klabunde *et al.*, 1990;). The degree to which L-arginine analogues are able to inhibit the vasodilation induced by Ach has also been variable, prompting some authors to propose additional mechanisms of action for this vasodilator in their preparations (Gold *et al.*, 1989; Bellan *et al.*, 1991; Ross *et al.*, 1991). The dose and duration of treatment have also been reported to alter the relative effect of L-arginine analogues on baseline vascular tone in comparison to their effects on the response to Ach (Bellan *et al.*, 1991). Furthermore, the relative potencies of two of these agents, LNA and N^G-monomethyl-L-arginine (LNMMA), in the in-vivo canine femoral circulation has been shown to differ from that predicted from in-vitro studies (Kirkeboen *et al.*, 1992). Differences in species, vessel type, agent used, dose and duration of treatment may all, therefore, contribute to these apparent discrepancies.

Three L-arginine analogues were used in the current study. We found that exposure of the diaphragmatic vasculature to equimolar concentrations of these three analogues increased baseline vascular resistance to a similar extent. In addition, LNA and ArgSA, in the concentration used, attenuated the vasodilation induced by Ach but did not increase phrenic vascular resistance beyond the baseline values. These results indicate that LNA and ArgSA did not completely reverse Ach-induced vasodilation. Moreover, these findings suggest that in the indomethacin pretreated canine diaphragmatic circulation, the vasodilation induced by Ach infusion is mediated partly by augmentation of NO release and that these L-arginine analogues are specific inhibitors of this effect. We speculate also that part of the Ach-induced phrenic vasodilation is mediated by NO-independent mechanisms such as endothelium-derived relaxing factor (EDRF, Komori and Vanhoutte, 1990). In isolated rat vessels, Ach induces endothelium-dependent hyperpolarization which partially mediate the vasodilatory effect of Ach (Van de Voorde et al., 1992).

***L-arginine*:**

Endothelium dependent relaxing factor/NO is synthesized from the guanido nitrogen of L-arginine and molecular oxygen by the NADPH and calmodulin dependent action of NO synthase (NOS). Citrulline is a coproduct of this reaction. FMN, FAD, heme and tetrahydrobiopterin are co-factors (Nathan 1992). Substrate levels adequate to support ongoing NO synthesis are maintained by uptake of extracellular L-arginine and through the synthesis of L-arginine by a process linked to the release of NO (Mitchell *et al.*, 1990a). Endothelial cells can generate L-arginine from at least two sources. These include the peptidyl L-arginine pool

which is available through the action of peptidyl arginine deimidase (Thomas & Ramwell, 1988) and recycling of accumulated L-citrulline to L-arginine through the intermediate formation and subsequent cleavage of argininosuccinate (Hecker *et al.*, 1990). Intracellular levels of L-arginine, therefore, normally remain high (0.1-1 mM, approximately 30 times the apparent Km for purified NOS, (Pollock *et al.*, 1991)) even during prolonged stimulation of NO release (Mitchell *et al.*, 1990b).

In isolated vessel preparations, the effect of administration of exogenous L-arginine on vascular smooth muscle tone has been variable. In preparations in which vasodilation was elicited, intracellular L-arginine had been depleted either because of prolonged (> 2hrs) preparation time (Shini & Vanhoutte, 1991, Sun *et al.*, 1992) or by continuous stimulation of NO synthesis in arginine free media (Gold *et al.*, 1989). In fresh preparations no effect of L-arginine is observed (Shini & Vanhoutte, 1991; Sun *et al.*, 1992).

In the majority of blood perfused tissue preparations (Thomas *et al.*, 1989; Fortes *et al.*, 1990; Gardiner *et al.*, 1990; Lahera *et al.*, 1990), infusion of L-arginine has had no effect on vascular resistance. Nevertheless, in the pial circulation, exogenous L-arginine, but not D-arginine administration has resulted in vasodilation which is reversible by the topical administration of LNAME (Morikawa *et al.*, 1992). In the human forearm, furthermore, Panza et al. (Panza *et al.*, 1993) found that infusion of L-arginine, but not D-arginine, enhanced the vasodilator response to acetylcholine, although such treatment had no effect on baseline vascular resistance. The role of extracellular L-arginine availability as a rate limiting factor in endothelial NO synthesis under physiological conditions, therefore, varies depending upon the tissue and the species under study. Our current finding that neither arginine isomers significantly altered

vascular resistance indicates that L-arginine availability does not normally limit basal NO release in the canine diaphragmatic circulation.

L-glutamine:

In cultured endothelial cells, Sessa et al. (Sessa *et al.*, 1990) found that L-glutamine resulted in significant (46.5%) inhibition of EDRF release as detected by bioassay. The effect was observed over a concentration range of 0.1 - 2.0 mM, with maximum effect at concentrations of 0.2 mM and above. L-glutamine exerted this action through inhibition of intracellular conversion of L-citrulline to L-arginine. It did not interfere with the conversion of L-Arg-L-Phe or L-Argsucc to L-arginine nor did it inhibit the uptake of L-arginine into the endothelial cells. The inhibitory action of L-glutamine on L-citrulline conversion is most likely effected by allosteric interaction with argininosuccinate synthetase or by competitive interference due to the structural similarity between these two amino acids.

In the current study we found that L-glutamine, at a final concentration in the perfusing blood of 1mM, produced a small but significant increase in diaphragmatic vascular resistance. The exact mechanism behind the increase in phrenic vascular resistance after L-glutamine infusion is not clear. Based on the experiments of Sessa et al., one may speculate that L-glutamine inhibits basal NO release by preventing the conversion of L-citrulline to L-arginine. However, L-arginine requirements for basal NO synthesis can also be provided through an influx of intracellular L-arginine. Our experiments also indicated that L-glutamine infusion did not attenuate the vasodilatory response to stimulation of NO release by Ach. These results suggest that during Ach infusion, intracellular L-arginine concentration may not be sufficiently reduced

by L-glutamine to influence NOS activity. Alternatively, other sources of L-arginine may become more important or else conversion of L-citrulline to L-arginine by an as yet unknown transamination reaction may be activated during stimulation of NO production.

In summary, modulation of basal NO release by the endothelial cell plays an important role in the regulation of baseline diaphragmatic vascular resistance. Extracellular L-arginine availability does not appear to be rate limiting in this process. Intracellular recycling of L-citrulline, however, is likely to be an important source of substrate for this reaction under basal conditions. The L-arginine analogues, LNA and ArgSA are potent and specific inhibitors of basal NO release in the canine phrenic circulation.

ACKNOWLEDGEMENTS

The authors thank S. Nuara for his technical assistance. M. Ward is a fellow of the Parker B. Francis Foundation. S. Hussain is a scholar of the Canadian Heart and Stroke Foundation. The study was funded by a grant from the Medical Research Council of Canada.

REFERENCES

Aisaka, K., Gross, S.S., Griffith, O.W. & Levi, R. (1989). N^G-methylarginine, a potent pressor agent in the guinea pig: does nitric oxide regulate blood pressure in vivo? *Biochem. Biophys. Res. Commun.* **160,** 881-886

Aubier, M., Murciano, D., Menu, Y., Boczkowski, J., Mal, H. & Pariente, R. (1989). Dopamine effects on diaphragmatic strength during acute respiratory failure in chronic obstructive pulmonary disease. *Ann. Int. Med.* **110,** 17-23

Bellan, J.A., Minkes, R.K., McNamara, D.B. & Kadowitz P.J. (1991). N^W-nitro-L-arginine selectively inhibits vasodilator responses to acetylcholine and bradykinin in cats. *Am. J. Physiol.* **260,** H1025-1029

Bellan, J.A., McNamara, D.B. & Kadowitz, P.J. (1993). Differential effects of nitric oxide synthesis inhibitors on vascular resistance and responses to acetylcholine in cats. *Am. J. Physiol.* **264,** H45-H52

Bogle, R.G., Moncada, S., Pearson J.D. & Mann, G.E. (1992). Identification of inhibitors of nitric oxide synthase that do not interact with the endothelial cell L-arginine transporter. *Br. J. Pharmacol.* **105,** 768-770

Busse, R., & Mulsch, A. (1990). Calcium-dependent nitric oxide synthesis in endothelial cytosol is mediated by calmodulin. *FEBS Lett.* **265,** 133-136

Forstermann, U., Pollock, J.S., Schmidt, H.H.H.W., Heller, M. & Murad, F. (1991). Calmodulin-dependent endothelium-derived relaxing factor/nitric oxide synthase activity is present in the particulate and cytosolic fractions of bovine aortic endothelial cells. *Proc. Natl. Acad. Sci. U.S.A.* **88,** 1788-1792

Fortes, Z.B., Oliviera, M.A., Scivoleto, R., Carvalho, M.H.C., De Nucci, G. & Nigro, D. (1990). Nitric oxide release may be involved in the microcirculatory response to acetylcholine. *Eur. J. Pharmacol.* **182,** 143-147

Gardiner, S.M., Compton, A.M., Kemp, P.A., & Bennett, T. (1989). Regional and cardiac haemodynamic responses to glyceryl trinitrate, acetylcholine, bradykinin and endothelin-1 in conscious rats: effects of N^G-nitro-L-arginine. *Br. J. Pharmacol.* **101,** 632-639

Gardiner, S.M., Compton, A.M., Bennett, T., Palmer, R.M.J. & Moncada, S. (1990). Control of regional blood flow by endothelium-derived nitric oxide. *Hypertension Dallas* **15,** 486-492

Gold, M.E., Wood, K.S.,Buga, G.M., Byrns, R.E. & Ignarro, L.J. (1989). L-arginine causes whereas L-argininosuccinic acid inhibits endothelium-dependent vascular smooth muscle relaxation. *Biochem. Biophys. Res. Commun.* **161,** 536-543

Gross, S.S., Stuehr, D.J., Aisaka, K., Jaffe, E.A., Levi, R. & Griffith, O.W. (1990). Macrophage and endothelial cell nitric oxide synthesis: cell-type selective inhibition by N^G-aminoarginine, N^G-nitroarginine and N^G-methylarginine. *Biochem. Biophys. Res. Commun.* **170,** 96-100

Hecker, M., Sessa, W.C., Haris, H.J., Anggard, E.E. & Vane, J.R. (1990). The metabolism of L-arginine and its significance for the biosynthesis of endothelium-derived relaxing factor: Cultured endothelial cells recycle L-citrulline to L-arginine. *Proc. Natl. Acad. Sci. U.S.A.*, **87,** 8612-8616

Hussain, S.N.A., Roussos, C. & Magder, S. (1989). In-situ, isolated, perfused and innervated left hemidiaphragm preparation. *J. Appl. Physiol.* **67,** 2141-2146

Kaley, G., Koller, A., Rodenburg, J. M., Messina, E.J. & Wolin, M.S. (1992). Regulation of arteriolar tone and responses via L-arginine pathway in skeletal muscle. *Am. J. Physiol.* **262,** H987-H992

Kelm, M. & Schrader J. (1990), Control of coronary vascular tone by nitric oxide. *Circ. Research* **66,** 1561-1575

Kirkeboen, K.A., Naess, P.A., Christensen, G. & Kiil, F. (1992). Importance of nitric oxide in canine femoral circulation: comparison of two NO inhibitors. *Cardiovas. Res.* **26,** 357-361

Klabunde, R.E., Ritger, R.C. & Helgren, M.C. (1990). N^G-monomethyl-L-arginine causes systemic vasoconstriction and cardiac depression in anesthetized dogs. *Pharmacologist* **32,**145

Koller, A. & Kaley, G. (1990) Role of endothelium in reactive dilatation of skeletal muscle arterioles. *Am. J. Physiol.* **259,** H1313-H1316

Koller, A., Sun, D., Messina, E. J., & Kaley, G. (1993). L-arginine analogues blunt prostaglandin-related dilation of arterioles. *Am. J. Physiol.* **264,** H1194-H1199

Komori, K. and Vanhoutte, P.M. (1990). Endothelium-derived hyperpolarizing factor. *Blood Vessels* 27:238-245.

Lahera, V., Salom, M.G., Fisken-Olsen, M.J., Raij, L. & Romero, J.C. (1990). Effects of N^G-monomethyl-L-arginine and L-arginine on acetylcholine renal response. *Hypertension Dallas* **15,** 659-663

Lamontagne, D., Pohl, U. & Busse, R. (1991). N^G-Nitro-L-arginine antagonizes endothelium-dependent dilator responses by inhibiting endothelium-derived relaxing factor release in the isolated rabbit heart. *Pflugers Arch.* **418,** 266-270

Macklem PT & Roussos CS (1977). Respiratory muscle fatigue: a cause of respiratory failure? *Clin Sci Mol Med.* **53,** 419-422

Mitchell, J.A., Hecker, M. & Vane J.R. (1990a). The generation of L-arginine in endothelial cells is linked to the release of endothelium-derived relaxing factor. *Eur. J. Pharmacol.* **176,** 253-254

Mitchell, J.A., Hecker M., Anggard E.E. & Vane (1990b). Cultured endothelial cells maintain their L-arginine level despite the continuous release of EDRF. *Eur. J. Pharmacol.*, **182,** 573-576

Morikawa, E., Rosenblatt S. & Moskowitz M.A. (1992). L-arginine dilates rat pial arterioles by nitric oxide-dependent mechanisms and increases blood flow during focal cerebral ischaemia. *Brit. J. Clin. Pharmacol.* 905-907

Mugge, A., Lopez, J.A.G., Piegors, D.J., Breese, K.R. & Heistad D.G. (1991). Acetylcholine-induced vasodilation in rabbit hindlimb in vivo is not inhibited by analogues of L-arginine. *Am. J. Physiol.* **260,**H242-247

Nathan C. (1992). Nitric oxide as a secretory product of mammalian cells. *FASEB J.* **6,**3051-3064

Panza, J.A., Casino, P.R, Badar, D.M. & Quyyumi, A.A. (1993). Effect of increased availability of endothelium-derived nitric oxide precursor on endothelium-dependent vascular

relaxation in normal subjects and in patients with essential hypertension. *Circulation* **87,** 1475-1481

Persson, M.G., Gustafsson, L.E., Wiklund, N.P., Hedqvist, P. & Moncada, S. (1990). Endogenous nitric oxide as a modulator of rabbit skeletal muscle microcirculation. *Br. J. Pharmacol.* **10,** 463-466

Pollock, J.S., Forstermann, U., Mitchell, J.A., Warner, T.D., Schmidt, H.H.H.W., Nakane, M. & Murad, F. (1991). Purification and characterization of particulate endothelial derived relaxing factor synthase from cultured and native endothelial bovine aortic endothelial cells. *Proc. Nat. Acad. Sci., U.S.A.*, **88,** 10480-10484

Ross, G., Chaudhuri, G., Ignarro, L.J. & Chyu K.-Y. (1991). Acetylcholine vasodilation of resistance vessels in vivo may not entirely depend on newly synthesized nitric oxide. *Eur. J. Pharmacol.* **195,** 291-293

Rubanyi, G.M., Lorenz, R.R. & Vanhoutte P.M. (1985). Bioassay of endothelium-derived relaxing factor. *Am. J. Physiol.* **215,** H1077-H1080

Sessa, W.C., Hecker, M., Mitchell, J.A. & Vane J.A. (1990). The metabolism of L-arginine and its significance for the biosynthesis of endothelium-derived relaxing factor: L-glutamine

inhibits the generation of L-arginine by cultured endothelial cells. *Proc. Natl. Acad. Sci. U.S.A.* **87,** 8607-8611

Shini, V.B. & Vanhoutte P.M. (1991). L-arginine evokes both endothelium-dependent and -independent relaxations in L-arginine-depleted aortas of the rat. *Circ. Res.* **68,** 209-216

Sun, D., Messina, E.J., Koller, A., Wolin, M.S. & Kaley, G. (1992). Endothelium-dependent dilation to L-arginine in isolated rat skeletal muscle arterioles. *Am. J. Physiol.* **262,** H1211-H1216

Supinski, G., Dimarco, A., Ketai, L., Hussein, F. & Altose, M. (1988) Reversibility of diaphragm fatigue by mechanical hyperperfusion. *Am. Rev. Respir. Dis.* **138,** 604-609

Thomas, G. & Ramwell, P.W.(1988). Peptidyl arginine diminase and endothelium dependent relaxation. *European J. Pharmacol.* **153,** 147-148

Thomas, G., Cole, E.A. & Ramwell, P.W. (1989). N^G-monomethyl-L-arginine is a nonspecific inhibitor of vascular relaxation. *Eur. J. Pharmacol.* **170,** 123-124

Thomas, G. & Ramwell, P.W. (1992). Interaction of Non-arginine compounds with the endothelium-derived relaxing factor inhibitor, N^G-monomethyl-L-arginine. *J. Pharmacol. Exp. Ther.* **260,** 676-679,

Vallance, P., Collier, J. & Moncada S. (1989). Effects of endothelium-derived nitric oxide on peripheral arteriolar tone in man. *Lancet* **2**, 997-1000

Van de Voorde, J., Vanheel, B. and Leusen, I. (1992). Endothelium-dependent relaxation and hyperpolarization in aorta from control and renal hypertensive rats. *Circ. Res.* 70:1-8.

Vargas, H.M., Cuevas, J.M., Ignarro, L.J. & Chaudhuri, G. (1991). Comparison of the inhibitory potencies of N^G-methyl-, N^G-nitro- and N^G-amino-L-arginine on EDRF function in the rat: Evidence for continuous basal EDRF release. *J. Pharmacol. Exp. Ther.* **257,** 1208-1215

White, D.G., Drew, G.M., Gurden, J.M., Penny, D.M., Roach, A.G. & Watts, I.S. (1993) The effect of N^G-nitro-L-arginine methyl ester upon basal blood flow and endothelium-dependent vasodilatation in the dog hindlimb. *Br. J. Pharmacol.* **108,** 763-768

FIGURE LEGENDS:

Figure 1

Change in phrenic arterial perfusion pressure following infusion of N^G-nitro-L-arginine methyl ester (LNAME, $6 \bullet 10^{-4}$M), N^G-nitro-L-arginine (LNA,$6 \bullet 10^{-4}$M), argininosuccinic acid (ArgSA, $6 \bullet 10^{-4}$M) and L-glutamine (LGlut, 10^{-3}M). * $p < 0.05$; ** $p < 0.01$ for the change compared to baseline perfusion pressure.

Figure 2

A representative tracing of the changes in phrenic perfusion pressure in response to $6 \bullet 10^{-4}$M LNAME.

Figure 3

Effects of N^G-nitro-L-arginine (LNA, $6 \bullet 10^{-4}$M), argininosuccinic acid (ArgSA, $6 \bullet 10^{-4}$M) and L-glutamine (LGlut, 10^{-3}M) on the changes in phrenic arterial perfusion pressure during acetylcholine (Ach, 10^{-5}M) and sodium nitroprusside (SNP, 2 μg/ml) infusion. *$p < 0.05$ compared with response to vasodilator alone.

Figure 4

Effects of L-arginine and D-arginine on baseline phrenic arterial perfusion pressure.

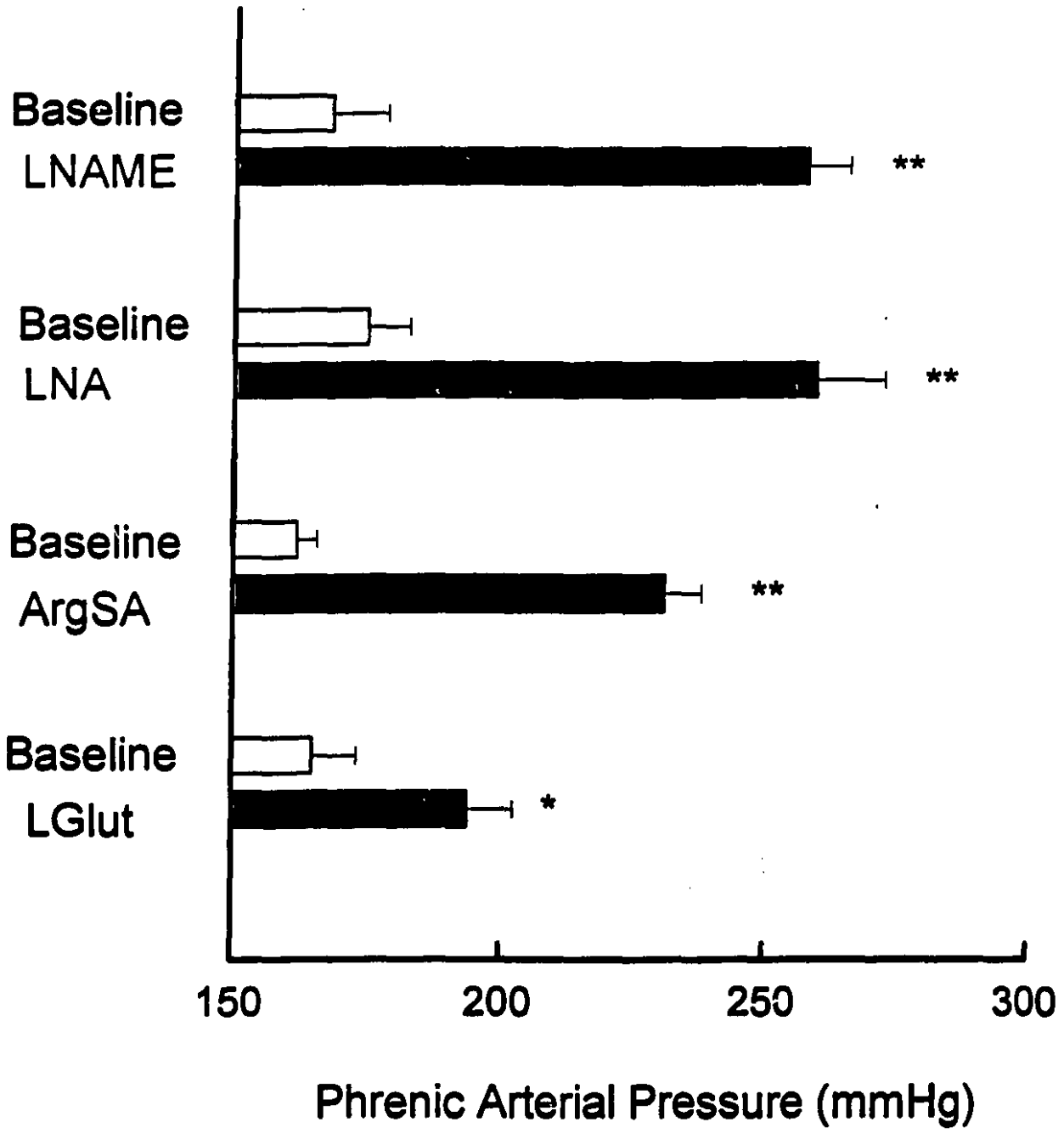
Baseline
LNAME
**
Baseline
LNA
**
Baseline
ArgSA
**
Baseline
LGlut
*
150
200
250
300
Phrenic Arterial Pressure (mmHg)

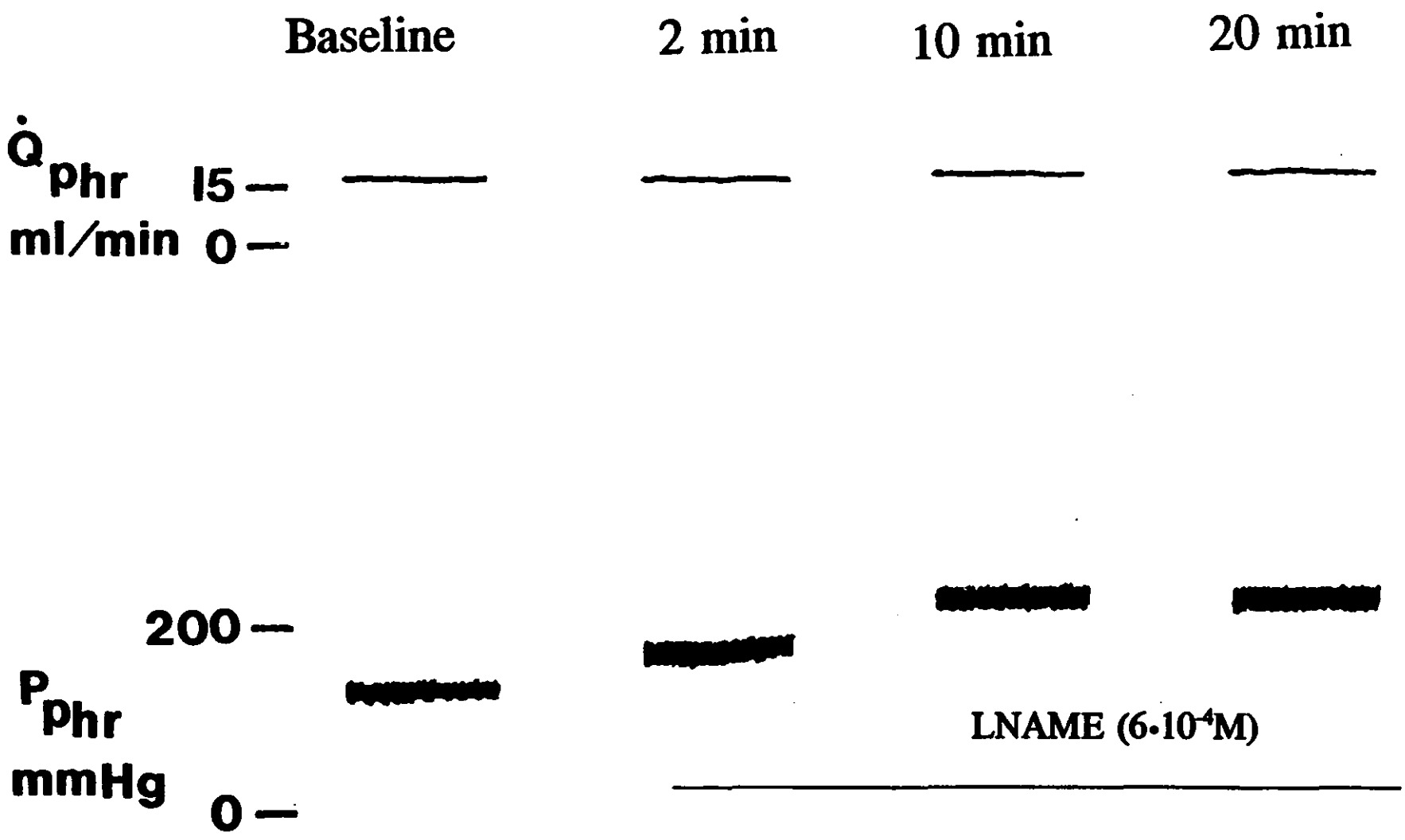
Baseline
2 min
10 min
20 min
$\dot{Q}_{Phr}$
15
ml/min
0
200
P_{Phr}
mmHg
0
LNAME ($6 \cdot 10^{-4}$M)

Figure 2

Figure 3

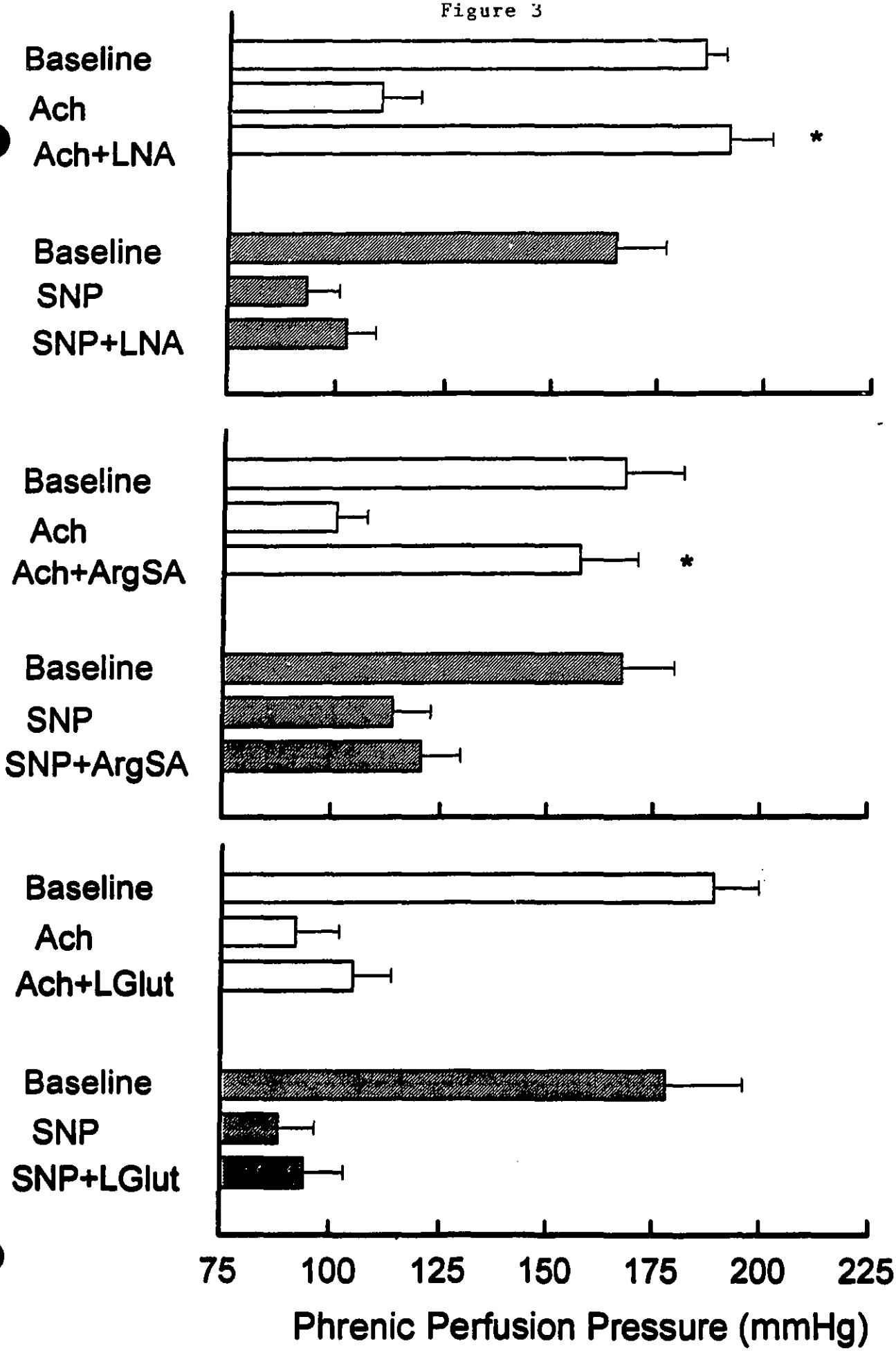
Baseline
Ach
Ach+LNA
*
Baseline
SNP
SNP+LNA
Baseline
Ach
Ach+ArgSA
*
Baseline
SNP
SNP+ArgSA
Baseline
Ach
Ach+LGlut
Baseline
SNP
SNP+LGlut
75
100
125
150
175
200
225
Phrenic Perfusion Pressure (mmHg)

Figure 4

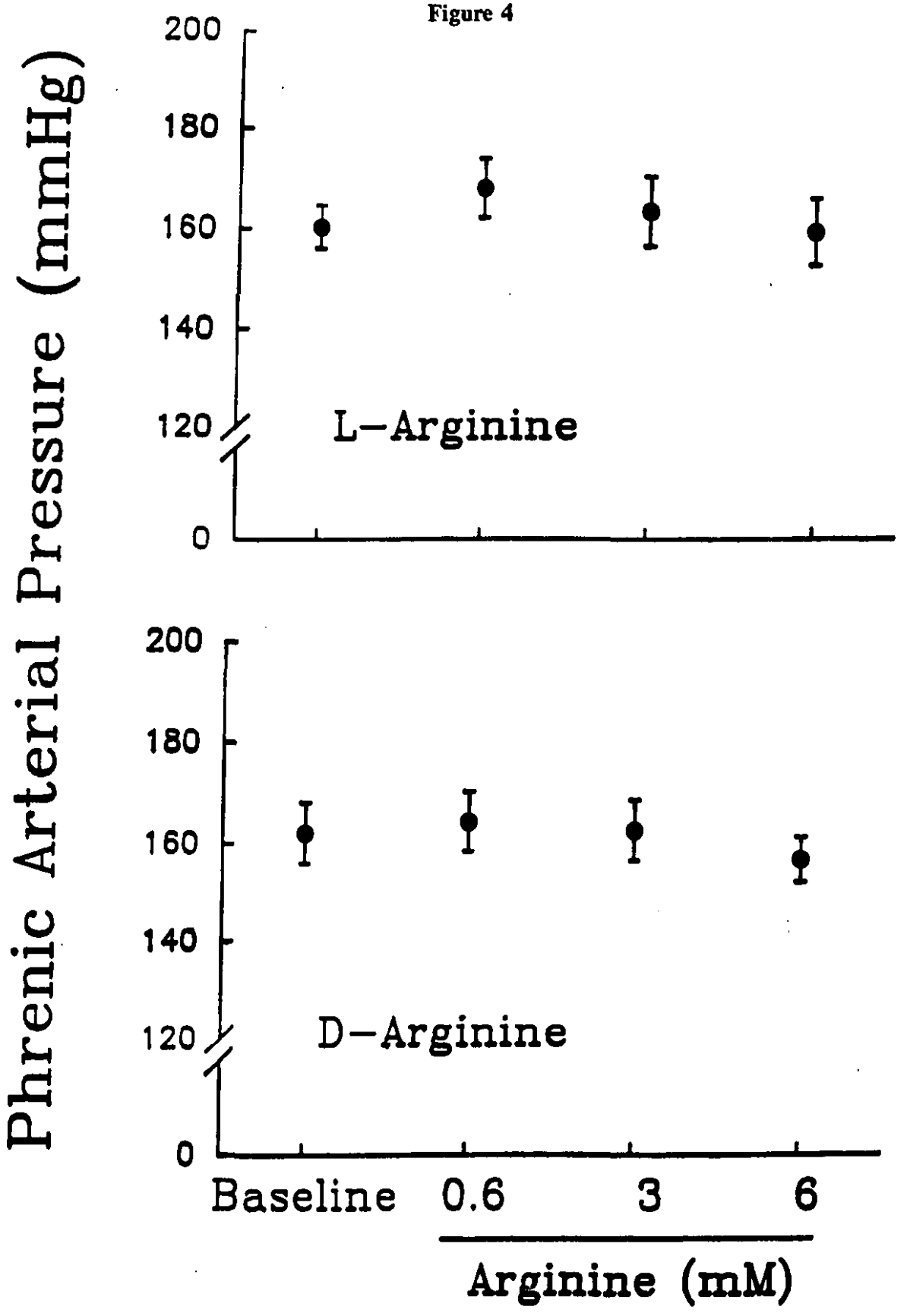
Phrenic Arterial Pressure (mmHg)
200
180
160
140
120
0
L-Arginine
D-Arginine
Baseline
0.6
3
6
Arginine (mM)

The Role of Endothelium-Derived Relaxing Factor in Reactive Hyperaemia in the Canine Diaphragm

Michael E. Ward, Sheldon A. Magder and Sabah N.A. Hussain
Journal of Applied Physiology 74: 1606-1612, 1993

ABSTRACT

We studied the effect of N^G-nitro-L-arginine (L-NA) on reactive hyperaemia in the vascularly isolated hemidiaphragm of anaesthetized dogs pretreated with indomethacin. In 9 animals, the diaphragm was autoperfused from the left femoral artery. Phrenic arterial flow was interrupted for 10-120 s during a control period and after 20 minutes of L-NA infusion ($6 \cdot 10^{-4}$M). Post-occlusive flow and duration of hyperemia during the control period increased progressively with increasing occlusion duration. Following L-NA infusion, baseline and post-occlusive flow in response to all occlusions declined significantly compared with control values. However, when normalized as % of baseline flow, post-occlusive flow remained similar to that found during the control period. By comparison, the duration of reactive hyperemia was significantly shortened by L-NA infusion. In 5 animals, we repeated the same protocol during pump-perfusion of the diaphragm at a fixed flow rate. L-NA infusion increased baseline and post-occlusive phrenic resistance in response to all occlusion durations, however, post-occlusive phrenic resistance as % of baseline remained similar to control values. In addition, hyperemia durations in response to 60 and 120 s occlusions were shortened significantly by L-NA infusion. We conclude that 1) Endothelium derived relaxing factor (EDRF) plays an important role in the regulation of baseline vasomotor tone in the diaphragm 2) Modulation of EDRF release contributes to the reactive vasodilatory response to transient vascular occlusion in the diaphragm.

Key Words: respiratory muscles, respiration, EDRF, endothelium, vasomotor control,

INTRODUCTION

Reactive hyperaemia is the vasodilator response to transient vascular occlusion. The magnitude and duration of vasodilation vary in different vascular beds. The greatest response is in tissues with high metabolic demands such as the myocardium and skeletal muscle. The response is modified by tissue temperature (21), intravascular pressure (15) and occlusion duration (5). These observations have led to the theory that the synergistic interaction of myogenic and metabolic control mechanisms determines the post-occlusive change in vascular tone (5).

Recently, endothelium derived relaxing factors (EDRF) have been recognized as a major determinant of the changes in vessel diameter in response to changes in blood flow and to a variety of chemical mediators (eg: acetylcholine, ATP, ADP, bradykinin, histamine, serotonin, noradrenaline, thrombin). Since vascular occlusion is accompanied by the most dramatic fluctuations in flow likely to be encountered under physiologic conditions and since many of the proposed mediators of metabolic control also influence EDRF release, it is not surprising that modulation of EDRF release has been proposed as one of the underlying mechanisms (1,17,20). Studies of the role of EDRF in reactive hyperaemia, however, have yielded conflicting results. Chemical de-endothelialization (saponin) in dog hindlimb (17) and injury of arteriolar endothelium (light-dye techniques (7)) in rat cremasteric muscle have been reported to reduce peak post occlusive vasodilation. Inhibition of EDRF synthesis by N^G-monomethyl-L-arginine infusion, in contrast, has not been found to alter peak post-occlusive changes in microvascular resistance in cat hindlimb muscle (1) nor to affect the increase in arteriolar diameter following a 15 second occlusion in rat cremaster muscle (20). As a result the role played by the EDRF

system in reactive hyperaemia remains controversial.

Since the diaphragm contracts rhythmically, its vascular bed is regularly exposed to wide fluctuations in transmural pressure, particularly when the ventilatory load is increased. The response to transient occlusion is, therefore, likely to play a more important role in determining the diaphragm's ability to efficiently match substrate availability to utilization than in other skeletal muscles. It is the goal of this study to determine the effect of inhibition of EDRF synthesis on the duration and magnitude of the reactive vasodilator response of the diaphragmatic vasculature in order to further evaluate the role of this pathway in control of diaphragm blood flow.

METHODS

Animal Preparation: Fourteen mongrel dogs weighing 28.7 ± 1.3 kg (SE) were anaesthetized with sodium thiopental (10 mg/kg) followed by α-chloralose (60-80 mg /kg). Supplemental doses of α-chloralose were given as needed to eliminate the jaw tone but maintain knee reflexes. The animals were supine, intubated with a cuffed endotracheal tube and mechanically ventilated (tidal volume 15 ml/kg, frequency of 15 /min). Supplemental O_2 was supplied through the inspiratory line and arterial PO_2 maintained above 100 mmHg. Positive end-expiratory pressure (PEEP) (5 cm) was applied at the expiratory line. A catheter was placed in the aorta via the right carotid artery to monitor arterial pressure (P_{ar}) and another catheter was placed in the right femoral vein to administer fluids. Core body temperature was kept constant at approximately 37° C by a heating pad placed under the animal.

Isolated left hemidiaphragm: In all animals, we used the in-situ vascularly isolated left hemidiaphragm preparation developed by Hussain et. al. (4). The completeness of vascular isolation in this preparation was confirmed in previous studies (4) by the inability to identify collateral vessels during Lissamine Green B injection and the absence of response of the diaphragmatic vasculature to systemic epinephrine infusion. The lower six ribs and interspaces on the left side were exposed by dissecting the abdominal rectus, external oblique and latissimus dorsi muscles. Each interspace was incised (5-10 cm long) and the incision was extended as near as possible to the origin of the costal diaphragm. Intercostal vessels were then ligated and the ribs were removed. A midline incision was made in the xiphisternal cartilage to expose the left internal mammary artery, which was then ligated. A lateral abdominal incision was made just caudal to the inferior margin of the costal diaphragm. This incision extended from the midline to the inferior margin of the last rib, which was cut at the left costophrenic angle. The two halves of the diaphragm were divided through a midline incision extending from the xiphisternal cartilage to the central tendon. The ribs and cartilages of the free costal margin were secured by silk threads to 3 metal bars, 5 cm long. Each bar was attached through its center to a thumbscrew that was attached to a force transducer (Grass model FT10). To ensure independent movement of the bars, we severed the interconnecting rib portions. Each transducer was mounted on a rack-and-pinion adjustable clamp. These clamps were attached horizontally to a rigid metal frame surrounding the animal's thorax. To eliminate contraction of the left diaphragm, we sectioned the left phrenic nerve close to its exit from the diaphragm. Resting length of each diaphragmatic segment was adjusted to be equal to that measured upon removing the ribs. The diaphragm was dissected free and weighed at the end of the experiment.

Phrenic arterial pressure and flow measurement: The stomach, liver, spleen, and left kidney were retracted through the abdominal incision to expose the left phrenic artery. This artery was dissected free from the surrounding tissue 4 to 6 cm above the adrenal gland. The proximal part of the artery was ligated, and a polyethylene catheter (PE 160, 1.14 mm ID, 1.57 mm OD, 3 cm long) was introduced into the distal portion. A side port was placed at the entrance of the catheter into the phrenic artery for measurement of phrenic perfusion pressure (P_{phr}). The catheter was connected to an electromagnetic flow probe (Carolina Medical Electronics, 1.91 mm ID). Phrenic arterial flow measured by the probe was designated as Q_{phr}. The other side of the probe was connected to a 15-cm-long polyethylene tube (4 mm ID, 6 mm OD) which, in turn, was connected to a Y-shaped connection. One arm of the Y connection was connected to a catheter in the left femoral artery so that the diaphragm could be autoperfused by diverting blood flow from the left femoral artery through the catheter-probe system to the left phrenic artery. The other arm of the Y connection was secured via two three-way stopcocks and an extension, to a non-pulsatile pump (Cole Palmer Instruments, model 7523-00) which was used to pump perfuse the left phrenic artery at a fixed rate with arterial blood from the right femoral artery. The stopcocks were connected through short polyethylene tubes to two 5-ml syringes mounted on a constant infusion pump (Harvard Apparatus, model 940) which was used to infuse vasoactive drug solutions into the phrenic circulation. All animals were heparinized after catheterizing the phrenic artery.

Drugs: To block prostaglandin synthesis, all animals received indomethacin (Sigma Chemicals) 5 mg/kg intravenously, 30 minutes before beginning the experimental protocol. Acetylcholine

chloride (Ach) and sodium nitroprusside (SNP) were dissolved in normal saline to obtain concentrations of 10^{-3} M and 200 μg/ml respectively. To inhibit EDRF (nitric oxide) synthesis, we used an L-arginine analogue, N^G-nitro-L-arginine (L-NA) which was dissolved in saline to obtain a concentration of $6 \cdot 10^{-2}$ M. These concentrations refer to the solutions contained in the 5 ml syringes of the Harvard infusion pump. The infusion rate was set at 1/100th of the phrenic arterial flow rate. The concentrations delivered to the diaphragmatic vasculature, therefore, represent a 100 fold dilution of these. Phenylephrine was diluted in saline to a concentration of 0.04 mg/ml and the infusion rate titrated to obtain the desired effect on phrenic vascular resistance. All drugs were obtained from Sigma Chemicals (St. Louis, MO) and fresh stock solutions were prepared immediately before each experiment.

Experimental Protocol:

Specificity of L-NA: We first assessed the capacity of L-NA to reverse endothelium-dependent (Ach-induced, n=6) and endothelium-independent (SNP-induced, n=4) vasodilation in this preparation. Following a 30-minute stabilization period during which the left diaphragm was autoperfused through the femoral arterial catheter, the diaphragm was then pump-perfused (Cole Parmer) at the flow rate recorded during the previous period of autoperfusion. Two 5-ml syringes containing saline were placed in the infusion pump and the pump speed was set at 1/100th of the phrenic arterial flow. After 5 minutes, in four animals, one of these syringes was replaced with a syringe containing SNP (200 μg/ml). After 4 minutes of SNP infusion, when P_{phr} had stabilized, the second saline syringe was replaced with one containing L-NA ($6 \cdot 10^{-2}$ M) and the SNP was also continued. Infusions were stopped after 20 minutes. In six animals, this

protocol was performed with Ach infusion (10^{-3} M) instead of SNP infusion.

Effect of L-NA on reactive hyperaemia: In 9 animals the effect of L-NA on the reactive hyperaemic response was assessed during autoperfusion at the natural flow rate with P_{phr} fixed by the animals systemic blood pressure. Phrenic arterial flow was interrupted for 10, 20, 30, 60 and 120 s by clamping the femoral arterial catheter. Occlusion periods were separated by five minutes and the order of presentation of the occlusions was randomized.

In 5 animals the diaphragm was then pump-perfused at a flow rate identical to the autoperfusion rate so that the reactive hyperaemic response could be assessed under conditions of constant flow. Occlusions were performed by simultaneously occluding the phrenic arterial catheter (distal to the Y connector) and opening the femoral arterial clamp so as to divert the right femoral arterial blood delivered by the Cole Palmer pump from the left phrenic artery to the left femoral artery. This was done so that when the phrenic arterial occlusion was released flow was immediately reestablished at its preocclusion rate. Occlusions were maintained for 10, 20, 30, 60 and 120 s separated by 5 minutes and were performed in random order. The vascular responses to occlusions performed before L-NA infusion under conditions of constant pressure (autoperfusion) and constant flow (pump perfusion) were designated as the control responses.

We next assessed the effect of L-NA on the reactive hyperaemic response. With phrenic arterial flow still being provided by the Cole Parmer pump, saline was infused into the phrenic circulation using the infusion pump at a rate equal to $1/100^{th}$ of the phrenic arterial flow for 3 minutes. One of the saline syringes was then replaced with a syringe containing L-NA ($6 \cdot 10^{-2}$ M) and infused for 20 minutes. It was unnecessary to continue L-NA infusion beyond this

because its effect is long lasting (see below).

In 5 animals, phrenic arterial occlusions were then performed during pump perfusion as described above for the control group. Pump perfusion was then stopped and a 10-minute stabilization period during which the diaphragm was autoperfused was allowed. In all 9 animals the phrenic arterial occlusions during autoperfusion were then repeated.

Arterial blood gases were measured immediately following the stabilization periods of autoperfusion before and after L-NA infusion.

Effect of phenylephrine on reactive hyperaemia: To determine the effect of changing baseline vascular resistance on reactive hyperaemia, we studied the effect of phenylephrine in 4 animals. Phrenic arterial occlusions (10, 20, 30, 60 and 120 s) were performed during autoperfusion as described above. Phenylephrine was infused into the phrenic artery using the Harvard pump at a rate which resulted in a reduction in phrenic arterial flow approximately comparable to that observed in the L-NA group (42% of baseline, see below). The phrenic arterial occlusions were then repeated.

Data analysis: Baseline Q_{phr} and P_{phr} were measured before each occlusion period. The diaphragmatic vascular resistance (R_{di}) calculated as the ratio of driving pressure to flow (P_{phr}/Q_{phr}) was measured prior to the occlusions (baseline), at the point of maximum post-occlusive Q_{phr} during autoperfusion, and at the point of minimum post-occlusive P_{phr} during pump perfusion. The minimum post-occlusion R_{di} during both auto and pump-perfusion was then expressed as % of the baseline value. The duration of the reactive vasodilation was measured

as the time from the release of the arterial occlusion to the return to baseline Q_{phr} (autoperfusion) or P_{phr} (pump perfusion). The reactive hyperaemic volume for each occlusion period was calculated as the time integral of Q_{phr} ($\int Q_{phr} \cdot dt$) above the baseline Q_{phr} during autoperfusion.

All data are presented as mean ± SE. Comparison between and within interventions were performed by analysis of variance (ANOVA). Differences were further evaluated by the Student-Newman-Keuls test. $P < 0.05$ or less were considered significant.

RESULTS

Arterial pH, PO_2, and PCO_2 averaged 7.34 ± 0.03, 128.0 ± 12.7 mmHg and 35.9 ± 4.31 mmHg respectively during the control period and were unchanged following L-NA infusion.

Ach and SNP infusion: Baseline mean P_{art}, P_{phr}, and Q_{phr} were 165.0 ± 9.4 mmHg, 195.8 ± 21.6 mmHg and 26.6 ± 3.2 ml/100g/min, respectively. Ach infusion reduced P_{phr} by 80.0 ± 14.1 mmHg ($P<0.01$ compared with baseline). When L-NA was added, P_{phr} increased above the baseline value by 15.0±7.3 mmHg. By comparison, SNP infusion reduced P_{phr} by 71.6 ± 9.2 mmHg ($P<0.01$). When L-NA was infused along with SNP, P_{phr} remained lower than baseline values by 62.5 ± 9.8 mmHg which was not different than that observed before L-NA infusion. Accordingly, infusion of L-NA reversed Ach-induced vasodilation completely, whereas SNP-induced vasodilation was not significantly affected.

Effect of L-NA on reactive hyperaemia:

Autoperfusion: ***Control:*** Baseline mean P_{art}, mean P_{phr}, Q_{phr} and R_{di} before the 10 s occlusion were 153.0 ± 4.9 mmHg, 152.7 ± 5.3 mmHg, 19.8 ± 1.7 ml/100g/min and 8.1 ± 0.6

mmHg/ml/100g/min, respectively. Peak post-occlusive Q_{phr} in response to 10, 20, 30, 60 and 120 s occlusions increased to 31.9±2.8, 32.2±2.7, 33.7±3.1, 40.2±3.6 and 50.3±3.0 ml/100g/min, respectively. Only after 60 and 120 s occlusions did peak post-occlusive Q_{phr} increase higher than after 10 s occlusion ($P<0.05$, 0.01, respectively). Figure 1 (top) illustrates the minimum R_{di} (as % of baseline) following the arterial occlusions. Thirty, 60 and 120 s occlusions induced greater reductions in R_{di} compared with that measured after 10 s occlusion ($P<0.05$). Increasing the duration of occlusion produced a progressive increase in reactive hyperemia duration reaching a mean value of 62.0 ± 6.4 s in response to 120 s occlusion (figure 1 middle). Reactive hyperemic volume also increased with increasing occlusion duration (figure 1 bottom).

Post L-NA infusion: Baseline values of mean P_{art}, P_{phr}, Q_{phr} and R_{di} measured before the 10 s occlusion averaged 154.0 ± 6.5 mmHg, 155.6 ± 9.2 mmHg, 8.0 ± 1.1 ml/100g/min and 23.3 ± 3.9 mmHg/ml/100g/min. L-NA infusion reduced baseline Q_{phr} significantly to 42% of control values ($P<0.01$), however, transient increases in flow still occurred after the occlusions with peak post-occlusive Q_{phr} after 10, 20, 30, 60 and 120 s occlusions averaging 12.6±2.2, 17.8±4.4, 19.3±5.1, 24.1±6.3 and 27.1±6.1 ml/100g/min, respectively. After L-NA infusion, post-occlusive Q_{phr} in response to any given occlusion duration was significantly lower than the control values. However, when minimum R_{di} is expressed as % of the baseline value (figure 1 top), the post-occlusive dilation post L-NA were not significantly different from the control period. Reactive hyperaemia duration and volume during the L-NA period rose with increasing higher occlusion durations but were always lower than those measured during the control period (figure 1 middle and bottom).

Pump perfusion: ***Control:*** Baseline values of mean P_{art}, P_{phr}, Q_{phr} and R_{di} averaged 159.0 ± 6.5 mmHg, 183.4 ± 28.3 mmHg, 21.0 ± 2.1 ml/100g/min and 9.0 ± 1.3 mmHg/ml/100g/min. P_{phr} transiently fell following all occlusions. Minimal P_{phr} following the 10, 20, 30, 60 and 120 s occlusions averaged 145.2±18.9, 142.0±17.9, 138.4±18.3, 132.7±17.0 and 112.0±15.0 mmHg, respectively. Minimal R_{di} (as % of baseline) declined with increasing occlusion duration reaching 57.2 ± 3.8% after 120 s occlusion. Increasing occlusion durations also resulted in a progressive rise in reactive hyperemia duration reaching 85.6 ± 9.8 s in response to 120 s occlusion ($P < 0.05$ compared with 10 s occlusion, figure 2 bottom).

Post L-NA infusion: Baseline values of mean P_{art}, P_{phr}, Q_{phr} and R_{di} measured before 10 second occlusion averaged 160.2 ± 12.8 mmHg, 276.2 ± 17.7 mmHg, 21.0 ± 2.1 and 14.0 ± 1.9 mmHg/ml/100g/min, respectively. Vascular resistance still declined and hyperemia duration still increased after all occlusions. Minimal P_{phr} in response to 10, 20, 30, 60 and 120 s occlusions averaged 209.8 ± 19.6, 216.0±21.6, 210.0±20.2, 180.0±20.5 and 150.0±29.5 mmHg, respectively. Occlusion durations longer than 30 s produced a progressive decline in minimal R_{di} reaching 47.2% of baseline after 120 s occlusion (figure 2 top). At any given occlusion duration, minimal R_{di} (as % of baseline) during the L-NA period was not different from control (figure 2 top). By comparison, the duration of reactive vasodilation which followed 60 and 120 s occlusions were shorter than those measured in the control period ($P < 0.05$, figure 2, bottom).

Effect of phenylephrine on reactive hyperaemia:

Phenylephrine infusion increased baseline R_{di} from 9.5 ± 2 to 30.6 ± 2.2 mmHg/ml/100g/min. The effect of phenylephrine lasted a significant period of time with

baseline R_{di} being unchanged (29.5 $\pm$ 3 mmHg/ml/100g/min) 10 minutes after discontinuation of the infusion. The effects of increasing baseline R_{di} by infusing phenylephrine on the post-occlusion vasodilation are shown in figure 3. At any given occlusion duration following phenylephrine infusion, minimal R_{di} (as % of baseline) was smaller than control values but the duration of reactive hyperaemia was unaffected (figure 3).

DISCUSSION

The main findings of this study are:

1) L-NA inhibits endothelium-dependent but not endothelium-independent vasodilation in the diaphragm. 2) L-NA infusion resulted in a significant increase in baseline diaphragmatic vascular resistance. 3) L-NA decreased peak reactive flow during autoperfusion or minimum post-occlusion perfusion pressure during pump perfusion. The reduction in the peak vasodilation was in proportion to the change in baseline vascular resistance. 4) L-NA reduced the duration of the reactive vasodilation at all occlusion durations during autoperfusion and for occlusion durations above 30 s during pump perfusion.

Critique:

The aortic pressures recorded during the current studies were higher than are generally observed in anaesthetized dogs. We attribute this to the choice of anaesthetic; our dogs were anesthetized with α-chloralose instead of the more commonly used barbiturates. Borgdorf et al. (2) have commented on a similar difference in aortic pressure between these two agents in cats.

We found phrenic perfusion pressure to be higher during pump perfusion than during autoperfusion. In the cat hindlimb, a switch from autoperfusion to pump perfusion has been shown to be associated with a fall in vascular resistance (2). Following treatment with

indomethacin, however, pump perfusion resulted in an increase in resistance (2) suggesting the release of a non-prostaglandin vasoconstrictor substance. Since the animals in our current study were pretreated with indomethacin, the increase in resistance during pump perfusion may represent a similar phenomenon. Another possibility is that basal EDRF release is reduced during pump perfusion as a result of elimination of the shear stress fluctuations which accompany pulsatile flow.

Comparison with phenylephrine: It is difficult to predict the effect of increased baseline vascular tone on the response to transient occlusion. On one hand, if the same vasoconstrictor influence were active in the post-occlusion period as under baseline conditions, one might expect a reduction in the peak response in proportion to the change in baseline resistance. On the other hand, a vessel with a smaller initial diameter would demonstrate a greater post-occlusive response than one beginning from a larger diameter if the reactive vasodilation was near maximum or if the relationship between vascular smooth muscle tension and vessel diameter were curvilinear. Increasing the baseline vascular resistance with phenylephrine reduced the peak change in R_{di}. The increase in baseline R_{di}, by inhibition of baseline EDRF release may, therefore, have accounted for some of the effect of L-NA. During phenylephrine infusion, however, minimum R_{di} (as % of baseline) was lower than the control value at all occlusion durations (figure 3). By comparison, minimum R_{di} (% of baseline) observed in response to all occlusion durations was not influenced by L-NA infusion (figures 1 and 2). Therefore, inhibition of EDRF release appears to have altered the peak response, since, if L-NA had no effect other than increasing baseline vascular tone, a greater degree of vasodilation would be expected.

One might reasonably expect the change in baseline resistance to alter the duration of the reactive vasodilation as well. Since the peak response is smaller, the time to recover should be shorter. Alternatively, if the main factor determining the duration is the metabolic state of the muscle, a longer duration might be expected in order to compensate for the smaller magnitude of the vasodilation. In fact, the most striking difference between the effects of phenylephrine and L-NA was the complete lack of effect of phenylephrine on the duration of the post-occlusive vasodilation. The time required for return of vascular tone following occlusion is apparently not influenced by the baseline condition of the vessels.

Role of basal EDRF release: L-NA is known to inhibit the EDRF pathway by competitive inhibition of the formation of nitric oxide (NO) from the guanido nitrogen moiety of L-arginine (14). In addition, L-NA is more potent than N-monomethyl-L-arginine (L-NMMA) and its effect is not completely reversed by L-arginine (11,12). This high potency and poor reversibility has been attributed to a high affinity of L-NA for the NO-synthase and to the fact that the nitroguanidino moiety of L-NA renders it more hydrophobic, therefore more likely to be taken up and "trapped" than L-arginine (12). L-NA does not reduce nitroglycerine or nitroprusside induced vasodilation, therefore, direct interference at points in the pathway distal to soluble guanylate cyclase have been excluded. In the current study, L-NA infusion into the phrenic artery produced a significant inhibition of EDRF-dependent dilation (Ach) but not of EDRF-independent dilation (SNP), supporting a similar effect in the diaphragmatic circulation as in these other models.

Basal release of NO in the isolated heart preparation has recently been documented (6).

In the skeletal muscles, there is indirect evidence supporting a role for EDRF in the regulation of basal vascular tone. For instance, Koller et al. (7) found vasoconstriction in rat cremasteric muscle following light-dye injury to the endothelium. Vallance et al. (19) found decreased blood flow in the human forearm following intravascular infusion of NMMA and Persson et al. (16) have shown NMMA to reduce microvascular diameters in rabbit tenuissimus muscle. Consistent with this evidence, we have found the baseline resistance of the diaphragmatic vasculature to increase significantly during both autoperfusion and during perfusion at constant flow suggesting a role for modulation of basal EDRF synthesis in the control of resting smooth muscle tone in this vascular bed as well.

EDRF in reactive hyperaemia: Assessments of the importance of the endothelium in reactive hyperaemia in skeletal muscle have varied depending on the preparation and the method used to impair the production of endothelium derived mediators. Sagach and Tkachenko (17) attempted to selectively inhibit endothelium dependent relaxation in the dog femoral artery by injection of saponin. This significantly reduced the peak flow following the release of arterial occlusions of 5 to 120 s duration. In rat cremaster muscle, Wolin et al. (20), found no change in the reactive increase in arteriolar diameter in response to a 15 s occlusion following treatment with NMMA and hydroquinone. Bjornberg et al. (1) have commented that blockade of EDRF synthesis with NMMA did not alter reactive hyperaemia in the cat hindlimb but did not provide data to support this conclusion. Koller and Kaley (9) produced endothelial injury in rat cremasteric muscle arterioles by light-dye techniques. This resulted in a marked attenuation of the post-occlusion increase in arteriolar diameter. In contrast, baseline arteriolar diameter

decreased only slightly and the increase in arteriolar diameter during occlusion was unchanged. They concluded that the peak response is a function of an initial myogenic vasodilation followed by further endothelium-dependent flow-sensitive dilation (8).

In the diaphragmatic circulation we found that L-NA reduced the peak reactive vasodilation to a greater extent than could be accounted for by its effect on baseline vascular resistance. In agreement with the findings of Koller and Kaley (9), our results support a role for flow sensitive vasodilation in generating the peak reactive vasodilation. When flow is unrestricted (autoperfusion), vasodilation is accompanied by increased flow and shear stress. When flow is fixed (pump perfusion) vasodilation results in a reduction in blood velocity (and vessel wall shear stress). If the peak vasodilation is, in part, dependent upon vasodilator factors released in response to high flow or shear stress, the magnitude of the reactive response should be smaller under conditions of fixed flow. This was indeed the case (compare figures 1 and 2).

The role of the endothelium in determining the duration of post-occlusive vasodilation has not been extensively evaluated. Koller and Kaley (9) have reported that, after endothelial injury, the duration of the hyperaemic response is decreased at short (20 s) but not at longer (80 s) occlusion durations. They proposed that, following the initial vasodilation, normal vascular tone is restored under the influence of metabolic factors which act independent of the endothelium and which are of increasing importance as the duration of the preceding occlusion is increased. This interpretation is compatible with previous observations. Johnson et al. (5) found that the increase in reactive hyperaemic volume with increasing occlusion duration is more dependent on the rise in duration than in the degree of vasodilation suggesting that the duration of the hyperaemia is related to the degree to which the tissue is deprived of nutrients during the

occlusion. Similarly, Bjornberg et al. (1) found that changing arteriolar transmural pressure without interrupting flow could reproduce the vasodilator response to occlusions of up to 30 s. They concluded that myogenic mechanisms predominate in the response to brief occlusions but that for longer occlusions metabolic factors must play a role.

Despite fairly wide acceptance of this explanation, no specific metabolite, has yet been identified to which mediation of reactive hyperaemia may be clearly ascribed. O_2 tension has been shown to influence peak post-occlusive flow and the duration of reactive vasodilation (18). A role for the direct effects of CO_2, H^+ and other byproducts of anaerobic metabolism on vascular smooth muscle has also been proposed (10). Finally, adenosine, possibly through effects on prostaglandin release (3,13), and prostaglandins themselves, have also been implicated as mediators of reactive hyperaemia. Blockade of these pathways by theophylline (3) or indomethacin (22), respectively, has been shown to attenuate the magnitude and duration of post-occlusive vasodilation in some preparations.

We found that inhibition of EDRF release in the diaphragmatic vasculature decreases the duration of post-occlusion hyperaemia at all occlusion durations during autoperfusion and at longer occlusion durations (greater than 30 s) during pump perfusion. The finding that the effect of L-NA was less pronounced when flow was maintained constant suggests that flow sensitive EDRF release may play a role in determining the duration of the response. L-NA shortened the reactive vasodilation for long occlusions even when flow was fixed. EDRF, therefore, appears to be involved in aspects of reactive hyperemia widely considered to be determined by factors of metabolic origin. This raises the possibility that some of the vascular changes which accompany alteration of the metabolic state of the muscle are mediated indirectly through

modulation of endogenous nitric oxide synthesis.

ACKNOWLEDGMENTS

The authors thank S. Nuara for his technical assistance. The study was funded by a grant from the Medical Research Council of Canada. M. Ward is a fellow of the Parker B. Francis Foundation. S. Hussain is a scholar of The Heart and Stroke Foundation of Canada.

REFERENCES

1. Bjornberg, J., U. Albert and S. Mellander. Resistance responses in proximal arterial vessels, arterioles and veins during reactive hyperaemia in skeletal muscle and their underlying regulatory mechanisms. Acta Physiol. Scand. 139: 535-550, 1990

2. Borgdorf, P., P. Sipkema, and N. Westerhof. Pump perfusion abolishes autoregulation possibly via prostaglandin release. Am. J. Physiol. 255: H280-H287, 1988

3. Carlsson, I., A. Sollevi and A. Wennmalm. The role of myogenic relaxation, adenosine and prostaglandins in human forearm reactive hyperaemia. J. Physiol. 389: 147-161, 1987.

4. Hussain S.N.A., C. Roussos, and S. Magder. In situ isolated perfused and innervated left hemidiaphragm preparation. J Appl Physiol 67:2141-2146, 1989

5. Johnson, P.C., K.S. Burton, H. Henrich and U. Henrich. Effect of occlusion duration on reactive hyperemia in sartorius muscle capillaries. Am. J. Physiol. 230: 715-719, 1976

6. Kelm, M. and J. Schrader. Control of coronary vascular tone by nitric oxide. Cir. Research 66: 1561-1575, 1990

7. Koller, A., E.J. Messina, M.S. Wolin and G. Kaley. Effects of endothelial impairment on arteriolar dilator response in vivo. Am. J. Physiol. 257: H1485-H1489, 1989

8. Koller A. and G. Kaley. Endothelium regulates skeletal muscle microcirculation by a blood flow velocity-sensing mechanism. Am. J. Physiol. 258: H916-H920, 1990

9. Koller A. and G. Kaley. Role of endothelium in reactive dilatation of skeletal muscle arterioles. Am. J. Physiol. 259: H1313-H1316, 1990

10. Kontos, H.A. and Patterson J.L. Carbon dioxide as a major factor in the production of reactive hyperaemia in the human forearm. Clin. Sci. 27: 143-154, 164

11. Lambert, L.E., J.P. Whitten, B.M. Baron, H.C. Cheng, N.S. Doherty and I.A. McDonald. Nitric Oxide synthesis in the CNS, endothelium and macrophages differs in its sensitivity to inhibition by arginine analogues. Life Sci. 48: 69-75, 1991

12. Mugge, A., Lopez, J.A.G., D.J. Piegors, K.R. Breese and D.D. Heistad. Acetylcholine-induced vasodilation in rabbit hindlimb in vivo is not inhibited by analogues of L-arginine. Am. J. Physiol. 260:H242-H247, 1991

13. Miura, M.S., S. Tominaga and K. Hashimoto. Potentiation of reactive hyperaemia in the coronary and femoral circulation by the selective use of 2,6-bis(diethanolamino)4,8-

dipiperidinopyrimido(5,4,-d)pyrimidine. Arzneim. Forsch. 17:976-979, 1967

14. Mulsch A. and R. Busse. N^G-Nitro-L-arginine (N^5-[imino(nitro-amino)methyl]-L-ornithine) impairs endothelium-dependent dilations by inhibiting cytosolic nitric oxide synthesis from L-arginine. Nauyn-Schmiedeberg's Arch. Pharmacol. 341:143-147, 1991

15. Patterson, G.C. Role of intravascular pressure in the causation of reactive hyperemia in the human forearm. Clin. Sci. 15: 17-25, 1956

16. Persson, M.G., L.E. Gustafsson, N.P. Wiklund, P. Hedqvist and S. Moncada, Endogenous nitric oxide as a modulator of rabbit skeletal muscle microcirculation. Br. J. Pharmacol. 10: 463-466, 1990

17. Sagach, V.F. and M.N. Tkachenko. Role of the endothelium in the development of reactive hyperemia. Biull. Eksp. Biol. Med. 108: 421-423, 1989

18. Tuna, R.F., L. Lindbom and K.E. Arfors. Dependence of reactive hyperemia in skeletal muscle on oxygen tension. Am. J. Physiol. 233:H289-H294, 1977

19. Vallance, P., J. Collier and S. Moncada. Effects of endothelium-derived nitric oxide on peripheral arteriolar tone in man. Lancet 2: 997-1000, 1989

20. Wolin, M.S., J.M. Rodenburg, E.J. Messina and G. Kaley, Similarities in the pharmacological modulation of reactive hyperemia and vasodilation to hydrogen peroxide in rat skeletal muscle arterioles: Effects of probes for endothelium-derived mediators. J. Pharmacol. Exp. Ther. 253: 508-512, 1990

21. Yonce, L.R. Effect of temperature on reactive hyperemia in skeletal muscle. Am. J. Physiol. 202: 1055-1058, 1962

22. Weiner, R., E.J. Messina, J. Rodenburg and G. Kaley. Indomethacin reduces skeletal muscle vasodilation induced by exercise and ischemia. Artery 3:52-57, 1977

FIGURE LEGENDS

Fig. 1 *top:* Minimum phrenic vascular resistance (% of baseline) following phrenic arterial occlusions during autoperfusion. Post L-NA, refers to minimum post-occlusion resistance following N^G-nitro-L-arginine infusion.

Middle: Duration of the reactive vasodilation in response to phrenic arterial occlusions during autoperfusion. Note the significant effect of L-NA on hyperemia duration.

Bottom: Reactive hyperemic volume (area above the flow-time curve above baseline flow) in response to phrenic arterial occlusions during autoperfusion.

Fig 2. *Top:* Minimum phrenic vascular resistance (% baseline resistance) following phrenic arterial occlusions during pump perfusion. Post L-NA, refers to minimum post-occlusion resistance following N^G-nitro-L-arginine infusion.

Bottom: Duration of reactive vasodilation in response to phrenic arterial occlusions during pump perfusion. Note the significant shortening of hyperemia in response to L-NA infusion.

Fig.3 *Top:* Minimum phrenic vascular resistance (% of baseline) following phrenic arterial occlusion during the control period and after phenlyephrine infusion.

Bottom: Duration of reactive hyperemia in response to phrenic arterial occlusions during the control period and after phenylephrine infusion.

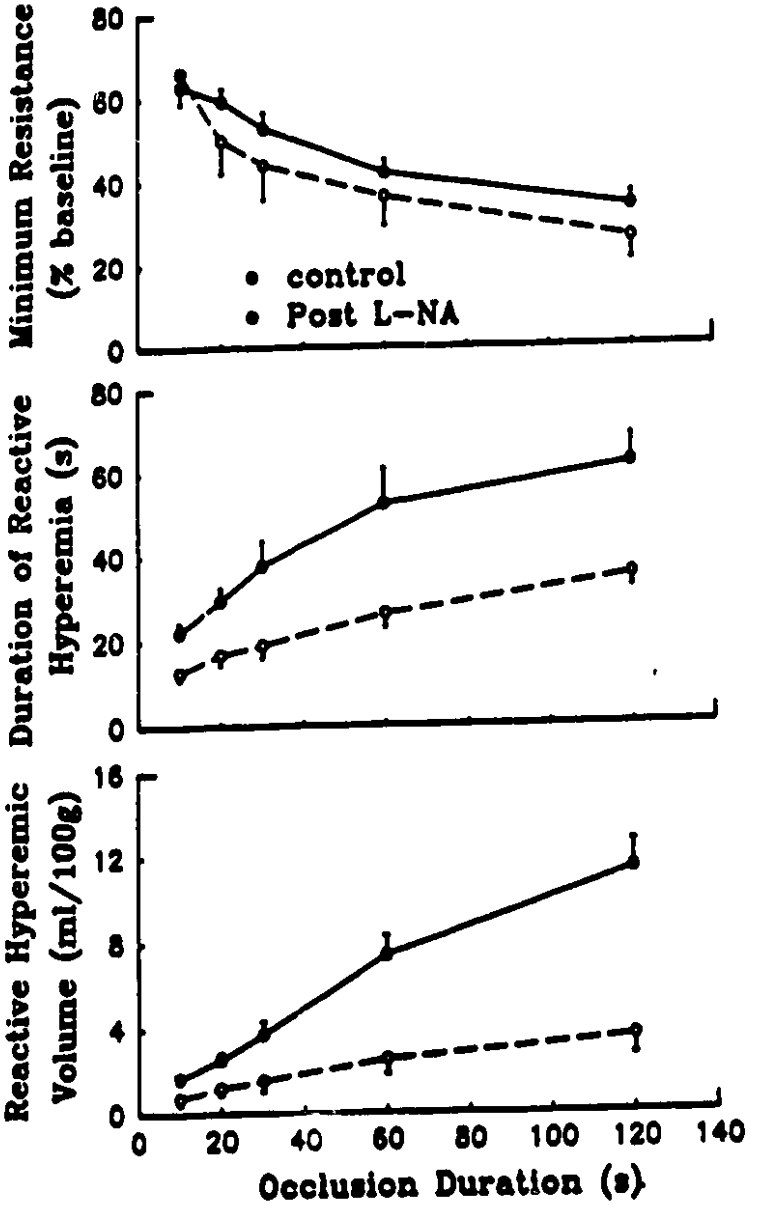
Minimum Resistance (% baseline)
80
60
40
20
0
control
Post L-NA
Duration of Reactive Hyperemia (s)
80
60
40
20
0
Reactive Hyperemic Volume (ml/100g)
16
12
8
4
0
0
20
40
60
80
100
120
140
Occlusion Duration (s)

Figure 2

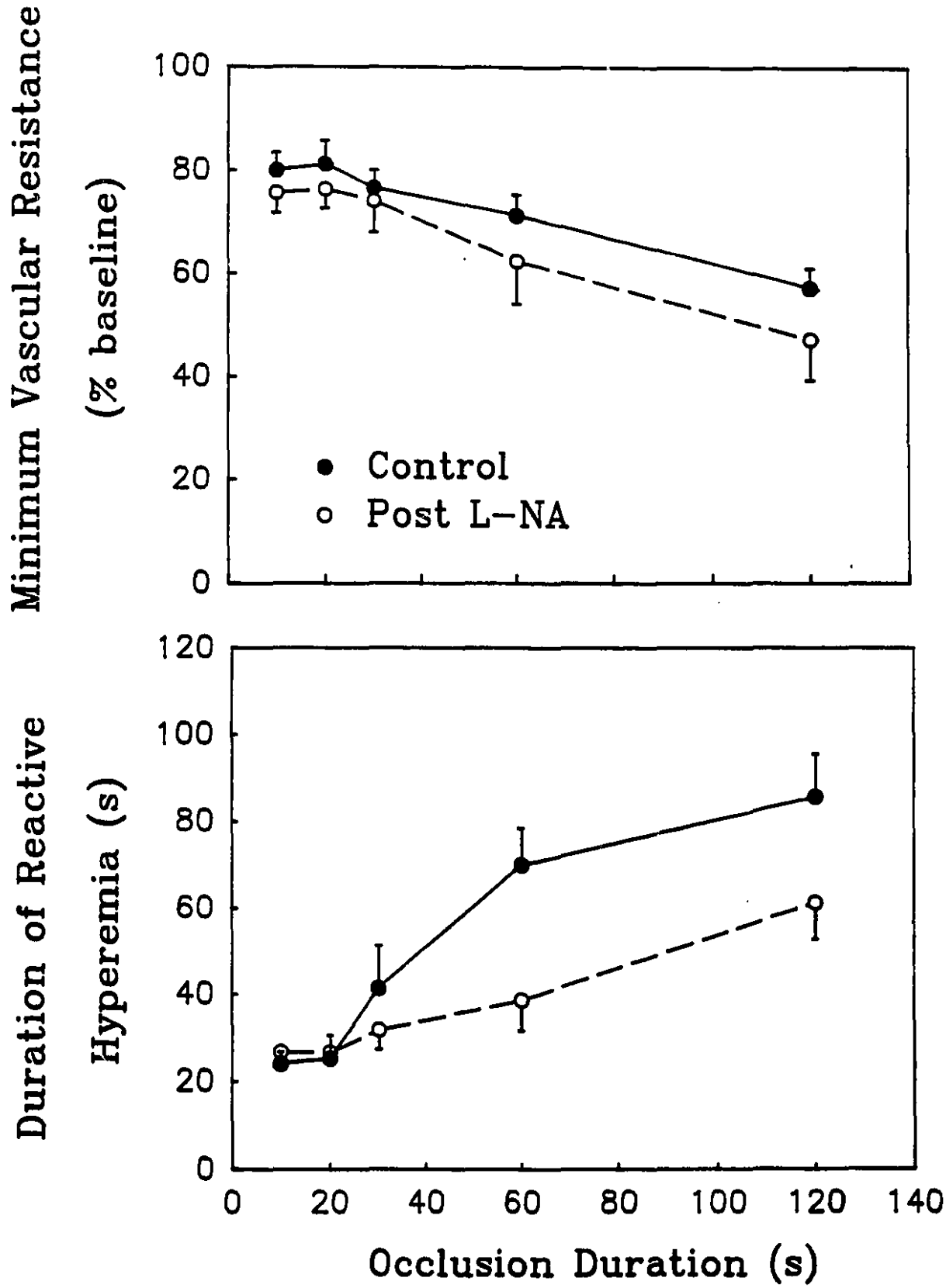
Minimum Vascular Resistance
(% baseline)
100
80
60
40
20
0
Control
Post L-NA
Duration of Reactive
Hyperemia (s)
120
100
80
60
40
20
0
0
20
40
60
80
100
120
140
Occlusion Duration (s)

Figure 3

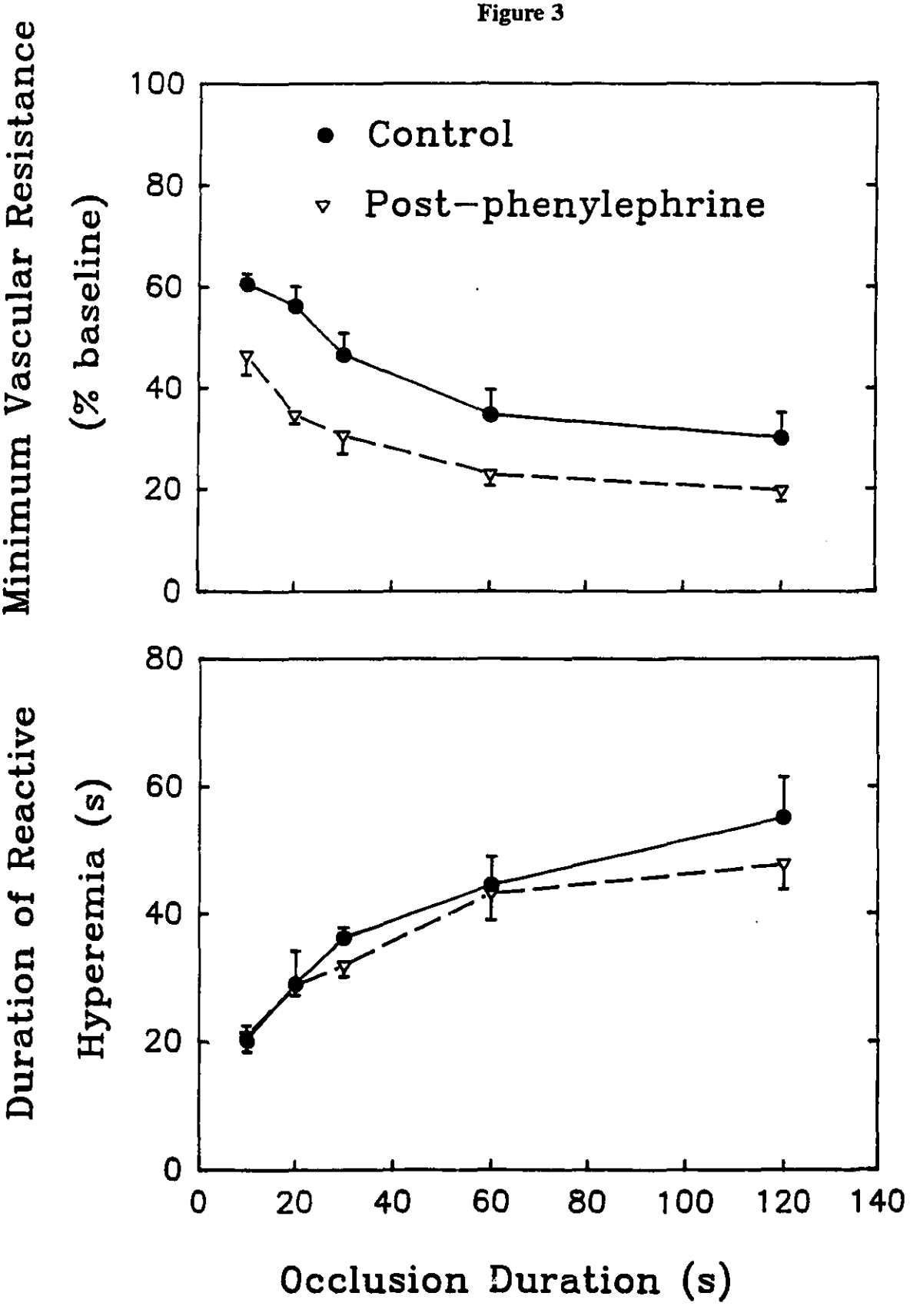
Minimum Vascular Resistance
(% baseline)
100
80
60
40
20
0
Control
Post−phenylephrine
Duration of Reactive
Hyperemia (s)
80
60
40
20
0
0
20
40
60
80
100
120
140
Occlusion Duration (s)

Effect of Inhibition of Nitric Oxide Release on the Diaphragmatic Oxygen Delivery-Consumption Relationship

Michael E. Ward and Sabah N.A. Hussain
Journal of Critical Care 1994 - In Press

ABSTRACT

Purpose: in the vascularly isolated resting and contracting (3 Hz) canine hemidiaphragm, we tested the hypothesis that nitric oxide (NO) is an important regulator of diaphragmatic O_2 extraction. **Methods:** the effect of intra-arterial infusion of an NO-synthase inhibitor, N^G-nitro-L-arginine (LNA), on the critical O_2 delivery (QO_2di,c) below which O_2 consumption becomes dependent on O_2 supply was assessed in two groups of animals in which either saline or LNA ($6 \cdot 10^{-4}$M) was infused into the phrenic artery over 20 minutes. The diaphragm was then perfused either by left femoral arterial blood (autoperfusion) or by pump perfusion with blood from the femoral artery. QO_2di was reduced by stepwise haemorrhage in the autoperfusion groups and by reducing the pump rate in the pump perfusion groups. **Results:** During autoperfusion, QO_2di,c in the saline and LNA treated groups were not different (0.88 ± 0.15 and 0.98 ± 0.12 ml/min/100g, respectively) for the resting diaphragm. Critical O_2 extraction ratios were not different (64.5 ± 9.9 and $67.8 \pm 6.4\%$, respectively). In the saline group, QO_2di,c during 3 Hz stimulation was 5.03 ± 0.9 ml/min/100g. In the LNA group, diaphragm flow was lower than the saline group and no critical O_2 delivery was found. In the pump-perfused contracting diaphragm, QO_2di,c in both groups did not differ (3.1 ± 0.5 and 4.05 ± 0.65 ml/min/100g respectively). O_2 extraction ratios at these O_2 deliveries were different ($63.3 \pm 5.2\%$ and $77.4 \pm 4.3\%$, respectively). However, NO-synthase inhibition had no effect on maximum diaphragmatic O_2 extraction ratio. **Conclusions:** these results indicate that NO release is an important modulator of the tone of diaphragmatic resistance vessels but it does not appear to regulate the processes by which O_2 extraction is enhanced to compensate for decreased O_2 delivery.

INTRODUCTION:

According to the metabolic theory of blood flow regulation, compensation for decreased oxygen delivery involves progressive recruitment of vessels as a result of differential sensitivity to metabolic mediators of vasodilation (6). Initially, an increase in capillary density serves to improve O_2 extraction. Worsening tissue oxygenation is associated with dilation of upstream resistance and conductance vessels to augment tissue blood flow. Recently, modulation of endothelial synthesis of nitric oxide (NO) has emerged as one of the most important mechanisms by which resistance and conductance vessel tone is regulated (14,4). As such, NO release is important in the coupling of oxygen delivery to metabolic rate in highly aerobic tissues which depend mainly on increasing blood flow to meet increases in O_2 demand. For example, inhibition of endothelium dependent vasodilation in the rabbit hindlimb is associated with a shift in tissue PO_2 toward lower values (22) and a reduction in hindlimb oxygen consumption (23). In the myocardium, analogues of the NO precursor, L-arginine, have been found to reduce O_2 consumption and increase lactate production (24) and to alter the relationship between myocardial O_2 uptake and coronary flow (34). It is not known, however, whether or not modulation of endogenous NO synthesis also contributes to the regulation of capillary flow and, thereby, plays a part in determining the limits of oxygen extraction.

The respiratory muscles are also highly aerobic and are obliged to continue to contract rhythmically under clinical conditions associated with reduced O_2 delivery. Since these muscles are responsible for the maintenance of oxygen availability to the entire body, the mechanisms responsible for maintaining their O_2 supply in proportion to demand are central to survival. In the diaphragmatic circulation, inhibition of NO synthesis has been shown to attenuate both active

and reactive hyperaemic responses (36,12). These findings support a role for NO pathway in matching diaphragmatic O_2 delivery to its metabolic requirements. As with other tissues, however, the degree to which NO release participates in the normal enhancement of O_2 extraction in response to tissue hypoxia is unknown. We postulated that endogenous NO release may enhance O_2 extraction by reducing the heterogeneity of blood flow within the diaphragm, attenuating arteriovenous and diffusional shunts and preventing microvascular plugging. The goal of this study, therefore, is to test the hypothesis that NO release is an important regulator of diaphragmatic O_2 extraction. To achieve this goal, we constructed the relationship between diaphragmatic O_2 delivery and O_2 consumption in two groups of animals; normal (saline infusion) and a second group in which diaphragmatic NO synthesis was inhibited by an L-arginine analogue. Under normal conditions, when O_2 delivery to a certain organ declines, O_2 consumption remains constant as a result of an increase in tissue O_2 extraction. At a certain O_2 delivery, the increase in O_2 extraction can no longer maintain tissue O_2 uptake constant and hence further reduction in O_2 delivery will result in limitation of O_2 consumption. We reasoned that if endogenous NO synthesis is an important modulator of diaphragmatic O_2 extraction, then inhibition of NO synthesis will reduce critical diaphragmatic O_2 delivery resulting in an abnormal dependence of O_2 consumption on blood flow. We used two methods to reduce diaphragmatic O_2 delivery. Firstly, we lowered perfusion pressure by stepwise hemorrhage. This method allows normal physiological processes such as autoregulation to occur. On the other hand, the release of catecholamines in response to systemic hypotension may interfere with the intrinsic ability of the diaphragm to extract O_2. To avoid this particular problem, we reduced diaphragmatic O_2 delivery locally by pump-perfusing the phrenic artery with arterial blood. By adjusting the rate

of the pump, we were able to match the exact values of diaphragmatic O_2 delivery in normal and NO synthesis-inhibited group. On the other hand, pump-perfusion have several disadvantages such as reducing the ability of the tissues to autoregulate local blood flow in relation to metabolic demands. Moreover, pump-perfusion is usually associated with a relatively high capillary pressure which may result in tissue edema which, in turn, may influence capillary flow and O_2 extraction.

Finally, to assess whether or not elevation of phrenic vascular resistance per se after NO synthase inhibition had any effect on the ability of the diaphragm to extract O_2, we studied the relationship between diaphragmatic O_2 delivery and O_2 consumption in a separate group of animals in which phrenic vascular resistance was raised by infusing α-adrenergic agonist (phenylephrine).

METHODS:

Animal Preparation: Studies were performed in 34 mongrel dogs (average weight 29.2 kg, range 25 to 31 kg) which were anaesthetized with sodium thiopental (10 mg/kg) followed by α-chloralose (60-80 mg/kg). Supplemental doses of α-chloralose were given as needed to eliminate jaw tone but maintain knee reflexes. To block prostaglandin synthesis, all animals received indomethacin (Sigma Chemicals) 5 mg/kg intravenously. The animals were supine, intubated with a cuffed endotracheal tube and mechanically ventilated (tidal volume 15 ml/kg, frequency adjusted to maintain arterial PCO_2 between 38 and 42 mmHg). Supplemental O_2 was supplied through the inspiratory line and arterial PO_2 maintained above 100 mmHg. Positive end-expiratory pressure (PEEP, 5 cmH_2O) was applied at the expiratory line. A catheter was placed

in the aorta via the right carotid artery to monitor arterial pressure (P_{art}) and another catheter was placed in the right femoral vein to administer fluids. Core body temperature was kept constant at approximately 37° C by a heating pad placed under the animal.

Isolated left hemidiaphragm: The left hemidiaphragm was vascularly isolated as reported previously (12). Briefly, the intercostal vessels and the left internal mammary artery were ligated and the lower left ribs were removed. Through an abdominal incision, the two halves of the diaphragm were divided. The ribs and cartilages of the free costal margin were secured by silk threads to 3 metal bars attached through their centres to force transducers (Grass model FT10). To ensure independent movement of the bars, we severed the interconnecting ribs. The stomach, liver, spleen, and left kidney were retracted to expose the left phrenic artery. This artery was ligated proximally and a polyethylene catheter (PE 160, 1.14 mm ID, 1.57 mm OD, 3 cm long) was introduced into the distal portion. Phrenic arterial perfusion pressure (P_{phr}) was measured from a side port in this catheter. The catheter was connected to an electromagnetic flow probe (Carolina Medical Electronics, 1.91 mm ID). The pressure-flow relationship of the catheter-probe system was linear over the range of flows in the study with conductance = 2.6 ml/min/mmHg. Phrenic arterial flow measured by the probe was designated as Q_{phr}. The other side of the probe was connected to a Y shaped connector, one arm of which was connected to a catheter in the left femoral artery, thereby allowing the diaphragm to be perfused with blood flow diverted this source. The other arm of the Y was connected via a constant perfusion pump to a catheter in the right femoral artery. The diaphragm could thereby be pump perfused using a constant flow pump (Cole-Parmer Masterflex No. 7523-00, head No. 7016-20, No. 16 tubing)

with blood from the right femoral artery by clamping the left femoral arterial catheter. Drugs were administered to the phrenic circulation through a side port in the Y connector. All animals were heparinized after catheterizing the phrenic artery.

To sample phrenic venous blood, a polyethylene catheter (PE280, 2.15 mm ID, 3.25 mm OD) was introduced into the left inferior phrenic vein through the left femoral vein and secured by a silk suture through the central tendon. The venous blood was collected in a container and reinfused through the femoral venous line.

The temperature of the diaphragm was monitored continuously using a temperature probe fixed to its surface (Mon-a-therm, Model 6000, Zimmer of Canada Ltd., Mississauga, Ont.) and maintained between 37.5 and 38.5°C using a heat lamp. At the end of the experiment the animals were exsanguinated and the diaphragm was dissected free and weighed.

Phrenic nerve stimulation: Bipolar electrodes were placed around the left phrenic nerve close to its exit from the diaphragm. The electrodes were connected through an isolation unit (Grass SIU5) to a stimulator (Grass S48). Maximum stimulation of the left diaphragm was achieved by delivering a single stimulus (0.2 ms duration) with progressively increasing voltage. The voltage output was then set 2 volts higher than the last voltage found to produce an increment in diaphragm tension. During contraction periods, the left phrenic nerve was stimulated continuously at 3 Hz for 3 minutes.

Oxygen Delivery and Consumption Measurements: phrenic arterial and venous blood O_2 contents (CaO_2, CvO_2,di, respectively) were measured with a co-oximeter (Instrumentation

Laboratory IL-182). CaO_2 was multiplied by Q_{phr} to obtain the O_2 delivery to the left hemidiaphragm (QO_2di). The oxygen consumption of the left hemidiaphragm (VO_2,di) was calculated as the product of the phrenic arteriovenous O_2 content difference (Ca-Cv)O_2,di and Q_{phr}. All values were normalized for tissue weight.

Experimental Protocol: Following a 30 minute stabilization period during which the left diaphragm was autoperfused from the left femoral artery, pump perfusion was begun, as described above, at the flow rate recorded during the previous period of autoperfusion. Using a Harvard infusion pump, either saline or a $6 \cdot 10^{-2}$ M solution of N^G-nitro-L-arginine (LNA) was infused into the phrenic circulation at a rate equal to $1/100^{th}$ of the phrenic arterial flow as described above for 20 minutes. The infusion was then stopped and the diaphragm either autoperfused or pump perfused with arterial blood according the protocols described below. In a separate group, phenylephrine was infused into the phrenic artery at a rate adequate enough to increase phrenic vascular resistance by a similar magnitude to that elicited by LNA infusion (approximately 30% of baseline values). The diaphragm was pump-perfused throughout the experiment in this group and the infusion rate of phenylephrine was adjusted during the reduction in phrenic flow (see below).

***Group 1; autoperfusion*:** This group consisted of 14 dogs, 7 saline and 7 LNA treated animals. Pump perfusion was discontinued and autoperfusion of the diaphragm from the left femoral artery was re-established. P_{phr} and Q_{phr} were recorded and arterial and phrenic venous blood samples were drawn. Stepwise haemorrhage was then begun by withdrawing blood in 50

to 100 ml aliquot from the right femoral arterial line. Haemorrhage was continued until the animal could no longer maintain a stable blood pressure. This resulted in the performance of 8 to 10 stages of haemorrhage in each animal. After steady state was reached at each stage, P_{phr} and Q_{phr} were again recorded and arterial and phrenic venous blood samples drawn. The phrenic nerve was then stimulated as described above and the measurements were repeated at the end of the contraction period at each stage.

***Group 2; Pump Perfusion*:** This group consisted of 20 dogs, 6 saline, 8 LNA and 6 phenylephrine treated animals. The diaphragm was pump perfused with arterial blood from the right femoral artery at the flow rate recorded during the initial period of autoperfusion. P_{phr} and Q_{phr} were recorded and arterial and phrenic venous blood samples were drawn. The perfusion rate, and thereby, diaphragmatic O_2 delivery, was then reduced in a stepwise fashion resulting in 9 to 12 approximately equal decrements in flow, the final stage representing the lowest possible pump flow setting. The exact number of stages and magnitude of the decrements in each animal depended on the initial flow rate. After steady state was reached at each stage, P_{phr} and Q_{phr} were again recorded and arterial and phrenic venous blood samples drawn. The phrenic nerve was then stimulated as described above and the measurements were repeated at the end of the contraction period at each stage.

Data Analysis: The diaphragmatic O_2 delivery at which VO_2di (resting and contracting) became supply dependent was calculated for each animal. In those cases in which a biphasic relationship between O_2 delivery and O_2 consumption could be clearly identified the critical O_2

the diaphragmatic O_2 delivery was plotted on the x axis against the corresponding O_2 consumption on the y axis. The data were sorted as O_2 delivery and O_2 consumption pairs with increasing O_2 delivery. All possible regression lines were then calculated as the data was grouped pair by pair into high and low O_2 delivery subsets. The pair of lines which resulted in the smallest sum of squared residuals was used in further calculations. The critical O_2 delivery was then determined by solving the equations describing the regression lines for the values of these variables at the point of intersection (31).

The critical O_2 extraction ratios at the point of onset of delivery dependence of VO_2di (resting and contracting) were calculated as the ratios of the respective phrenic arteriovenous O_2 content differences to the arterial O_2 content when the critical point corresponded to a direct measurement of O_2 delivery. When this was not the case, the critical extraction ratio was estimated by linear interpolation using values measured during the two stages bracketing the point of critical O_2 delivery. The O_2 extraction ratios for the diaphragm (resting and contracting) were calculated as the ratios of the respective arteriovenous O_2 content differences to the arterial O_2 content during the initial and final stages of each experiment. The maximum O_2 extraction ratio was taken as the highest which was recorded.

Differences among mean values for the resting and contracting diaphragmatic variables were evaluated using one way analysis of variance (ANOVA). If the ANOVA revealed significant ($p < 0.05$) differences among the means, the differences between individual means were tested post-hoc using the Student Newman Keuls procedure. P values less than 0.05 were considered significant. All values are reported as means $\pm$ SEM.

RESULTS:

Autoperfusion: Figures 1 and 2 illustrate the relationships between O_2 delivery and O_2 consumption for the resting and contracting diaphragm in each animal. In the saline infused group (figure 1), a critical O_2 delivery could be identified for both the resting and contracting diaphragm in all animals. In the LNA infused group, a "critical point" could be identified only in the resting diaphragm and the QO_2di at this point was not significantly different from that in the saline infused group. In contrast, in the contracting diaphragm, all animals in which LNA was infused into the phrenic circulation, demonstrated dependence of VO_2di on QO_2di over the entire range of blood flows recorded (figure 2).

Tables 1 and 2 present the mean values for Q_{phr}, P_{phr}, QO_2di, VO_2di, extraction ratio, phrenic venous PO_2 and the generated tension (contracting diaphragm only) recorded initially, at the "critical point" below which VO_2di became dependent on QO_2di and during the final stage of the experiment for each group. The initial QO_2di in the LNA treated group was similar to the critical QO_2di in the saline infused group.

The maximum recorded extraction ratios for the resting diaphragm were $77.4\pm4.0\%$ and $74.0\pm8.4\%$ in the saline and LNA treated groups, respectively. For the contacting diaphragm the maximum extraction ratios were $94.1\pm2.2\%$ and $88.4\pm5.5\%$ in the saline and LNA infused groups, respectively. Differences between saline and LNA treated groups were not significant.

Pump Perfusion: No critical point could be identified for the resting muscle during pump perfusion, following either saline or LNA infusion (figures 3 & 4). In the contracting diaphragm, 5 out of 6 animals in the saline infused group (figure 3) and 5 out of 8 animals in

the LNA infused group (figure 4) demonstrated a biphasic QO_2di - VO_2di relationship.

Tables 3 and 4 present the mean values for Q_{phr}, P_{phr}, QO_2di, VO_2di, extraction ratio, phrenic venous PO_2 and the generated tension (contracting diaphragm only) recorded initially, at the "critical point" below which VO_2di became dependent on QO_2di and during the final stage of the experiment for each group. In the contracting diaphragm, the VO_2di and the extraction ratio at the point of onset of delivery dependence of VO_2di was higher in the LNA treated group than in the saline group (Table 4). The critical QO_2di for the two groups were not different.

The maximum recorded extraction ratios for the resting diaphragm were $59.2\pm7.2\%$ and $71.2\pm5.1\%$ in the saline and LNA treated groups respectively. For the contacting diaphragm the maximum extraction ratios were $89.9\pm5.1\%$ and $91.9\pm1.8\%$ in the saline and LNA infused groups respectively. Differences between saline and LNA treated groups were not significant.

By design, phrenic vascular resistance at rest and during 3Hz stimulation of the phrenic nerve was increased by 30% of the saline value after phenylephrine infusion. The initial values for Q_{phr}, P_{phr}, QO_2di, VO_2di, and extraction ratio of the resting diaphragm after phenylephrine infusion averaged 42.1 ± 3.0 ml/100g/min, 350.0 ± 12.2 mmHg, 8.2 ± 3.1 ml/100g/min, 0.23 ± 0.13 ml/100g/min and $2.8\pm1.8\%$, respectively. Like the saline and LNA groups, no critical point could be identified for the resting muscle during pump perfusion following phenylephrine infusion, however, a biphasic relationship between QO_2di and VO_2di was found in all animals during 3Hz stimulation. The initial values for Q_{phr}, P_{phr}, QO_2di, VO_2di, and extraction ratio of the contracting diaphragm after phenylephrine infusion averaged 42.1 ± 3.0 ml/100g/min, 266.7 ± 6.8 mmHg ($P<0.01$), 8.2 ± 3.1 ml/100g/min ($P<0.01$), 5.1 ± 0.5 ml/100g/min ($P<0.05$) and $63.5\pm8.6\%$ ($P<0.05$ compared with the saline group). In addition

to increasing the critical QO_2di (6.16±0.42 ml/100g/min, $P<0.05$ compared with saline), phenylephrine infusion increased VO_2di (5.4±0.35 ml/100g/min, $P<0.05$) and extraction ratio (87.8±1.2 %, $P<0.05$) at the critical QO_2di. Maximum extraction ratio (94.9±6.1 %), however, was not different from the saline group. Diaphragmatic tension in response to 3Hz stimulation after phenylephrine infusion was not different from that of the saline group.

DISCUSSION:

The main findings of this study are: 1) Inhibition of endogenous NO synthesis in the autoperfused and pump-perfused diaphragm increased resting vascular resistance resulting in a decrease in flow and an increase in perfusion pressure, respectively. 2) Inhibition of NO release attenuated the active vasodilator response to 3 Hz stimulation in both the autoperfused and pump perfused diaphragm. 3) The critical diaphragmatic O_2 delivery of the autoperfused resting diaphragm or the pump perfused contracting (3 Hz) diaphragm was not affected by NO inhibition. 4) Uniike NG inhibition, increasing phrenic vascular resistance of the contracting diaphragm by an α-adrenergic agonist (phenylephrine) resulted in a significant increase in critical diaphragmatic O_2 delivery during pump perfusion. 5) The maximum extraction ratio in the autoperfused and pump perfused diaphragm, resting or contracting, was not influenced by NO inhibition or α-adrenergic stimulation..

Critique:

It can be argued that the procedure of isolating the left hemidiaphragm may induce a state of hypoperfusion of the diaphragm and consequently leads to an abnormal dependence of

diaphragmatic O_2 uptake on O_2 delivery especially in the autoperfused groups. However, we believe that the diaphragm is adequately perfused in our preparation because diaphragmatic blood flow and O_2 uptake for the resting diaphragm are comparable to those measured in the intact diaphragm. Moreover, the values of critical diaphragmatic O_2 delivery in the autoperfused resting diaphragm in the saline group were similar to those measured in limb muscles (30,2) In addition, the initial O_2 supply-independence of diaphragmatic O_2 uptake in the resting and contracting diaphragms indicate that initial diaphragm O_2 uptake was not limited by the blood flow. Finally, measurements of phrenic venous-arterial lactate differences (data not shown) indicate that lactate production by the resting and contracting diaphragms was negligible at initial values of blood flow and O_2 delivery. Only when O_2 delivery was reduced below the critical values did lactate production by the diaphragm increase. Inspite of these evidence, we must emphasize that our results applies only to the condition of isolated diaphragm preparation.

LNA has been shown to competitively inhibit the synthesis of NO from the guanido nitrogen moiety of L-arginine (18). LNA inhibits the activity of both the constitutive form of NO synthase which is present in endothelial cells and the cytokine inducible form present in endothelial and smooth muscle cells (32). L-NA does not reduce nitroglycerine or nitroprusside induced vasodilation (18), therefore, direct interference at points in the pathway distal to soluble guanylate cyclase have been excluded. In a previous study (12), we have demonstrated that L-NA infusion into the phrenic artery produced significant inhibition of endothelium dependent vasodilation (acetylcholine) but not of endothelium independent vasodilation (Sodium nitroprusside), supporting a similar effect in the diaphragmatic circulation as in these other models. Following LNA administration according to the protocol employed in the current study,

inhibition of endothelium dependent vasodilation persists for at least 2 hours (36,12).

In some preparations, prostaglandins have been found to participate in reactive hyperaemia (16) exercise hyperaemia (10), and the vasodilation which accompanies increases in blood flow velocity (15). In addition, the fact that pump perfusion interferes with normal autoregulation in the cat hind limb and this effect is reversed by indomethacin (1) suggests that variations in prostaglandin release may enhance differences between pump and autoperfused groups. Furthermore, in cultured endothelial cells prostacyclin and NO release are coupled (19) and a vascular interaction between these mediators, similar to their synergistic effect on platelet activation (26), cannot be excluded. We, therefore, chose to avoid these confounding effects by pretreatment of all animals with indomethacin.

Although it would be preferable to study spontaneous diaphragmatic contraction, variations in respiratory drive related to anaesthesia and changes in arterial pressure result in unpredictable fluctuations in diaphragmatic O_2 demand. We, therefore, chose to increase VO_2di by stimulating the phrenic nerve at a constant frequency (3 Hz) in order to maintain O_2 demands as constant as possible throughout the experimental protocol. The VO_2di values measured during 3 Hz stimulation in the current study are comparable to those reported to during increased activation of the diaphragm by moderate inspiratory resistive loading in spontaneously breathing dogs (28,29,27). Higher frequencies of stimulation result in the generation of high intramuscular pressure which limit blood flow during muscle contraction and are associated with a rapid decline in tension as a result of diaphragmatic fatigue (11). Using 3 Hz stimulation frequency, we observed no decline in tension until the final stage of the experiments.

NO and blood flow regulation

Infusion of LNA into the phrenic artery resulted in a significant increase in baseline vascular resistance as reflected by a decrease in Qphr in the autoperfused groups and an increase in Pphr compared to the saline treated group when the diaphragm was pump perfused. In addition, the decrease in diaphragmatic vascular resistance in response to 3 Hz stimulation was lower in the LNA treated groups than in those treated with saline. These findings are compatible with previous data showing increased baseline vascular tone following infusion of L-arginine analogues (36,35,3) and the continuous basal release of nitric oxide by direct spectrophotometric measurement (33). In addition to removal of the vasodilator influence of basal NO release, treatment with LNA may have altered the response of the diaphragmatic circulation in two other ways. First, inhibition of NO release may have enhanced the availability and effects of neurally-released catecholamines (5,17). Second, NO inhibition may have unmasked intrinsic myogenic vasoconstriction (24,5). According to this hypothesis, shear stress-induced dilation and myogenic constriction interact as two opposing positive feedback mechanisms to regulate resistance vessel tone. The removal of one of these renders vascular tone unstable due to the progressively enhanced effects of the opposing mechanism (8).

Under conditions of constant pressure perfusion (autoperfusion) the change in vascular resistance resulting from inhibition of NO synthesis placed the contracting diaphragm on the descending limb of its' O_2 delivery-consumption relationship. This indicates that modulation of nitric oxide release is an important mechanism by which diaphragmatic resistance vessel tone is adjusted in response to increases in metabolic rate.

NO and O_2 uptake

Intraarterial infusion of NO inhibitors has been shown in several preparations to reduce O_2 uptake (22,23,24,34). This reduction is due, in part, to inhibition of resistance vessel dilation response to increased metabolic activity (12). Oxygen availability, however, is also regulated at the level of the terminal arterioles governing capillary flow. In the models proposed by Granger (6), differential sensitivity to metabolic mediators of vasodilation among microvessels of differing diameter results initially in an increase in capillary density and an improvement in extraction ratio in response to hypoxia with upstream resistance vessels being recruited later on. Both recruitment of unperfused capillaries and intraregional redistribution of capillary flow are possible mechanisms by which alterations in terminal arteriolar tone may modify oxygen extraction (25,9). In a study of arteriolar diameters in the rabbit tenuissimus muscle, Persson et al. (20,21) found that superfusion with N^G-monomethyl-L-arginine reduced terminal arteriolar diameter in the resting muscle. This treatment did not, however, affect the post contraction vasodilation of the terminal arterioles. They, therefore, concluded that modulation of NO synthesis does not contribute to the metabolic regulation of terminal arteriolar tone in that preparation. Oxygen extraction during muscle contraction was not evaluated in these studies.

In the current study, we found that, during autoperfusion, the critical diaphragmatic O_2 delivery and extraction ratio were unaffected by treatment with LNA in the resting muscle as were the maximum O_2 extraction ratios under both resting and contracting conditions. During pump perfusion the critical oxygen extraction ratio was, if anything, higher in the LNA treated group, the O_2 uptake of the contracting muscle became delivery limited at the same QO_2di as

was observed in the saline infused animals and the maximum oxygen extraction ratio was unaffected. These findings, therefore, support the assertion that NO does not play a role in metabolic vasodilation of the terminal arterioles governing flow through nutritive capillaries.

In the pump perfused contracting diaphragm, the VO_2di initially and at the onset of delivery dependence of O_2 uptake were higher in the LNA infused group than in the saline infused group despite the fact that similar diaphragmatic tensions were generated (table 4). Several factors may have altered the relationship between tension and O_2 uptake. A difference between the two groups in the magnitude and velocity of shortening cannot be excluded since these parameters were not measured. Another possible explanation is that the phrenic artery perfusion pressure at a given value of O_2 delivery was higher in the LNA treated group and this may have increased the internal work load which the muscle must overcome during contraction (7). In addition to a higher VO_2di, however, the critical O_2 extraction ratio observed in the LNA treated group was also higher than in the saline group. This could occur only if the slope of the relationship between O_2 delivery and uptake were increased and indicates that inhibition of nitric oxide synthesis enhanced O_2 extraction.

This finding raises the possibility that the regulation of flow through nutritive and non-nutritive capillaries may involve different mechanisms. The existence of two populations of capillaries differing anatomically and functionally has been demonstrated. In rat skeletal muscle, Potter and Groom (25) identified a population of long, low velocity capillaries with diameters clustered around 5.5 μm and a smaller population of shorter capillaries with a modal diameter of 7.5 μm. Subsequently, Harrison (9) calculated that, despite their smaller numbers, the large diameter (high flow) capillaries, which contribute little to gas exchange, may carry up to 71%

of the total muscle blood flow. Since redistribution of nutritive and non-nutritive flow in response to a metabolic stimulus (13) requires directionally opposite changes in tone of the terminal arterioles governing flow through these two types of capillaries, differential control mechanisms must be proposed. Higher flow through the non-nutritive channels may be associated with higher basal NO release. Modulation of NO concentrations may, therefore, be an important mechanism by which non-nutritive flow is controlled whereas the vasoactive effects of other metabolic byproducts may predominate in regulating flow through nutritive capillaries. If this were the case, inhibition of NO synthesis would be expected to result in vasoconstriction predominantly of the non-nutritive channels. An increase in bulk flow would, then, be accompanied by a relatively greater increase in exchange vessel perfusion and O_2 extraction would be higher. Further studies are indicated to substantiate this hypothesis.

ACKNOWLEDGEMENTS:

The authors thank S. Nuara for his technical assistance. M. Ward is a fellow of the Parker B. Francis Foundation.

REFERENCES:

1. Borgdorff, P., P. Sipkema, and N. Westerhof. Pump perfusion abolishes autoregulation possibly via prostaglandin release. Am. J. Physiol. 255: H280-H287, 1988

2. Bredle, D.L., R.W. Samsel, P.T. Schumacker and S.M. Cain. Critical O_2 delivery of skeletal muscle at high and low PO_2 in endotoxemic dogs. J. Appl. Physiol. 66: 2553-2558, 1989.

3. Ekelund, U., and S. Mellander. Role of endothelium-derived nitric oxide in the regulation of tonus in large-bore arterial resistance vessels, arterioles and veins in cat skeletal muscle. Acta Physiol. Scand. 140: 301-309, 1990

4. Furchgott, R.F. and Zawadzki, J.V. The obligatory role of endothelial cells in the relaxation of arterial smooth muscle by acetylcholine. Nature 288: 373-376, 1980

5. Gonzalez, C., C. Martin, E. Hamel, E. Galea, B. Gomez, S. Lluch, and C. Estrada. Endothelial cells inhibit the vascular response to adrenergic nerve stimulation by a receptor-mediated mechanism. Can. J. Physiol. Pharmacol. 68: 104-109, 1990

6. Granger, H.J., A.H. Goodman, and B.H. Cook. Metabolic models of microcirculatory regulation. Fed Proc. 34: 2025-2030, 1975

7. Gregg D.E. Effect of coronary perfusion pressure or coronary flow on oxygen usage of the myocardium. Circ. Res. 13: 497-500, 1963

8. Griffith, T.M. and D.,H. Edwards. Myogenic autoregulation of flow may be inversely related to endothelium-derived relaxing factor activity. Am. J. Physiol. 258: H1171-H1180, 1990

9. Harrison, D.K., S. Birkenhake, S.K. Knauf, and M. Kessler. Local oxygen supply and blood flow regulation in contracting muscle in dogs and rabbits. J. Physiol. 422: 227-243, 1990

10. Herbaczynska-Cedro, K. J. Staxzewska-Barczak, and H. Janczewska. Muscular work and the release of prostaglandin-like substances. Cardiovascular Res. 10: 413-420, 1976

11. Hussain, S.N.A. and S.A. Magder. Diaphragmatic intramuscular pressure in relation to tension, shortening, and blood flow. J. Appl. Physiol. 71: 159-167, 1991

12. Hussain S.N.A., Stewart, D.J., Ludemann, J.P. and S.A. Magder. Role of endothelium-derived relaxing factor in active hyperemia of the canine diaphragm. J. Appl. Physiol. 72: 2393-2401, 1992

13. Hyman C., Independent control of nutritional and shunt circulation. Microvasc. Res.

3: 89-94, 1971

14. Ignarro, L.J. Biological actions and properties of endothelium-derived nitric oxide formed and released from artery and vein. Circ. Res. 65: 1-15, 1989

15. Koller A. and G. Kaley. Prostaglandins mediate arteriolar dilation to increased blood flow velocity in skeletal muscle microcirculation. Circ. Res. 67: 529-534, 1990

16. Messina, E.J., Weiner, R. and Kaley G. Arteriolar reactive hyperemia: Modification by inhibitors of prostaglandin biosynthesis. Am. J. Physiol. 232: H571-H575, 1977

17. Miller, V.M., Interactions between neural and endothelial mechanisms in control of vascular tone. News Physiol. Sci. 6: 60-63, 1991

18. Mulsch A. and R. Busse, N^{G}-Nitro-L-arginine (N^{5}-[imino(nitro-amino)methyl]-L-ornithine) impairs endothelium-dependent dilations by inhibiting cytosolic nitric oxide synthesis from L-arginine. Nauyn-Schmiedeberg's Arch. Pharmacol. 341: 143-147, 1991

19. Nucci, G., R.J. Gryglewski, T.D. Warner, and J.R. Vane. Receptor-mediated release of endothelium-derived relaxing factor and prostacyclin from bovine aortic endothelia cells is coupled. Proc. Natl. Acad. Sci. 85: 2334-2338, 1988

20. Persson, M.G., L.E. Gustafsson. N.P. Wiklund, P. Hedqvist, and S. Moncada. Endogenous nitric oxide as a modulator of rabbit skeletal muscle microcirculation in vivo. Br. J. Pharmacol. 100: 463-466, 1990

21. Persson, M.G., N.P. Wiklund, and L.E. Gustafsson. Nitric oxide requirement for vasomotor nerve-induced vasodilation and modulation of resting blood flow in muscle microcirculation. Acta Physiol. Scand. 141: 49-56, 1990

22. Pohl, U. and Busse, R. Reduced nutritional blood flow in autoperfused rabbit hindlimbs following inhibition of endothelial vasomotor function. In: Resistance Arteries, edited by Halpern, W., Pegram, B., Bryaden, J., Mackey, K., Mclaughlin, M. and Osol, G. New York: Ithaca, Perinatology, 1988, p. 10-16

23. Pohl, U. and D. Lamontagne. Impaired tissue perfusion after inhibition of endothelium-derived nitric oxide. Basic Res. Cardiol. 86: 97-105, 1991

24. Pohl, U., D. Lamontagne, E. Bassenge and R. Busse. EDRF antagonizes myogenic autoregulation in the vasculature of isolated rabbit hearts. Am. J. Physiol. 1992. (in press)

25. Potter, R.F., and A.C. Groom. Capillary diameter and geometry in cardiac and skeletal muscle studied by means of corrosion casts. Microvascular Res. 25: 68-84, 1983

26. Radomski, M.W., Palmer, R.M.J., and S. Moncada. The anti-aggregating properties of vascular endothelium: interactions between prostacyclin and nitric oxide. Br. J. Pharmacol. 92: 639-646, 1987

27. Reid, M.B., and R.L. Johnson, Jr., Efficiency, maximal blood flow, and aerobic work capacity of canine diaphragm. J. Appl. Physiol. 54: 763-772, 1983

28. Robertson, C.H.Jr., M.A. Pagel, and R.lL. Johnson Jr., The distribution of blood flow, oxygen consumption, and work output among the respiratory muscles during unobstructed hyperventilation. J. Clin. Invest. 59: 43-50, 1977

29. Rochester, D.F., and G. Bettini, Diaphragmatic blood flow and energy expenditure in the dcg. J. Clin. Invest. 57: 661-672, 1976

30. Samsel, R.W., D.P. Nelson, W.M. Sanders, L.D.H. Wood and P.T. Schumacker. Effect of endotoxin on systemic and skeletal muscle O_2 extraction. J. Appl. Physiol. 65: 1377-1382, 1988.

31. Samsel, R.W. and P.T. Schumacker. Determination of the critical oxygen delivery from experimental data: sensitivity to error. J. Appl. Physiol. 64: 2074-2082, 1988

32. Schini V.B. and P.M. Vanhoutte. Inhibitors of calmodulin impair the constitutive but

not the inducible nitric oxide synthase activity in the rat aorta. J. Pharmacol. Exp. Ther. 261: 553-559, 1992

33. Schror, K., S. Forster, and I. Woditsch. On-line measurement of nitric oxide release form organic nitrates in the intactg coronary circulation. Nauyn-Schmiedegerg's Arch. Pharmacol. 344: 240-246, 1991

34. Ueeda, M., Silvia, S.K., and R.A. Olsson. Nitric oxide modulates coronary autoregulation in the guinea pig. Circ Research 70: 1296-1303, 1992

35. Vallance, P., J. Collier and S. Moncada. Effects of endothelium-derived nitric oxide on peripheral arteriolar tone in man. Lancet 2: 997-1000, 1989

36. Ward, M.E., Magder, S.A., and S.N.A. Hussain. Role of endothelium-derived relaxing factor in reactive hyperaemia in the canine diaphragm. J. Appl. Physiol. 1992 (in press)

Table 1: Initial, critical and final values in the autoperfused, saline and LNA infused resting diaphragm.

AUTOPERFUSION

RESTING

		Qphr	Pphr	QO_2di	VO_2di	ER	PvO_2di
		ml/min/100g	mmHg	ml/min/100g	ml/min/100g	%	mmHg
Saline:	Initial (n=7)	25.0±3.6	151.7±13	4.74±1.1	0.26±0.08	5.5±1.6	67.7±6.4
	Critical (n=7)	4.6±0.6	55.0±2.9	0.88±0.15	0.58±0.16	64.5±9.9	33.2±2.1
	Final (n=7)	2.62±0.8	34.2±3.3	0.46±0.13	0.34±0.08	77.4±4.0	29.8±3.3
LNA:	Initial (n=7)	8.42±1.9*	153±5	1.49±0.39*	0.18±0.04	13.6±2.2*	60.5±3.3
	Critical (n=7)	5.30±0.8	90±15*	0.98±0.12	0.68±0.10	67.8±6.4	37.6±4.1
	Final (n=7)	2.1±0.4	40±3.4	0.35±0.06	0.26±0.05	74.0±8.4	31.0±1.8

Qphr, phrenic arterial flow; Pphr, phrenic arterial pressure; QO_2di, diaphragmatic O_2 delivery; VO_2di, diaphragmatic O_2 consumption; ER, O_2 extraction ratio; PvO_2di, phrenic venous O_2 tension. * significantly different ($p < 0.05$) from saline infused group.

Table 2: Initial, critical and final values in the autoperfused, saline and LNA infused contracting diaphragm.

AUTOPERFUSION

CONTRACTING

		Qphr ml/min/100g	Pphr mmHg	QO_2di ml/min/100g	VO_2di ml/min/100g	ERdi %	PvO_2di mmHg	Tension g
Saline:	Initial (n=7)	42.5±4.8	151.7±13	8.25±1.6	4.64±0.77	57.6±2.4	34.6±3.2	84±12
	Critical (n=7)	25.1±3.3	105.0±7.1	5.03±0.9	4.08±0.78	81.7±4.3	23.9±1.9	81±15
	Final (n=7)	6.32±1.7	34.2±3.3	1.05±0.3	0.94±0.28	92.0±2.4	21.7±2.1	35±8
LNA:	Initial (n=7)	29.0±7.0*	152.5±5.0	4.9±1.2*	3.3±0.95	69.1±4.6*	27.4±2.5*	87±15
	Final (n=7)	4.8±1.2	40±3.6	0.88±0.12	0.76±0.2	87.4±5.5	20.1±3.2	36±9

Qphr, phrenic arterial flow; Pphr, phrenic arterial pressure; QO_2di, diaphragmatic O_2 delivery; VO_2di, diaphragmatic O_2 consumption; ER, O_2 extraction ratio; PvO_2di, phrenic venous O_2 tension. * significantly different ($p < 0.05$) from saline infused group.

Table 3: Initial, critical and final values in the pump perfused, saline and LNA infused resting diaphragm.

PUMP PERFUSION

RESTING

		Qphr ml/min/100g	Pphr mmHg	QO_2di ml/min/100g	VO_2di ml/min/100g	ER %	PvO_2di mmHg
Saline:	Initial (n=6)	22.3±3.1	167±21	4.1±0.4	0.24±0.05	5.8±1.1	76.0±4.2
	Final (n=6)	4.24±0.55	32.5±12	0.75±0.12	0.44±0.09	59.2±7.2	34.4±2.3
LNA:	Initial (n=8)	24.0±2.7	293±19*	5.1±0.6	0.19±0.08	3.6±1.3	90±9.4
	Final (n=8)	4.56±0.76	44.8±8.7	0.86±0.10	0.61±0.08	71.2±5.1	34.8±4.0

Qphr, phrenic arterial flow; Pphr, phrenic arterial pressure; QO_2di, diaphragmatic O_2 delivery; VO_2di, diaphragmatic O_2 consumption; ER, O_2 extraction ratio; PvO_2di, phrenic venous O_2 tension. * significantly different ($p < 0.05$) from saline infused group.

Table 4: Initial, critical and final values in the pump perfused, saline and LNA infused contracting diaphragm.

PUMP PERFUSION

CONTRACTING

		Qphr	Pphr	QO_2di	VO_2di	ERdi	PvO_2di	Tension
		ml/min/100g	mmHg	ml/min/100g	ml/min/100g	%	mmHg	g
Saline:	Initial (n=6)	22.3±3.1	120±10.6	4.1±0.4	2.11±0.30	50.2±2.0	33.8±1.3	73±7
	Critical (n=5)	15.5±1.8	81.0±9.5	3.1±0.5	1.92±0.25	63.3±5.2	28.4±2.1	79±6
	Final (n=6)	4.24±0.55	9.2±0.8	0.75±0.12	0.63±0.11	83.7±4.1	21.4±2.8	34±8
LNA:	Initial (n=8)	24.0±2.7	151±14*	5.1±0.6	3.26±0.26*	65.0±4.6*	31.1±3.2	82±11
	Critical (n=5)	18.6±2.7	109±8*	4.05±0.65	3.1±0.5*	77.4±4.3*	27.8±2.0	87±12
	Final (n=8)	4.56±0.76	26.1±4.3*	0.86±0.10	0.79±0.09	91.4±3.7	18.7±2.6	46±8

Qphr, phrenic arterial flow; Pphr, phrenic arterial pressure; QO_2di, diaphragmatic O_2 delivery; VO_2di, diaphragmatic O_2 consumption; ER, O_2 extraction ratio; PvO_2di, phrenic venous O_2 tension. * significantly different ($p < 0.05$) from saline infused group.

FIGURE LEGENDS

Figure 1.

Individual oxygen delivery-consumption relationships for the autoperfused, resting (Rest) and contracting (3Hz) diaphragm following infusion of saline into the phrenic artery.

Figure 2.

Individual oxygen delivery-consumption relationships for the autoperfused, resting (Rest) and contracting (3Hz) diaphragm following infusion of N^G-nitro-L-arginine into the phrenic artery.

Figure 3.

Individual oxygen delivery-consumption relationships for the pump perfused, resting (Rest) and contracting (3Hz) following infusion of saline into the phrenic artery.

Figure 4.

Individual oxygen delivery-consumption relationships for the pump perfused, resting (Rest) and contracting (3Hz) diaphragm following infusion of N^G-nitro-L-arginine into the phrenic artery.

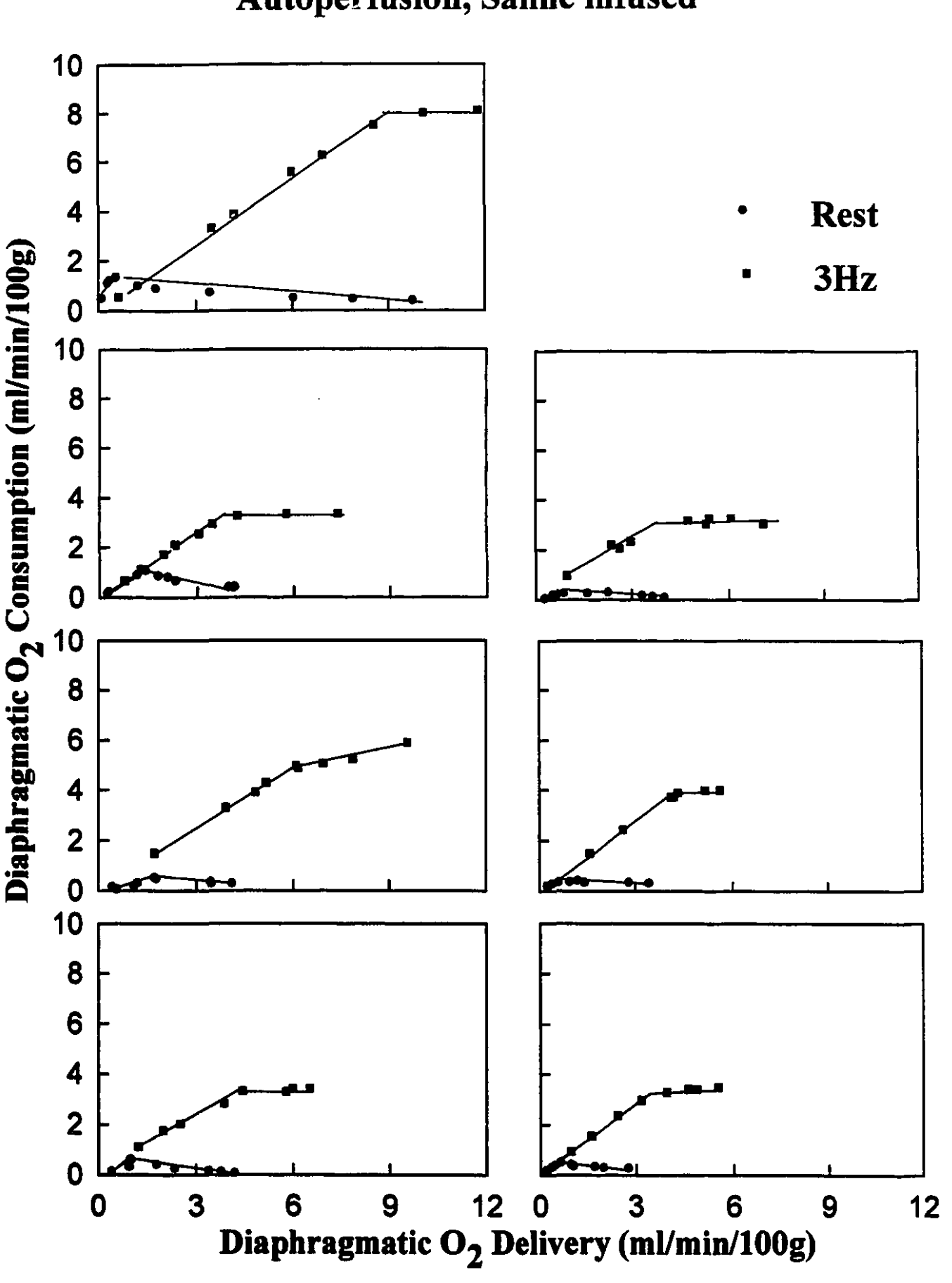
Autoperfusion, Saline infused
Rest
3Hz
Diaphragmatic O_2 Consumption (ml/min/100g)
Diaphragmatic O_2 Delivery (ml/min/100g)
0
2
4
6
8
10
0
3
6
9
12

Figure 2

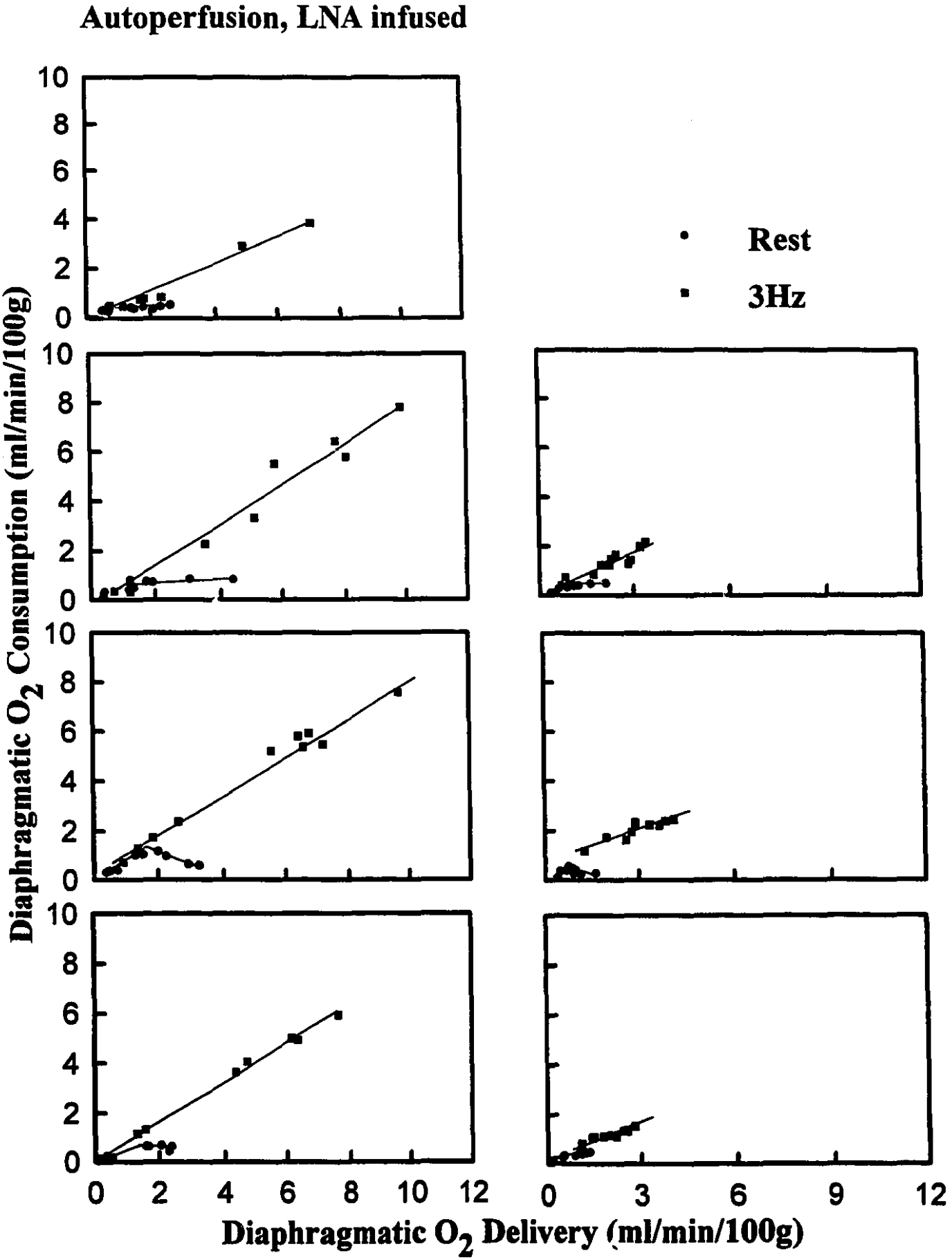
Autoperfusion, LNA infused
Rest
3Hz
Diaphragmatic O_2 Consumption (ml/min/100g)
Diaphragmatic O_2 Delivery (ml/min/100g)
0
2
4
6
8
10
12
3
9

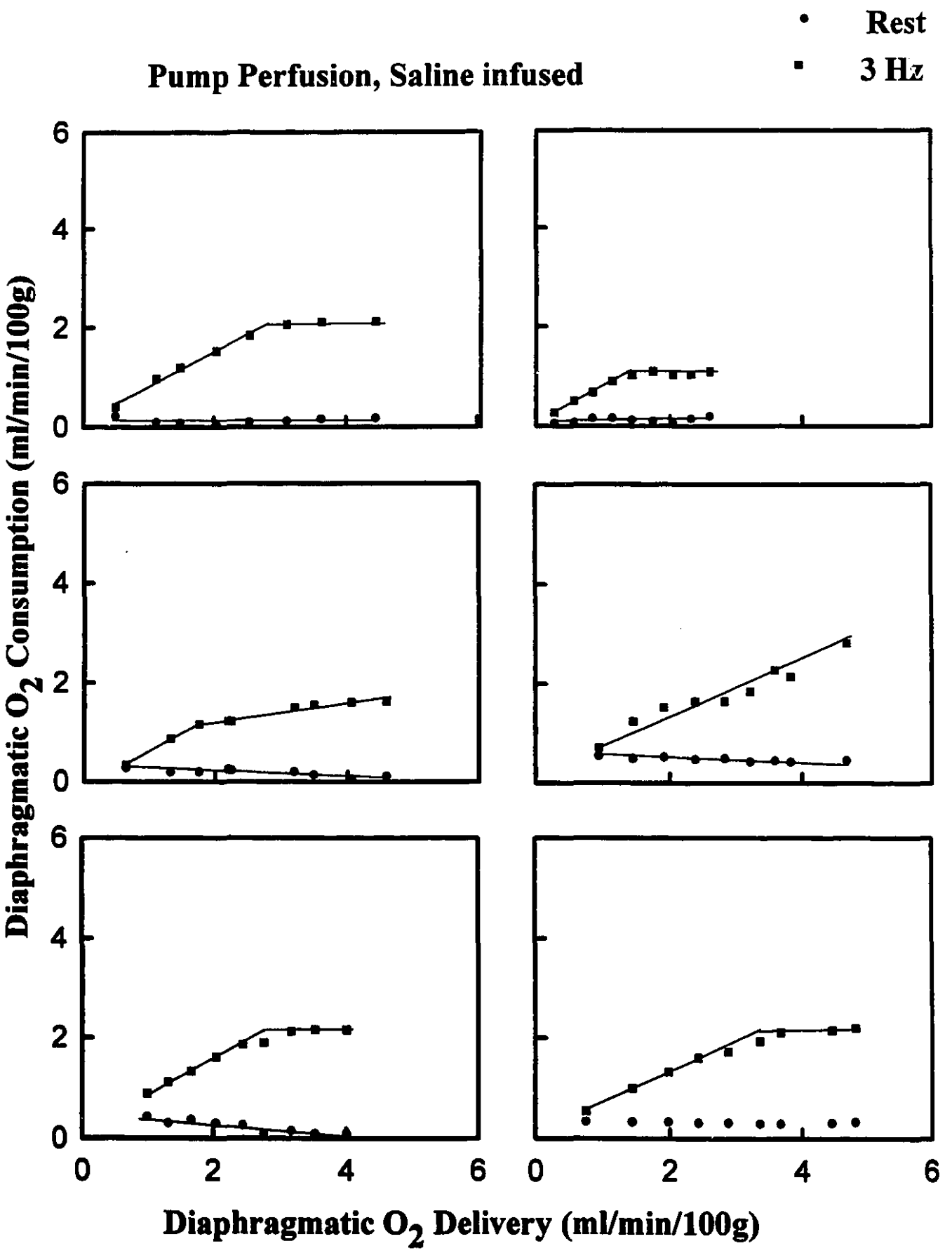
Rest
3 Hz
Pump Perfusion, Saline infused
Diaphragmatic O_2 Consumption (ml/min/100g)
Diaphragmatic O_2 Delivery (ml/min/100g)
0
2
4
6

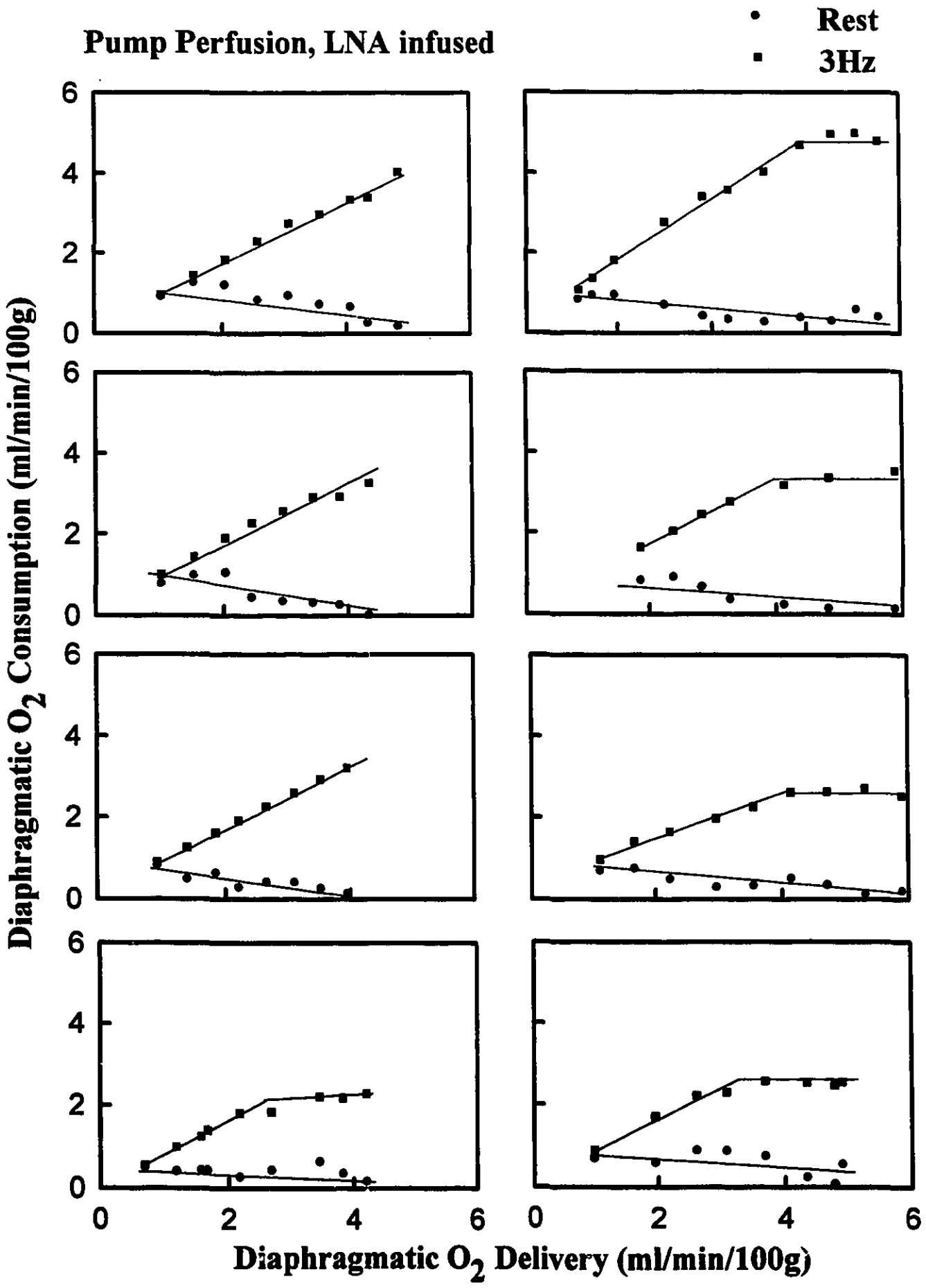
Pump Perfusion, LNA infused
Rest
3Hz
Diaphragmatic O_2 Consumption (ml/min/100g)
Diaphragmatic O_2 Delivery (ml/min/100g)
0
2
4
6

CHAPTER 6: Summary and Conclusions

Summary and Conclusions

The studies presented in this thesis evaluate the processes by which the respiratory muscles perform the work of ventilation and by which the metabolic substrates required for this work are supplied. These mechanisms determine the role which failure of the respiratory muscles to sustain their work load plays in the development of respiratory failure. In chapter two, a model of chest wall function is presented. This model represents an advance over previous conceptualizations in that it recognizes the rib cage as a system comprised of two mechanically linked but anatomically and functionally distinct units. Within the framework of this model, and relying on the mathematical analysis to which it gives rise, the strength of the mechanical linkage between rib cage compartments and the separate actions of the respiratory muscles was determined in humans. The mechanical linkage between pulmonary (upper, lung apposed) and abdominal (lower, abdomen apposed) rib cage compartments was found to be stronger than had been predicted from animal studies. During quiet breathing, the force resulting from rib cage muscle contraction, and the force exerted on the pulmonary rib cage as a result of displacement of the abdominal rib cage contributed approximately equally to the pressure inflating the lungs. These findings indicate that the interaction between rib cage compartments is important and suggest a new mechanism by which alterations of chest wall function may contribute to the pathophysiology of respiratory failure. For example, processes which interfere with transmission of intraabdominal pressure to the abdominal rib cage (eg: pneumothorax, pleural effusion, hyperinflation) or which alter the interaction between the rib cage compartments (eg: trauma, ankylosis) may reduce the capacity of the chest wall to convert respiratory muscle contraction into ventilation of the lungs.

Another factor which influences the manner in which the respiratory muscles interact with each other is their pattern of neural activation. In chapter three, a study on the effect of activation of small fiber phrenic afferents on minute ventilation, ventilatory timing and the pattern of recruitment of the respiratory muscles is discussed. These fibers, activated by mechanical deformation and by the chemical byproducts of muscular metabolism transmit neural impulses arising in the diaphragm to the respiratory centres of the brain. They are, therefore, well situated to mediate reflex adjustments in the distribution of motor output among the respiratory muscles. Electrical activation of these fibers in spontaneously breathing dogs was found to stimulate ventilation through both an increase in respiratory frequency and tidal volume. The increase in breathing frequency was associated with a preferential reduction in expiratory time. The effect on respiratory muscle activity was inhomogeneous. Of the muscles active in inspiration, the increase in activity of the genioglossus muscle was much greater than that observed in the diaphragm, rib cage muscles or alae nasi. Of the muscles active in expiration, transversus abdominis activity increased greatly whereas triangularis sterni activity remained virtually unchanged. These changes suggest a role for reflexes involving phrenic small afferent fibers in redistributing the ventilatory load among respiratory muscle groups. In addition the pattern of activation and the effects on ventilatory timing suggest that these reflexes may provide a mechanism by which diaphragm length and velocity of shortening may be optimized to enhance muscular efficiency.

In chapter 4, two studies are discussed. In the first of these studies the effect of increasing blood flow independent of oxygen delivery on diaphragm fatigue is evaluated. The rate of development of fatigue was dependent on the flow rate per se. Therefore, although the

maintenance of diaphragm oxygen delivery is necessary to sustain a given level of metabolic activity, blood flow itself is an important factor in maintaining diaphragm contractility. In the second study, the dependence of diaphragm oxygen consumption on oxygen delivery is explored. The critical level of diaphragm oxygen delivery, at which oxygen uptake becomes supply dependent was the same for the resting diaphragm as for the average of the non-diaphragmatic tissues. In the contracting diaphragm, however, this point is reached at a far higher systemic oxygen delivery than for the other tissues. These findings suggest that the respiratory muscles, because their continued rhythmic contraction is obligatory, may be particularly sensitive to reductions in systemic oxygen delivery. This provides an explanation for the observation that respiratory failure develops early in shock states, before dysfunction of other tissues becomes life limiting.

In Chapter 5 the results of three studies are reported. The goal of these studies is to determine the role which endothelial nitric oxide release plays in regulating diaphragmatic blood flow and oxygen uptake. Nitric oxide release was inhibited in the diaphragmatic circulation by infusion of N^G-nitro-L-arginine. This treatment was found to increase baseline diaphragmatic vascular resistance. It also reduced the magnitude and duration of the reactive vasodilatory response to transient phrenic arterial occlusion. In the contracting diaphragm, inhibition of nitric oxide release increased the uptake of oxygen at a given oxygen delivery. That is, the extraction of oxygen was increased. This enhancement of oxygen extraction was also noted at the point of onset of delivery dependence of diaphragmatic oxygen consumption. These findings indicate an important role for the endothelial nitric oxide pathway in regulating basal diaphragmatic blood flow and suggest that it may mediate, in part, the vascular responses to metabolic stimuli.

Claims of Originality

Claims of Originality

Chapter 2

The study presented in this chapter represents an original application of a new model of chest wall mechanics to the analysis of chest wall motion in spontaneously breathing humans. In contrast to previous models this analysis incorporates a two compartment, flexible rib cage. The new knowledge added to the literature by the work comprising this chapter includes the following points:

1) The strength of the mechanical linkage between the upper (pulmonary) and lower (abdominal) rib cages in humans is greater than has previously been recognized and has been predicted by previous animal studies.

2) The relationship between degree of chest wall distortion and the force tending to restore the relaxation configuration of the chest wall is curvilinear. This means that the increment in restoring force for a given increase in distortion increases progressively with increasing degree of distortion.

3) As a result of the strength of mechanical linkage between pulmonary and abdominal rib cages, small distortions represent significant contributions to the pressure inflating the upper rib cage and lungs.

4) The analysis presented allows, for the first time, calculation of the contribution of the pressure generated by the rib cage muscles to inflation of the respiratory system. During spontaneous breathing in normal subjects, the pressure resulting from rib cage distortion and that generated by the rib cage muscles contribute equally to the total pressure required to inflate the lung and the pulmonary rib cage.

5) The analysis developed in this chapter permits the transdiaphragmatic pressure to be partitioned between insertional and non-insertional components. In normal subjects during quiet breathing, the insertional component of the transdiaphragmatic pressure is significant, comprising 40% of the total pressure across the diaphragm.

Chapter 3

The following new findings were contributed to the literature as a result of the work presented in this chapter:

1) Reflex interactions between the diaphragm and ribcage muscles, abdominal muscles and upper airway muscles exist and are mediated by small fibre afferents travelling in the phrenic nerve.

2) The increase in inspiratory muscle activity evoked by phrenic afferent stimulation is not homogeneous. While activation of the diaphragm, parasternal intercostal and alae nasi muscles increases to approximately the same extent, the genioglossus muscle is disproportionately recruited. This may be an important for protection of patency of the upper airway during intense diaphragmatic contraction.

3) The increases in expiratory muscle activation by phrenic afferent stimulation is also differentially distributed. Specifically, there is dissociation between the effects on the rib cage and abdominal expiratory muscles. Triangularis sterni activity is unaffected by phrenic afferent stimulation while the transversus abdominis is strongly recruited. This differential activation pattern may play a role in protecting the mechanical advantage of the diaphragm.

Chapter 4

The work included in this chapter contributes the following the new knowledge to the literature:

1) Increasing diaphragm blood flow retards development of diaphragmatic fatigue induced by intermittent submaximal contractions. This effect results from the increase in blood flow itself and is independent of alterations in diaphragmatic oxygen delivery.

2) At a level of activity resulting in a diaphragmatic oxygen consumption comparable to that observed during the application of moderate resistive loads, the critical systemic O_2 delivery for the diaphragm is higher than that for the rest of the body.

3) Critical diaphragmatic O_2 delivery and the critical O_2 extraction ratio for the resting diaphragm did not differ from those of the non-diaphragmatic tissues. These values increase levels above those for the non-diaphragmatic tissues during stimulated diaphragmatic contraction.

Chapter 5

The studies in this chapter evaluate the role of nitric oxide in regulation of diaphragmatic blood flow and oxygen transport. The new knowledge contributed by the studies comprising this chapter includes:

1) Inhibition of nitric oxide synthesis by infusion of the L-arginine analogues increases the baseline vascular resistance of the phrenic circulation in vivo.

2) Infusion of L-arginine and D-arginine at physiological pH have no effect on baseline diaphragmatic vascular resistance. This indicates that basal nitric oxide formation in the diaphragmatic vasculature is not limited by the availability of extracellular L-arginine.

4) Infusion of L-glutamine into the diaphragmatic circulation increases baseline vascular resistance. This suggests an important role for the intracellular recycling of L-citrulline as a source of L-arginine in the basal synthesis of nitric oxide in this vascular bed.

5) Inhibition of nitric oxide synthesis decreases the maximum change in diaphragmatic resistance and the duration of the vasodilation which follows transient occlusion of phrenic arterial blood flow. This finding suggests a role for nitric oxide in the metabolic regulation of blood flow in this vascular bed.

6) In the contracting diaphragm, nitric oxide inhibition increases the oxygen consumption and the oxygen extraction ratio at the critical point at which oxygen consumption becomes dependent on oxygen delivery. This suggests a role for the nitric oxide pathway in regulating oxygen delivery at the level of the intramuscular vasculature.

7) The critical diaphragmatic oxygen delivery and the maximum oxygen extraction ratio of the diaphragm are not affected by inhibition of nitric oxide synthesis.